

PROSTATE CANCER AND BONE HEALTH

Catherine Handforth

Submitted in accordance with the requirements for the
degree of Doctor of Philosophy

Department of Oncology and Metabolism
The Medical School
University of Sheffield

October 2021

Acknowledgements

Firstly, I would like to thank all the patients and volunteers that agreed to participate in the ANTELOPE study, without them, this would not have been possible. I am grateful to the Weston Park Hospital Cancer Charity who funded ANTELOPE.

To my supervisors Prof Brown and Dr Walsh, thank you for your support, encouragement and belief that I could do this. I am hugely appreciative of the opportunities given to me since 2015, which have extended beyond the work done in this thesis. I am especially grateful that you did not get too cross(!) about repeated maternity leaves, and for Dr Walsh who provided clinical oversight at the CRF.

To Margaret, you have been amazing throughout my time in Sheffield. I have really appreciated your wisdom and help with bone imaging and radiation protection. I am especially grateful for all the time you have invested in scan analysis, for carrying on after tricky times, and in the post-covid era, helping me pin down all the data. Thankyou also to Selina for your help with the scans at the CRF.

A special thankyou to Angela Green; for your enthusiasm for ANTELOPE, for helping me to untangle the logistics and practicalities, for doing a brilliant job recruiting controls, and help with matching. I am grateful to Julie Walker, Abiola Ali and Jill Thompson, for helping ensure things ran smoothly and that samples and paperwork were in the right places. Thank you to Claire Ward who helped at a key time to recruit participants to group A, to Fatma Gosseil for helping with the serum analysis, to Richard Jacques for the help with ANCOVA and Eugene McCloskey for help with FRAX calculations.

To Steve, thank you for sharing your proteomics wisdom with me, for supporting me through the laboratory project, and for truly empathising with the difficulties that come with managing parenting, sleeplessness and trying to get work done! To Ana and Maria, I am truly grateful for all the time you invested in me, for your advice, patience, and all the moral support. Thank you for teaching me everything in the lab, you somehow managed to transform me from someone who didn't know one end of a pipette from the other into some sort of laboratory scientist able to plan their own experiments. I am especially grateful for all the time you spent with me trying work out why things didn't work, and what I had done wrong!

To Amy and Elisavet, I appreciated having you around more than you know! Thank you for all the coffees, chat and support you gave me when things were tricky.

To my parents, thank you for all you have invested in me, for believing in me, and for all the support you have given me. To Josh, Sam and Reuben, thank you for the hugs, the fun and the silliness, and for keeping me going when it was just really difficult. It is hard to believe that I started this journey before you were around. I hope that I have shown you that working hard is worth it, and that if you are determined enough, you can achieve anything!

And finally to my Harry. You are incredible and I could not have done this without you. Thank you for all that you have sacrificed in order for me to be able to do this, for your patience, being a superb dad and for stepping in when I was not around. Your love and moral support has enabled me to keep on going. What a journey. Six years later, finally, I can say that it is done.

The candidate confirms that the work submitted in this thesis is her own and that appropriate credit has been given where reference has been made to the work of others.

This copy has been supplied on the understanding that it is copyright material and that no quotation from the thesis may be published without proper acknowledgement.

Statement of attribution

ANTELOPE study

Prof Brown and Dr Walsh obtained funding for the ANTELOPE study from the Weston Park Hospital Cancer Charity. The original study protocol was written by Prof Brown and Dr Walsh, I was involved in subsequent amendments. I applied for and secured ethical approval and arranged local research and development approvals. I obtained medical imaging and medical physics approval. I was responsible for site file maintenance, submission of amendments and general study management. I wrote the participant information sheets, consent form, bone health questionnaire, CRF and other supporting documentation.

I was responsible for study recruitment; I recruited group B participants and approximately half of group A. The urology research nurse Claire Ward recruited the remainder of group A participants (whilst I was on maternity leave). I recruited group C participants from email and poster advertisements, the rest were recruited by Angela Green, research sister at the Northern General NIHR Clinical Research Facility (NGH CRF) from an existing database of healthy volunteers. I kept the study recruitment and screening log up to date.

Study visits were booked by the research sisters at the Clinical Research Facility; Angela Green, Julie Ward and Abiola Ali. Study visits were carried out by a researcher; either myself or one of the research nurses. Study visits included eligibility checking, informed consent, anthropometric measurements, serum sample collection and processing, tests of physical performance and muscle strength, ensuring questionnaire completion and arranging participant expenses. Mrs Jill Thompson helped with some of the serum sample processing, and arranged storage at the CRF and transfer to the University of Sheffield Biorepository. I collected all data for prostate cancer diagnosis and treatment from clinical records.

All DXA and Xtreme CT scans were carried out by Dr Margaret Paggiosi and Selina Bratherton who established the scanning protocols. Where possible, I observed these scans. Scan analysis and finite element analysis were performed by Dr Paggiosi and Selina Bratherton.

Serum biochemistry analysis and sex hormone analyses were carried out at the Department of Clinical Chemistry, Sheffield Teaching Hospitals. Fatma Gossiel performed the automated biochemical analysis for the biomarkers of bone turnover in the Bone Biochemistry Laboratory, Medical School, the University of Sheffield.

I was responsible for ensuring that study documentation was complete and for addressing data queries. I helped to design the study database with the data manager at the Cancer Clinical Trials Centre at Weston Park Hospital, Janet Horsman. Data entry was done by Carol Crabtree and Richard Lloyd at the Cancer

Clinical Trials Centre. Scan data were downloaded directly from the scanners by Dr Margaret Paggiosi.

I carried out statistical analysis for the study, ANOVA and ANCOVA for comparison of between group changes was done by Richard Jacques, statistician at the School of Health and Related Research, University of Sheffield. FRAX risk calculation was performed by an existing computer-based algorithm, by Dr Helena Johansson.

Biomarkers of prostate cancer bone metastasis

Prostate cancer cell lines were obtained and cell lysates were prepared by Dr Steven Wood, senior research associate, University of Sheffield. I undertook protein assays, western blots, image analysis and data analysis. For the IHC work, FFPE TMA slides were prepared by Maria Oliva, research technician, and Maggie Glover sectioned these to prepare slides for IHC. I undertook antigen retrieval, immunoprobng, slide scanning and image analysis myself.

Prof Brown, Dr Walsh and Dr Wood provided advice and guidance throughout this work.

.

Publications

List of publications during PhD training

Brown JE, Handforth C, Compston JE, Cross W, Parr N, Selby P, Wood S, Drudge-Coates L, Walsh JS, Mitchell C, Collinson FJ et al. Guidance for the assessment and management of prostate cancer treatment-induced bone loss. A consensus position statement from an expert group. *Journal of Bone Oncology*, 2020; 100311-100311

Handforth C, D'Oronzo S, Coleman R, Brown JE. Cancer treatment and bone health. *Calcified tissue international*: 2018:102 (2) p 251-264

Handforth C, Burkinshaw R, Freeman J, et al. Comprehensive geriatric assessment and decision making in older men with incurable but manageable (chronic) cancer. *Supportive care in cancer* (2019) 27: 1755-1763

Salawu A, Handforth C, Brown JE. Bone targeted therapies in prostate cancer (chapter). In: *Management of prostate cancer: a multidisciplinary approach*. p 343-356. Jan 2017. Springer.

Table of Contents

Acknowledgements.....	ii
Statement of attribution.....	iv
Publications.....	vi
Table of Contents.....	vii
List of Tables.....	xiv
List of Figures.....	xvi
Outline of thesis.....	1
Abstract.....	2
List of Abbreviations.....	3
Chapter 1: Introduction.....	7
1.1 Bone anatomy and determinants of bone strength.....	7
1.1.1 Types of bone tissue.....	7
1.1.2 Bone tissue composition.....	8
1.1.3 Determinants of bone strength.....	9
1.1.4 Bone geometry.....	12
1.1.5 Bone microarchitecture.....	12
1.1.6 Bone tissue material properties.....	13
1.2 Bone biology and physiology.....	14
1.2.1 Osteoblasts.....	14
1.2.2 Bone lining cells.....	15
1.2.3 Osteocytes.....	15
1.2.4 Osteoclasts.....	16
1.2.5 Bone turnover.....	18
1.2.6 Biomarkers of bone turnover.....	19
1.2.7 Regulation of bone turnover.....	23
1.3 Prostate cancer.....	24
1.3.1 Epidemiology and survival.....	24
1.3.2 Referral and clinical management pathway.....	24
1.3.3 Diagnosis.....	25
1.3.4 Staging and risk stratification.....	25
1.4 Prostate cancer treatment.....	27
1.4.1 Conservative management.....	27
1.4.2 Curative treatments.....	27

1.4.3 Management of metastatic prostate cancer	28
1.4.3.1 Hormone sensitive disease	28
1.4.3.2 Castration resistant disease	29
1.4.4 Androgen deprivation therapy.....	29
1.4.4.1 Production and activity of testosterone	29
1.4.4.2 Indications for ADT.....	30
1.4.4.3 Methods of ADT	30
1.4.4.4 Adverse effects of ADT.....	33
Bone density and microarchitecture	33
Hot flushes	41
Metabolic consequences.....	41
Body composition	41
Cardiovascular risk.....	41
Fatigue.....	41
Neuropsychological	42
Sexual dysfunction.....	42
1.5 Metastatic prostate cancer	45
1.5.1 Bone metastases	45
1.5.1.1 Epidemiology and clinical sequelae	45
1.5.1.2 Classification of bone metastases.....	46
1.5.1.3 Pathophysiology.....	46
1.6 Management of bone health in men with PC.....	49
1.6.1 Lifestyle modifications	49
1.6.2 Bone-targeted treatments	50
1.6.2.1 Bisphosphonates.....	50
1.6.2.2 Denosumab	51
1.6.2.3 Other therapies	51
1.7 Osteoporosis	52
1.7.1 Epidemiology.....	52
1.7.2 Aetiology and risk factors.....	52
1.7.3 The role of androgens and oestrogens in bone homeostasis.....	53
1.7.4 Osteoporosis in men	54
1.7.5 Diagnosis	55
1.7.6 Fracture risk assessment.....	56
1.7.7 Fracture risk assessment in men with prostate cancer	57
1.7.8 Management of osteoporosis in men.....	62

Chapter 2: Assessment of bone loss in men receiving treatment for prostate cancer (ANTELOPE)	64
2.1 Introduction	64
2.1.1 Factors that affect bone density and turnover	65
2.1.2 Sarcopenia.....	66
2.1.2.1 Prostate cancer and sarcopenia.....	69
2.1.2.2 Frailty in men with prostate cancer	71
2.1.3 Assessment of body composition, muscle function and strength	72
2.1.3.1 Body composition	72
2.1.3.2 Muscle function and strength	72
Grip strength.....	72
The short physical performance battery (SPPB)	73
2.1.4 Assessment of bone structure and microarchitecture	74
2.1.4.1 Dual X-ray absorptiometry (DXA).....	74
2.1.4.2 Basic principles	74
2.1.4.3 Limitations of DXA.....	75
2.1.5 Computed tomography.....	78
2.1.6 High resolution computed tomography	78
2.1.7 Finite element methods.....	79
2.1.8 High resolution imaging techniques used in prostate cancer	83
2.2 ANTELOPE study methods	84
2.2.1 Overall aim and rationale for ANTELOPE	84
2.2.2 Study design	84
2.2.3 Study location, funding and approval	85
2.2.4 Recruitment and informed consent.....	85
2.2.5 Inclusion and exclusion criteria.....	86
2.2.6 Study assessments and schedule.....	90
2.2.6.1 Anthropometric measurements	90
2.2.6.2 Prostate cancer and treatment details	90
2.2.6.3 Serum samples	90
2.2.6.4 Bone health questionnaire.....	91
2.2.6.5 Tests of muscle function	91
2.2.6.6 Frailty assessment	92
2.2.7 ANTELOPE bone imaging procedure	94
2.2.7.1 DXA.....	94

Image acquisition and quality control	94
Study procedure	94
Image analysis.....	95
2.2.7.2 High resolution peripheral quantitative computed tomography.....	97
Image acquisition and quality control	97
Study procedure	97
Image reconstruction and analysis	98
2.2.7.3 HR-CT T12 vertebra	103
2.2.8 Study data management.....	103
2.2.9 Outcomes of interest	103
2.2.10 ANTELOPE statistical analysis.....	105
Chapter 3: ANTELOPE results (I) the effect of androgen deprivation on mobility, muscle mass and function and bone biomarkers.....	106
3.1 Screening and recruitment	106
3.1.1 Baseline assessment	110
3.1.1.1 Participant demographics	110
3.1.1.2 Bone health and fracture risk	110
3.1.1.3 Prostate cancer details.....	111
3.1.1.4 ADT administration and timing.....	111
3.1.1.5 Mobility, falls and frailty	115
3.1.2 Assessment of muscle function and strength.....	118
3.1.3 Changes in body composition	122
3.1.4 Results of serum tests	128
3.1.4.1 Vitamin D status	128
3.1.4.2 Measurement of sex hormones.....	128
3.1.4.3 Biomarkers and regulators of bone turnover	130
3.2 Summary of key findings from this chapter	134
Chapter 4: ANTELOPE results (II) the effect of androgen deprivation therapy on bone density and microarchitecture	135
4.1 Results	135
4.1.1 Change in in lumbar spine and hip bone mineral density and bone mineral content by DXA.....	135
4.1.2 Change in radius volumetric density and microarchitecture by HR-pQCT	142
4.1.3 Finite element analysis.....	151
4.2 Summary of key findings from this chapter	156

Chapter 5: ANTELOPE: Overall discussion	157
5.1 Study recruitment and retention	157
5.2 Changes in sex hormones	158
5.3 Bone health	158
5.4 Fracture risk	159
5.5 Prevalence of frailty	160
5.6 Tests of physical function	161
5.7 Changes in body composition	163
5.8 Changes in biomarkers of bone turnover	166
5.8.1 Resorption and formation markers in non-metastatic prostate cancer	166
5.8.2 Resorption and formation markers in metastatic prostate cancer	167
5.9 ADT and osteoclast activity	168
5.10 ADT and osteocyte activity	169
5.11 Conclusion: the effects of ADT on biomarkers of bone turnover	170
5.12 Changes in areal bone mineral density	171
5.13 Changes in volumetric bone density	174
5.14 Changes in bone microarchitecture	176
5.15 Changes in bone strength	177
5.16 Strengths of study	178
5.17 Study limitations	179
5.2 ANTELOPE: Main conclusions and future work	180
5.3 Overall conclusion	186
Chapter 6: Potential biomarkers of metastatic bone disease in prostate cancer	187
6.1 Overview	187
6.2 Introduction	187
6.2.1 Use of bone biomarkers in men with PC and metastatic bone disease	188
6.2.1.1 Diagnosis and prognostication	188
6.2.2 Biomarkers predictive of response to therapy	189
6.2.3 Novel approaches to biomarker discovery in PC bone metastases	189
6.2.3.1 Circulating tumour cells, tumour DNA and micro RNA....	189
6.2.3.2 Proteomics	190

6.2.4 Potential protein biomarkers of cancer metastasis to bone	192
6.2.4.1 Macrophage capping protein (CAPG)	192
Structural features and mechanism of action	192
Role in cancer biology	192
CAPG in prostate cancer.....	193
CAPG and cancer metastasis.....	193
6.2.4.2 GAIP interacting protein C terminus member 1 (GIPC1).....	193
Structural features and mechanism of action	193
Role in cancer biology	194
Role as a biomarker	194
Studies in prostate cancer.....	195
6.2.4.3 Dedicator of cytokinesis protein 4 (DOCK4)	197
Structural features and mechanism of action	197
DOCK family proteins and cancer biology	200
DOCK4 and tumorigenesis.....	200
DOCK4 as a clinical biomarker	200
Studies of DOCK in prostate cancer	201
6.2.5 Prostate cell lines and in vitro models	201
6.2.5.1 Prostate cancer cell lines	202
LNCaP	202
C4, C5 and C4-2 cell lines.....	203
The C4-2B and C4-2B4 cell lines.....	203
PC3 and PC3M cell lines	204
6.2.6 Hypothesis and aims	204
6.3 Materials and methods	208
6.3.1 Cell culture	208
6.3.2 Preparation of cell lysate	208
6.3.3 Protein assay	208
6.3.4 Western blotting	208
6.3.5 Optimisation.....	209
6.3.6 Immunohistochemistry	212
6.3.6.1 Preparation of slides	212
6.3.6.2 Verification of target proteins	212
6.3.7 Statistical analysis	213
6.4 Results	217
6.4.1 CAPG.....	217
6.4.1.1 Verification by western blot.....	217
6.4.2 GIPC1	220
6.4.2.1 Verification by western blot.....	220
6.4.2.2 Verification by immunohistochemistry	223

6.4.3 DOCK4	228
6.4.3.1 Verification by western blot.....	228
6.4.3.2 Verification by immunohistochemistry	231
6.4.4 Overall summary of analysis	236
6.5 Discussion.....	238
6.5.1 CAPG.....	238
6.5.2 GIPC1	240
6.5.3 DOCK4	241
6.5.4 Strengths of this study	242
6.5.5 Study limitations	243
6.6 Conclusions and recommendations for future work	243
Overall summary of thesis.....	245
Bibliography.....	248

List of Tables

Table 1: Key biomarkers of bone turnover	21
Table 2: Prostate cancer risk stratification	26
Table 3: Methods used to achieve androgen deprivation	32
Table 4: Studies that have investigated of the effect of ADT on BMD in men with PC published since 2000	35
Table 5: Key studies of 12 month areal BMD change associated with ADT	40
Table 6: Key studies of the effect of ADT on body composition.....	43
Table 7: Summary of studies that have used FRAX to determine the fracture risk in ADT-treated men	60
Table 8: Definitions of sarcopenia	68
Table 9: Micro FE analysis outcomes derived from HR-QCT.....	81
Table 10: Summary of study inclusion and exclusion criteria.....	88
Table 11: Definition used for frailty	93
Table 12: ANTELOPE outcomes of interest from HR-pQCT.....	101
Table 13: Summary of screening and recruitment by study group	109
Table 14: Participant demographics at baseline	112
Table 15: Baseline risk factors for fracture, and risk calculation	113
Table 16: Prostate cancer staging and treatment in group A and B participants...	114
Table 17: Prevalence of frailty at baseline and at 12 months	116
Table 18: 12-month change in grip strength and SPPB score	119
Table 19: Comparison of groups A and C for change in grip strength and SPPB	120
Table 20: Baseline and 12 month measures of body composition	123
Table 21: Comparison of the mean change in body composition	125
Table 22: Change in serum sex hormones	129
Table 23: 12 month change in biomarkers and regulators of bone turnover	131
Table 24: Comparison of the 12 month change in serum biomarkers and regulators of bone turnover.....	133
Table 25: 12-month change in areal BMD	137
Table 26: Comparison of mean change in BMD and BMC	139
Table 27: Change in volumetric bone mineral density and bone microarchitecture.....	144
Table 28: Comparison of microarchitecture change	147
Table 29: Finite element analysis outcomes from HR-pQCT at the distal radius ...	152
Table 30: Comparison of finite element outcomes	154

Table 31: Contribution of ANTELOPE data to our current understanding of the effects of ADT on bone, body composition, frailty and physical performance.....	182
Table 32: Studies of the protein expression of a primary tumour as a biomarker of BM	191
Table 33: Prostate cancer cell lines used	206
Table 34: Primary and secondary antibodies used for immunoprobng, dilutions and optimal conditions used for film development	211
Table 35: Primary and secondary antibodies used for immunohistochemistry.....	216
Table 36: Quantification of CAPG identified by western blot.....	219
Table 37: Quantification of GIPC1 identified by western blot	221
Table 38: Verification of GIPC1 using IHC	224
Table 39: Average GIPC1 DAB intensity across cell lines	225
Table 40: Average GIPC1 DAB positive cells across cell lines.....	226
Table 41: Quantification of DOCK4 identified by western blot	229
Table 42: Verification of DOCK4 using IHC.....	232
Table 43: Average DOCK4 DAB intensity across cell lines.....	233
Table 44: Average DOCK4 DAB positive cells across cell lines	234
Table 45: Overall summary of biomarker results.....	237

List of Figures

Figure 1: A force-displacement curve (stress-strain) from mechanical testing of a bone.	10
Figure 2: Determinants of bone strength.	11
Figure 3: Osteoclast activity	17
Figure 4: Androgen action and main regulatory pathway	31
Figure 5: The 'vicious cycle' of prostate cancer cell bone metastases	48
Figure 6: The FRAX fracture risk assessment tool.....	58
Figure 7: Assessment of fracture risk and intervention thresholds.....	59
Figure 8: Aetiology of sarcopenia in men with prostate cancer.	70
Figure 9: DXA scanner scintillation detector array system.	77
Figure 10: The finite element process	82
Figure 11: The ANTELOPE study assessment schedule.....	89
Figure 12: Patient positioning for DXA and example images.	96
Figure 13: Patient positioning for DXA and example images.	99
Figure 14: Motion artefact grading used for HR-pQCT scan analysis.	100
Figure 15: ANTELOPE primary and secondary outcomes.	104
Figure 16: Summary of ANTELOPE screening, recruitment and retention	108
Figure 17: The prevalence of frailty.	117
Figure 18: 12-month change in maximal grip strength and total SPPB score.	121
Figure 19: 12-month change in lean mass and fat mass, and BMI by DXA.	126
Figure 20: 12-month change in trunk and upper limb lean mass and fat mass by DXA.	127
Figure 21: 12-month change in hip and lumbar spine BMD.	140
Figure 22: 12-month change in total body BMD and BMC measurements.....	141
Figure 23: 12-month change in vBMD by HR-pQCT at the distal radius.....	148
Figure 24: Plots of the 12-month change in cortical microarchitecture at the distal radius by HR-pQCT.....	149
Figure 25: 12-month change in trabecular microarchitecture at the distal radius by HR-pQCT.	150
Figure 26: 12-month change in estimates of bone strength and stiffness at the distal radius by HR-pQCT.	155
Figure 27: Summary of important future research questions in ADT-treated men with PC	185
Figure 28: Activity of GIPC1.....	196
Figure 29: Regulation of DOCK proteins by ELMO.....	198

Figure 30: DOCK4 mechanisms of action.	199
Figure 31: Hypothesis for the relationship between the prostate cancer cell lines and expression of potential biomarkers of BM.	207
Figure 32: Western blot analysis for biomarker validation.	210
Figure 33: Immunohistochemistry using heat antigen retrieval.	214
Figure 34: A standard IHC run with DOCK4 and GIPC.	215
Figure 35: CAPG protein quantified by western blot.	218
Figure 36: GIPC1 protein identified by western blot.	222
Figure 37: IHC images for GIPC1 and DAB intensity.	227
Figure 38: DOCK4 quantification by western blotting.	230
Figure 39: IHC images for DOCK4 and DAB intensity.	235

Outline of thesis

Chapter one

General introduction

Chapter two

ANTELOPE study: introduction and methods

Chapter three

ANTELOPE results (I): screening, recruitment and demographics, cancer information and fracture risk The effect of ADT on frailty, fracture risk, tests of muscle function and physical performance, and serum bone biomarkers.

Chapter four

ANTELOPE results (II): the effects of ADT on bone density, microarchitecture, structure and strength.

Chapter five

ANTELOPE discussion, summary and conclusions

Chapter six

Biomarkers of prostate cancer bone metastases. Introduction to biomarkers, methods, results, discussion and conclusions

Abstract

Introduction

Both prostate cancer (PC) and its treatment have important effects on bone and body composition. Three distinct mechanisms affect bone; androgen deprivation therapy (ADT); use of chemotherapy and systemic glucocorticoids (GC), and bone metastases (BM). Work undertaken in this thesis investigates the effect of ADT on bone density, microarchitecture, strength, physical performance, frailty, biomarkers of bone turnover and body composition. The second section explores the role of biomarkers in predicting the development of PC BM.

Methods

The ANTELOPE trial recruited men receiving ADT or ADT and chemotherapy/GC for PC, and healthy controls. A comprehensive bone health assessment was undertaken at baseline and 12 months to identify changes associated with ADT. The biomarker discovery project applied proteomic methods to PC cell lines to quantify the expression of CAPG, GIPC1 and DOCK4 proteins and sought to relate expression to their predicted metastatic potential.

Results

ADT was associated with loss of bone density at all skeletal sites. There was significant loss of volumetric density at the radius, along with microarchitectural deterioration and reduced bone strength and stiffness. ADT increased bone turnover, and led to sarcopenic obesity with marked effects in upper limb composition. Frailty increased and physical performance and strength deteriorated in association with ADT.

The biomarkers GIPC1 and DOCK4 showed differential expression across PC cell lines and may have a role in the early stages of metastasis, but do not appear to predict BM development.

Conclusions

ADT has profound effects on bone density, structure, strength and body composition, and has important effects on frailty and physical performance. Assessment of bone health is an unmet need in this population and must be incorporated into clinical practice to reduce risk of fractures and their associated morbidity and mortality. Studies should explore the effects of bone targeted therapies on density and microstructure in order to select the most appropriate treatment for this population.

Proteomic techniques allow the identification of predictive biomarkers of BM in PC, and further work should explore GIPC1 and DOCK4 in PC cell lines and tissue models.

List of Abbreviations

ADT	Androgen deprivation therapy
AGE	Advanced glycation end products
AN(C)OVA	Analysis of (co)variance
AR	Androgen receptor
AS	Active surveillance
ATP	Adenosine triphosphate
BALP	Bone alkaline phosphatase
BC	Breast cancer
BM	Bone metastases
BMD	Bone mineral density
BMP	Bone morphogenetic protein
BP	Bisphosphonate
BSP	Bone sialoprotein
BTM	Biomarkers of bone turnover
CAB	Complete androgen blockade
CAPG	Macrophage-capping protein
CES-D	Center for Epidemiological Studies-Depression
CI	Confidence Interval
CRPC	Castration resistant prostate cancer
CSF1	Colony stimulating factor 1
CT	Computed tomography
CTC	Circulating tumour cells
ctDNA	Circulating tumour DNA
CTIBL	Cancer treatment induced bone loss
CTX	C-terminal telopeptide of type 1 collagen
DAB	3,3'-Diaminobenzidine
DHEA	Dihydroepiandrosterone
DHT	Dihydrotestosterone
DKK	Dickkopf-related protein
DMEM	Dulbecco's Modified Eagle Medium
DOCK	Dedicator of cytokinesis protein 4 (DOCK4)
DPD	Deoxypyridinoline
DXA	Dual-energy X-ray absorptiometry

EBRT	External beam radiotherapy
ECLIA	Electrochemiluminescence Immunoassay
ECM	Extracellular matrix
ELISA	Enzyme-linked immunosorbent assay
FCS	Fetal calf serum
FEA	Finite Elements Analysis
FFPE	Formalin fixed paraffin-embedded
FGF	Fibroblast growth factor
FN	Femoral neck
FSH	Follicle stimulating hormone
GC	Glucocorticoid
GEF	Guanine nucleotide exchange factor
GIPC1	GAIP interacting protein C terminus member 1
GnRH	Gonadotrophin releasing hormone
GTP	Guanosine-5'-triphosphate
HIF1	Hypoxia inducible factor 1
HR	Hazard Ratio
HRCT	High resolution computed tomography
HR-pQCT	High-resolution peripheral quantitative computed tomography
HSPC	Hormone sensitive prostate cancer
HTA	Human Tissue Authority
IHC	Immunohistochemistry
ILGF	Insulin-like growth factor
IMRT	Intensity modulated radiotherapy
IOF	International Osteoporosis Foundation
IT	Intervention threshold
LDL	Low density lipoprotein
LH	Luteinising hormone
LHRH	Luteinising hormone releasing hormone
LRP	Low-density lipoprotein receptor-related protein
LS	Lumbar spine
(m)CRPC	(metastatic) castration resistant prostate cancer
(m)HSPC	(metastatic) hormone sensitive prostate cancer
MCSF	Macrophage colony stimulating factor

miRNA	microRNA
MMP	Matrix metalloproteinases
MOF	Major osteoporotic fracture
MRI	Multi-parametric magnetic resonance imaging
MW	Molecular weight
NGS	Normal goat serum
NHS	National Health Service
NICE	National Institute for Health and Care Excellence
NOGG	National Osteoporosis Guideline Group
NTX	N-terminal telopeptide of type 1 collagen
OC	Osteocalcin
ONJ	Osteonecrosis of the jaw
OPG	Osteoprotegerin
OS	Overall survival
PBS	Phosphate buffered saline
PC	Prostate cancer
PDGF	Platelet derived growth factor
PET	Positron emission tomography
PFS	Progression free survival
PICP	Procollagen type I C propeptide
PINP	Procollagen type I N propeptide
PSA	Prostate specific antigen
PTH	Parathyroid hormone
PTH-r	Parathyroid hormone receptor
PTHrp	Parathyroid hormone related peptide
QALY	Quality adjusted life year
RANK	Receptor activator of nuclear factor kappa-B
RANK	Receptor activator of nuclear factor kappa-B ligand
RCT	Randomised Controlled Trial
Runx2	Runt related transcription factor 2
SCID	Severe combined immunodeficient
SDS PAGE	Sodium dodecyl-sulfate polyacrylamide gel electrophoresis
SE	Standard error
SERM	Selective oestrogen reuptake modulator

SHBG	Sex hormone binding globulin
SRE	Skeletal related event
SST	Serum separating tube
TBS	Trabecular bone score
TBV	Trabecular bone volume
TCF	T cell factor
TCL	Total cell lysate
TGFβ	Transforming growth factor beta
TH	Total hip
TMA	Tissue microarray
TNM	Tumour Node Metastasis (classification system)
Trap5b	Tartrate resistant acid phosphatase type 5b
uPA	Urokinase plasminogen activator
VEGF	Vascular endothelial growth factor
VF	Vertebral fracture
WHO	World Health Organisation
Wnt	Winged (signalling pathway)
WW	Watchful waiting

Chapter 1: Introduction

This chapter will provide a general introduction to this thesis. It will explain basic bone anatomy, physiology, and metabolism. It will also provide a thorough overview of prostate cancer, with a focus on the effects of androgen deprivation therapy and metastatic bone disease on bone health. This chapter will also explain the mechanisms and management of osteoporosis in men, including the role of fracture risk assessment.

1.1 Bone anatomy and determinants of bone strength

The adult human skeleton is comprised of more than 200 bones, and provides structural support, facilitates movement and protects vital organs. It regulates mineral homeostasis and acid-base balance, serves as a reservoir for growth factors and cytokines, and is the site of haematopoiesis within the bone marrow compartment. Long bones have a hollow shaft (diaphysis), a flared metaphysis below the growth plate, and a rounded epiphysis ¹.

1.1.1 Types of bone tissue

Macroscopically, bone tissue can be divided into cortical bone and trabecular bone. Approximately 80% of the adult human skeleton is comprised of cortical bone ². This is predominantly found in the diaphysis of long bones and is responsible for the mechanical function of the skeleton. Trabecular bone is mostly found in the axial skeleton between the cortices of smaller bones such as the scapulae and vertebrae. Trabecular bone is surrounded by a cortical shell, but the cortical thickness (and the ratio of cortical to trabecular bone) depends on the location in the skeleton. For example, cortical bone comprises 95% of bone tissue at the radius (higher cortex to trabecular bone volume ratio), compared with only 25% in the vertebral bodies ¹. In general, there is a higher cortex to trabecular bone volume ratio in diaphyseal areas than in metaphyseal areas ³.

Cortical bone consists of a series of dense, parallel concentric osteons and has an outer periosteum and an inner surface covered by endosteum ^{1,4}. A network of Haversian and Volkmann's canals contain capillaries and nerve fibres, and facilitate the supply of energy and nutrients ⁵. The periosteal surface is where appositional growth and damage repair occur. Bone formation typically exceeds resorption here, and as a consequence, bone diameter increases with ageing ⁶. The inner endosteal surface experiences a greater rate of bone turnover due to biomechanical forces and exposure to cytokines ¹. Bone resorption exceeds formation here, and the bone marrow compartment expands over time.

In general, cortical bone is stiffer and able to resist higher stress than trabecular bone, but it is also more brittle ^{3,7,8}. It has a more uniform pattern of biomechanics, strength and stiffness than trabecular bone. Cortical porosity is defined as the average fraction of void volumes within the cortical bone volume, usually around 5% ⁹. Increased cortical

porosity is observed when bone turnover is increased, and it is associated with reduced strength and stiffness^{10,11,12}. Cortical porosity contributes to an increased risk of fracture, independent of bone density and other fracture risk factors^{10,13}.

Trabecular bone is more metabolically active than cortical bone and has a much larger surface area¹. It is comprised of a network of lamellar bone plates and rods that are interspersed throughout the tissue, and is less dense, homogenous and parallel than cortical bone². Trabecular bone obtains its blood supply via diffusion from the bone marrow compartment⁴. It varies widely in strength and stiffness even within a small area, due to its heterogeneity in structure and apparent density. In general, trabeculae size and shape, and their connectivity and orientation (a measure of anisotropy, where properties depend on direction of load) are significant contributors to bone strength.

The stiffness and strength of cortical and trabecular bone depend on the direction of the load that is applied. Bone is most able to withstand compression loads, is able to withstand tension loads to some degree, and is least able to resist shear loads^{14,15}.

1.1.2 Bone tissue composition

The majority of bone is comprised of an organic matrix which consists predominantly of type 1 collagen fibres^{16,17}. The remainder is comprised of proteoglycans and non-collagenous proteins which have a role in matrix mineralisation and regulation of bone cell differentiation and function¹⁸. The main function of bone matrix is to provide tensile strength, reflected by an increased fracture risk in those with abnormal type 1 collagen^{19,20}.

Type 1 collagen is produced by osteoblast cells from procollagen. This polypeptide consists of an N-terminal pro-peptide, a central collagen domain and a C terminal pro-peptide. Following post-translational modification, procollagen is transported through the Golgi apparatus and secreted from the cell into the extracellular matrix²¹. It is cleaved of the N and C-terminals to produce a triple helix. This consists of two identical $\alpha 1(I)$ chains and a third structurally similar but genetically different $\alpha 2(I)$ chain. Each chain is composed of around 1000 amino acids and has cross links (formed by hydrogen bonds) between hydroxyproline and other charged residues. These mature collagen molecules undergo spontaneous self-assembly into linear collagen fibrils, which are grouped in bundles to form collagen fibres²¹. Inter-molecular and inter-fibrillar cross-links²² help to maintain the polypeptide chains in a closely organised fibrillar structure.

The inorganic fraction of bone accounts for around 60% of bone tissue by weight, and around 40% of bone volume^{17,23}. It is comprised of hexagonal hydroxyapatite crystals of calcium and phosphate which can vary in size or in composition¹⁶. Mineralisation is a key determinant of bone strength, and refers to the process by which an inorganic substance (hydroxyapatite) precipitates in an organic matrix scaffold (type 1 collagen predominant bone matrix). Bone mineralisation occurs in two phases. Primary mineralisation of newly formed bone occurs during the bone remodelling cycle

(described later), and secondary mineralisation after the remodelling cycle has been completed, where there is a gradual increase in crystal size and number ^{1,24}.

1.1.3 Determinants of bone strength

The ability of bone to carry out its mechanical function is determined by its strength ²⁵. When strain on a bone reaches a critical limit, it is unable to be effectively dissipated, micro-cracks form, and accumulation of these ultimately leads to bone failure (fracture).

There are four mechanical terms that can describe the load- carrying behaviour of bone, and these can be derived from a stress-strain curve when bone undergoes testing (figure 1) ^{26,27}. Bone strength is the maximum force that a bone can withstand and is represented by the maximum height of the curve. The area under the curve is a combination of bone toughness (an approximate estimate of the energy that is required to cause bone failure) and resilience which is the amount of stored elastic energy. The fourth key property is bone stiffness, which is how a bone responds to an initial load, and is represented by the maximum slope of the stress strain curve. Bone stiffness prevents a bone from bending and buckling in response to strain ²⁸.

A well-established hierarchical group of material properties are the key determinants of bone strength and are shown in figure 2. These include; whole bone geometry and bone mass (bone size and shape, the amount and distribution of bone tissue, and cortical thickness); bone microarchitecture (trabecular architecture, cortical parameters such as porosity); and biophysical properties of bone tissue (such as the mineral to matrix ratio and mineral crystal size, degree and types of collagen cross links, the ability to repair microdamage) ²⁹. It therefore follows that bone strength can be impaired by deficits in one or more of the above properties of bone. However, their relationship with overall bone strength is complex, and all determinants must be considered together. For example, properties which may contribute to a bone having increased resistance to compression may be deleterious when a different force (such as bending) is applied ³⁰. Equally, many properties have a U shaped association with bone strength; such as the degree of mineralisation (too little mineralisation causes weakness, whilst excess mineralisation causes brittleness and decreased elastic strength) ^{31,32}.

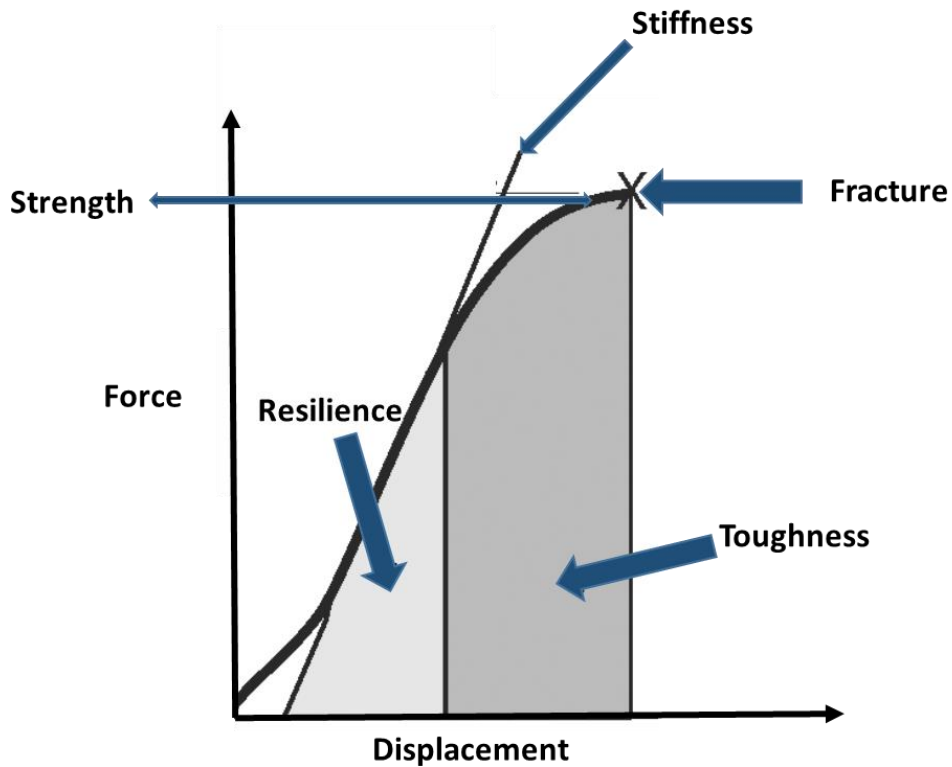


Figure 1: A force-displacement curve (stress-strain) from mechanical testing of a bone.

The height of the curve represents bone strength, which is the maximum load that a bone can sustain. The total area under the curve is comprised of the material toughness (the amount of energy required to break the material, known as the plastic modulus) and resilience (the amount of stored elastic energy). The maximum slope of the curve indicates the bone stiffness, which is also known as the Young's modulus. This is the ratio between the stress applied to bone and the strain which occurs as a result; a higher Young's modulus denotes a stiffer material (more force is required to produce the same strain when compared to a less stiff material)³³. Indicated by X, the yield point is a transition point when the strains can no longer be dissipated, and which results in permanent structural damage (fracture). Figure adapted from Hart, NH et al²⁸.

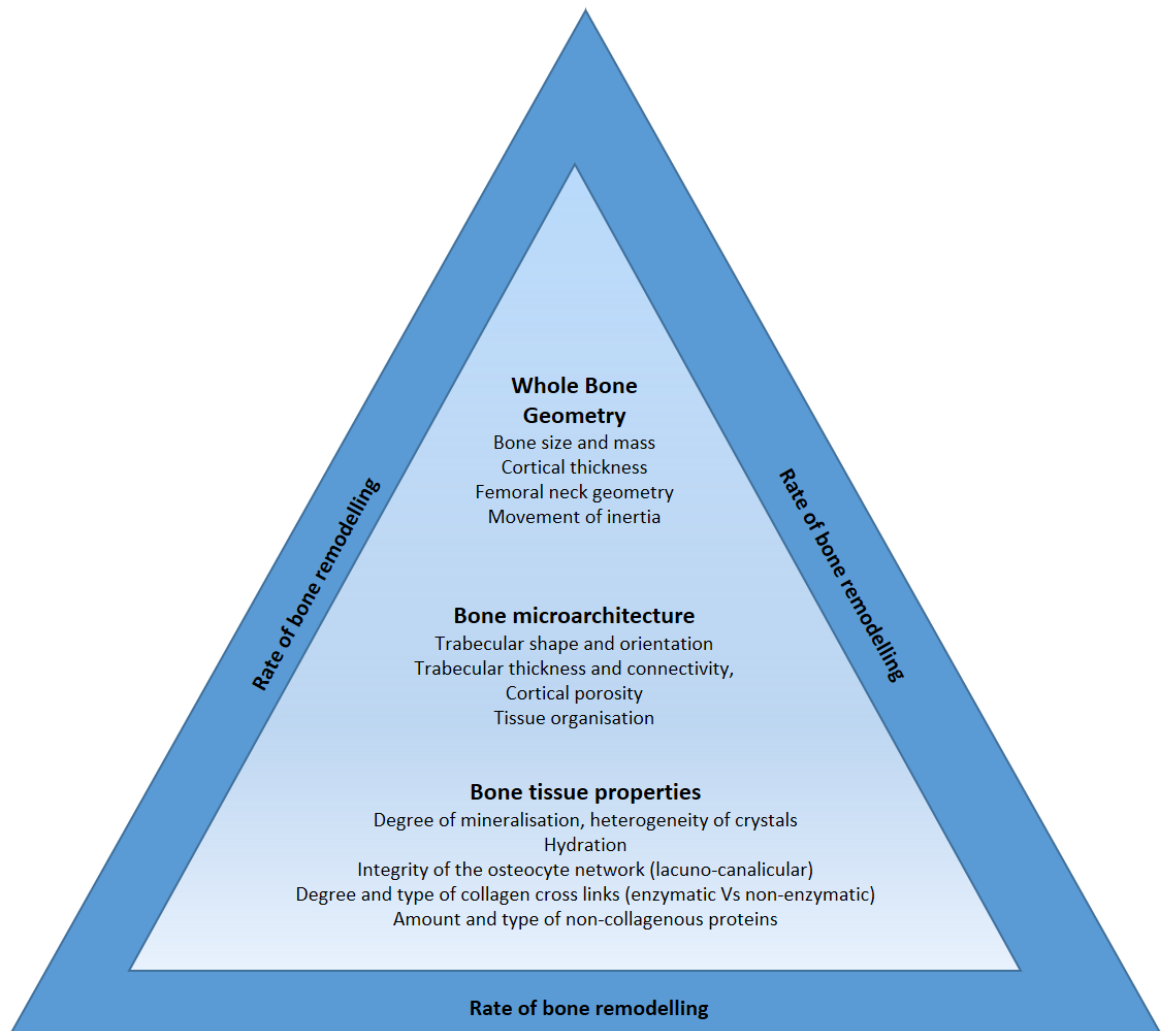


Figure 2: Determinants of bone strength.

An established bone strength framework demonstrates the material properties of bone strength ¹¹. At the top of the pyramid and supported by the other elements, the macrostructural and morphological features of bone are represented. The centre of the pyramid contains the microarchitectural properties of the cortical and trabecular components, and the base of the pyramid is represented by the relative amount and biophysical properties of the inorganic and organic components. In addition, the rate of bone remodelling (which may be affected by many other factors) is a key contributor to bone strength. Alterations in any one, or a combination of any of these can have a significant impact on overall bone strength.

1.1.4 Bone geometry

Bone geometry refers to its size, shape, cortical thickness, and cross sectional area. These factors determine the distribution of bone mass and the ability of bone to withstand forces such as bending and torsion²⁸. Increased cortical perimeter and thickness are predictive of higher bone strength and a reduced risk of fracture^{34,35}. It has been suggested that increases in bone diameter that are associated with age and menopause may be a compensatory mechanism for the changes seen in trabecular architecture and bone mass, allowing bone strength to be maintained^{36,37}. Femoral neck geometry affects the forces that are transmitted in the event of a fall³⁸, and femoral neck parameters have been incorporated into fracture risk estimation by software³⁹.

1.1.5 Bone microarchitecture

Bone microarchitecture refers to both trabecular and cortical parameters. Features of trabecular microstructure include the trabeculae orientation, thickness and spacing, and also their degree of connection with each other⁴⁰. When bone is resorbed, trabecular bone is often affected more than cortical bone due to its greater surface to volume ratio. Trabeculae shift from plate shapes to thinner rods, and their separation increases. Thinning leads to progressive perforation, loss of connectivity and reduced number of trabeculae, which compromises bone strength^{26,41}. This is most significant in bones with a high proportion of trabecular bone such as vertebrae, where the trabecular bone volume is thought to explain more than 90% of their variability in compressive strength, and can influence bone strength independently of BMD^{42,43}. Trabecular bone volume (TBV) decreases along with age; studies in humans have suggested approximately one quarter of TBV is lost between the ages of 20 and 90 years⁴⁴. The factors underlying this decrease seem to differ in men and women; the former experience decreased trabecular thickness, whilst the latter display a decrease in number and separation⁴⁴.

Cortical bone thickness and integrity contributes significantly to bone strength. The cortex bears between 30-90% of axial loads at the ends of long bones, the distal radius and the vertebrae. Assessment of cortical bone parameters predicts bone strength more accurately than bone mineral density measurement. Cortical bone mass, area and thickness are predictive of fracture risk at various skeletal sites⁴⁵.

Cortical porosity can reflect either an increased number or diameter of Haversian canals, or both of these. It is defined as the average fraction of void volumes within bone, and is reported as a percentage⁹. Cortical porosity increases with age and varies between individuals with the same BMD¹⁰. Increased cortical porosity is associated with reduced stiffness, toughness, elasticity and ability to absorb impact energy^{45,46,47,48}. It has also been observed that the mechanical properties of bone are highly sensitive to small changes in its cortical porosity; for example, a change in porosity from 10 to 15% reduces the elastic modulus (material stiffness) of a bone by almost half⁴⁶.

1.1.6 Bone tissue material properties

The properties of bone tissue comprise the relative amount and biophysical properties of both the organic and the inorganic (matrix) components. A key feature of the organic matrix is post translational crosslink formation between type 1 collagen fibres, which can occur via enzymatic and non-enzymatic mechanisms.

Enzymatic crosslinks are considered to be beneficial to the mechanical properties of collagen²¹. They are generated via both lysyl oxidase and lysyl hydroxylases, which aids the formation of crosslinks such as pyridinoline and deoxypyridinoline²¹, which are indicators of collagen maturity that can be used as markers of bone resorption⁴⁷.

Non-enzymatically generated collagen crosslinks include advanced glycation end products (AGEs) and pentosidine, and these accumulate with age and in disease (such as osteoporosis)^{48,49,50}. Glycation is mediated by aldose or ketose sugars (or other metabolites) which react with free amino groups in lysine, hydroxylysine and arginine residues and lead to formation of protein adducts or promotion of cross-linkage²¹. The presence of AGEs is associated with deterioration in bone mechanical properties; increased brittleness; accumulation of micro-damage, a reduction in toughness and increased fracture risk^{11,51,52}.

In addition to the type of crosslinks, other factors may influence the mechanical properties of collagen. These include; the amount and type of non-collagenous proteins⁵³, the orientation of collagen fibres⁵⁴ and the number and type of crosslinks present^{55,56}.

The degree of bone matrix mineralisation also has an important influence on bone strength³¹. In general, an increase in bone mineralisation is associated with increased strength and elastic modulus (even when other parameters of bone strength are the same). Mineralisation is linked to the speed at which new bone is synthesised and old bone is broken down (bone turnover); when this is rapid, recently formed bone is resorbed before there is time for adequate secondary mineralisation⁵⁷. Conversely, in very low bone turnover states there is excess mineralisation which can be harmful and compromise strength. In this situation, the reduced removal of old and extensively mineralised bone makes bone brittle and reduces its elastic properties, and facilitates the development and proliferation of micro-cracks and subsequent structural failure⁵⁸. An important clinical manifestation of this mechanism occurs when bisphosphonates are used to suppress bone turnover. A well described adverse effect of bisphosphonates is the incidence of atypical fractures⁵⁹; and bone tissue at these sites has been shown to be heavily mineralised⁶⁰.

In addition to the degree of mineralisation, the morphology of hydroxyapatite crystals is also a determinant of bone strength. Increased strength is associated with an increase in crystal size heterogeneity⁶¹, this reduces with ageing in humans, in those with fragility fractures, and in the long term use of bisphosphonates^{60,62}.

1.2 Bone biology and physiology

There are four principal types of bone cell; osteoblasts, osteoclasts, osteocytes and bone lining cells.

1.2.1 Osteoblasts

Osteoblasts are multinucleated cuboidal cells that are located on the surface lining of bone, and constitute 4-6% of all bone cells⁶³. They are derived from mesenchymal stem cells in the bone marrow and their principal role is to produce the organic bone matrix⁶⁴. They differentiate into mature osteoblasts via either intramembranous or endochondral ossification⁶⁵. The functional role of osteoblasts is reflected in their morphology; they display many characteristics of protein synthesising cells such as abundant rough endoplasmic reticulum, mitochondria, secretory vesicles and prominent Golgi apparatus⁶⁶.

Commitment of stem cells to the osteoprogenitor/ osteoblast cell lineage is dependent on the expression of specific genes such as bone morphogenetic protein, SOX9 and members of the Wntless (Wnt) pathway^{67,65}. The key transcription factor in the commitment of mesenchymal progenitor cells to the osteoblast lineage is the runt-related transcription factor 2 (Runx2)^{63,68}. Pre-osteoblast differentiation into mature cells occurs in three phases; the first involves proliferation and expression of fibronectin, collagen, transforming growth factor beta 1, and osteopontin⁶³. Stage two occurs when cells exit the cell cycle, begin to differentiate and show alkaline phosphatase activity (pre-osteoblast)⁶⁸. The third stage involves maturation and morphological changes and secretion of proteins including type 1 collagen and bone matrix proteins⁶⁵.

The process of new bone formation takes between 4 and 6 months. Bone matrix is synthesised by osteoblasts in two main phases; the deposition of matrix and mineralisation. Matrix is formed by the secretion of collagen, non-collagenous proteins as well as proteoglycans⁶⁹. Mineralisation begins when there is release of matrix vesicles from the apical membrane of osteoblasts, which bind to proteoglycans in the newly formed bone matrix²⁴. Calcium and phosphate ion mobilisation is also mediated by osteoblasts; they secrete enzymes that degrade proteoglycans (calcium containing) and alkaline phosphatase degrades phosphate containing compounds. Calcium ions are taken up into matrix vesicles via annexin channels whereas the phosphate ions are released inside matrix vesicles²⁴. Nucleation of these ions leads to the formation of the hydroxyapatite crystals. The fibrillar phase of mineralisation occurs when supersaturation of calcium and phosphate ions inside the matrix vesicles leads to their rupture and spread to the surrounding matrix⁷⁰.

Regulation of the osteoblast cell lineage, and their differentiation and maturation is complex, and involves multiple genes (Runx2, osterix, Sox9) as well as physical forces (such as shear stress, vibration, compression and bending) which induce

osteoblastogenesis⁷¹. Other important regulators include bone morphogenic proteins (BMPs)⁷², growth factors, Vitamin D receptor and parathyroid hormone^{63,65,68,87}. Mature osteoblasts eventually undergo apoptosis (between 50-70% of cells) or terminal differentiation⁷⁴. Those that have encircled themselves within bone matrix differentiate into osteocytes, those that remain on the surface of bone facing towards the periosteum become bone lining cells.

1.2.2 Bone lining cells

Bone lining cells contain scarce cytoplasm and few organelles, are metabolically inactive, and are found on the surfaces of bones⁷⁵. Some have membrane processes that extend into canaliculi, and gap junctions are widely seen between adjacent cells and also between lining cells and neighbouring osteocytes. Their role is not entirely clear, but may involve coupling bone formation with resorption, regulation of crystal growth in bone, and a physical role as a barrier between extracellular fluid and bone^{66,76}.

1.2.3 Osteocytes

Osteocytes account for over 90% of the total bone cells in the adult skeleton, and have a life span of up to 25 years. Cell bodies of osteocytes are found in lacunae surrounded by mineralised bone matrix and cellular morphology is dependent on the type of bone inhabited⁷⁷. The osteoblast to osteocyte transition process is accompanied by structural and morphological changes; a reduction in the number of organelles, an increase in the nucleus:cytoplasm ratio, reduction in cell size, a decrease in protein secretion, and the development of cytoplasmic processes⁷⁸.

The podoplanin protein (E11/gp38) is important in the development of osteocyte cytoplasmic processes that project into canaliculi and form the lacuna-canalicular system. Gap junctions between cells facilitate intercellular communication and nutrition, and the complex interconnected network allows osteocytes to act as mechanosensors^{79,80}. Osteocytes also produce secondary messengers and paracrine factors in response to mechanical stimulus^{81,82}.

In addition to their role as mechanoreceptors, osteocytes recruit osteoclasts to sites of remodelling when they undergo apoptosis⁸³. Osteocyte cell death is increased in conditions such as osteoporosis, osteoarthritis, use of glucocorticoids, low oestrogen states, and oxygen deprivation (such as during periods of immobilisation)⁸². Inhibition of osteocyte cell death occurs with the use of oestrogen, drugs such as bisphosphonates, and some forms of mechanical loading^{82,84}. Osteocyte autophagy is a degradation of lysosomes that facilitates recycling of cellular products, it can either preserve viability of cells (through self-preservation of cells during unfavourable conditions) or can lead to cell death⁸². The viability of osteocytes is an important determinant of bone homeostasis and maintenance of strength; apoptosis is essential for normal bone remodelling and repair of damage, however excess apoptosis contributes to bone loss and fragility.

The Wnt/ beta catenin pathway regulates both osteocyte viability and function. Selective deletion of beta catenin in osteocytes increases the activity of osteoclasts and generates a porous bone phenotype ⁸⁵. Osteocyte β catenin is required for the expression of anti-osteoclastogenic factors such as osteoprotegerin (OPG) ⁸². Osteocytes highly express the negative regulators of the Wnt/ β catenin pathway sclerostin and DKK1 ⁸⁶. Sclerostin is encoded by the SOST gene, and has anti-anabolic effects on bone formation, it is believed to be an antagonist of lipoprotein receptor 5 (a positive regulator of bone mass) ^{89,87}. SOST mutations are associated with higher bone mass in humans ⁸⁸. A reduction in sclerostin expression is observed with mechanical loading and PTH ^{89,90}.

1.2.4 Osteoclasts

Osteoclasts are giant multinucleated cells that have numerous mitochondria and lysosomal vacuoles ⁹¹. Their plasma membrane has a characteristic ruffled border, with a large surface area for intra- and extracellular exchange ⁹². Osteoclasts migrate from the bone marrow to the bone surface at various skeletal sites and their primary function is bone resorption. Osteoclasts also produce clastokines and cytokines involved in regulation of the haematopoietic stem cell niche ⁹³. Disorders of osteoclast formation or activity such as osteoporosis, inflammatory arthritis, and osteopetrosis demonstrate their importance in maintaining normal bone homeostasis ⁶⁹.

Active osteoclasts at sites of bone remodelling are highly polarised cells. Activation induces structural changes such as rearrangement of the actin cytoskeleton, and formation of a tight junction between the bone matrix surface and basal membrane to form a sealed compartment⁹¹. Osteoclast attachment to matrix proteins is mediated by integrins ^{94 95}. Once osteoclasts have attached to bone a sealed resorption compartment is formed shown in figure 3. This compartment is acidified by release of organic acids from the ruffled border which degrade hydroxyapatite crystals ⁹⁶. Exocytosis of lytic enzymes from the ruffled border such as matrix metalloproteinases, Cathepsin K and tartrate resistant acid phosphatase erode the inorganic bone components ⁹¹. Degradation products are transcytosed through the cell and released from the plasma membrane into the extracellular space ^{94,97}.

Multiple genes regulate osteoclastogenesis and can prevent development and/or function of the osteoclast ⁹¹. Two other important factors in the activation of osteoclasts are macrophage colony-stimulating factor (M-CSF) and receptor activator of nuclear factor kappa β ligand (RANKL) ⁹¹. M-CSF binds to its receptor in osteoclast precursors which stimulates their proliferation and prevents apoptosis ⁹⁸. RANKL is expressed by osteoblasts, osteocytes and stromal cells; it binds to the RANK receptor on osteoclast precursor cells and induces osteoclastogenesis ⁹⁹. The RANK/RANKL interaction has other important downstream effects that contribute to the function of osteoclasts and their precursors ¹⁰⁰. A key inhibitor of the RANK/RANKL interaction is osteoprotegerin (OPG) which is produced by fibroblasts, osteoblasts and stromal cells ¹⁰¹.

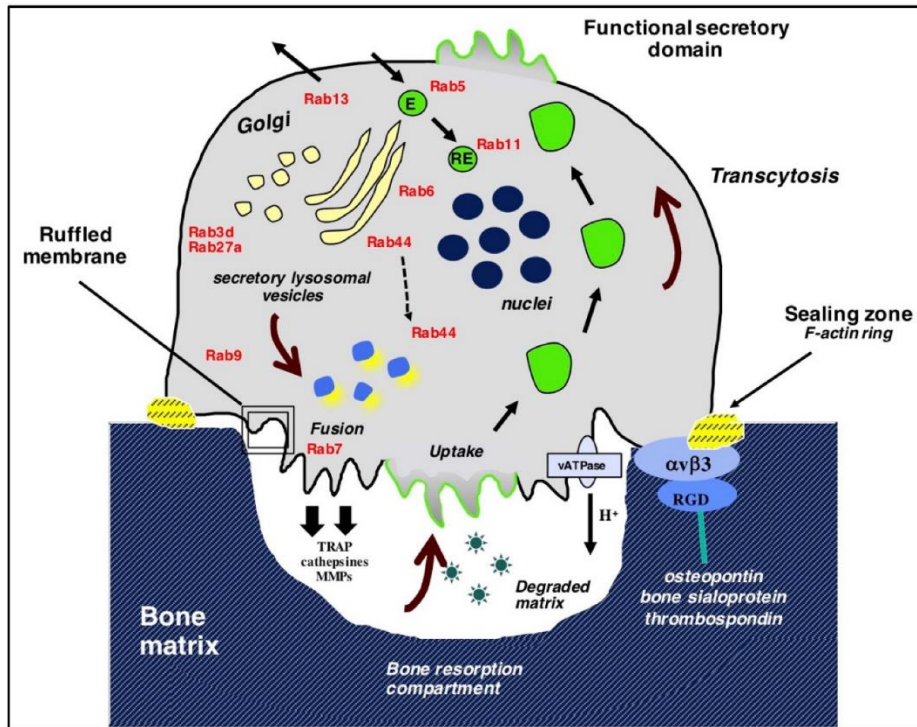


Figure 3: Osteoclast activity

Upon contact with bone, the osteoclast undergoes structural change and forms a sealed compartment (Howship's lacuna). The osteoclast becomes polarised via matrix-derived signals transmitted by integrins. The ruffled border secretes organic acids to produce an acidic microenvironment which mobilises bone mineral that can subsequently undergo enzymatic degradation, and the products of this are transcytosed through the cell in vesicles and released at the plasma membrane. Figure taken from Roux et al¹⁰².

1.2.5 Bone turnover

Bone modelling refers to the modifications in bone size and shape that begin in early skeletal development. Bone formation and bone resorption are uncoupled, and bone is removed from one skeletal site and new bone is formed at another to bring about major change in bone architecture.

Remodelling refers to the continuous process by which bone is resorbed and re-formed at the same skeletal site. This is a tightly coupled process both spatially and temporally; there is minimal net change in bone volume and the bone structure remains constant. It has been estimated that up to 10% of the adult human skeleton is replaced each year, and each cycle of remodelling lasts between 120-200 days¹⁰³. Multiple systemic and local factors regulate remodelling. Physiological remodelling allows for damage repair, prevents the accumulation of excessively mineralised bone, and also maintains mineral homeostasis¹⁰⁴.

A basic multicellular unit (BMU) is an anatomical term which refers to an active site of bone remodelling. It comprises osteoclasts, osteoblasts, a vascular supply¹⁰⁵. Traversing and encasing this compartment is a canopy of bone cells, which forms a specialised microenvironment¹⁰⁶. The bone remodelling cycle has five distinct and sequential phases, activation, resorption, reversal, formation and termination.

Activation occurs when an initiation signal is detected from mechanical stress or hormonal influence. Targeted remodelling refers to the specific removal of damaged bone¹⁰⁷. Mechanical strain applied to bone results in structural damage; sensed by osteocytes and transduced into biological signals⁸². Damage to bone matrix triggers osteocyte apoptosis and the release of paracrine factors that stimulate angiogenesis and recruit osteoclasts. Non-targeted remodelling occurs in response to changes in systemic hormones such as PTH, and does not target a specific skeletal site¹⁰⁷. PTH is released which activates protein kinase intracellular signalling and regulates the release of factors that promote bone resorption¹⁰⁸.

The resorption phase is a response by osteoclasts to signals generated by osteocytes or hormones, and has a duration of between eight and ten days. Osteoblasts release chemokines that attract osteoclast precursors¹⁰⁹. Osteoblasts modulate their expression of master osteoclastogenesis cytokines; RANKL expression is upregulated to promote the proliferation and differentiation of osteoclast precursors, and there is a reduction in OPG expression to remove its inhibitory effect on osteoclastogenesis⁹⁹. Increased osteoblast expression of CSF-1 promotes proliferation and survival of osteoclasts, and directs their motility and cytoskeletal organization⁹⁷. Once activated, osteoclasts attach to exposed integrin vitronectin receptors on the bone surface to form Howships lacunae, acidify the compartment and release proteolytic enzymes (described previously)¹¹⁰. The resorption phase is terminated by the programmed cell death of osteoclasts.

The reversal phase involves a switch from bone resorption to formation, and lasts for around one month. The resorbed bone surface is prepared for new matrix deposition, and signalling pathways that couple resorption to formation are activated. A mononuclear cell of osteoblastic lineage 'reversal cell' removes fragments of digested collagen matrix from the bone surface ¹¹¹. This leads to the formation of a non-mineralised cement line to enhance osteoblast adherence ¹¹². The coupling of bone formation to resorption is essential to prevent net bone loss; it involves factors from the bone matrix, osteoclasts, osteoclast membrane factors and structural changes brought about by the osteoclast on bone tissue surface ¹¹³.

Bone formation phase has been described previously, and lasts for around four months. It occurs in two parts; secretion of the type 1 collagen matrix by osteoblasts (along with multiple other non-collagenous proteins) and its subsequent mineralisation ⁶⁹. Important regulation of this phase occurs via PTH and mechanical strain which both inhibit osteocyte expression of sclerostin (which usually binds to LEP 5/6 to inhibit Wnt signalling) and increases bone formation ⁸⁶. The final phase of the bone remodelling cycle is termination. Once mineralisation is complete, osteoblasts undergo apoptosis, differentiate into bone lining cells or terminally differentiate into osteocytes ⁶⁹.

1.2.6 Biomarkers of bone turnover

Biomarkers of bone turnover (BTM) are a group of proteins, protein degradation products and enzymes that are released into the circulation during bone remodelling. They reflect the number and activity of osteoblasts and osteoclasts and can be measured non-invasively in serum or urine. They have been incorporated into many trials involving patients with metabolic bone disorders, however, their role in routine clinical practice is yet to be established. The most widely used biomarkers are listed in table 1.

Biomarkers of bone formation include bone-specific alkaline phosphatase (BALP), procollagen type 1 N terminal propeptide (PINP), procollagen type 1 C terminal propeptide (PICP), and osteocalcin (OC) ¹¹⁴⁻¹¹⁷.

PINP and PICP are cleaved from the procollagen molecule during its conversion to collagen. They are used as indicators of type 1 collagen deposition, and PINP has been more extensively investigated. PINP is released into the intracellular space and can be measured in the circulation using antibody assays. PINP is the preferred bone formation marker recommended by the International Osteoporosis Foundation (IOF) and the UK National Osteoporosis Guideline Group (NOGG).

Osteocalcin (OC) is the most abundant non-collagenous protein in bone and accounts for 2% of total body protein. OC is synthesised by osteoblasts and used as a marker of their function, serum levels correlate with improvements seen in bone density when

bone targeted therapies are used. Levels of OC also decrease rapidly and significantly with the use of oral glucocorticoids (GC).

Key biomarkers of bone resorption include the carboxy-terminal and amino-terminal crosslinked telopeptides of type 1 collagen (β CTX1 and NTX1) and bone sialoprotein (BSP). Other resorption markers are deoxypyridinoline, hydroxyproline, hydroxylysine and pyridinoline, however these are not routinely used, due to lack of specificity and difficulties in measurement ¹¹⁸.

Degradation of type 1 collagen during bone resorption produces β CTX1 and NTX1, both of which have been the subject of extensive investigation and are widely used biomarkers. β CTX1 is highly sensitive and specific and is the recommended resorption biomarker endorsed by clinical guidelines. It can also be used to monitor response to anti-osteoporosis treatments; β CTX1 levels reduce by 50-80%, and reach maximum suppression after 2 months. β CTX1 is also useful in the evaluation of glucocorticoid induced changes in bone turnover, the initiation of glucocorticoids is associated with a rapid increase in β CTX1 which peak after a week. β CTX1 is measured in serum via enzyme-linked immunosorbent assay (ELISA) and can also be measured in urine.

The amino-terminal crosslinked telopeptide of type 1 collagen (NTX-1) can be measured in either serum or urine. Urinary NTX has been used in studies to assess fracture risk in certain patient populations, and although it does not require serum sampling (as β CTX1 does), the 24hr collection of urine can provide practical challenges. β CTX1 levels are affected by food intake (20% postprandial reduction) and requires fasting measurement. Other resorption biomarkers include osteoclast specific enzymes such as tartrate-resistant acid phosphatase 5b (TRAP5b) and Cathepsin K, which may reflect the number and activity of osteoclasts.

Clinical studies that measure BTM must account for other factors that affect their levels in serum or urine. Many resorption markers exhibit diurnal variation and are often highest early in the morning ¹¹⁹. A postprandial decrease occurs in virtually all BTMs, with a greater effect on resorption markers (apart from Trap5b), which experience a 20-40% reduction compared with 10% fall in formation markers ¹¹⁵. BTMs are also increased by; recent fracture (resorption markers rapidly increase followed by a gradual increase in formation markers); during the winter; with increasing age and following the menopause ^{120, 121, 122}. The overall balance of biomarkers alters after exercise (increase in formation and decrease in resorption markers); immobilisation (increase in resorption and decrease in formation) and the use of GCs where there is a rapid and dose-dependent decrease in markers of formation ¹¹⁷. Simple measures can help to circumvent some of these effects; for example by seeking to obtain fasted serum samples early in the morning, and asking individuals to avoid alcohol or exercise ¹¹⁶.

Table 1: Key biomarkers of bone turnover

Formation biomarkers <small>114–117</small>			
Biomarker	Origin	Action	Features
Bone-specific alkaline phosphatase (BALP)	Osteoblast plasma membrane	Enzymatic degradation of pyrophosphate (mineralisation inhibitor)	Low intra-individual variation Not affected by renal impairment Minimally affected by feeding Minimal changes seen with use of bone targeted medications
Procollagen type 1 N terminal propeptide (PINP); procollagen type 1 C terminal propeptide (PICP)	Proliferating osteoblasts and fibroblasts	Cleaved from procollagen by proteases during type 1 collagen formation	Low intra-individual variability Small circadian rhythm Significant changes with bone targeted treatments allow for use in treatment monitoring Can be affected by renal failure or metastatic bone disease (decreased clearance) Relatively expensive PINP is the preferred formation biomarker
Osteocalcin (OC)	Major non-collagenous protein, produced by osteoblasts during bone formation	Influences osteoid mineralisation Provides negative feedback during remodelling	Large variation: inter-laboratory / -assay. Affected by renal function and vitamin K/ Has circadian variability. Reflects late osteoblast activity
Resorption biomarkers			
Biomarker	Origin	Action	Features
Deoxypyridinoline (DPD)	Mature type 1 collagen	Cross link released during the breakdown of mature type 1 collagen	Bone-specific measure of collagen degradation Not affected by feeding Does not require plasma sample Circadian variation 24hr urine collection required
Collagen type 1 cross-linked C-telopeptide (CTX1)	Type 1 collagen (isomerisation to β aspartyl occurs in mature collagen)	Cleaved from type 1 collagen by cathepsin-K during bone resorption	Large circadian variation Substantial change seen with bone-targeted treatments and with fasting Preferred biomarker for resorption

Collagen type 1 cross-linked N-telopeptide (NTX1)	Type 1 collagen	Cleaved from type 1 collagen by cathepsin-K during bone resorption	Only a small change seen with feeding Large circadian variation Affected by hepatic and renal dysfunction
Tartrate resistant acid phosphatase 5b (Trap5b)	Enzyme cleaved by proteases into isoform b. Present in ruffled border of osteoclasts	Cleaves type 1 collagen into fragments	Circadian variation Affected by exercise Very specific to osteoclast activity
Cathepsin K	Protease in ruffled border of resorbing osteoclasts	Cleaves telopeptide and helical regions of type 1 collagen	Specific biomarker of osteoclastic activity Requires further clinical validation

1.2.7 Regulation of bone turnover

Multiple factors affect the differentiation, maturation, migration and activity of bone. Key regulators include the receptor activator of nuclear factor kappa (RANK), its ligand (RANKL) and osteoprotegrin (OPG) ¹⁰⁰.

RANK is a transmembrane signalling receptor and a member of the TNF superfamily ¹²³. It is expressed by osteoclast precursors and mature osteoclasts. The ligand for RANK (RANKL) is highly expressed by bone marrow stoma cells and osteoblasts ¹²⁴. The interaction between RANK/RANKL stimulates the differentiation of osteoclast precursors and activation of mature osteoclasts ¹²⁵. The interaction between RANK and RANKL generates anti-apoptotic signals to osteoclasts to promote their survival and induce osteoclastogenesis ⁹¹.

Osteoprotegrin (OPG) is produced by osteoblasts, and acts as a soluble decoy receptor to RANKL. It competes with RANK for RANKL binding sites to inhibit osteoclast activation ¹²⁶. OPG expression is downregulated in the presence of bone resorbing factors and upregulated by bone formation factors such as oestrogen, TGF β , and Wnt pathway activation ¹²⁷.

Dickkopf 1 (DKK1) is secreted by osteoblasts and osteocytes and inhibits Wnt signalling, osteoblastogenesis and bone formation ¹²⁸. DKK1 binds to the LRP5/6 receptor and its cell surface co-receptor (Kremen-1) and deactivates them. It also inhibits Wnt-mediated recruitment of mesenchymal cells to the osteoblast lineage and prevents the Runx2/Osterix interaction required for the maturation of osteoblast precursor cells ¹²⁸.

Sclerostin is a potent inhibitor of bone formation that is encoded by the SOST gene, secreted by osteocytes and binds to LRP5/6 on osteoblasts ^{89,88}⁸⁶. It acts as a competitive inhibitor; it prevents Wnt from binding to the Frizzled–LRP5/6 receptor complex and prevents osteoblast differentiation, proliferation and activity ¹²⁹. In humans, sclerostin levels increase with ageing, and in renal impairment. Osteosclerosis is a rare disorder characterised by a mutation in the SOST gene; affected individuals have a hyperostotic skeleton that is resistant to fracture and high levels of BTM ¹³⁰.

The inhibitory effects of sclerostin and DKK can be neutralized by their respective antibodies, thus activating the Wnt signalling pathway downstream. These are both potential targets for drug treatments that promote bone formation. A monoclonal antibody against sclerostin (romosozumab) is available in some countries, but has not been approved for use in the UK.

1.3 Prostate cancer

1.3.1 Epidemiology and survival

Prostate cancer (PC) is the commonest cancer in the United Kingdom (UK) ¹³¹ and will affect 1 in 8 men during their lifetime ¹³². More than 48,000 men are diagnosed with PC in the UK each year, it is responsible for almost 12,000 deaths and is the second leading cause of cancer mortality in men ¹³¹. The incidence of PC increases with age; more than one third of cases occur in those aged over 75 years, and the incidence peaks in those aged 75-79 years. The incidence has increased by around 40% over the past three decades; current projections suggest that more than 77,000 new cases will be diagnosed in the UK in 2035 ¹³¹.

In addition to age, the other main risk factors for PC are ethnicity (more common in black African and Afro-Caribbean men) and family history ^{133,134}. Obesity (a body mass index of $>30\text{kg}/\text{m}^2$) has been associated with more aggressive and advanced forms of PC ¹³⁵.

Survival rates from PC have improved significantly over the past fifty years. Five and ten year age-standardised survival rates in the 1970s were 37% and 24% respectively, whereas current estimates are between 84-85% ^{131,136}. This change can be attributed to multiple factors; population change, patient education and awareness campaigns, access to prostate specific antigen (PSA) testing, introduction of screening programmes and advances in hormonal and systemic anticancer treatments. These have all played an important role in the shift towards greater awareness, earlier diagnosis and increased cancer-specific survival.

Improved PC survival has shifted the perception of PC amongst many clinicians towards that of a chronic illness. An estimated 400,000 men in the UK are currently living with or after PC ¹³²; and therefore the long term consequences of cancer and its treatments are becoming increasingly important ¹³⁷.

Population screening for PC is a subject of controversy ¹³⁸. Autopsy studies have found that between a third and half of men aged over 70 have PC, which suggests that a significant proportion of PC is not clinically significant ^{139,140}. Screening may reduce overall PC mortality, however it risks over-diagnosis and overtreatment, is not currently recommended in the UK ^{141,142}. The risk of clinically significant PC depends upon many factors and risk calculation tools are available to estimate this ^{143,144}.

1.3.2 Referral and clinical management pathway

In the United Kingdom, the NHS has rapid diagnostic and referral pathways for individuals with suspected cancer. The majority of referrals are from primary care, and patients are reviewed in clinics where there is rapid access to expert clinicians and diagnostic investigations. Cancer care is co-ordinated by local site-specific multi-disciplinary teams (therefore prostate cancer is managed by the urology team

multidisciplinary meeting). This comprises an administration team, radiologists, pathologists, urologists, clinical and medical oncologists and specialist nurses. The ongoing involvement of specialities depends on the cancer stage, the performance status of a patient, and selection of treatment. The prostate cancer continuum is vast and there are multiple different management strategies that depend on both patient factors and, treatment intent.

1.3.3 Diagnosis

PC is suspected on the basis of symptoms, PSA measurement and digital rectal examination. PSA is a complex tumour marker, it is organ specific but not cancer-specific^{145,146}. Important features of PSA include its density (serum PSA level divided by prostate volume, the higher density the more likely that the PC is clinically significant); velocity (absolute annual increase in serum PSA); doubling time and the free/total PSA ratio¹⁴⁵. Magnetic resonance imaging is the imaging modality of choice, and is recommended before targeted biopsy^{147,148}.

1.3.4 Staging and risk stratification

PC is staged using the TNM tumour classification system¹⁴⁹ and biopsy samples are evaluated using the International Society of Urological Pathology Consensus recommendations¹⁵⁰. The Gleason score is calculated by determining the predominant pattern of differentiation, which ranges from 1 (well differentiated) to 5. The dominant pattern gives the primary grade and first part of the score, and the second part of the score is the secondary grade, these are added to give a total score¹⁵⁰. A Gleason score of 8 or more is considered high risk, more likely to represent a poorly differentiated and aggressive tumour. A recent re-grading system has been proposed to limit the number of grades to 5¹⁵¹. A combination of the T stage, PSA level and Gleason score can be used in risk stratification (table 2)^{145,151}.

Further staging investigations (cross-sectional imaging and a bone scan) are recommended in intermediate and high risk PC in men who are suitable for treatment^{152,153}. Novel imaging methods such as prostate-specific membrane antigen PET-CT may improve diagnostic accuracy¹⁵⁴.

Metastatic PC is associated with an increased cancer-specific mortality (5 year survival in this group is 49% compared with more than 95% in men without metastatic PC) and men with visceral metastases have a particularly poor prognosis¹⁵⁵. Between 17 and 34% of men diagnosed with PC in the UK have metastatic disease at the time of diagnosis¹³¹. The most common site of metastasis is bone; more than 80% of those with metastatic disease have bone involvement¹⁵⁶. Other frequent sites of PC metastasis are lymph nodes, liver, thorax and brain^{14,157}.

Table 2: Prostate cancer risk stratification

Localised			Locally advanced
Low risk	Intermediate risk	High risk	
PSA <10ng/mL, and Gleason grade 1 and cT1-2a disease	10-20ng/mL or Gleason grade 2/3 or cT2b	>20ng/mL or Gleason grade 4/5 or cT2c	Any PSA Any Gleason grade cT3 or T4 or node positive disease

1.4 Prostate cancer treatment

The PC continuum is vast, and includes localised PC, locally advanced PC, metastatic disease, newly diagnosed and recurrent disease, and both hormone sensitive and resistant disease. The morbidity associated with each treatment strategy can be significant, and many men will not benefit from curative treatment ¹⁵⁸. The management of PC therefore varies considerably, and treatment decisions are individualised and evidence based ^{145,152,153}.

1.4.1 Conservative management

Conservative strategies aim to reduce over-treatment of PC and include watchful waiting (WW) and active surveillance (AS). AS aims to achieve the correct timing for curative treatment in those with localised PC and a life expectancy in excess of 10 years ¹⁴⁵. It involves close monitoring until there is evidence of disease progression which meets pre-defined thresholds ¹⁵⁹. WW may be offered to those not suitable for, or willing to undergo curative treatment, and is carried out until there is evidence of local or systemic progression, at which point when treatment may be offered ^{145,152}.

1.4.2 Curative treatments

Curative management of PC involves either radical prostatectomy or radical radiotherapy. Large randomised controlled trials (RCTs) have compared the two approaches in men with localised disease, and results have been mixed ^{160,161}. Prostatectomy can be performed as an open procedure or by laparoscopic or robotically assisted laparoscopic techniques ¹⁵³. Radical radiotherapy is offered to men with localised disease, and is offered along with hormone therapy in those with localised high risk or locally advanced PC. The gold standard for external beam radiotherapy is the use of intensity modulated (IMRT) or image guided techniques ¹⁵³. Radiotherapy can be given with neo-adjuvant, concurrent or adjuvant androgen deprivation therapy (ADT, discussed below) in men with intermediate or high risk localised, or locally advanced disease ^{145,152,153}. Radiotherapy-associated pelvic toxicity can be acute or late, can have significant impact on quality of life, and includes urinary (dysuria, frequency, haematuria, retention) gastrointestinal (diarrhoea, rectal bleeding, proctitis) and general (nausea, malaise) effects ^{162,163}.

1.4.3 Management of metastatic prostate cancer

1.4.3.1 Hormone sensitive disease

Primary ADT is the first line treatment for hormone sensitive metastatic PC ¹⁶⁴. ADT will be discussed in detail in section 1.4.4 below. The addition of an antiandrogen to achieve complete androgen blockade (CAB) may provide a small survival benefit in selected patients ^{165,166}.

Data from large, multi-centre RCTs significantly changed the management of hormone sensitive metastatic prostate cancer (HSMPC) from 2015. Many men now receive early treatment with systemic anticancer therapies in addition to ADT.

The CHARTED study randomised 790 men with metastatic PC to ADT or ADT given with six cycles of docetaxel (75mg/m² given three weekly within 3 months of ADT initiation) ¹⁶⁷. The combination of chemotherapy and ADT was associated with improved overall survival (OS); median 57.6 months in the chemotherapy and ADT arm compared with 44 months ADT arm (HR 0.61 (95% CI 0.47-0.80, p<0.001)). STAMPEDE (Systemic Therapy in Advancing or Metastatic Prostate Cancer: Evaluation of Drug Efficacy) is a multi-arm, multistage phase III study designed to test whether the addition of various treatments to ADT improves OS ¹⁶⁸. The addition of chemotherapy to ADT improved OS compared with ADT alone (60 Vs 45 months, HR 0.76, 95% CI 0.62-0.92, p=0.005) in men with metastatic PC. A third study (GETUG-15) found that docetaxel and ADT improved both PSA and radiographic progression free survival (PFS) compared to ADT alone, although this did not translate into an OS benefit (HR 1.01, 95% CI 0.75-1.36, p =0.955) ¹⁶⁹.

Subsequent meta-analysis of these three trials included survival data for 2292 of the 3206 men (93%). The addition of docetaxel to ADT improved OS when data were combined (HR 0.77, 95% CI 0.68-0.87 p<0.0001), which resulted in a 9% absolute improvement in OS at 4 years ¹⁷⁰. Chemotherapy was also associated with improved failure-free survival (HR0.64 95% CI 0.58-0.70; p<0.0001) and a 16% reduction in absolute failure rates after 4 years. These results have been confirmed by further meta-analysis, and been practice changing ^{152,171,172}. In those who are fit for systemic treatment, docetaxel and ADT has become the standard treatment in men with mHSPC ¹⁵³.

In the era of COVID-19, there has been a shift to use oral anticancer therapies in an effort to reduce hospital and clinic attendances. An alternative to chemotherapy in the HSMPC setting is abiraterone acetate. This is converted in vivo to abiraterone, which inhibits the CYP17A1 complex required for adrenal and testicular androgen synthesis ¹⁷³. The addition of abiraterone to ADT improves OS compared with ADT alone in men with mHSPC ¹⁷⁴. Most recently, data from the PEACE-1 trial suggest that the combination of abiraterone, ADT and docetaxel given upfront to men with mHSPC improves both PFS and OS, compared with standard treatment ¹⁷⁵. Abiraterone may also have a role in the earlier stages of disease; recent STAMPEDE trial data in men with

high risk localised PC suggest that the addition of abiraterone for two years after diagnosis improved metastasis-free, cancer-specific and overall survival when compared with standard treatment ¹⁷⁶.

Enzalutamide is a novel androgen receptor signalling inhibitor ¹⁷⁷. In men with mHSPC, enzalutamide improves PFS and OS ^{178,179}. Apalutamide is a competitive inhibitor of androgen signalling, and is the subject of ongoing clinical trials ¹⁸⁰.

1.4.3.2 Castration resistant disease

ADT continues when PC becomes castration resistant. Prospective data are lacking but it is likely that there is a modest benefit from continuing ADT which outweighs the adverse effects ^{145,181}. Studies of systemic therapies in mCRPC have included men with ongoing androgen suppression. Discussion of the choice, timing and sequence of available therapies extends beyond the scope of this thesis, but may include abiraterone, enzalutamide and docetaxel ^{182,183 184,185} and second line cabazitaxel ¹⁸⁶.

Radium-223 is a calcium mimetic that forms a complex with hydroxyapatite in areas of high bone turn over, and releases energy as α particles that deliver high energy radiation within a short radius. In the ALSYMPCA trial, men with metastatic bone disease treated with radium-223 had as a significant improvement in OS compared with placebo (14.9 vs 11.3 months, HR 0.70, $p < 0.001$). Radium was also protective against fractures and bone complications, improved pain and quality of life ¹⁸⁷. On the basis of these results it gained approval for use in clinical practice. However subsequent data suggest that the combination of radium and abiraterone may increase the risk of fracture and negatively affect survival ¹⁸⁸.

An ongoing trial (EORTC1333/PEACEIII) is investigating the combination of enzalutamide and radium-223, and has reported concerning interim data regarding fracture. The addition of radium-223 to enzalutamide increased the 1-year cumulative fracture rate, but no fractures occurred when patients started treatment with a bone-protecting agent before radium-223 administration ¹⁸⁹. The final results may lead to a change in practice, and the recommendation that all such men with mCRPC receive bone protection as standard of care.

1.4.4 Androgen deprivation therapy

1.4.4.1 Production and activity of testosterone

PC is a hormone sensitive disease and cells exhibit excess activation of androgen signalling pathways ^{112,190}. Knowledge of androgen synthesis and regulation pathways is important to frame our understanding of PC treatments. The hypothalamic–pituitary–gonadal axis regulates the production of testosterone from Leydig cells in the testes ¹⁹¹. Gonadotrophin releasing hormone (GnRH) is released in the hypothalamus and binds to receptors in the anterior pituitary gland which releases luteinising hormone (LH) and follicle stimulating hormone (FSH) (figure 4). In men, LH

stimulates the production of testosterone from the Leydig cells in the testes¹⁹¹. This system forms a negative feedback loop when testosterone levels rise (figure 4b). The testes produce more than 90% of circulating testosterone and the remaining 5-10% is produced by the adrenal cortex¹⁹¹. Adrenal testosterone is produced from cholesterol derivatives such as pregnenolone, 17-hydroxypregnenolone, androstenedione and dehydroepiandrosterones (DHEA), DHEA and androstenedione can also undergo aromatisation to oestrogens¹⁹¹.

Once in the circulation, testosterone is mostly bound to sex hormone binding globulin (SHBG) and albumin, and only the free form of testosterone (1-2%) can enter prostate cells¹⁹². Testosterone is transported across the cell membrane and converted by 5 α reductase enzymes into its more potent form 5 α -dihydrotestosterone (DHT)¹⁹³. DHT binds to the intracellular androgen receptor with high affinity, this complex is subsequently translocated into the nucleus to promote the expression of target genes involved in PC growth and survival¹⁹³.

1.4.4.2 Indications for ADT

The development and initial progression of PC depends upon androgenic stimulation, and therefore androgen deprivation therapy (ADT) is the mainstay of initial therapy. It is offered in various clinical scenarios within the PC disease spectrum; to control disease in men not fit for curative treatment; alongside radiotherapy in men with intermediate, high risk or locally advanced PC, and in metastatic PC where the disease is initially hormone sensitive^{145,152,153}. Approximately 40-45% of men with PC will receive ADT at some stage in their cancer treatment pathway^{194,195}.

1.4.4.3 Methods of ADT

ADT is achieved with gonadotrophin-releasing hormone agonists or antagonists, anti-androgens or surgical castration via bilateral orchiectomy (table 3). ADT is associated with a rapid fall in serum testosterone levels to castration levels, defined as <20 ng/dL (although there are historical and clinical trial differences in this definition)^{145,196}. In men with advanced PC, initiation of ADT provides a period of remission in around 90% of patients with a fall in serum PSA¹⁹⁷. However after an average of 2 years the disease can progress to castration resistant prostate cancer (CRPC), where there is disease progression despite castration levels of testosterone^{172,198}.

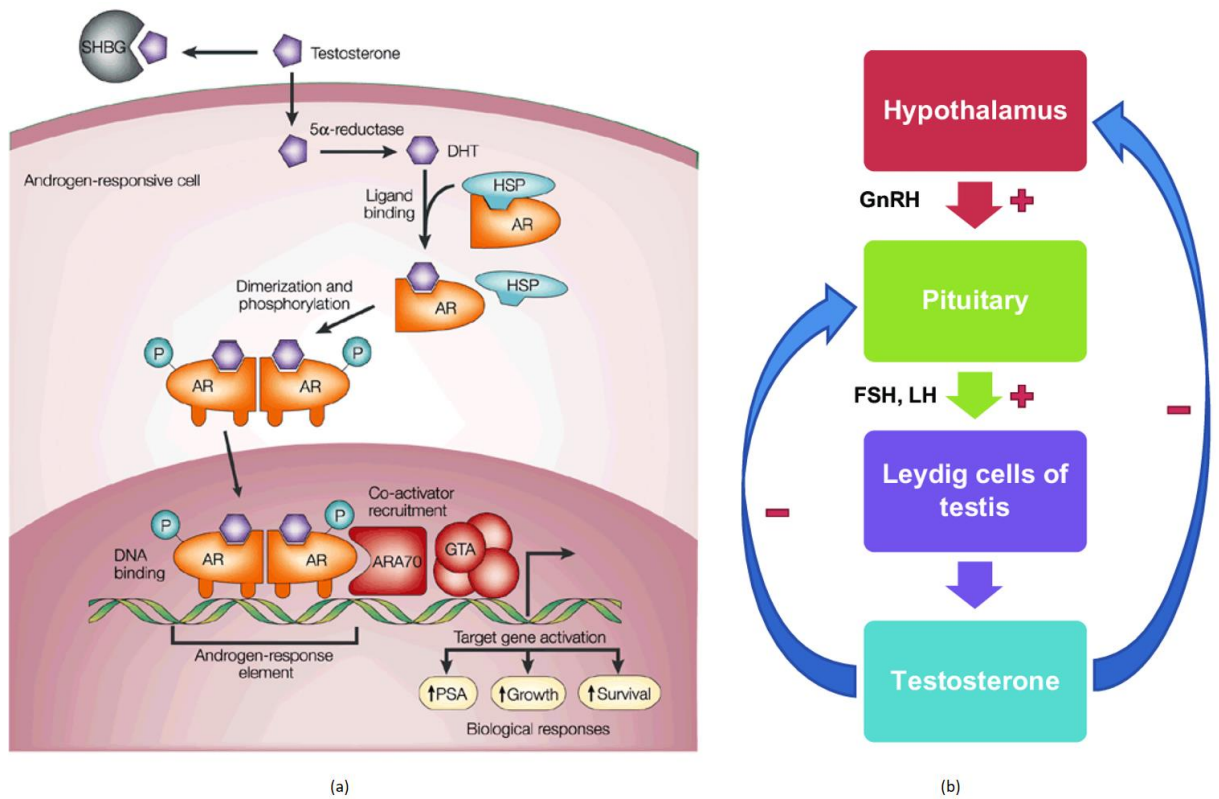


Figure 4: Androgen action and main regulatory pathway

Figure 4(a): Androgen action. Circulating testosterone is mostly bound to sex hormone binding globulin, although can also be bound to albumin. The remaining 1-2% of testosterone is free, and can enter prostate cells and undergoes enzymatic conversion to the active form 5 α -dihydrotestosterone (DHT). This is ten times more potent than testosterone in terms of its ability to activate transcription. DHT binds to the androgen receptor (AR) in the cytoplasm, which causes it to dissociate from heat shock proteins. Subsequent phosphorylation and dimerisation of the AR occurs in the cytoplasm before the ligand-receptor complex translocates into the nucleus. Here, it binds to androgen response elements in the promoter regions of target genes that are involved in the growth, survival and production of PC¹⁹³. Image in figure 4a taken from Feldman et al¹⁹⁹. **Figure 4(b):** Hypothalamic-pituitary-gonadal axis in males. Gonadotrophin releasing hormone (GnRH) is produced by neurones in the hypothalamus, stimulates the synthesis and release of luteinizing hormone (LH) and follicle stimulating hormone (FSH) from the anterior pituitary gland into the circulation. LH acts via receptors on testicular Leydig cells to regulate the production of testosterone. High levels of testosterone act as a negative feedback to inhibit further release of GnRH.

Table 3: Methods used to achieve androgen deprivation

Method	Mechanism of action	Important features
Surgical castration	Bilateral orchiectomy removes testicular testosterone production	Simple, cheap, irreversible. Rapidly reach castration levels of testosterone (< 12hrs) Potential psychological consequences
GnRH agonists (Leuporelin, Goserelin)	Target the LHRH receptor in the anterior pituitary gland. Continuous, non-pulsatile LHRH agonists stimulate the receptor and generate a transient surge in testosterone. After this, there is receptor downregulation over 2-3 weeks, reduction in LH and suppression of testicular testosterone production.	These are given as subcutaneous injection or implant, and are associated with an initial flare of testosterone (clinical manifestations such as bone pain, acute bladder outlet obstruction, obstructive renal failure, spinal cord compression, and hypercoagulation) ²⁰⁰ . Requires pre- and concurrent treatment with antiandrogen to minimise the effects of flare, usually for 4-6 weeks in total. Castration levels of testosterone are reached in 2-4 weeks.
GnRH antagonists (Degarelix)	Competitively binds to LHRH receptor and inhibits downstream LH signalling to suppress testosterone secretion. No initial surge in testosterone.	Testosterone suppression is achieved in 2-3 days. A loading dose is given, and monthly subcutaneous injections thereafter. Approved by NICE for use in advanced PC and spinal metastases- as there is no flare there may be a reduced risk of spinal cord compression ²⁰¹ .
Non-steroidal antiandrogens (Bicalutamide, Flutamide)	Block the androgen receptor to reduce effects of testosterone signalling in the cell. Do not reduce the level of serum testosterone, and are less effective than LHRH therapies in metastatic PC.	Used concomitantly with LHRH agonists to reduce the impact of testosterone flare. Used in combination with an LHRH agonist/antagonist to achieve complete androgen blockade (CAB) in metastatic PC. Also used in localised PC in those who wish to avoid metabolic, sexual and skeletal adverse events associated with other forms of ADT ²⁰² . Bicalutamide shows the most favourable safety and tolerability profile. All have the potential for significant liver toxicity ¹⁴⁵ .
Steroidal antiandrogen (Cyproterone)	Block the androgen receptor to reduce effects of testosterone signalling in the cell	Cyproterone acetate was the first licensed anti-androgen. Important adverse effects are cardiovascular and hepatotoxicity ¹⁴⁵ .

1.4.4.4 Adverse effects of ADT

ADT is associated with important adverse effects which can have significant impact on general health, treatment tolerance, compliance and quality of life.

Bone density and microarchitecture

One of the most important effects of ADT is on bone metabolism. Following initiation of ADT, serum testosterone and oestrogen levels fall rapidly and significantly, and reach a nadir within 2-4 weeks. Sex hormone deficiency leads to loss of bone mineral density (BMD) which is greatest during the first year of ADT. In general, there is between 5-8% BMD loss over the first 12 months of ADT, depending on the study methods and skeletal site^{203-205 206}. (table 4 and 5). In contrast to this, the annual age-related BMD loss is 0.5-1.0% in men, (compared with 1-2% in postmenopausal women)^{207, 208}. ADT-associated bone loss is often super-imposed on other co-morbid conditions, and often increased age, the combination of all of these increases the risk of skeletal complications.

There is considerable heterogeneity in published studies that have investigated the effect of ADT on BMD; in regards to the study size and design, population of men, length of ADT at the time of comparison, length of follow-up and the skeletal sites assessed. Data are available from cross sectional and longitudinal studies, and also from the control arm of intervention studies where ADT/placebo was used as the control arm. Recent studies are summarised in table 4. Studies that have reported data for BMD changes observed after 12 months of ADT are shown in table 5.

In addition to early bone loss from ADT, BMD continues to decrease whilst androgen suppression continues. Loss of BMD ultimately leads to osteopenia and osteoporosis, and increases the risk of fracture (and associated morbidity and mortality). In one study of 390 men, the prevalence of osteoporosis was 35% in hormone naïve patients, 43% after 2 years of ADT, and 81% after 10 years²⁰⁹. A recent meta-analysis of 1,394 men with PC on ADT from 13 studies reported the prevalence of osteoporosis to be between 9 and 53%²¹⁰. This compares with a prevalence of 4%-37% in hormone naïve men with PC²¹¹ and 5-10% in healthy older men without PC^{212,213}.

The pattern of BMD loss that occurs with ADT seems to differ from other causes of bone loss, as it is more likely to affect the distal radius most^{214,215}. The addition of radius to standard hip and spine BMD measurements classifies a third more men with PC and on ADT as having osteoporosis than would otherwise be detected²¹⁴. The apparent greater BMD loss at the radius could either be due to artificial increases at the hip or spine from osteoarthritis, or because the amount of trabecular bone (with greater remodelling and therefore more susceptible to loss) at the distal radius increases with ageing^{208,210,219}. Unfortunately, many prospective studies in men receiving ADT for PC have measured BMD at the hip and spine only, and BMD loss may have been under-estimated.

Changes in bone microarchitecture also occur as a result of treatment with ADT. Microarchitectural deterioration is a key determinant of bone strength and an important consideration in bone quality assessment and fracture risk prediction. There are many factors in addition to BMD that contribute to the risk of fracture in the general population (this will be discussed later in more detail), and in men with PC, the use of standard BMD techniques may lead to as many as 90% of men with clinical osteoporosis being misclassified²¹⁷. Recent studies have associated ADT with increased porosity at cortical bone, trabecularization of cortical bone and loss of trabecular bone^{215,218}. When the trabecular bone score was used to assess bone quality in men with ADT, 43% and 27% had highly and partially degraded microarchitecture respectively, after 12 months ADT²¹⁹.

There appears to be an increased risk of fracture as a result of ADT-associated changes in bone density and strength, although many of the data come from retrospective analysis²²⁰⁻²²². A study of 50,000 men with PC found that there were significantly more fractures at all sites in men on ADT compared to controls 5 years after diagnosis (19.4% Vs 12.6%, $p < 0.001$)²²¹. A population-based study compared 6,954 men with PC on ADT with 13,128 men with PC and no ADT and 159,662 age matched healthy controls²²³. Compared to men without PC, the PC ADT group had an increased risk of any fracture (HR 1.4 95% CI 1.28-1.53) as well as hip fracture (HR 1.38 95% CI 1.20-1.58) and major osteoporotic fracture (HR 1.44 95% CI 1.28-1.61), and those with PC not on ADT had no change in their fracture risk. Similar findings were reported in a previous study of 47,000 men, with an odds ratio for fracture of 1.7 (1.2-2.5; $P < 0.01$) with ADT, compared with healthy men²²⁴. This study also found that PC itself (including no ADT) was a risk factor for all fractures (OR 1.8, 95% CI 1.6-2.1) and hip fracture (OR 3.7, 95% CI 3.1-4.4).

A large prospective cohort study in 180,000 older men included almost 7,000 with PC on ADT, and 13,000 with PC not on ADT²²³. Almost 11,000 fractures were identified over 270,300 patient years. Application of multivariate regression analysis to population registry data found that men treated with ADT were found to have a significantly increased risk of any fracture (HR 1.40 95% CI 1.28-1.53), hip fracture (1.38 (1.20-1.58)) and MOF (1.44 (1.28- 1.61) compared with healthy men and men with PC not on ADT.

Fractures in men with PC have a negative correlation with survival²²⁵. Studies have consistently reported increased mortality compared with men with PC not on ADT, and with the non-PC age matched population. Men with PC on ADT that experience hip fracture are more than twice as likely to die than men without PC (HR 2.4 95%CI 2.29 to 2.60), especially in the first 30 days (HR 5.64, 95% CI 4.16 to 7.48)²²⁶. Fracture at any site within the first 4 years of PC diagnosis significantly impacts overall survival, and is associated with a 40% increase in mortality compared to no fracture²²⁷.

Table 4: Studies that have investigated of the effect of ADT on BMD in men with PC published since 2000

Author (year)	Study groups and population	n	Follow-up	Significant findings
Yuasa (2009) ²²⁸	Men with PC on ADT and a non-ADT group (non-metastatic PC)	201	Cross sectional	Men in the ADT group has significantly lower BMD at the LS, FN and TH than the hormone naïve group ($p = 0.08, 0.02$ and <0.01 respectively).
Kiratli (2001) ²²⁹	Men receiving ADT compared with those on ADT for 2,4,6,8 and 10 years, and age matched healthy controls	36	Cross-sectional	ADT was associated with lower hip BMD than no ADT ($p<0.02$). Those who had not started ADT had similar BMD to age matched healthy controls. Decrease in hip BMD correlated with longer duration of ADT and was evident for up to 10 years
Morote (2007) ²⁰⁹	Men with non-metastatic PC, a hormone naïve group were compared to men who had 2, 4, 6, 8 and 10 years of ADT	390	Cross-sectional	The prevalence of osteoporosis was 35.5% in hormone naïve men, 42.9% after 2 years ADT, 49.2% after 4 years, 59.5% at 6 years and 80.6% after 10 years.
Galvão (2009) ²³⁰	Men receiving ADT for PC and age matched healthy controls	118	Cross sectional	The ADT group had significantly lower BMD for all measurements compared to the healthy controls; TB ($p<0.013$), upper limb ($p=0.002$), lower limb ($p=0.013$) and TH ($p=0.034$)
Stoch (2001) ²³¹	Men with PC on ADT for at least 6 months, men with PC not receiving ADT, and age-matched healthy controls	157	Cross sectional	In men with PC, BMD was significantly lower in ADT group compared with those not receiving ADT, at spine, hip and forearm ($p=0.01, p<0.05$ and $p=0.01$, respectively)
Basaria (2002) ²³²	Men with PC receiving ADT for >12 months, men with PC not	58	Cross sectional	Significantly lower BMD at LS and TB in ADT group compared to no ADT and healthy control group ($p<0.0001$ and $p=0.03$). BMD was inversely related to the duration of ADT.

	receiving ADT, and age matched healthy controls			
Yamada (2008) ²³³	Men with PC receiving ADT for at least 3 months, receiving CAB, a CAB and estramustine group, and healthy controls	204	Cross sectional	BMD at distal radius was significantly lower in the ADT group than healthy controls ($p < 0.016$).
Wang (2017) ²³⁴	Men with PC on acute ADT (<6 months), chronic ADT (>6 months), former ADT and no ADT (controls)	88	6 months	At baseline, TB BMD was significantly lower in the chronic ADT group compared with former ADT and controls ($p = 0.03$). After 6 months, there was significant loss of BMD at ultradistal forearm in the acute ADT (-4.08%, $p = 0.012$) and chronic ADT groups (-2.7% $p = 0.026$). Those in acute ADT group had a significant reduction in TB BMD (-2.99%, $p = 0.032$). Former ADT users had increased LS and FN BMD compared to current ADT users
Galvão (2008) ²³⁵	Men with non-metastatic PC receiving ADT, prospective	72	36 weeks	BMD significantly decreased from baseline at TH ($p < 0.001$), TB ($p < 0.001$), LS ($p < 0.001$) and in the upper limb ($p < 0.001$)
Lee (2005) ²³⁶	Men with PC who were initiating ADT (65%) or had been on ADT for median of 18 months (35%)	65	12 months	BMD loss at TH was 1.9% \pm 2.7% in all groups of men, ($p < 0.001$ in the group that had no previous ADT)
Poulsen (2019) ²³⁷	Men with PC starting ADT, prospective longitudinal study	105	2 years	BMD decreased by 2.0% and 4.6% at LS, 2.3% and 5.2% at FN and 2.1% and 4.2% at TH after 12 and 24 months respectively. The prevalence of osteoporosis increased from 10% at baseline to 22% at 2 years
Morote (2006) ²³⁸	Prospective longitudinal study in men with non-metastatic PC	62	2 years	ADT was associated with significant loss of BMD over 12 months at all skeletal sites measured ranging from 2.29% to 5.55% ($p < 0.001$).

	starting ADT, and age matched men with PC not receiving ADT.			
Preston (2002) ²³⁹	Prospective longitudinal study of men with PC on ADT compared with age matched controls	78	2 years	At baseline, only BMD at the distal forearm was significantly different between the two groups; and was lower in the PC group (p=0.003). At 24 months, there was greater BMD loss in the ADT group at the distal forearm (p<0.0005), FN (p<0.0056). TH BMD increased in the control group (0.8% ±0.5%) and decreased in the ADT group (-7.1% ±1.0%, p=0.0018), the same was true at the LS (+1.1% ±0.6% for controls and -0.2% ± 0.8% with ADT, p=0.079).
Ziaran (2013) ²⁴⁰	Prospective longitudinal study of men with locally advanced PC starting ADT compared with age matched healthy controls,	185	2 years	At baseline, the ADT group had lower baseline BMD than controls at the LS (p=0.022) and TH (p=.028). After 12 months, BMD loss at the LS and TH were significantly greater in the ADT group (p<0.004 and p<0.001 respectively). After 24 months, there was greater loss of BMD with ADT, at the LS (p<0.001), TH (p<0.001) and FN (p= 0.37).
Bergström (2016) ²⁴¹	Men with PC starting ADT (orchiectomy or LHRH analogue) and healthy controls	38	36 months	After 12 months, BMD loss at FN was 0.037g/cm ² in the orchiectomy group (p=0.010), 0.027gcm ² in LHRH group (p=0.027), whilst there was a non-significant gain in BMD in controls.
Daniell (2000) ²⁴²	Men with PC starting ADT, on ADT for 3-5 years, after orchiectomy and age matched healthy controls, prospective longitudinal study	26	42 months	FN BMD was higher in healthy men at baseline, compared with men with PC. Following orchiectomy mean BMD at FN decreased by 2.4% and 7.6% at 1 and 2 years, and after ADT started by 3.4% and 6.5% after 1 and 2 years respectively. ADT was associated with mean 1.4%-2.6% BMD loss per between 3-8 years of treatment

Wadhwa (2009) ²⁴³	Prospective longitudinal study of men with newly diagnosed PC initiating ADT	618	7 years	At baseline, the prevalence of osteoporosis was 41%. In 124 men with normal BMD at baseline, 1.2% (p=0.018) was lost after 12 months, 6.5% by 3 years (p<0.001) and 12.7% by 6 years (p<0.054). Men with osteopenia and osteoporosis at baseline lost 1.8% (p<0.001) and 0.5% (p=0.362) BMD after 12 months, and 14% and 2.2% after 6 years of ADT (p=0.8 for both).
Key intervention studies where ADT (<12 months) was used as the control arm				
Smith (2001) ²⁰⁵	Men with locally advanced or recurrent PC starting ADT. Open label study comparing ADT alone Vs ADT and pamidronate	47	48 weeks	Men in the ADT alone group experienced significant BMD loss at 48 weeks, compared with baseline BMD. Mean BMD loss was 3.3% ±0.7% at LS 2.1% ±0.6% at trochanter, 1.8% ±0.4% at TH (p<0.0001). Mean BMD at FN did not change significantly (P=0.87). Mean loss of trabecular BMD at LS in ADT group was 8.5% ±1.8% (p<0.001)
Satoh (2009) ²⁰⁶	Men with hormone naïve metastatic PC starting ADT were randomised to receive zoledronate or placebo	40	12 months	No difference between groups at baseline. At 6 months there was more significant loss in controls compared to zoledronate group, BMD loss at LS (4.6% ±1.0%, p=0.002) TH (2.2% ±0.5% p=0.0025) and femoral neck (0.7% ± 0.1% p 0.0063) in the control group At 12 months, mean BMD loss was 8.2% ± 1.8% at LS (p=0.0004), 4.6% ± 1.0% at TH (p <0.0008) and 1.8% ± 0.4% at FN (p=0.039)
Israeli (2007) ²⁴⁴	Men with non-metastatic PC who had started ADT <12 months or had recent orchiectomy, randomised to zoledronate or placebo	215	12 months	After 12 months mean BMD in the placebo group significantly decreased at LS and TH (p<0.001% for both) compared to zoledronate group.
Diamond (2001) ²⁰⁴	Men with metastatic PC treated with CAB, randomised to receive placebo or	31	12 months	In the CAB/placebo group, mean loss of BMD was 2.3% ±0.7% at FN and 3.3% ±1.5% loss at trochanter using DXA, and 5.7% ±1.6% loss at LS using QCT

	pamidronate, and compared to a control group with PC not receiving ADT			
Smith (2003) ²⁴⁵	Men with non-metastatic PC starting ADT, randomised to receive zoledronate or placebo	106	12 months	In the ADT/placebo group BMD decreased from baseline by 2.2% ±0.9% at LS (p=0.012), 2.1% ±0.7% at FN (p=0.011), 2.7% ±0.8% at trochanter (p=0.001), 2.8% ± 0.6% at TH (p=0.001) and 5.7% ± 1.4% at non dominant forearm (p=0.003).
Ryan (2006) ²⁴⁶	Men with non-metastatic PC, randomised to zoledronate or placebo.	120	12 months	The ADT/placebo group had mean BMD loss of 2.4% at FN (95% CI 1.0-3.7%, p=0.006), 2.4% at TH (95% CI 1.5-3.3% p<0.0001) and 2.1% at LS (95% CI 0.5-3.7%, p=0.01).
Ryan (2007) ²⁴⁷	Men with PC, starting ADT or had started <12 months, randomised to placebo or zoledronate	42	12 months	The ADT/placebo group had mean BMD loss of 3.2% (1.5-5.0%, p< 0.001) at FN, and non-significant loss at the LS of 2.2% (95% CI 0.6-4.9%, p= 0.12).
Klotz (2013) ²⁴⁸	Men with localised PC starting ADT, randomised to alendronate or placebo	186	12 months	The ADT/placebo group had mean BMD loss of 1.89% at LS, 2.06% at TH, and 1.18% at FN, BMD increased in the alendronate group, the difference between groups was significant (p< 0.0001).
Choo (2013) ²⁰³	Men with non-metastatic PC receiving radiotherapy and ADT, randomised to placebo or risedronate	104	1 and 2 years	Mean LS BMD loss in ADT/placebo group was 5.77% at 1 year, and 13.55% at 2 years, compared with 0.12% and 0.85% in the risedronate group (p 0.25 and 0.05).
Abbreviations: BMD: bone mineral density; TH: total hip; FN: femoral neck; TB: total body; LS :lumbar spine				

Table 5: Key studies of 12 month areal BMD change associated with ADT

Author (year)	Lumbar spine	Total hip	Femoral Neck	Forearm
Smith (2001) ²⁰⁵	-3.3% ±0.7%	-1.8% ±0.4%	No change	
Diamond (2001) ²⁰⁴	-5.7% ±1.6%	NR	-2.3% ±0.7%	-
Smith (2003) ²⁴⁵	-2.2% ±0.9%	-2.8% ± 0.6%	-2.1% ±0.7%	-5.7% ± 1.4%
Ryan (2006) ²⁴⁶	-2.1% (0.5-3.7%)	-2.4% (1.5-3.3%)	- 2.4% (1.0%-3.7%)	-
Ryan (2007) ²⁴⁷	No change	NR	-3.2% (1.5-5.0%)	-
Bhoopalam (2009) ²⁴⁹	-3.13%	NR	NR	-
Klotz (2013) ²⁴⁸	-1.89% (SD 4.31)	-2.06% (SD 5.71)	-1.18% (SD 16.5%)	-
Choo (2013) ²⁰³	5.77 ±4.66%	NR	NR	-
Lee (2005) ²⁵⁰	NR	-1.9% +- 2.7	NR	-
Wadhwa (2008) ²⁴³	NR	NR	NR	-1.2%
Poulson (2019) ²³⁷	2.0%	2.1%	2.3%	-
Israeli (2007) ²⁴⁴	2.0%	2.1%	NR	-
Satoh (2009) ²⁰⁶	8.2% ± 1.8%	4.6% ± 1.0%	1.8% ± 0.4%	-

*Using QCT NR= Data not reported

Hot flushes

Hot flushes are caused by ADT via inappropriate stimulation of the hypothalamic thermoregulatory centre which results in peripheral vasodilatation, and affect between 40 and 80% of ADT treated men^{251, 252}. There may be a reduction in frequency and intensity of flushes with the use of antiandrogens, serotonin re-uptake inhibitors, low dose oestrogen, high dose gabapentin and alternative therapies^{253,254,255}.

Metabolic consequences

ADT has been associated with alterations in lipid metabolism²⁵⁶, insulin resistance²⁵⁷ and diabetes^{258,259,260}. Metabolic syndrome is more prevalent in men with PC receiving ADT than PC controls, and may affect half of those treated with long term ADT²⁵⁶. Diagnosis of metabolic syndrome requires three or more of the following; waist circumference >102cm, serum triglyceride levels > 1.7mmol/L, blood pressure >130/80mmHg, high-density lipoprotein (HDL) cholesterol < 1mmol/L, in addition to hyperglycaemia or the use of medication to control hyperglycaemia²⁶¹.

Body composition

ADT has also been associated with changes in body composition. There is a progressive decrease in lean body mass and gain in fat mass. This combination of features is termed sarcopenic obesity, and appears to be more prevalent in ADT-treated men aged over 70 years²⁶². A summary of the key studies that have investigated the effect of ADT on body composition can be seen in table 6. Sarcopenia is discussed in more detail in chapter two (section 2.1.2). Meta-analysis reported a mean 7.71% increase in fat mass (95% CI 4.27%-11.15%) and a 2.82% reduction in lean mass (95% CI -3.64 to -2.01%) associated with ADT²⁶³. Changes in physical performance have also been observed in men receiving ADT using tests of muscle function and strength²⁶⁴. Exercise and resistance training programmes may mitigate the effects of ADT on metabolism and body composition, however published studies have been limited by their size and design, and results have been mixed^{265,266}.

Cardiovascular risk

Cardiovascular morbidity is an important consideration when initiating ADT, especially in older men. It is the most common cause of mortality in men with PC and it exceeds cancer-specific mortality^{267,268}. The association between ADT and risk of cardiovascular disease and myocardial infarction is controversial, and it is not clear if the risk is increased by ADT^{259,269,270,271}. As with all treatments, the risks and benefits of ADT need to be discussed with individual patients²⁷².

Fatigue

Clinically significant fatigue affects more than 40% of men that have started ADT and seems to worsen over time²⁷³. Exercise interventions can help to alleviate

this, and improve quality of life ²⁷⁴ . The UK National Institute for Health and Care Excellence (NICE) recommend that all men due to start ADT should be offered access to a 12 week supervised resistance and aerobic exercise programme ¹⁵³. Another important cause of fatigue in men receiving ADT is anaemia, although the degree to which anaemia contributes to fatigue in ADT treated men is unclear.

Neuropsychological

ADT may increase the risk of stroke ²⁶⁰, cognitive impairment, poor visual and immediate memory, working memory and visuospatial awareness ^{275,276,277} . Between 25-50% of men starting ADT (or a family member) have reported cognitive difficulties related to the start of ADT ^{278,279}. However, the data vary between studies, and have included heterogenous populations, have and important design and methodological differences. ²⁸⁰.

Changes in mood can include irritability, problems with concentration and attention or anxiety, along with depressive symptoms such as poor appetite, insomnia and intrusive thoughts ²⁷⁹. One study of men receiving ADT found that 12.8% met clinical criteria for depression ²⁸¹. However, in the context of an individual with cancer and with other co-morbid conditions it is difficult to assess the specific contribution of ADT to mood; there are likely to be multiple factors involved.

Sexual dysfunction

ADT suppresses serum testosterone which reduces libido and causes erectile dysfunction in more than 90% of men on ADT, and has significant effects on quality of life ^{232,282}. These effects can be mitigated by using shorter durations of ADT or intermittent treatment, but these are not recommended when survival may be compromised ²⁸³. NICE guidelines recommend that all men receiving ADT have access to psychosexual and erectile dysfunction clinics ¹⁵³.

Table 6: Key studies of the effect of ADT on body composition

Author (year)	Study population and design	N	Follow-up	Main findings
Smith (2001) ²⁸⁴	Men with PC starting ADT	22	3 months	Total fat mass increased by 1.7kg (± 9.6 kg p<0.008). Lean body mass reduced by 1.7kg (± 6.0 kg p=0.016)
Smith (2006) ²⁸⁵	Men with locally advanced PC starting CAB	25	12 weeks	Mean body fat mass increased by 4.3% (± 1.3 %) from baseline p=0.002
Boxer (2005) ²⁸⁶	Retrospective analysis, men with PC on LHRH-agonist were compared to men without PC	55	6 months	ADT group experienced gain in % body fat ($+9.5\% \pm 0.13\%$ p<0.001) whereas the control group had a small decrease in % body fat ($-3.8\% \pm 0.08$, p= 0.02). ADT group experienced loss of skeletal muscle mass (-2.3 kg ± 0.03 kg p<0.001) and lean mass (-2.1 kg ± 0.03 kg p<0.001) with no change in controls
Galvão (2008) ²⁸⁷	Longitudinal observational study of men with PC on CAB	72	36 weeks	Whole body lean mass decreased by 2.4% ($\pm 0.4\%$ p<0.01). Total fat mass increased by 13.8% ($\pm 2.3\%$, p<0.001)
Smith (2002) ²⁸⁸	Longitudinal observational study of men with non-metastatic, locally advanced or recurrent PC treated with leuprolide	40	48 weeks	Serum testosterone decreased by 96.3% ($\pm 0.4\%$ p<0.001). Weight increased by 2.4% ($\pm 0.8\%$ p=0.005). % body fat mass increased by 9.4% ($\pm 1.7\%$ p<0.001). % lean body mass decreased by 2.7% ($\pm 0.5\%$ p<0.001). Increased subcutaneous abdominal fat ($3.9\% \pm 1.2\%$ p = 0.003) but not intra-abdominal fat
Lee (2005) ²⁵⁰	Prospective observational study of men with PC on ADT	65	12 months	Lean body mass decreased by 2.0% $\pm 3.3\%$ p<0.001. Fat mass increased by 6.6% $\pm 9.4\%$ p<0.001

Smith (2008) ²⁸⁹	Observational study of men with recurrent or locally advanced PC starting leuprolide	26	12 months	Fat mass increased by 11.2% ($\pm 1.5\%$ $p < 0.001$). Lean mass decreased by 3.6% ($\pm 0.5\%$ $p < 0.001$). Total abdominal fat area increased by 16.5% ($\pm 2.6\%$ $p < 0.001$) 94% was due to accumulation of subcutaneous fat
Hamilton (2010) ²¹⁸	Prospective observational study in men starting ADT	26	12 months	Increase in total fat mass +3400g (± 870 g $p < 0.001$). Loss of total lean mass -1900g (± 50 g, $p < 0.001$)
Greenspan (2005) ²⁹⁰	Prospective observational study in men with PC on ADT <6 and > 6 months, no ADT, healthy controls	195	12 months	Significant changes in body composition only detected in men in the <6 month ADT group after 12 months. Lean mass reduced by 3.5% ($\pm 0.5\%$ $p < 0.001$) and total body fat increased by 10.4% ($\pm 1.7\%$ $p < 0.001$)
Smith (2004) ²⁰²	Open label study of men with PC on bicalutamide or leuprolide	52	12 months	Fat mass increased by 11.1% ($\pm 1.3\%$, $p < 0.01$) with leuprolide and by 6.4% ($\pm 1.1\%$ $p < 0.01$) with bicalutamide
Berruti (2002) ²⁹¹	Men with non-metastatic PC starting ADT	35	12 months	Total fat mass increased by 19% ($p < 0.001$) and lean mass decreased by 1.9% ($p < 0.001$)
Smith (2004) ²⁹²	Prospective observational study of men starting ADT	79	48 weeks	1.8% increase in weight ($\pm 0.5\%$, $p < 0.001$) and total fat mass increased by 11.0% ($\pm 1.7\%$ $p < 0.001$). Lean mass decreased by 3.8% ($\pm 0.6\%$, $p < 0.001$)
Chen (2005) ²⁹³	Case control study in men with PC on ADT and age-matched healthy men	109	N/A	Men with PC had higher body weight, a higher % body fat (30% Vs 26% $p < 0.05$) compared with healthy controls
Basaria ²⁹⁴ 2002	Cross sectional study of men on ADT (>12 months), men with PC not on ADT, and age matched healthy men	58	NA	The ADT group had higher fat mass (32.2% $\pm 5.4\%$) compared to the PC and no ADT group (26.2% $\pm 6.0\%$) and healthy controls (22.4% $\pm 4.1\%$) $p < 0.0001$
Abbreviations: CAB: complete androgen blockage				

1.5 Metastatic prostate cancer

The population of men with metastatic PC is heterogenous. It includes men with newly diagnosed hormone sensitive PC (HSMPC), men with localised or locally advanced disease which has progressed to castration resistance (CRPC), and those who have experienced a relapse following curative treatment. Prognosis in the context of metastatic PC is multifactorial; co-morbid conditions, location and volume of metastases, performance status, frailty, Gleason score and response to initial treatment all affect survival. The most common site of PC metastasis is bone, other frequently involved sites are distant lymph nodes, liver, thorax and brain ¹⁵⁶.

1.5.1 Bone metastases

1.5.1.1 Epidemiology and clinical sequelae

Metastatic bone disease affects 10-20% of men at the time of PC diagnosis, more than 80% of men with CRPC ²⁹⁵, and more than 90% of men who develop metastatic PC ^{296,157}. Bone lesions typically develop in the lumbar spine, ribs, and pelvis, and their pattern of spread follows the distribution of adult red bone marrow, and can subsequently progress to involve adjacent cortical bone ²⁹⁷. The classic radiological appearance of PC-associated BM is of an osteosclerotic lesion secondary to osteoblastic bone formation ²⁹⁸. Histomorphometric analysis demonstrates increased bone formation around tumour cell deposits, combined with unbalanced osteolytic activity and areas of eroded bone surface ²⁹⁹.

Biomarkers of bone turnover (both resorption and formation) are increased, their levels correlate with the degree of skeletal involvement ³⁰⁰. Consequent uncoupled resorption and formation is detrimental to bone strength, and net bone loss increases the risk of clinical complications ^{301,302}. Such complications are known as skeletal-related events (SREs), and are associated with significant morbidity and mortality. SREs include; pathological fracture, malignant spinal cord compression and the need for surgery or radiotherapy to bone ³⁰³. More than half of men with PC and untreated BM will experience a SRE ^{304,305}, the most frequent are the need for radiotherapy (around two thirds of all SREs) and pathological fracture ^{306,307}. Risk factors for SRE are the number of metastatic sites (more than three), previous SRE, pain from BM, and disease progression ³⁰⁸⁻³¹⁰.

SREs have multiple adverse consequences for individuals, such as increased pain, decreased health-related quality of life (which includes physical, functional, mental and emotional wellbeing), loss of function and/or independence, a greater incidence of anxiety and depression and significantly worse survival ^{225,311,312,313}. There is also a substantial economic burden from SREs, which arises from increased health service utilisation (inpatient and outpatient episodes, diagnostic tests), the need for interventions (radiotherapy, surgery or bone-targeted medications) and additional care that may be required ^{306,314}.

1.5.1.2 Classification of bone metastases

In general, bone metastases (BM) may be classified as osteolytic, osteoblastic or mixed, depending on the mechanism of bone remodelling disruption. The bone remodelling cycle has been described in section 1.2.5; normal bone homeostasis is maintained by a state of equilibrium between bone formation and resorption, and regulated by the influence of cytokines and growth factors.

Metastatic PC is usually associated with the development of osteoblastic BM. Although these BM are predominantly bone-forming, the risk of fracture is increased as the new bone formed lacks strength. BM with an osteoblastic phenotype may also be associated with small cell lung cancer and Hodgkin's lymphoma. Although the radiographic appearances are of dense and sclerotic bone, there is dysregulation of both bone formation and resorption. The underlying mechanisms involve signalling via bone morphogenetic proteins (BMPs) – including BMP2, -4, -6 and -7, as well as, fibroblast growth factor and TGF β , with the result of osteoblast activation and their osteogenic differentiation.

Osteolytic BM are associated with destruction of normal bone, and found in individuals with breast and renal cancers, melanoma, non-small cell lung cancer, thyroid cancer and Non-Hodgkin's lymphoma³¹⁵. Key drivers of osteolytic BM are cancer cell production of PTHrP, and RANK-L expression, along with reduced secretion of OPG. In addition, cancer cells that become established in bone release and upregulate Wnt family members, endothelin-1, BMPs and TGF β to drive the cycle of bone destruction described below and shown in figure 5.

1.5.1.3 Pathophysiology

The development of metastatic bone disease is a multi-step process, that requires PC cells to detach from the primary tumour, invade blood or lymphatic vessels, travel in the circulation to bone and invade and proliferate. At sites of metastasis, there are a series of complex interactions with bone cells, that promote colonization of bone by PC cells.

Cancer cell escape and dissemination is a vital step in metastatic progression. PC cells produce matrix metalloproteinases (MMPs) which degrade the extracellular matrix proteins and have a role in angiogenesis^{316,317}. Cancer cells penetrate the basement membrane and invade either blood or lymphatic vessels to escape the confines of the primary tumour. High levels of MMPs have been observed in metastatic PC and are associated with worse outcomes³¹⁸.

PC cell adhesion and invasion is mediated by the expression of chemokines such as CXCR4 which facilitate bone invasion via CXCL12 expressed by bone marrow stromal cells³¹⁹. Chemokines induce MMPs, down-regulate their tissue inhibitors, and are also important regulators of angiogenesis via interaction with vascular endothelial growth factor (VEGF)³²⁰. PC cells also highly express protease activated

receptor 1 which alters the expression of integrin $\alpha\beta3$ required for PC cell adhesion to vascular endothelium and for osteoclast-mediated bone resorption³²¹. Cadherin-11 is another important adhesion molecule highly expressed in PC BM, but not found in non-skeletal metastases, and increases cell migration and invasiveness^{322,323}.

In addition to cell escape, migration and invasion, PC cells must proliferate and form metastatic deposits via interactions between cancer cells, bone cells and matrix. Initially proposed by Paget in 1889, the 'seed and soil' hypothesis forms the basis of our current understanding of cancer growth in bone³²⁴. It describes the preferential interaction between 'seeds' (metastatic cancer cells) and the 'soil' (the environment) to facilitate cancer growth and progression³²⁴. An autocatalytic 'vicious cycle' of bone destruction becomes established at sites of metastasis and is shown in figure 5; PC cells produce proteins such as parathyroid hormone-related peptide (PTHrP) which up-regulates RANKL and inhibits OPG production by osteoblasts, leading to osteoclast activation^{325,326}.

Accelerated bone resorption and other physical factors within bone (such as hypoxia and low pH) aids the release of factors that promote PC cell growth, proliferation and survival (figure 5)³²⁶. There is also simultaneous upregulation of PC cell expression of osteoblast stimulatory factors, those that directly affect osteoblast function (such as platelet-derived growth factor (PDGF), fibroblast growth factor (FGF), insulin-like growth factor-1 (IGF1), bone morphogenic proteins (BMPs), TGF- β and Wnt) and those that affect osteoblast function indirectly through modification of the bone microenvironment, such as VEGF and endothelin 1^{327,328}. Osteoblast stimulatory factors are frequently elevated in men with PC and metastatic bone disease^{329,326}. Two other important PC-specific growth factors are prostate-specific antigen (PSA) and urokinase plasminogen activator (uPA), which are both serine proteases produced by PC cells^{330,331,332}.

Other factors in the bone microenvironment contribute to PC metastasis. PC cells release exosomes which are small membrane-enclosed vesicles containing mRNA, micro-RNA and DNA, which mediate intercellular communication during the formation of bone metastasis^{333,334}. Specific miRNAs isolated from PC cells increase OPG/RANKL expression, upregulate MMPs and promote metastatic colonisation³³⁵. Hypoxic signalling in the bone microenvironment is mediated by hypoxia-inducible factor 1 (HIF1), which enhances the invasive potential of cancer cells³³⁶. HIF-1 results in the transcription of hypoxia response genes involved in angiogenesis, cancer cell apoptosis and production of growth factors and cytokines; cancer cells are able to thrive under such conditions³³⁷. Extracellular pH in bone is important; acidification facilitates osteoclast absorption and increases secretion of proteins that degrade the ECM such as cathepsin and MMPs, which promote metastasis³³⁸. Metastatic cancer cells produce lactic acid to create an acidotic bone compartment that favours their colonisation and progression.

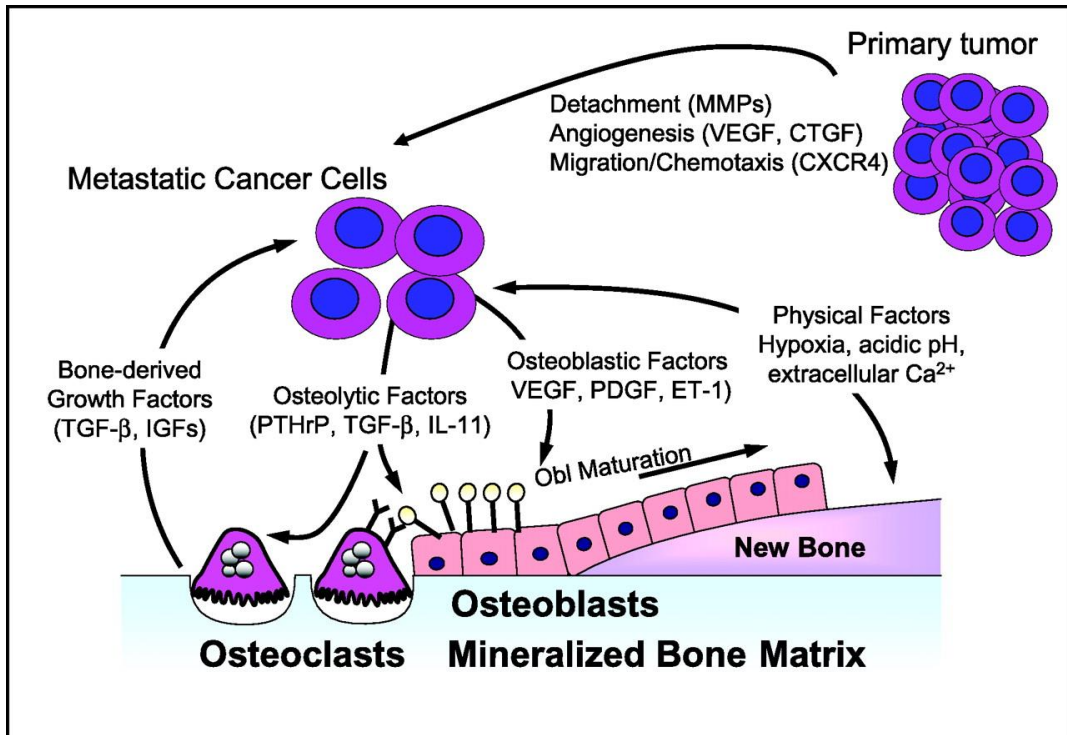


Figure 5: The 'vicious cycle' of prostate cancer cell bone metastases

Tumour cells migrate to bone and survive under the influence of factors such as; MMPs, chemokine receptor 4 (CXCR4), vascular endothelial growth factor (VEGF), and connective tissue growth factor. Physical factors within the bone microenvironment activate PC cell expression of osteoblast stimulatory factors (VEGF, ET-1, BMPs, PDGF). PC cells also produce osteoclast stimulatory factors (PTHrP, TGFβ 1) that act via increased production of RANKL by osteoblasts, lymphocytes and stromal cells. Activation of bone resorption releases a host of bone-derived growth factors that are usually immobilised in bone, and promotes prostate cancer cell growth and survival. Image reproduced from Guise et al ³²⁶.

1.6 Management of bone health in men with PC

There are three significant insults to bone health in men with PC. Cancer treatment-induced bone loss (CTIBL) is associated with ADT and increases the risk of osteoporosis and fracture. GCs are used alongside chemotherapy and adversely affect bone. Metastatic bone disease in some men predisposes men to SREs and their associated morbidity and mortality.

1.6.1 Lifestyle modifications

Despite the potential adverse consequences of ADT for bone health, evidence suggests that many patients have limited knowledge of osteoporosis, and are not actively engaged in taking measures to optimise their bone health^{339,340}. Guidance for the monitoring and management of CTIBL in men with PC has been published by various expert groups and societies, although there is variation in the specific recommendations^{341,342,343,344,345,153}. A recent survey of clinicians suggests that adherence to guidelines and knowledge and awareness of CTIBL remains sub-optimal³⁴⁶.

Men with PC should consider lifestyle changes such as smoking cessation and reduction in alcohol intake to optimise their bone health³⁴⁷. Vitamin deficiency or insufficiency are common, and calcium and vitamin D supplementation may reduce bone loss, and is associated with a reduction in falls and fractures in non-cancer populations. Supplementation with calcium and vitamin D has been included in the control arm of intervention studies investigating CTIBL. However a review of 12 PC studies found that men receiving supplements at current recommended doses (500–1,000 mg calcium and 200–500 IU vitamin D per day) continue to lose bone, suggesting that these doses are insufficient to prevent bone loss³⁴⁸. Further studies are needed to determine the safety and efficacy of higher doses in this population.

Exercise can mitigate adverse effects of ADT such as fatigue, low mood, impaired cognition, increased fat mass and sarcopenia^{349–351}. Sarcopenia is a particular problem in the PC patient population receiving ADT, as it increases the risk of falls on a background of pre-existing and acquired low BMD^{262,352}. ADT has also been associated with frailty which is predictive of hospitalization, development of disability, and falls^{353,354}. Regular weight bearing exercise is recommended in all men with PC receiving ADT; in the UK, NICE guidelines recommend a supervised 12 week aerobic exercise programme for all men in this situation³⁵⁵.

There is clear evidence to support the benefit of exercise training in ADT-treated men. Combined resistance and aerobic exercise is advocated by national and international guidance^{172,355}. However, there is a lack of evidence to suggest that routine referral and participation is standard practice, and a lack of clarity of how best to embed exercise referral pathways into standard PC care³⁵⁶. The STAMINA trial was designed to investigate the acceptability and feasibility of incorporating

supervised exercise into NHS pathways. Despite the effects of the covid-19 pandemic, supervised exercise was acceptable to patients and clinicians, and had a positive impact on lifestyle and physical measures³⁵⁷. The ongoing trial aims to determine both the clinical efficacy and economic impact of an adapted exercise intervention in ADT-treated men³⁵⁸.

1.6.2 Bone-targeted treatments

Bone targeted treatments vary in their mechanism of action and their pattern of activity. They have two main indications; for the prevention of CTIBL, and to reduce the risk of skeletal related events. The dose intensities and scheduling in men with PC are different to those used to treat metabolic bone disorders.

1.6.2.1 Bisphosphonates

Bisphosphonates (BP) are pyrophosphate analogues that have a high affinity for mineralised bone matrix. They bind selectively to hydroxyapatite at sites of active bone metabolism, and are released and internalised by osteoclasts during bone resorption³⁵⁹. Their mechanism of action depends upon their nitrogen content, which is associated with higher potency. Non-nitrogen containing BP (such as clodronate) act as metabolized cytotoxic molecules in the osteoclast, which leads to osteoclast apoptosis³⁵⁹. Nitrogen containing BP include zoledronate, ibandronate and pamidronate, which inhibit the enzyme farnesyl diphosphonate synthase³⁶⁰. This impairs the ability of the osteoclast to bind to bone, to maintain its characteristic brush border and to acidify bone, which compromises bone resorption. BP vary in their action at skeletal sites depending on the affinity with which they bind hydroxyapatite. Some are more effective at the spine than the hip, and their impact on cortical and trabecular bone differs^{360,361,362}.

Studies have investigated the role of BP in the prevention of CTIBL in ADT-treated men. When compared to placebo, zoledronate improves BMD at the lumbar spine and hip after 12 months of ADT, and is also associated with a reduction in BTM^{244,245,363}. However meta-analysis of published data has been limited by heterogeneity in study design, populations and follow-up, and studies have been underpowered to detect clinically important endpoints (such as fracture). No BP are currently approved for the prevention of CTIBL in men with PC.

Zoledronate may also reduce the risk of SREs in men with metastatic PC. In men with CRPC and bone pain, there was a 36% reduction in SRE incidence ($p=0.002$) and time to first SRE ($p=0.009$) with zoledronate compared with placebo, and a reduction in bone pain³⁰⁸. However in the HSMPC setting, zoledronate does not appear to affect bone endpoints or survival^{364,365}. In the UK, NICE PC guidelines suggest that zoledronate can be considered in men with mCRPC to minimise risk of SRE or treat pain, however, stronger recommendations were not made due to a lack of evidence of survival benefit¹⁵³.

BPs are usually fairly well tolerated. Adverse effects include flu like symptoms, gastrointestinal disturbance, hypocalcaemia, atypical fracture and osteonecrosis of the jaw (ONJ) ³⁶⁶. The risk of ONJ depends upon the dose used (higher doses are used to prevent SREs than to treat metabolic bone disorders), the frequency and duration of BP and dental factors. ONJ affects up to 6% of men with PC receiving BP, and guidelines recommend dental assessment and intervention before BP are initiated and good dental hygiene throughout treatment ^{367,368,369}.

1.6.2.2 Denosumab

Denosumab is a monoclonal antibody that is specific to RANKL and inhibits osteoclast activity. In contrast to BPs it is not incorporated into bone matrix and bone turnover is not suppressed after its cessation. As a consequence, treatment cessation increases the risk of rebound fractures. Other adverse effects include hypocalcaemia and ONJ. Compared with placebo, denosumab significantly increased BMD at all skeletal sites and reduced the incidence of vertebral fractures in ADT-treated men with non-metastatic PC ^{281,370}. It is currently NICE-approved for the prevention of CTIBL in men with PC. Denosumab may also be used in men with metastatic PC to delay the time to SRE; a large phase III trial found denosumab was superior to zoledronic acid in delaying the median time to first SRE (20.7 months Vs 17.1 months, $p=0.0002$) ³⁷¹.

1.6.2.3 Other therapies

Selective oestrogen receptor modulators may improve BMD in men receiving ADT ^{372,373}, however they are not recommended for use due to safety concerns. Men with CRMPC and symptomatic BM may also be treated with Radium-223 (described previously) as monotherapy or in combination with ADT ¹⁸⁷. The other main management options for those with bone pain include palliative radiotherapy and opiate-based analgesia.

1.7 Osteoporosis

1.7.1 Epidemiology

Osteoporosis is a major health, social and economic concern. It is defined by the WHO as 'a progressive systemic skeletal disease characterised by low bone mass and microarchitectural deterioration of bone tissue, with a consequent increase in bone fragility and susceptibility to fracture'³⁷⁴. Fragility fractures result from low energy mechanical forces that would not ordinarily cause fracture. Osteoporosis is responsible for 9 million fractures annually worldwide³⁷⁵ and more than 300,000 fractures in the UK each year³⁷⁶. More than 30% of women and 20% of men in the UK will sustain an osteoporotic fracture in their lifetime³⁷⁷, which has a projected annual cost to the NHS of £2.2 billion by 2025³⁷⁸. Approximately one third of all osteoporotic fractures occur in men, who have an estimated lifetime risk of between 10% and 25%.

The most common sites of fracture are the vertebral bodies, distal radius, proximal femur and humerus. Hip fractures account for more than 20% of UK orthopaedic inpatient beds³⁷⁷. They are associated with loss of independence (almost half will be unable to live independently) and significant mortality (20% at 1 year)³⁷⁹. Vertebral fractures are important as they are the commonest fracture associated with skeletal fragility, and are associated with significant morbidity, mortality and other adverse health outcomes^{380,381}.

1.7.2 Aetiology and risk factors

In all individuals with osteoporosis, there is an imbalance in bone resorption and formation with a greater increase in resorption and net bone loss. Risk factors for primary osteoporosis include; increased age, female sex, white or asian race, low BMI, family history of osteoporotic fracture, early menopause, sedentary lifestyle, excessive alcohol, caffeine and tobacco use, and low calcium and/or vitamin D intake³⁸². Secondary osteoporosis arises as a consequence of disordered endocrine or metabolism (for example hypogonadism and hyperthyroidism), malabsorption, rheumatoid arthritis, renal impairment, and certain medications (such as glucocorticoids, antiepileptics, and ADT)³⁸². Fracture risk assessment tools are widely used, and will be described later.

Glucocorticoids (GCs) are the commonest cause of secondary osteoporosis³⁸³. Long term GC therapy is used to treat a range of systemic conditions in 1-2% of the population, and GC are also used in men with metastatic PC treated with systemic anticancer therapies^{384,385}. During chemotherapy, the usual dose is 10mg prednisolone per day (in addition to intravenous dexamethasone on the day of chemotherapy) for up to 6 months. Continuous oral GCs causes rapid bone loss and a significantly increased fracture risk. This occurs shortly after initiation of GC therapy (within 3–6 months), is dose-related and remains elevated for the duration

of therapy^{386,387}. The effects of intravenous and inhaled steroids are less clear. Osteoporosis associated with GC use is characterised by an early transient increase in bone resorption followed by decreased bone formation. In addition to loss of BMD, microarchitectural changes include loss of cortical thickness, increased trabecular separation and reduced number, and a reduction in bone stiffness^{383,388}.

Underlying mechanisms involve the upregulation of peroxisome proliferator-activated receptor gamma receptor 2 which directs precursor cells away from the osteoblast lineage, and effects on the Wnt/ β catenin signalling pathway^{389,390}. Sclerostin expression is increased with GC use. Deficiency or inhibition of sclerostin can maintain bone mass and integrity, even in conditions of GC excess³⁹¹. GCs also have direct effects on bone resorption, increasing the number and activity of osteoclasts³⁸³. The underlying condition for which long-term GCs are required may also have indirect effects on bone via chronic inflammation and pro-resorption cytokines. In addition to effects on bone, GCs also have adverse effects on muscle mass and function, leading to sarcopenia and an increased risk of falls³⁹².

1.7.3 The role of androgens and oestrogens in bone homeostasis

Androgens have direct effects on bone cells via the androgen receptor (AR), and indirect effects through aromatase-mediated conversion to oestrogen. Most of our knowledge of the effect of sex steroids on bone comes from studies in animal models. Caution is required in the application of results to humans for several reasons. Murine models lack SHBG which is a key regulator of the availability of free testosterone³⁹³, and may also permit greater fluctuations in sex hormone levels³⁹⁴. Mice also have relatively lower levels of free oestrogen than humans, and orchietomy-based models may result in the loss of other hormones required for bone such as inhibin A^{395,396}.

However, despite the limitations, mouse cell lines have provided important insights into the role of testosterone in bone by generating cell line-specific knockouts of aromatase enzyme and AR. In osteoblasts, AR-mediated testosterone signalling is important in trabecular but not cortical bone formation; loss of the AR decreased trabecular number and bone mass, and increased in trabecular separation, but did not affect cortical parameters^{397,398}. The direct role of testosterone in osteoclasts is less well established³⁹⁶. In osteocytes, AR are upregulated with increasing osteocyte differentiation, and AR knockout results in a deterioration of trabecular microarchitecture³⁹⁹. In human studies, those with androgen insensitivity syndrome (a partial or total lack of AR signalling) have a characteristic reduction in BMD that occurs regardless of oestrogen replacement^{400,401}.

The indirect effects of testosterone (from aromatisation to oestrogen) have been determined through the overexpression of aromatase in mouse models. This has been found to increase trabecular and cortical BMD, cortical thickness and a reduction in both osteoclast number and activity⁴⁰². In humans, aromatase

deficiency frequently presents with osteopenia or osteoporosis, and inhibition of aromatase is associated with low BMD ⁴⁰³.

In humans with sex steroid deficiency, oestrogen appears to play a greater role than testosterone in the suppression of bone resorption, and this may be independent of FSH secretion ⁴⁰⁴. The effects of oestrogen on bone resorption may be mediated via regulation of RANKL production by osteoblasts. Serum testosterone and oestrogen may also have differential effects on the mechanisms involved bone resorption; such as their ability to prevent increases in collagen degradation products, and effect on osteoclast-specific enzymes.

Large population based studies have sought to determine the relationship between circulating androgens and oestrogens, BMD and fracture risk. The osteoporotic fractures in men (MrOS) study included cohorts of men aged over 65 in Sweden, United States and Hong Kong with a spectrum of hypogonadal states. Low serum oestrogen was associated with low BMD and increased risk of fracture ⁴⁰⁵. Higher SHBG levels were also associated with an increased fracture risk (but did not affect BMD). Men with reduced serum free testosterone had an increased risk of fracture, however did not have an overall reduction in BMD ⁴⁰⁶. Overall, the men with the highest risk of fracture had a combination of low free testosterone, low oestrogen and high SHBG ⁴⁰⁷. These findings were confirmed when hypogonadal men in the Framingham study were compared to eugonadal men. Men with the highest oestradiol levels had the highest BMD, and those with the lowest oestradiol levels had the highest risk of hip fracture ⁴⁰⁸. Other studies have reported similar results, although notably the Dubbo study found that it was testosterone rather than oestrogen that increased the fracture risk, particularly at the hip ⁴⁰⁹. Although testosterone appears to be less important than oestrogen in BMD, it has an independent contribution to male muscle strength and physical performance. Reduced testosterone has been associated with falls in older men which is another component of overall fracture risk ⁴¹⁰.

1.7.4 Osteoporosis in men

In early adult life, fractures are more common in men than women, and are mostly traumatic ⁴¹¹. A major determinant of bone mass in later life is peak bone mass, which is usually achieved by the end of the third decade ⁴¹². Genetic factors account for over half of the variability in peak bone mass, and other important influences are the timing of, and hormonal changes associated with puberty and lifestyle factors ^{413,414}. When peak bone mass is achieved, men have larger bone size, bone density and cortical bone mass than women.

Ageing is associated with altered bone turnover and an increase in resorption relative to formation with net BMD loss ⁴¹⁵. In men, 1% of BMD is lost per year following the attainment of peak bone mass (from around the age of 40) ^{416,417}., and the most rapid decline in BMD occurs in men aged 74 - 79 years ⁴¹⁸.

Compared with age-matched women, bone resorption is less rapid in older men, although smoking and weight loss can cause significant acceleration of this in both ⁴¹⁹. Physical changes in bone size and shape are thought to account for some of the gender differences in bone strength. In both men and women, there is increased bone resorption at the endocortical surface, an increase in periosteal bone deposition and circumference and loss of cortical thickness ^{36,420}. Periosteal apposition is greater in men than women, which offsets endosteal bone loss to a greater extent and ultimately reduces the stress applied to bone ^{421,422}.

In addition to BMD loss and changes in bone size and shape, bone strength is compromised by age-related microarchitecture deterioration. In general, cortical porosity increases, there is trabecularisation of cortical bone and decreased trabecular thickness ^{416,423}. Men and women experience different patterns of microarchitectural change ⁴⁴. In men, reduced bone formation predominates and there is trabecular thinning, but their number and connectivity remain fairly constant ⁴²⁴. In women, bone resorption is greater, and there is loss of both trabecular number and connectivity, which have a greater overall impact on bone strength ⁴²⁵.

Age-related bone loss can also be accelerated by endocrine factors. A decline in sex steroid levels is associated with age, partly due to an increase in SHBG ^{426,427}. Free testosterone and oestradiol both help to maintain normal bone turnover ⁴²⁸, and oestrogen seems to be the more potent inhibitor of bone resorption ⁴²⁹. This is supported by treatment of older men with androgen supplements, which do not increase BMD ⁴³⁰. The risk of fracture in men has been strongly associated with serum oestrogen levels ⁴⁰⁸.

Bone loss may also occur due to age-related decreases in growth hormone and IGF-1 production ⁴³¹. IGF-1 drives of long bone growth and periosteal apposition and the serum concentration is positively associated with BMD ^{432,433}. Older men are also more likely to have renal impairment, vitamin D insufficiency and reduced gastrointestinal calcium absorption, all of which elevate PTH and increase resorption ^{434,435}.

1.7.5 Diagnosis

The WHO classification for osteoporosis is based upon bone mineral density (BMD) measurement in postmenopausal women using dual X-ray absorptiometry (DXA). Comparison of an individual patient BMD to the peak bone mass in young adults results in a standard deviation measurement known as the T score. Osteoporosis is defined as a T score of ≤ -2.5 and osteopenia (low bone mass) as a BMD T score between -1.0 and -2.5 ⁴³⁶. The same diagnostic criteria are used in men, as there is evidence to suggest that fracture risk is the same as in women, given the same BMD and age ^{437,438}. The T score diagnostic criteria for osteoporosis recognises the importance of BMD in the pathogenesis of fracture, and provide a framework for

use in epidemiological studies. There is strong correlation between BMD and the risk of fracture. For every reduction of 1 SD there is a 1.5-2 times increase in the risk of fracture^{439,440}. However BMD cannot be used in isolation, as many fragility fractures occur in individuals with normal BMD^{440,441,442}. Clinical factors have been incorporated into fracture risk assessment tools (used with or without BMD data) to determine the probability of fracture.

1.7.6 Fracture risk assessment

The most widely studied tool recommended by many clinical guidelines is the Fracture Risk Assessment Tool (FRAX)⁴⁴³. FRAX is based upon data from 12 prospectively studied population-based cohorts from Europe, Australia, Canada, the USA and Japan. Extensive follow-up included 250,000 patient years and approximately 5,000 fractures in over 60,000 men and women⁴⁴⁴. In contrast to other fracture risk calculators, FRAX can be directly calibrated to measure fracture incidence in a target population, and considers death as a competing risk⁴⁴⁵. The FRAX website for each country has a link to national guidelines for the management of osteoporosis, for example the UK website links to the National Osteoporosis Guideline Group (NOGG)^{446,447}.

An example case is shown in figure 6. Risk factors in the FRAX algorithm include; age, sex, weight, height, previous fracture, parental hip fracture, smoking, GCs, rheumatoid arthritis, secondary osteoporosis and alcohol intake, and it is applicable to people aged 40–90 years. FRAX estimates the 10-year probability of major osteoporotic fracture (MOF; a composite of hip, spine, forearm and proximal humerus fracture) and hip fracture.

Assessment of fracture risk provides probability data, and intervention thresholds (ITs) determine the appropriate management. This may be a recommendation for BMD assessment (if this has not been done), or for treatment to be initiated. ITs vary between populations, and depend upon the prevalence of risk factors, fracture incidence, healthcare resources and access to BMD testing⁴⁴⁶. As with all medical interventions, the efficacy of treatment must be balanced with its adverse effects, as well as the risks associated with non-intervention. The economic impact of intervention is also key; NICE uses the EQ5D to determine the number and cost of each quality adjusted life year (QALY) that is gained from an intervention, and to determine its cost effectiveness^{448,449}.

UK NOGG guidance recommends that FRAX is used without BMD to estimate fracture risk (figure 7a)⁴⁴⁷. Individuals at high risk are offered treatment, those with an intermediate risk undergo BMD assessment to refine their risk (figure 7b). This approach reduced hip fractures by 28% in the SCOOP study⁴⁵⁰, and significantly reduced fractures in women identified by FRAX as intermediate or high risk⁴⁵¹. It has also been found to be cost effective⁴⁵². The evidence in men is limited, but NOGG recommend that fracture risk is assessed in all those aged over

50 with fracture risk factors. The NOGG IT for osteoporosis treatment equates to a woman aged over 50 with a previous fragility fracture (where treatment without BMD assessment is cost effective), and the same threshold applies to men.

Important limitations of FRAX are that it does not incorporate the risk of falls (falls predict subsequent fracture independently of FRAX)⁴⁵³ or frailty markers^{454,455}. Assessment of BMD as a surrogate for bone strength does not identify individuals with normal BMD but abnormal bone geometry or microarchitecture. Novel techniques are the subject of ongoing investigation and may be used in the future to enhance risk assessment. One recent development is the use of the trabecular bone score (TBS; a measure of texture derived from DXA of the spine) to refine FRAX output⁴⁵⁶.

1.7.7 Fracture risk assessment in men with prostate cancer

Men with PC are at increased risk of fracture compared with the general population, and ADT increases this risk further⁴⁵⁷. Published consensus guidance recommends that all men starting ADT undergo FRAX risk assessment and subsequent BMD measurement and treatment if indicated³⁴⁵. NICE guidance for PC recommends that fracture risk is considered in all men. However there are no specific recommendations regarding the method of assessment, the timing in relation to ADT initiation or duration, or where the responsibility for undertaking this assessment lies¹⁵³.

A small number of studies have reported fracture risk in men with PC treated with ADT, and these are summarised in table 7. In general, the use of FRAX identified a large number of individuals at risk of fracture, than would otherwise have been identified by an isolated BMD measurement^{458,459,460}. Some evidence suggests that FRAX identifies a different group of men at risk of fracture to those with a low T score⁴⁶¹. In general, fracture risk in men with PC undergoing ADT is strongly associated with age, and a significant proportion of men have a risk of hip fracture that is sufficient to warrant intervention^{462,458–460,462–464}. However, most data are derived from relatively small cross sectional and retrospective studies in specific populations, and there is a lack of prospective data from randomised studies regarding fracture endpoints.

Calculation Tool

Please answer the questions below to calculate the ten year probability of fracture with BMD.

Country: **UK** Name/ID: [About the risk factors](#)

Questionnaire:

1. Age (between 40 and 90 years) or Date of Birth
Age: Date of Birth: Y: M: D:

2. Sex Male Female

3. Weight (kg)

4. Height (cm)

5. Previous Fracture No Yes

6. Parent Fractured Hip No Yes

7. Current Smoking No Yes

8. Glucocorticoids No Yes

9. Rheumatoid arthritis No Yes

10. Secondary osteoporosis No Yes

11. Alcohol 3 or more units/day No Yes

12. Femoral neck BMD (g/cm²)
Select BMD

BMI: 21.6
The ten year probability of fracture (%)

without BMD	
Major osteoporotic	5.7
Hip Fracture	1.8

Algorithms are available for over 60 countries

If available, BMD data can be entered here

10 year risk of fracture is shown here

Link to management guidance depending on country selected

Figure 6: The FRAX fracture risk assessment tool.

A screenshot showing the freely available online tool (<https://www.sheffield.ac.uk/FRAX/tool.aspx?country=9>). Fracture risk is shown when calculated in a 70-year old male with no other fracture risk factors (no BMD data included).

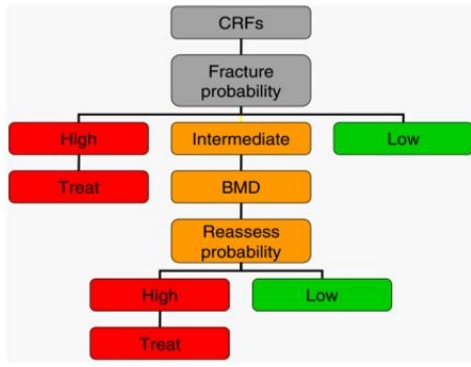


Figure 7(a)

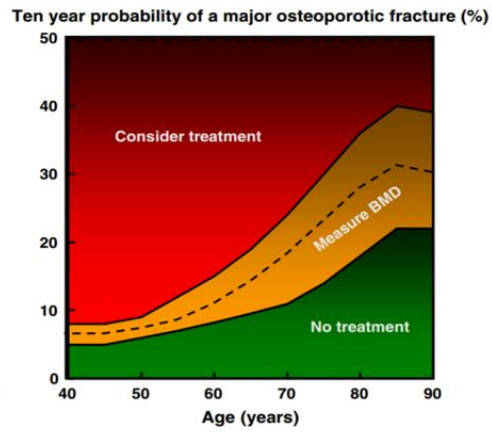


Figure 7(b)

Intervention Threshold

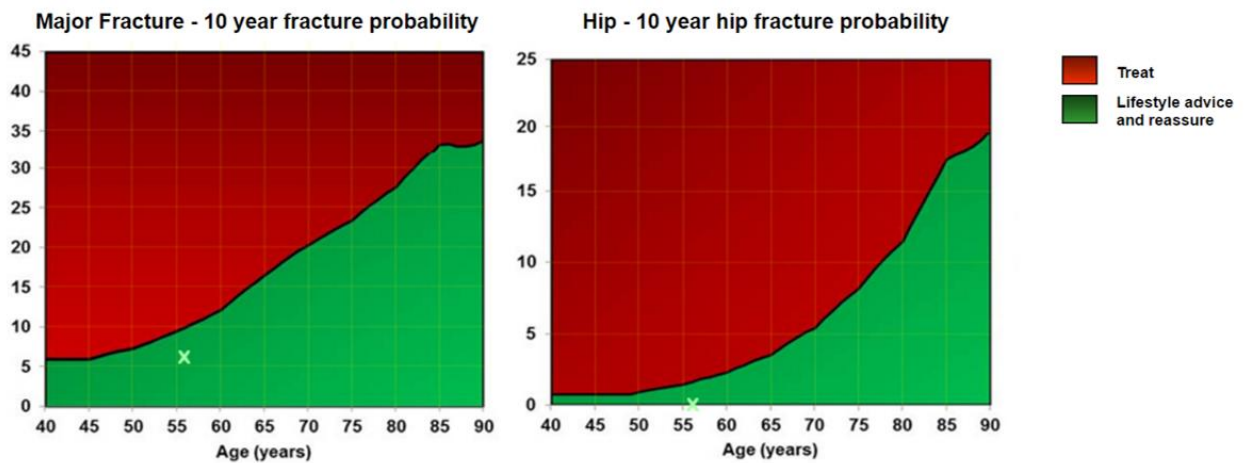


Figure 7(c)

Figure 7: Assessment of fracture risk and intervention thresholds

Images obtained from <https://www.sheffield.ac.uk/FRAX/tool.aspx?country=9>.

Figure 7a: algorithm for the use of clinical risk factors (CRFs) and bone mineral density. **Figure 7b:** NOGG guidance for the management of osteoporosis: based upon 10-year risk of major osteoporotic fracture. The dotted line shows the intervention threshold (the probability at which intervention is recommended). The orange shaded area shows the limits of fracture probabilities for the assessment of BMD (BMD assessment thresholds). **Figure 7c:** FRAX[®] intervention thresholds once BMD has been measured ⁴⁴³.

Table 7: Summary of studies that have used FRAX to determine the fracture risk in ADT-treated men

Author (year)	Study design and population	Methods	Main findings
Brown (2019) ⁴⁶⁵	Men with metastatic or high risk PC starting ADT	FRAX with CRF	34.8% were at intermediate/ high risk of fracture and required BMD assessment
Saylor (2010) ⁴⁵⁸	Cross sectional study in men with PC receiving ADT	FRAX with CRF, and FRAX with BMD	<p>Risk of hip fracture was 3.1%, risk of MOF was 12%. 51.2% of men had a risk of hip fracture above the IT.</p> <p>If ADT was excluded as a risk factor for secondary osteoporosis, 32.8% of men exceeded the IT and hip fracture risk was 1.8%.</p> <p>In men that had BMD measured, hip fracture risk was 0.9%, 15% of men exceeded IT. In this group, the FRAX risk of hip fracture without BMD was 2.4%, and 44% required treatment.</p> <p>Fracture risk and need for treatment was strongly influenced by increasing age</p>
Adler (2010) ⁴⁶¹	Cross-sectional study in men receiving ADT for non-metastatic PC	FRAX with and without BMD	<p>FRAX with BMD: risk of hip fracture was 1.6%, risk of MOF was 8.0%</p> <p>FRAX without BMD: risk of hip fracture was 3.8% and MOF was 12.3%</p>
Neubecker (2011) ⁴⁵⁹	Retrospective study of men with PC receiving ADT or about to start ADT, with reported height loss	FRAX with and without BMD	<p>22 men had VF, 17 of these were asymptomatic. Of these 22 men, only 59% would have been above the IT based on FRAX with BMD, and 73% when FRAX was used with BMD.</p> <p>Hip fracture risk using BMD was 3% and 4.5% in those without/with VF, without BMD was 4% and 6.8% in those with/without VF.</p> <p>MOF risk using BMD was 7.5% and 11% in those without/with VF, risk without BMD was 9.3% and 15% in those with/without VF</p>

Dhanapal (2011) ⁴⁶⁴	Retrospective review of men with PC receiving ADT	FRAX without BMD	Risk of MOF increased from 4% to 5.6% after starting ADT, and hip fracture risk increased from 1.3% to 2.2%. Compliance with guidelines was poor; 9% of those requiring BMD assessment had a DXA, <5% were started on calcium and Vitamin D supplements
James (2014) ⁴⁶⁰	Men with PC receiving ADT	FRAX without BMD for all FRAX with BMD in 94 men	FRAX without BMD identified 61.6% as being above the IT, risk of hip fracture was 4.0% and risk of MOF was 10%. FRAX with and without BMD identified 46.8% and 69.1% as requiring treatment respectively, compared with only 19% when T score was used in isolation.
Kawahara (2016) ⁴⁶⁶	Cross sectional, men with PC receiving ADT, or had brachytherapy/radiotherapy or surgery, some of which was combined with ADT	FRAX without BMD	Median risk of hip fracture was 2.7% and MOF was 7.9%, 52.7% had a hip fracture risk above the IT and 4% had a >20% risk of MOF ADT was associated with significantly higher risk of MOF and hip fracture (p<0.001 for both)
Ojeda (2017) ⁴⁶⁷	Prospective study in men with high risk PC receiving ADT	FRAX with BMD	Baseline fracture risk was 4% and 0.7% for MOF and hip fracture respectively. 4% had hip fracture risk above the IT
Miyawaza (2018) ⁴⁶³	Men with PC starting ADT	FRAX without BMD	Baseline risk of any fracture was 23% Risk of hip and MOF were 3.6% and 9.6%
Kojima (2019) ⁴⁶²	Men with PC receiving ADT	FRAX with BMD	55% had a T score of <-1.0. 23% had a >20% risk of MOF. 97% had a risk of hip fracture above the IT
Abbreviations: MOF: major osteoporotic fracture; BMD: bone mineral density; IT: intervention threshold; VF: vertebral fracture			

1.7.8 Management of osteoporosis in men

Over the last two decades there has been significant progress in the management of osteoporosis. National and international guidelines are available, risk assessment tools and treatment algorithms guide management, and bone targeted therapies are widely used. However data suggest that osteoporosis remains both under-diagnosed and under-treated, even after a fragility fracture, and that this is especially true in men ^{468,469,470,471}. The 'osteoporosis treatment gap' was highlighted in a recent study, where BMD was measured in just 9% of 2.3 million individuals who experienced a fracture ⁴⁷². Of these, 307,000 had a subsequent fracture, with a \$6.3 billion associated cost. A UK study of 27,542 individuals who had a first hip fracture found that 68% did not receive osteoporosis medication in the 6 months prior to, or in the year after fracture ⁴⁷¹.

Evidence based lifestyle measures to improve bone health have been incorporated into UK NOGG guidance ⁴⁴⁷. These have been discussed previously, and include regular weight-bearing exercise, smoking cessation, a reduction in alcohol intake, and assessment and reduction of the risk of falls.

The safety and efficacy of pharmacological treatments on BMD and BTM appear to be similar in men and women ⁴⁷³. However, the evidence base in men is limited and few studies have evaluated fracture risk in response to treatment. The indications for therapy in male osteoporosis are the same as those for women; those aged over 50 with a fragility fracture of the hip or spine, in those with osteopenia or osteoporosis, and in those with a high risk of fracture based on risk assessment ^{447,473}.

Bisphosphonates (BPs) are the commonest prescribed therapy for osteoporosis. In 2018, 120 BP prescriptions were generated per 1000 population in the UK ⁴⁷⁴. A range of BPs (including oral and intravenous therapies) have improved BMD and reduced fracture risk in men with osteoporosis, ^{475,476,477} hypogonadal men ⁴⁷⁸ and in androgen suppressed men with PC ³⁶³. Currently licensed BPs for male osteoporosis in the UK are alendronate, risedronate, zoledronic acid.

Denosumab (60mg every 6 months) is used for the treatment of osteoporosis in postmenopausal women and in men at increased risk of fracture ^{479,480}. In women, it reduces the incidence of vertebral, non-vertebral and hip fractures ⁴⁷⁹, and approval in men was based on a BMD bridging study ⁴⁸¹. In men with PC receiving ADT, denosumab improved BMD and reduced the incidence of VF ²⁸¹ (given at higher doses in men with metastatic bone disease, to prevent SREs). Cessation of therapy is associated with rapid decreases in BMD and requires careful management ⁴⁸².

Teriparatide (recombinant human PTH 1-34) is an anabolic agent that is administered via subcutaneous injection. It is approved for use in postmenopausal and GC-associated osteoporosis ^{483,484}, and in male osteoporosis based on data

from BMD bridging studies ⁴⁸⁵. It is most frequently used in those where other therapies are not tolerated, effective or are contraindicated ⁴⁴⁷. It's efficacy in hypogonadal men (including those receiving ADT) has not been established, in part due to the fact it is contraindicated in those with BM or who have received radiotherapy. Its use is restricted to 24 months due to an increased risk of osteosarcoma ⁴⁴⁷.

A range of novel agents are the subject of ongoing osteoporosis trials. These include cathepsin K inhibitors, anti-sclerostin antibodies, and antibodies to DKK-1 ⁴⁸⁶. The anti-sclerostin antibody romosuzumab was recently approved for use in postmenopausal women with severe osteoporosis. in Scotland (November 2020), and NICE is currently reviewing the evidence for its use ⁴⁸⁷. None of these treatments are currently available for men.

Chapter 2: Assessment of bone loss in men receiving treatment for prostate cancer (ANTELOPE)

2.1 Introduction

This chapter provides an introduction to the ANTELOPE study; assessment of bone loss in men receiving treatment for prostate cancer (PC). Factors that affect bone density will be outlined, along with tools available to assess muscle function and strength. This chapter will describe established and novel bone imaging techniques and will outline the ANTELOPE study methods.

ADT is the cornerstone of therapy for men with PC and the indications and adverse effects have been outlined in chapter one. ADT is associated with a rapid and profound fall in serum oestrogen and testosterone levels, disruption of the bone remodelling cycle and net bone loss. The reduction in BMD is most significant (between 5-8%) during the first year of therapy, and subsequent BMD loss is 1-4% throughout the duration of treatment^{238,246}. This BMD loss is super-imposed upon the usual age-related bone loss (approximately 1% per year) and may also be influenced by other factors such as co-morbidities, lifestyle and use of certain medications.

In addition to BMD loss, men with PC are at higher risk of fracture than men without PC, even in those who do not receive ADT²²⁴. There is also a significant dose-response between ADT and fracture risk²²¹. An important consequence of ADT is sarcopenia, which may further increase the risk of falls and subsequent fracture. Using FRAX, approximately one third of ADT treated men with PC are at intermediate or high risk of fracture⁴⁶⁵. Studies of FRAX in men with PC are limited in number and have varied in their methods. The use of clinical risk factors to determine the risk of fracture provides additional information to BMD data^{458,460,461}.

There is a disparity in the management of bone health between men with PC receiving ADT and women with breast cancer undergoing endocrine therapy. Both groups are at risk of both CTIBL and SRE from their underlying disease and from treatment. In women with breast cancer (BC) bone endpoints such as fracture and change in BMD have been widely incorporated into randomised clinical trials⁴⁸⁸. Established guidelines and algorithms for BMD assessment and management of bone health have been incorporated into clinical BC practice. In the UK, NICE guidelines for early and for advanced BC make specific recommendations for the use of dual-energy X-ray absorptiometry (DXA) scans and use of bone targeted therapies^{489,490}.

In men with PC undergoing ADT, awareness of bone health amongst patients and clinicians is suboptimal³³⁹. Guidelines for bone health assessment have varied,

adherence to them is poor, and there is no clear consensus as to which speciality should have overall responsibility for bone health assessment and optimisation^{345,346}. Recent publications have attempted to address this issue^{342,345,491,492}; it remains to be seen how these will impact the frequency of DXA, future use of fracture risk assessment tools and initiation of bone targeted therapies in ADT-treated men with PC.

2.1.1 Factors that affect bone density and turnover

In addition to the effects of PC and ADT on bone, other factors may also have significant impact. There were considered in the ANTELOPE study design, and in inclusion and exclusion criteria.

Increasing age is associated with loss of BMD, however only a few studies have investigated longitudinal BMD change in men⁴⁹³. The magnitude of BMD loss depends on the skeletal site, but appears to be around 1% per year with advancing age^{418,419}. In addition to loss of BMD, microarchitectural changes in older men (such as trabecular thinning) affect bone strength and fracture risk⁴⁹⁴.

Low BMI is associated with low BMD and an increased risk of fracture^{495,496}. In middle aged men, weight loss over three decades was associated with a significant reduction in hip BMD⁴⁹⁷. Almost one third of men in the lowest quartile of BMI at baseline who lost weight (5% or more) during the study had osteoporosis, whereas only 4% of those who gained weight had osteoporosis. In general, obesity (BMI >30kg/m²) is associated with a higher BMD, however its relationship with falls and fracture risk is complex. The risk of non-vertebral fractures appears to be higher in morbidly obese men (BMI >35kg/m²) than those with a BMI of 30-34.9kg/m² after adjustment for BMD⁴⁹⁸. The risk of fracture that is associated with obesity is also site dependent; there are fewer hip and vertebral fractures but a higher incidence of fracture at peripheral sites^{499,500}.

Vitamin D has direct and indirect actions on bone. The direct effects are mediated through effects on osteoblasts and osteoclasts. Vitamin D regulates osteoblast differentiation and affects key non-collagenous proteins that aid bone matrix formation⁵⁰¹. It induces pre-osteoclasts to produce macrophage colony-stimulating factor (M-CSF) to upregulate osteoclast proliferation and prevent their apoptosis. The indirect actions of vitamin D on bone occur via increased calcium and phosphate absorption from the intestine and renal tubule⁵⁰².

Vitamin D insufficiency (30-50nmol/L) and deficiency (<30nmol/L) are frequent in older adults⁵⁰³ and are also highly prevalent in men with PC⁵⁰⁴. Underlying mechanisms include; reduced synthesis, reduction in dietary intake, decreased intestinal absorption and less exposure to sunlight. The resulting negative calcium balance stimulates PTH secretion, enhances calcium absorption and increases bone resorption. Vitamin D deficiency has also been associated with muscle weakness, increased falls risk, poor physical performance and postural instability^{505,506}.

Supplementation with calcium and vitamin D has been used as the control arm in studies of bone targeted therapies in ADT-treated men⁵⁰⁷, however there is no convincing evidence that it is able to prevent bone loss.

A number of systemic conditions are important considerations when designing studies of changes in bone density, structure and strength. These include endocrine disorders (such as thyroid and parathyroid disorders, diabetes mellitus); collagen disorders⁵⁰⁸; conditions where bone remodelling is uncoupled; states of chronic inflammation⁵⁰⁹ and malabsorption.

As the commonest cause of secondary osteoporosis, continuous oral GC therapy causes bone loss and an increased risk of fracture. The pathophysiology (outlined in chapter 1) includes inhibition of osteoblast formation, promotion of osteoblast and osteocyte apoptosis and an increase in the number and activity of osteoclasts. Loss of BMD is most rapid during the first year of treatment (between 6-12%), subsequent loss of BMD is around 3% per year thereafter³⁸³. Microarchitectural changes include loss of cortical thickness, increased trabecular separation and reduced number, and a reduction in bone stiffness^{383,388,510}. Changes in BTM include an increase in resorption markers and a fall in formation markers; in particular, PINP is suppressed in a dose dependant manner⁵¹¹. Fracture risk is affected by the duration of GC use (cumulative dose) and current dose, and discontinuation of treatment is associated with a risk reduction⁵¹². The FRAX algorithm defines GC use as a fracture risk factor if an individual is currently exposed to oral GCs, or has taken them for more than 3 months at a daily dose of ≥ 5 mg prednisolone or equivalent^{443,513}. In addition to GCs, medications used in the management of epilepsy and metabolic bone disorders also alter bone metabolism⁵¹⁴.

2.1.2 Sarcopenia

Sarcopenia is the progressive loss of skeletal muscle mass and quality. There is a reduction in muscle mass and number of fibres, in addition to a shift in composition towards expression of slow fibre (type I) types and loss of precursor cells for type II fibres^{515,516}. Loss of fast type II fibres (required to mobilise ATP and create tension) causes muscle to fatigue easily. Loss of muscle strength that is related to loss of mass (in those with no neuromuscular deficit) is referred to as dynapenia⁵¹⁷. There is a lack of consensus regarding the specific definition and precise diagnostic criteria for sarcopenia. Recent publications have produced different consensus definitions (table 8), and made recommendations for assessment. The most recent of these were the updated EWGSOP guidelines, which also made recommendations for clinical practice and research⁵¹⁸.

Sarcopenia is common in older populations and contributes to frailty, falls, fractures, disability and increased mortality^{519,520,521,352,522}. Hospitalisation or a period of immobility following a fall causes dis-use atrophy, which precipitates

physical decline and may lead to loss of independence ⁵²³. The aetiology of sarcopenia is multi-factorial. With normal ageing, around one third of muscle mass is lost between the ages of 50 and 80 years ⁵²⁴. It is estimated that sarcopenia affects between 5-13% of the population aged between 60-70 years and more than half of those aged over 80 years ⁵²⁵. However, prevalence estimates vary in the literature due to study population heterogeneity and methods used to measure muscle mass (DXA is the gold standard, but CT, MRI and neurophysiological techniques may also be used). An indirect age-related change in muscle strength occurs via impaired growth hormone production, which reduces the anabolic effect of IGF-1 on muscle. In addition to ageing, other risk factors for sarcopenia are poor nutrition, sedentary lifestyle, chronic diseases, a reduction in circulating sex steroids, and use of certain medications ⁵²³.

In older cancer patients, the aetiology of sarcopenia is complex and multifactorial, and exacerbated by cachexia and cytokine-mediated degradation of muscle mass ⁵²⁶. Individuals with cancer have an increased metabolic rate and an underlying state of chronic inflammation, both of which lead to a reduction in protein synthesis and increased protein degradation ⁵²⁷. Individuals with cancer are also likely to have impaired nutrition and reduced physical activity as a result of their disease and/or treatment. The prevalence of sarcopenia varies between cancer types, stages and progress through treatment ⁵²⁸. Sarcopenia has been associated with increased toxicity to systemic anticancer treatments, cancer-related fatigue and increased mortality, independent of disease stage ^{529,530 531}. However, many studies in cancer patients have not assessed muscle strength to classify sarcopenia and have relied on radiological measurement of lean mass. The Society of Geriatric Oncology (SIOG) recommends geriatric assessment in all older cancer patients before treatment is initiated, and this should include assessments able to identify sarcopenia ⁵³².

Table 8: Definitions of sarcopenia

Group	Year	Proposed diagnostic criteria
European Working Group on Sarcopenia in Older People (EWGSOP) ^{533,534}	2010	Low skeletal muscle mass Either low muscle strength or low performance (for example gait speed) If only low mass is present = pre-sarcopenia 2 criteria are present = sarcopenia If all 3 criteria are present = severe sarcopenia
	2019	Three criteria; 1= low muscle strength (grip strength or chair stand), 2= low muscle quantity/quality, and 3= reduced physical performance (gait speed, timed up and go, or short physical performance battery) If low muscle strength is present in isolation: probable sarcopenia Low muscle strength and quality: sarcopenia All three criteria = severe sarcopenia
European Society for Clinical Nutrition and Metabolism Special Interest Groups (ESPEN-SIG) ⁵³⁵	2010	Low skeletal muscle mass Low muscle strength
International Working Group on Sarcopenia (IWGS) ⁵³⁶	2011	Low skeletal muscle mass and low muscle function measured by gait speed

2.1.2.1 Prostate cancer and sarcopenia

In men with PC, the aetiology of sarcopenia is multifactorial and the important aetiological factors are shown in figure 8. Older men may also have comorbidities that directly or indirectly affect body composition. Hypogonadism is a key mediator (total testosterone concentration > 2 SD below mean for young men), as serum testosterone correlates positively with lean mass⁵³⁷. Hypogonadism is present in 20% of all men aged between 60-80 years and 50% of those aged over 80 years, and is partially explained by an increase in SHBG with age^{538,539}. The initiation of ADT causes circulating testosterone and oestrogen to decrease further; they rapidly fall to castration levels. GCs are often used in PC treatment and also have a negative effect on lean mass⁵⁴⁰.

Prospective studies have investigated changes in lean and fat mass associated with ADT, and these were summarised in table 6 (chapter one). Continuous ADT is associated with simultaneous loss of skeletal muscle mass and gain of fat mass, a condition which is termed sarcopenic obesity. Meta-analysis of studies of ADT on body composition have reported a mean increase in weight of 2.1% (95% CI 1.4-2.9%), mean increase in fat mass of 7.7% (95% CI 4.3-6.9%), and decrease in lean mass by 2.8% (95% CI 3.6-2.0%). ADT has also been shown to affect lower limb muscle function, with a prominent decrease in peak hip flexor and knee extensor torque, mediated by decreased force from proximal muscles⁵⁴¹. In men with metastatic PC, sarcopenia may also reduce tolerance to chemotherapy and has been associated with worse cancer-specific survival^{542,543,544,545}. SIOG recommend that a comprehensive geriatric assessment is undertaken in all men with PC before treatment is initiated, and this should include measures of muscle strength and function⁵⁴⁶.

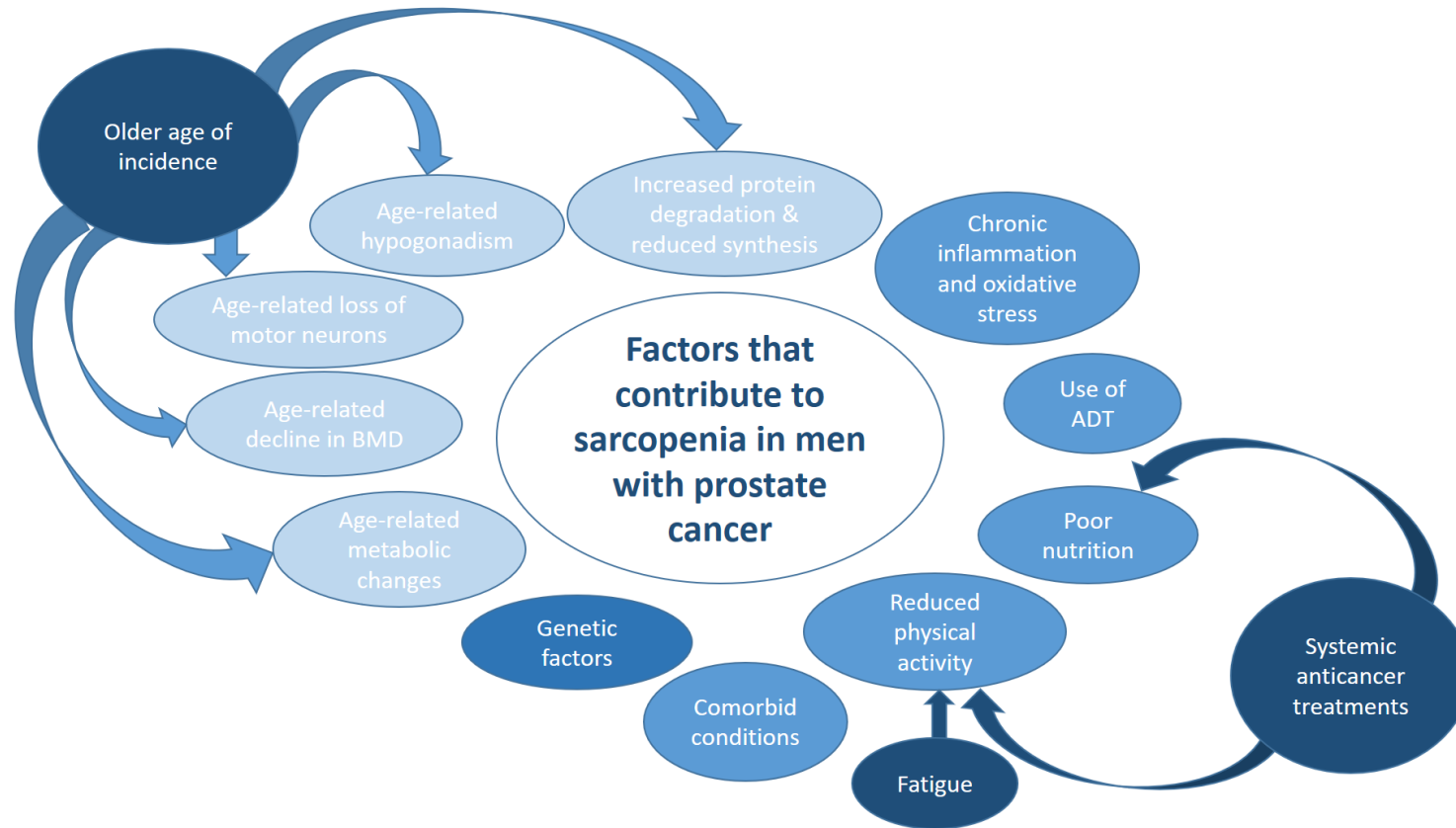


Figure 8: Aetiology of sarcopenia in men with prostate cancer.

The aetiology of sarcopenia in men with PC is complex and multifactorial. It includes genetic, lifestyle and age-related influences, in addition to the physiological and biological effects of cancer and its treatment.

2.1.2.2 Frailty in men with prostate cancer

In addition to changes in muscle strength and sarcopenia that are associated with ADT, another important consideration is frailty. This common geriatric syndrome is defined as a state of vulnerability to the poor resolution of homeostasis following a stressor event⁵⁴⁷. It is the consequence of cumulative deficits across multiple physiological systems, and has been associated with adverse outcomes in cancer patients, including increased mortality and intolerance to cancer treatment⁵⁴⁸. In an ageing population, the distinction between biological and chronological age and the identification of frail cancer patients is of increasing importance.

The diagnostic criteria for frailty depend on the model that is used; current evidence-based approaches are the phenotype model, comprehensive geriatric assessment (CGA) and the cumulative deficit model. The phenotype model identifies frailty when three or more of the following characteristics are present; unintentional weight loss, exhaustion, low energy expenditure, slow gait speed and weak grip strength³⁵³. Those with one or two characteristics are categorized as pre-frail. The cumulative deficit model defines frailty as the cumulative effect of individual deficits (clinical signs, symptoms, disease states, disabilities and abnormal laboratory test results)⁵⁴⁹, and CGA is a multidimensional, multi-disciplinary assessment process that is widely used in geriatric medicine⁵⁵⁰.

It is estimated that frailty affects between 40 and 50% of oncology patients, and a similar proportion are considered to be pre-frail⁵⁴⁸. Frailty assessment provides additional information to the assessment of performance status (the most frequent measure of fitness for treatment in oncology practice)⁵⁵¹. In ADT-treated men with PC, the prevalence of frailty is estimated to be between 6.4% and 60%, and a significant proportion are pre-frail^{548,552,553}. However, high quality epidemiological data are lacking in men with PC²⁴⁷. Importantly, there is also considerable overlap between the known physical toxicities of ADT (such as sarcopenic obesity, fatigue and changes in muscle strength) and frailty, and ADT may either directly cause or exacerbate pre-existing frailty or pre-frailty⁵⁵⁴.

Published guidelines for the assessment and management of older patients with PC are available⁵⁵⁵, however geriatric assessment (including frailty screening) is not routinely carried out in oncology practice in the UK. Failure to consider frailty and fitness in men with PC risks the under-treatment of older patients who are otherwise fit. Conversely, it may lead to the over-treatment of younger men (based on age criteria alone), some of whom may have underlying comorbid conditions and be less able to withstand standard treatments. In addition, health professionals report a lack of knowledge and confidence in managing and treating older cancer patients, and the current workforce is not designed to meet their needs^{556,557}. Recent initiatives such as the McMillan Cancer Support and Age UK Cancer Services Coming of Age report, NHS England's 2015-2020 cancer strategy

and recommendations from the UK Association of Cancer Physicians seek to improve cancer care and outcomes in older patients^{556,558}. McMillan Cancer Support has subsequently established an expert reference group to drive forward workforce and policy changes in order to achieve this⁵⁵⁹.

2.1.3 Assessment of body composition, muscle function and strength

2.1.3.1 Body composition

Standard clinical measurements of height and weight are used to determine body mass index (BMI, kg/m²) and identify individuals as underweight (BMI <18.5), normal weight (BMI 18.5-24.9), overweight (BMI 25-29.9kg/m²), obese (BMI 30-34.9kg/m²) or severely obese (BMI >35kg/m²) based on the WHO classification⁵⁶⁰. BMI is a widely available screening tool, but does not account for variation in fat and lean mass or adequately define risk of long term adverse health. In addition to BMI, waist and abdominal circumference and skinfold thickness may also be measured⁵⁶¹. Bioelectrical impedance is a more resource intense method, and produces estimates of body water and fat mass by measuring the resistance of the body as a conductor to a small alternating electrical current⁵⁶².

The commonest imaging technique used to determine body composition is dual-energy X-ray absorptiometry (DXA) and DXA will be described in greater detail later in this chapter. It is used to calculate the proportion of fat and lean tissue in a region of interest (this can include the whole body). It is limited by some technical aspects (such as variability between scanners) and the software used which makes inherent assumptions regarding levels of hydration and tissue density⁵⁶¹.

2.1.3.2 Muscle function and strength

Tests of balance and muscle strength in older individuals can determine functional status and degree of dependence, and can also predict multi-morbidity and mortality^{563,564,565}. Balance is a composite of multiple integrated body systems, and thorough assessment of balance includes static, dynamic (such as walking) and proactive and reactive elements⁵⁶⁶. Numerous tests can assess balance and/or muscle strength, and available tools range in their complexity, ease of use, sensitivity and specificity. Tests of grip strength, walking speed, sit-to-stand, and standing balance may predict both current and future health^{564,563,567}.

Grip strength

Grip strength declines after midlife and this accelerates with increasing age⁵⁶⁸. Loss of grip strength predicts functional decline, falls, disability, impaired quality of life and mortality in middle-aged and older adults^{569-571,572}. Cross sectional data suggest that it may also be a useful marker of frailty⁵⁷³. Assessment of grip strength has been recommended by the European Working Party on Sarcopenia in Older People (EWGSOP)³⁵² and it is measured quantitatively using a dynamometer.

The Jamar hand dynamometer has the most extensive normative data and is the most commonly cited.

Measurement of grip strength is simple, quick, and requires relatively inexpensive equipment. In most studies, strength is assessed three times in each hand⁵⁷⁴ which produces good to excellent test-retest reproducibility⁵⁷⁵ and excellent inter-rater reliability⁵⁷⁶. However, there is no standard protocol and variation in the methods used in published studies. There is some evidence that the dominant hand may have up to 10% stronger grip strength than the non-dominant hand, and assessment of both hands improves accuracy⁵⁷⁷. Positioning is also important as results may be elevated by supination of the forearm, flexion of the elbow to 90 degrees, and posture^{578,579,580}. Methods of instruction and encouragement by the assessor may also affect results⁵⁸¹, as well as the amount of time left between repeated measures⁵⁸². The time of day may also have an effect, with a circadian rhythm resulting in maximum strength first thing in the morning⁵⁸³.

The short physical performance battery (SPPB)

The short physical performance battery (SPPB) has been used to assess performance in community and hospital settings, and is recommended by the current EWGSOP guidance⁵³⁴. It comprises assessment of muscle strength, balance and mobility to provide a rapid and objective outcome measure. It involves walking at a normal pace, a balance task and chair stand test⁵⁸⁴. The reliability of SPPB is good and it has been validated with self-reported mobility and disability^{585,586}. Components of the SPPB have been shown to predict risk of falls⁵⁸⁷, loss of independence⁵⁸⁸ hospitalisation and mortality^{586,589}, and it is a sensitive measure of reduced lower limb performance⁵⁹⁰.

In a study of men with PC who had received ADT for at least 3 months, 56% of men had impairment in the SPPB across all components, and one fifth of men had experienced a recent fall⁵⁹¹. Another study compared SPPB scores in three groups of men with PC (no ADT, short term and long term ADT) and healthy controls without PC. Long term ADT was associated with a significantly lower score than short term or no ADT⁵⁹². A lower SPPB score has also been associated with impairment in instrumental activities of daily living (IADL) in older men with PC⁵⁹³.

2.1.4 Assessment of bone structure and microarchitecture

2.1.4.1 Dual X-ray absorptiometry (DXA)

DXA is a non-invasive quantitative imaging technique that is used to measure two dimensional (areal) BMD (aBMD) at the lumbar spine, hip and proximal femur. DXA scans are widely available and standard clinical practice. The BMD and T score outcomes directly relate to the WHO diagnostic criteria for osteoporosis; BMD at the hip is the most reliable measurement for estimating fracture risk^{594,595}. DXA provides an accurate assessment of response to treatment and changes in aBMD over time^{596,597}. Other non-BMD applications of DXA include; fracture risk assessment; vertebral fracture assessment; measurement of body composition⁵⁹⁸; hip geometry analysis⁵⁹⁹; and trabecular bone score⁶⁰⁰. DXA has important practical advantages such as; short scanning times and quick patient set up, low doses of radiation (approximately 32 μ Sv, equivalent to 5 days of natural background radiation), stable calibration, and the availability of reliable reference ranges⁵⁹⁷.

2.1.4.2 Basic principles

DXA relies upon the difference in attenuation of photon energy by bone mineral, compared with soft tissue⁶⁰¹. DXA scanners transmit beams of photons with high and low energies by alternating the voltage of the x-ray tube (kV switching). A fan shaped beam is generated by passing the beam through a collimator. Photons are then attenuated by absorption and scatter (Compton scatter), resulting in the loss of kinetic energy⁶⁰². In photoelectric absorption, the incident photon energy provides all its energy to an electron and disappears. In Compton scattering, only part of the photon energy transfers to an electron, and this interaction results in the production of a scattered photon with altered direction and reduced energy⁶⁰³. The x-ray attenuation coefficient depends on atomic number and photon energy.

The intensity of an incident beam depends on its photon energy and the composition, density and thickness of the material it passes through⁶⁰². Measurement of the transmission factors at two different (high and low) energies enables the areal densities (the mass per unit of projected area) of two different types of tissue to be inferred. For the purposes of DXA, these are considered to be bone mineral or hydroxyapatite, and soft tissue⁶⁰¹. Hydroxyapatite has a high density, includes higher atomic number elements such as calcium and phosphate and causes greater attenuation of photon energy than soft tissue elements (skin, fat, muscle, vasculature) which are predominantly comprised of oxygen, carbon and hydrogen molecules^{601,602}.

Transmitted photons pass through the body and reach a scintillation detector array system (figure 9), which converts the emerging x ray beams (which vary in energy) into light energies. These are detected by a photo diode and converted into electrical signals for image generation. An attenuation coefficient is calculated for

each pixel (R value) and is the ratio of attenuation at low and high energy beams. The standard equation for the calculation of attenuation of a beam passing through homogenous tissue is

$$I = I_0 \exp - (\mu M)$$

Where I is the intensity of the beam after it has been transmitted, I_0 is the beam intensity, μ is the linear mass attenuation coefficient of the tissue (cm^2g^{-1}) and M represents the area density (g/cm^2)⁶⁰². However, as the body is not a homogenous tissue, two separate compartments (bone and soft tissue) are modelled to calculate bone density.

For a given energy, the equation used for determination of attenuation in BMD calculations is

$$I = I_0 \exp - (\mu_{\text{BMB}} + \mu_{\text{SMS}}) \text{ (B represents bone and S is soft tissue)}$$

This can also vary depending on the beam energy, and requires separate equations to be used for low and high energy beams.

During the DXA scan, a bone profile is generated as a pixel map, with an edge detection algorithm used to delineate bone from soft tissue. Bone density is calculated for each pixel of the area that is scanned, the mean density of these is equivalent to the areal BMD (g/cm^2). The software identifies the bone area scanned, and can use this information along with the mean BMD to calculate the bone mineral content (BMC). This is measured in grams and is derived from multiplication of the BMD of an area by the total bone area.

The main outcome of interest from DXA is aBMD. From this, the clinically important T and Z scores are determined. These are gender specific standard deviations (SD), the T score quantifies how far the BMD lies from the mean value for young adults, whilst the Z score refers to a comparison between observed BMD and the population mean for someone of the same age. The standard equations used are:

$$\text{BMD T-score} = (\text{observed BMD} - \text{young normal BMD}) / (\text{SD of young normal BMD})$$

$$\text{BMD Z-score} = (\text{observed BMD} - \text{age and gender-matched BMD}) / (\text{SD of age and gender-matched BMD})$$

2.1.4.3 Limitations of DXA

The most significant limitation of DXA is the two-dimensional measurement which does not account for bone depth, and lacks detailed information regarding bone microarchitecture. BMD measurements may also be affected by increased bone marrow fat (such as those with a lower BMI), in individuals where fat distribution is non-homogenous, in those where the level of hydration is not constant throughout their lean mass, and when there is non-standard bone geometry^{604,605,606,607}. Most DXA scanners have a scan table weight limit (typically around 150kg) which excludes some patients from assessment. Accurate positioning can also be difficult

in overweight and obese patients, and may require scanning adaptations that can introduce error⁶⁰⁸.

DXA may also overestimate BMD, as age-related conditions such as osteoarthritis and aortic calcification may all falsely elevate BMD measurement⁶⁰⁹. This issue may be circumvented by the use of peripheral DXA (imaging sites such as the radius), which not only improves accuracy of BMD measurement, but may also identify additional patients with osteoporosis^{214,290}. Peripheral DXA may be particularly useful in men with PC, the distal radius is rarely affected by bone metastasis and forearm BMD is a strong predictor of fracture risk in men⁶¹⁰. However central DXA is more widely available, is able to provide information regarding body composition and the addition of peripheral DXA to central DXA measurement has implications on scanning times.

DXA results may also vary due to the use of different machines and scanning techniques. There is also the possibility of differences in calibration, as serial measurements rely on these factors remaining constant. These are usually overcome by quality control, and the use of standard phantoms. When BMD is measured for research purposes, the scanning conditions must remain constant wherever possible.

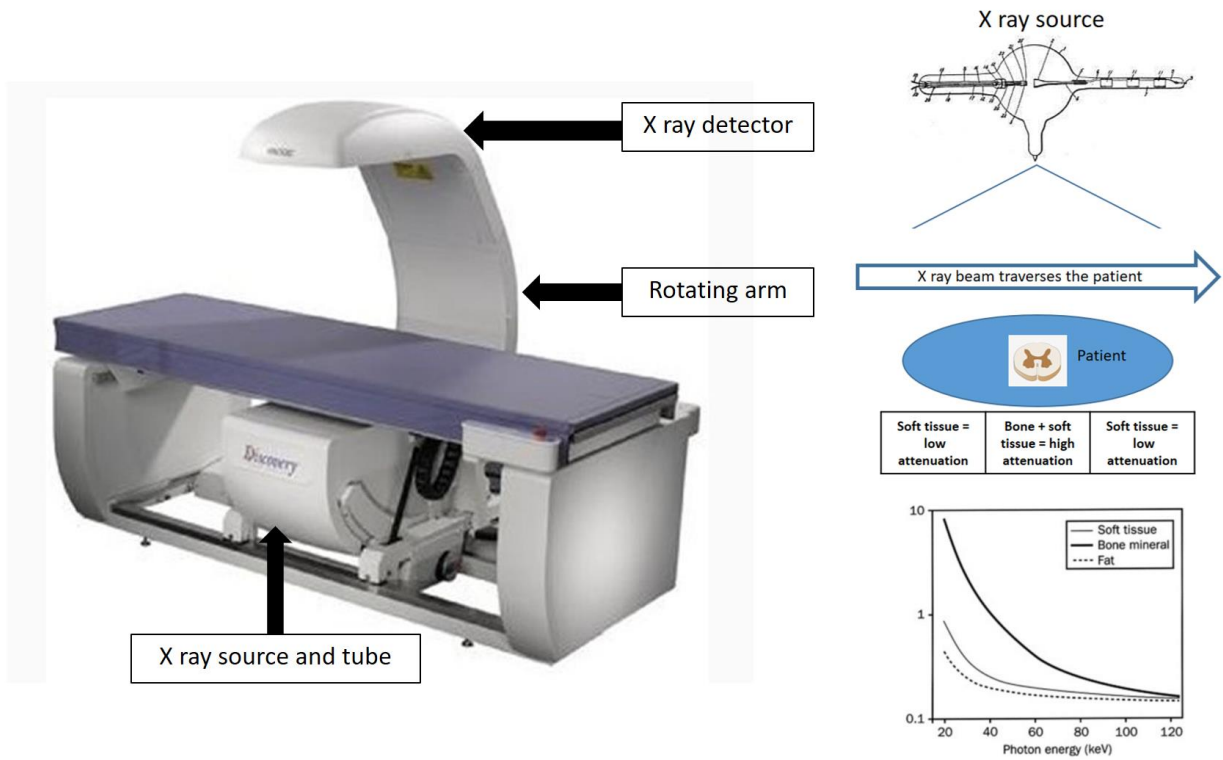


Figure 9: DXA scanner scintillation detector array system.

The components of a DXA scanner are shown above. As the x ray source moves over a patient, the x ray beam is attenuated by a greater or lesser degree, depending on the composition of the material it traverses. The attenuation of soft tissue (muscle, fat blood and skin) is similar, whereas bone mineral has a higher attenuation.

2.1.5 Computed tomography

Computed tomography (CT) is based upon the same principle as DXA, where calculation of tissue density is based upon the degree of attenuation of x ray beams. A standard CT scanner is used, and the X-ray beam is directed from the source through the body to a detector. The peak tube voltage (kilovolt peak, kVp) controls the beam quality, and is inversely proportional to the image quality. The tube current (milliamperes, mA, or microamperes, μ A) controls the number of photons and affects image density. Higher voltage and current improve the CT images but require a higher radiation dose to be delivered. Other key parameters are the scan integration time (ms, the exposure duration for each tomographic projection) and the slice thickness (mm or μ m, the smallest thickness of the two dimensional slices). Computer based algorithms such as the noise index are available to adjust images to an appropriate quality.

The attenuation profile is used to construct a three dimensional image on to a blank matrix ⁶¹¹. This achieves a true measurement of volumetric density, and also accounts for gradations of density within tissue. The degree of attenuation within each voxel is compared with the attenuation of water; the mean attenuation is then converted into Hounsfield units (HU; a scale that uses water as the reference value of zero). The tissue that gives rise to the most attenuation is bone. Each pixel is assigned a shade of grey based on the HU gradation.

Quantitative CT (QCT) is used to measure bone properties from CT images. Calibration phantoms containing rods of hydroxyapatite are imaged, and the mean attenuation for each compartment is calculated and used to convert the HU into BMD. Computer-based post imaging processing methods are used to calculate three dimensional vBMD and morphological parameters.

For the purposes of bone density assessment, CT has several advantages over DXA, most notably it produces a three dimensional volumetric measure of tissue density due to the detection of photons over multiple projections rather than a single projection. CT is also able to differentiate between cortical and trabecular bone compartments, is more accurate than DXA in assessing bone size and shape, and is able to distinguish between degenerative changes and extra-osseous calcification which may lead to inaccurate estimates using DXA. The principal disadvantages of CT compared with DXA are that a higher exposure to ionising radiation is required; relative expense; lower availability; and the inability to quantify bone material properties beyond mineral.

2.1.6 High resolution computed tomography

Advances in CT technology have led to the use of high resolution (HR) techniques with improved spatial resolution over a smaller field of view, improved signal to noise ratio and fast scan acquisition times ⁶¹². Studies that have used HR-CT have

significantly improved the understanding of changes in bone microstructure, stiffness and strength that occur in both health and disease.

High resolution peripheral quantitative computed tomography (HR-pQCT) measures bone size, geometry, density and microarchitecture at the tibia or radius, and is more sensitive than DXA in detecting osteoporosis^{613,614}. The only HR-pQCT machine currently able to measure human bone microarchitecture in vivo is the Xtreme CT (SANCO Medical AG, Brüttisellen, Switzerland). Analysis software is available to determine microarchitectural parameters, and finite element modelling (described later in this chapter) can be used to estimate bone stiffness and strength.

Most of the standard HR-pQCT measures are based upon those used in micro CT (μ CT) which is considered the gold standard⁶¹⁵. However, some measures are derived, as for example, the average voxel size of 80 microns is close to the average thickness of a human trabecula (therefore trabecular thickness cannot be directly measured)⁶¹⁶. There is good agreement between HR-pQCT and μ CT for the assessment of morphology⁶¹⁷, as well as cortical porosity and stiffness^{618,619,617}. The reproducibility of measures obtained by HR-pQCT is excellent and there is a low frequency of precision error (generally <1%)⁶²⁰.

The dose of radiation from a single HR-pQCT scan is $3\mu\text{sv}$ (equivalent to less than 1 day of average background radiation), and the scanning process usually takes 3 minutes⁶²⁰. Regular quality control (QC) identifies drift, scatter artefact and beam hardening that occurs as a result of decreased x-ray emission (decay)⁶²¹. An important limitation of HR-pQCT is motion artefact; even very small movements can significantly distort the images. Methods to grade and adjust for motion artefact have been developed, however in reality it is usually easier to repeat the scan where possible⁶²². The other main disadvantage of HR-pQCT is that it is limited to peripheral sites and unable to assess the spine, hip and proximal femur which are associated with a high frequency of fractures associated with metabolic bone disorders.

HR-CT at central sites is feasible; it has been used for assessment of human vertebrae microstructure, where it was found to provide additional information to DXA. The HR-CT vertebra protocol involves examinations at 120kV and 360mAs, and image reconstruction with a voxel size of $156\mu\text{m}$ and slice thickness of 300- $500\mu\text{m}$ ⁶²³. The major disadvantage is the high dose of radiation required (approximately 4.1mSv per scan, equivalent to 18 months of background radiation), which limits longitudinal assessment.

2.1.7 Finite element methods

Finite element (FE) analysis (FEA) involves a computer based simulation where mechanical loads are applied to a material to determine the stresses (internal force per unit area) and strains (deformations) inside a structure. The magnitude and

direction of these are affected by the load conditions, shape and internal architecture of the material, in addition to local material properties⁶²⁴. FE methods are widely used in engineering, to predict the conditions that would result in failure of a material. It is used when direct measurement is not possible, and was first applied to bone in the 1970s⁶²⁵.

The FE process is summarised in figure 10. The first stage involves a pre-processing step and generation of a computer aided design model. This defines the geometry and density of the material under investigation, and uses images generated by computed tomography. Once a model has been developed, a mesh is generated, which subdivides the structure into simple elements and connects it at key points. Other pre-processing steps include definition of the shape outline and application of boundary conditions (calculation of load applied and what subsequent constraints or reaction to the applied load occur)⁶²⁴. The material properties are assigned, based on either direct measurement or estimation based on a material's known properties⁶²⁶. Two important components of this are the Young's modulus (a measure of stiffness and resistance to elastic deformation under load which relates stress to the amount of strain) and the Poisson ratio; a ratio of lateral contraction to longitudinal extension of a material under longitudinal tensile stress⁶²⁷. Material properties are considered to be either linear or non-linear, and require different models. Using bone as an example material, the elastic modulus is typically well correlated with strength across a range of densities^{628,629}. However, estimates of yield stress (which can only be obtained from non-linear models) may improve predictions of strength as non-linear processes are involved in failure (fracture)^{629,630}. Once a CAD model is prepared, the next step involves computational processing, where the FE equations are assembled, followed by post-processing analysis, review and refinement.

Micro FE is a novel approach and allows calculation of the mechanical properties of bone as they relate to its microstructure⁶³¹. Cross sectional images from high resolution CT scans are stacked to create a three dimensional structure, which is combined with fully automated FE models⁶³². There are two main analysis techniques; each voxel in a reconstructed 3D image can be converted into equally shaped brick elements (voxel conversion method), and assigns them the elastic properties of bone tissue^{632,631}. The second method uses marching cubes, where voxels are subdivided into tetrahedron elements⁶³³. This creates a model with smooth trabecular surfaces, however adds complexity and may be less accurate than voxel conversion⁶³². Both methods produce extensive and complex models; for example, a single human vertebra may contain up to 60 million separate elements and the stress and strain can be determined at the level of an individual trabeculae. Special-purpose solvers have been developed to enable the automated solution of such large problems within a reasonable time frame. The main outcomes of micro FE analysis in bone are summarised in table 9.

Table 9: Micro FE analysis outcomes derived from HR-QCT

Outcome (abbreviation)	Units	Description
Stiffness	kN/mm	Resistance to deformation when applying a load; total reaction force divided by displacement
Estimated ultimate failure load (Est.Fail.Load)	kN	Maximum load the bone can bear before fracture
Mean trabecular Von Mises stress (Tb.VM)	MPa	Indicates whether combined stresses in the x, y and z directions in the trabeculae will cause failure
Mean cortical Von Mises stress (Ct.VM)	MPa	Indicates whether combined stresses in the x, y and z directions in the cortex will cause failure
Proximal trabecular/cortical load and distal trabecular/cortical load	All %	The distribution of the load between the cortical and trabecular compartments

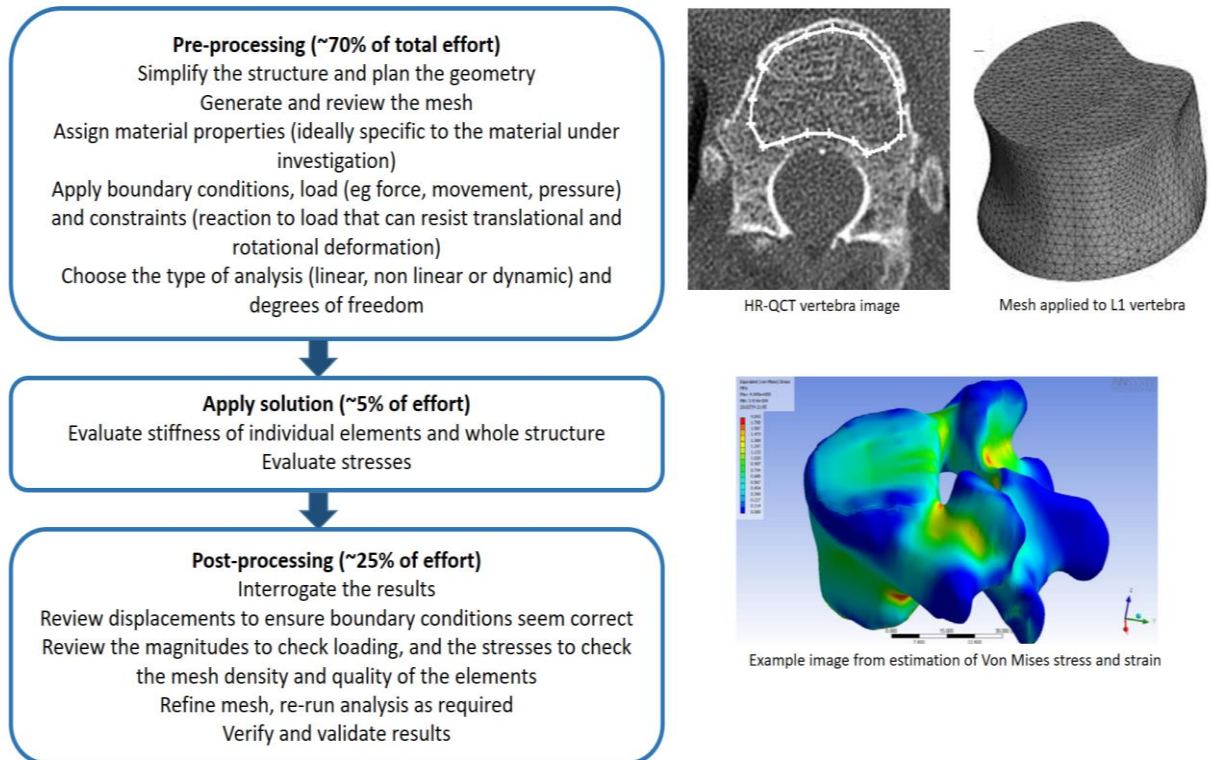


Figure 10: The finite element process

This is used for the estimation of material strength. The initial pre-processing step is the most time-consuming and requires consideration to be given to all of the conditions and properties, in order to generate an accurate model. The length of time taken to solve the problem is dependent upon the complexity of the model.

2.1.8 High resolution imaging techniques used in prostate cancer

Only a few studies have used HR techniques to investigate the effects of ADT on bone microarchitecture and strength. One study in men with PC initiating ADT measured the 12-month change at the radius and tibia using DXA and HR-pQCT²¹⁸. At baseline, 26 men with PC were compared to age matched healthy controls, and the only significant difference in density and microarchitecture was thinner trabeculae in men with PC ($p=0.007$). After 12 months, the ADT group had decreased total vBMD at the distal radius ($5.2\% \pm 5.4$, $p=0.001$), loss of cortical BMD ($11.3\% \pm 8.6\%$) and loss of trabecular density ($3.5\% \pm 6.0\%$). Both the cortical area ($-11.5\% \pm -8.8\%$) and the derived measure of cortical thickness decreased ($p=0.001$ for both) and cortical porosity was increased. Trabecular area increased ($1.7\% \pm 1.8\%$, $p=0.001$) and the trabecular number decreased, however there was no change in trabecular thickness. Similar findings were reported at the tibia, although the trabecular thickness increased at this site. Overall, there was a greater decline in volumetric BMD by HR-pQCT than areal BMD measured by DXA.

Another study investigated microarchitectural change over 2 years in 76 men with non-metastatic PC starting ADT randomised to bisphosphonate or placebo⁶³⁴. HR-pQCT at the distal radius demonstrated a decrease in total vBMD in both groups over 24 months, and that loss of cortical BMD exceeded loss of trabecular BMD. Trabecular number, thickness and separation remained fairly constant. When groups were compared, there was no significant difference at 12 or 24 months, suggesting that bisphosphonate treatment was not able to prevent deterioration in microstructure that is associated with ADT⁶³⁴.

A small cross sectional feasibility study of 22 men with PC used HR-pQCT and DXA within 6 months of ADT initiation⁶³⁵. Outcomes were correlated with duration of ADT and serum testosterone. Limited data suggest that trabecular vBMD and BV/TV may be negatively correlated with ADT duration, and positively correlate with serum testosterone levels.

A prospective cohort study has investigated the longitudinal change in bone microarchitecture and changes in sex steroids in 820 older men⁶³⁶. It included a small number of men with PC receiving ADT who underwent HR-pQCT at the tibia and radius at baseline, and after 4 and 8 years of follow-up. The ADT group were compared to the no ADT group; at both the radius and tibia ADT was associated with significant decreases in BMC, total vBMD, cortical vBMD, cortical thickness and area, whereas the trabecular area increased more rapidly with ADT.

High resolution micro MRI has also been used in men treated with ADT²¹⁷. Microarchitectural outcomes included the surface density, surface to curve ratio (the intactness of the trabecular network) an erosion index (the degree to which trabecular plates have deteriorated to become rods), and the bone to tissue volume ratio. More than a third of men had an undiagnosed vertebral fracture (VF),

the BV/TV and surface density were lower, and the erosion index was higher in men with moderate to severe VF. The addition of the MRI parameters to the DXA results improved the prediction of VF. The length of ADT was also associated with deterioration of microarchitectural parameters using micro MRI, but not with DXA.

In general, it seems that incorporation of HR techniques, and in particular the assessment of trabecular bone parameters provides useful information regarding bone strength and fracture risk in men receiving ADT. However, the numbers of men that have been included are small, access to scanners is limited, and prospective data are currently lacking.

2.2 ANTELOPE study methods

2.2.1 Overall aim and rationale for ANTELOPE

There is increasing awareness of the long term effects of cancer treatments, especially in PC where many men may live with their disease for a lengthy period of time. Recent publications and guidance are available, however routine assessment and consideration of bone health in men with PC is not incorporated into usual clinical practice. Published data to date has focussed on ADT and changes in aBMD, predominantly in those receiving bone targeted treatments. Only a few studies have applied HR imaging and FEA to investigate microarchitectural changes that are likely to be as important as aBMD in terms of bone strength. There is no published data on the change in bone parameters in men with hormone sensitive metastatic PC that are treated with ADT and docetaxel/prednisolone, which is currently offered to all newly diagnosed men who are fit for this treatment.

ANTELOPE (Assessment of bone LOSS in men receiving treatment for Prostate cancer) is designed to investigate the longitudinal change in bone density and microarchitecture in men with PC receiving continuous ADT, and included some men receiving chemotherapy in addition to ADT. Improved understanding of the effects of ADT on the properties of bone will help clinicians to better identify those at risk of fracture in whom bone-targeted therapies should be considered, and select the most appropriate therapy.

2.2.2 Study design

ANTELOPE is a prospective longitudinal case control study of changes in bone density, bone microarchitecture, body composition and muscle function and strength over 12 months in men with PC receiving ADT. Patient representatives had an important role in the study design process, and reviewed the study protocol, patient information sheet, bone questionnaire and advertising material.

ANTELOPE recruited three groups of men, and the study schedule is summarised in the trial schema (figure 11). Group A included those with localised or locally advanced PC due to commence (or had recently commenced) treatment with

continuous ADT. Men with recently diagnosed hormone sensitive metastatic PC were recruited to Group B; this group had recently started ADT and were due to start palliative chemotherapy with docetaxel and prednisolone. Group C were healthy men without PC and were matched by age and BMI to Group A.

A power calculation was based on the reported findings of a previous study that measured bone structural change in men with PC. With 90% power and 5% two-sided significance, 24 participants were required in each group to detect a standardised difference of 0.96 in change in volumetric BMD (primary outcome). To allow for a 10% drop out rate, and also in anticipation of the fact that some men in Group B (with more advanced disease) would have disease progression during the study period, ANTELOPE aimed to recruit 30 participants to each group. Any participant that was excluded at baseline or lost to follow-up was replaced by additional recruitment. ANTELOPE participants in Group B that developed progressive disease (and required change in treatment) during the study period had their second assessment brought forwards, provided that they had been on study for at least 6 months and wished to continue on study.

2.2.3 Study location, funding and approval

ANTELOPE was carried out within the University of Sheffield and Sheffield Teaching Hospitals NHS Foundation Trust and was funded by a grant from the Weston Park Hospital Cancer Charity. Participants visited the Clinical Research Facility at the Northern General Hospital (NGH) in Sheffield for study assessments. The departments of radiology and biochemistry at the NGH were used for CT scans and real time biochemistry. The end of study serum sample analysis was undertaken in the bone biochemistry laboratory in the University of Sheffield medical school and the biochemistry laboratory at the Royal Hallamshire Hospital in Sheffield.

ANTELOPE received approval from medical and clinical radiation experts, was approved by the South Yorkshire Research Ethics Committee in October 2016 and received HRA approval in November 2016. The study was sponsored by Sheffield Teaching Hospitals NHS Foundation Trust, with appropriate insurance and indemnity secured.

2.2.4 Recruitment and informed consent

Participants were recruited between January 2017 and November 2018. Group A were recruited from urology and clinical oncology outpatient clinics at the Royal Hallamshire and Weston Park Hospitals in Sheffield. Group B were recruited from medical oncology clinics at Weston Park Hospital. Group C were initially recruited from a database of healthy volunteers who had participated in previous studies at the academic unit of bone metabolism. Healthy controls were also recruited from those that responded to poster adverts displayed within the University of Sheffield, and email advertising via university distribution lists. All participants underwent assessment of bone and muscle function on two occasions, 12 months apart.

All potential participants received a patient information sheet prior to consent. All men provided written informed consent before any study procedure took place.

2.2.5 Inclusion and exclusion criteria

Key inclusion and exclusion criteria are listed in table 10, and sought to ensure that any differences in outcome were related to the differences in study groups. All participants were aged between 50 and 85 years at the time of first study visit, and had a WHO performance status of 0 (fully active and able to carry out all usual activities) or 1 (mildly symptomatic or slightly restricted in strenuous activity, able to undertake light housework). All were able to provide informed consent prior to any study procedures, and agreed to comply with the terms of the protocol. Participants were excluded if their body mass index (BMI) was less than 18.5 kg/m² or greater than 35.0 kg/m². All men had normal organ function on standard laboratory testing at baseline.

All participants in group A had histological confirmation of PC and had no evidence of metastatic disease. All group A participants were due to commence continuous ADT for a minimum of 12 months, and had the baseline study assessment within 4 weeks of ADT initiation. Although ADT has a rapid effect on bone turnover, this was a pragmatic choice and reflected the anticipated difficulty in recruiting this group and undertaking a separate assessment to their standard treatment in a different location. The majority of group A had received radiotherapy (to the prostate or pelvis) prior to study participation, or underwent radiotherapy during the study period.

Group B participants had newly diagnosed hormone sensitive PC, and had commenced ADT less than 3 months prior to study participation. The usual pathway for these patients (via urology clinics and urology multi-disciplinary team meetings) results in men attending oncology clinics some weeks after ADT initiation. Participants in this group had all started or were due to start disease-modifying chemotherapy with 6 cycles of docetaxel and prednisolone (10mg prednisolone daily and prophylactic dexamethasone prior to chemotherapy is the standard chemotherapy protocol). Those in group B included men with metastatic bone disease, however those with disease affecting the radius were excluded. In the event of an individual receiving palliative radiotherapy for bone pain, continued study participation was permitted, but it was recommended that future BMD assessment would avoid the treated site. Participants who developed bone pain during the study period could receive opiate based analgesia as required. Any participant that needed to start a bisphosphonate could have their follow-up assessment brought forwards if they had been on study for 6 months or more.

Group C participants were healthy men. Participants were matched by age (± 5 years), height (± 5 cm) and BMI (± 5 kg/m²) to Group A participants. This was done by hand using a matching table, and ensuring that towards the end of the study, we

recruited healthy control participants that were a good match for those recruited to Group A.

Exclusion criteria sought to ensure that none of the study participants had or experienced conditions that would affect bone metabolism. Individuals with known metabolic bone diseases or with conditions known to affect bone metabolism were excluded from participation (table 10). Those taking prescribed medications that affect bone health were also excluded, such as osteoporosis/ bone targeted therapies, radium-223, hormone treatments (other than ADT), oral corticosteroids (apart from chemotherapy-associated steroids for group B), and antiepileptic medications. Due to the effect on BTM, those who had experienced a fracture or undergone orthopaedic surgery within the past 12 months were unable to take part in ANTELOPE, in addition to those with arthritis, previous surgery to bone or skeletal abnormality that would prevent the acquisition of study measurements. ANTELOPE excluded individuals participating in any other clinical trial involving an investigational medicinal product and those with any concurrent or recent cancer (apart from PC in groups A and B) that could confuse study endpoints.

Anyone that was found to be at high risk of fracture based on the DXA results at their baseline visit was excluded from further participation, and referred to the Sheffield metabolic bone centre for ongoing management. GPs were also informed.

Table 10: Summary of study inclusion and exclusion criteria

Inclusion criteria
<p>All participants</p> <ul style="list-style-type: none"> • Male • Aged 50-85 years • WHO performance status 0-2 • Able and willing to comply with protocol terms and undertake trial assessments • BMI between 18.5 and 35kg/m² at baseline • Provide written informed consent prior to any trial-specific procedures • No evidence of significantly abnormal organ function on standard lab testing
<p>Group A only</p> <ul style="list-style-type: none"> • Histological confirmation of prostate cancer with no evidence of metastases • Has commenced ADT < 4 weeks before baseline visit (or due to commence) • No prior systemic therapy for prostate cancer
<p>Group B only</p> <ul style="list-style-type: none"> • Newly diagnosed hormone sensitive metastatic prostate cancer • Has been referred to oncologist for chemotherapy • Has commenced ADT <12 weeks before baseline visit (or due to commence)
Exclusion criteria
<p>All participants</p> <ul style="list-style-type: none"> • Known to have osteoporosis or other metabolic bone disease, or is receiving bone targeted therapy (such as bisphosphonate) • Has another systemic disease that affects bone metabolism including; hyperthyroidism, primary hyperparathyroidism, chronic liver disease, rheumatoid arthritis, inflammatory bowel disease or chronic malabsorption • Currently taking anti-epileptic medication • Has taken previous hormone treatment in past month (other than ADT) • Has had a fracture or orthopaedic surgery in the past 12 months • Arthritis, previous orthopaedic surgery or abnormality of radius, spine or hip • Any other cancer which could confuse the endpoints of the study • Current or recent (within 1 month) participation in another clinical trial involving a medicinal product (except STAMPEDE for Group B)
<p>Group A</p> <ul style="list-style-type: none"> • Takes oral systemic corticosteroids
<p>Group B</p> <ul style="list-style-type: none"> • Known to have bone metastases involving radius at baseline visit • Taking in excess of 2mg dexamethasone or 10mg prednisolone daily (this does not include steroids given alongside chemotherapy)
<p>Group C</p> <ul style="list-style-type: none"> • Takes oral systemic corticosteroids

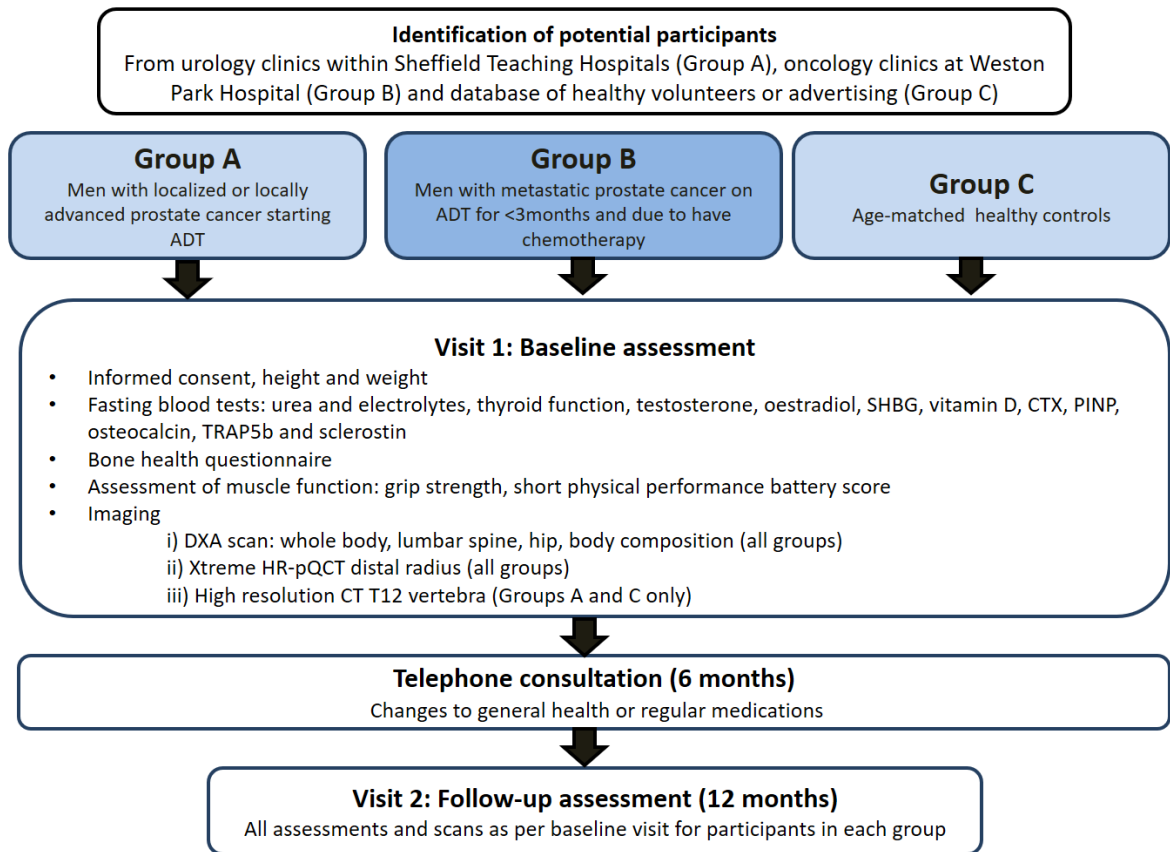


Figure 11: The ANTELOPE study assessment schedule.

An overview of the assessment process required for each participant. Two study visits were required, with a 6 month telephone call to ensure that the participant is eligible and willing to continue participation.

2.2.6 Study assessments and schedule

A summary of the study assessments is shown in figure 11. After an overnight fast, all study visits took place in the morning.

2.2.6.1 Anthropometric measurements

Anthropometric measurements were taken using a Harpenden stadiometer to measure height (to the nearest 0.1cm) and weight in kilograms (to the nearest 0.1kg), and body mass index (BMI) was calculated. Any participant found to have a BMI greater than 35kg/m² or less than 18.5kg/m² was excluded from further assessment and study participation.

2.2.6.2 Prostate cancer and treatment details

Details of PC diagnosis and staging for participants in groups A and B were obtained from electronic and paper clinical records by a study clinician, and also from the Sheffield Teaching Hospitals NHS Foundation Trust ICE laboratory reporting system. Information regarding prostate cancer treatment was obtained from electronic clinical records, from Aria radiotherapy software (group A) and from Chemocare prescriptions (group B).

2.2.6.3 Serum samples

A fasting 16ml blood sample was obtained. 5ml was collected in a SST tube and sent to the biochemistry laboratory within Sheffield Teaching Hospitals for real time measurement of serum urea and electrolytes and thyroid function. The remaining sample was left to clot for 30 minutes and centrifuged for 10 minutes at 3000 rpm at 4°C. Serum was divided into 0.25 ml aliquots and labelled with anonymised participant information. Samples were stored at -80°C at the NGH Clinical Research Facility, and were transferred in batches to the Sheffield Teaching Hospitals NHS Foundation Trust HTA licensed biorepository (license number 12182) at the Royal Hallamshire Hospital.

Batch analysis of serum samples from baseline and 12 months was undertaken at the end of the study. Testosterone, oestradiol and SHBG were measured using the Cobas e801 automated electrochemiluminescent immunoassay (ECLIA, Roche Diagnostics, Penzberg, Germany) in the biochemistry laboratory at the Royal Hallamshire Hospital.

The remaining serum tests were undertaken in the bone biochemistry laboratory within the Academic Unit of Bone Metabolism, University of Sheffield. The inter-assay coefficients of variation were <5% for all tests. The biomarkers of bone turnover (CTX and PINP), osteocalcin, and vitamin D were measured using the Cobas e411 automated ECLIA (Roche Diagnostics, Penzberg, Germany). Sclerostin was measured using an enzyme-linked immunosorbent assay (ELISA) (Cat no: BI-20492, Biomedica, Vienna, Austria), and TRAP5b was measured using the

BoneTRAP® ELISA (Cat no: SB-TR201A, Immunodiagnostic Systems Ltd, Boldon, United Kingdom).

2.2.6.4 Bone health questionnaire

Participants were asked to complete a bone health questionnaire. This included questions regarding fracture risk factors, medical history, drug history, calcium intake, family history of osteoporosis, and frailty screening questions.

2.2.6.5 Tests of muscle function

After a light meal, grip strength was measured using a digital hand dynamometer (Seahan Corp., Masan). Participants were seated, their forearm was held at 90 degrees to the upper body and their wrist not rotated when the measurement was taken. Each participant was asked to hold their maximum grip for 5 seconds, which was repeated three times for each hand with at least 30 seconds rest in between. The maximal grip strength from all six measurements was used for analysis.

Proximal muscle function was assessed using a chair stand test. Each participant sat on a chair with their feet on the floor, knees flexed and with their arms folded across their chest. They were asked to stand and sit five times without stopping, as quickly as possible and the time taken for the 5 stand and sit cycles was recorded to the nearest one hundredth of a second. If the participant was unable to complete 5 cycles, this was recorded along with the number of completed cycles.

The short physical performance battery (SPPB) score was calculated from a six metre walk, a narrow walk test and chair stand test. For the 6 metre walk, the participant was asked to walk along a six-metre long, marked course at their normal pace. The number of steps and time taken was recorded for two attempts, and the average time was recorded (to the nearest one hundredth of a second). The six metre course was subsequently narrowed to a width of 20cm, and each participant was asked to walk along and keep their feet within the marked lines. The narrow walk test was repeated three times, and the average time taken was recorded to the nearest one hundredth of a second. Deviations from the narrow path were documented.

The total SPPB score (potential range 0-12 points) was calculated once all participants had completed all study assessments and was based on three components. Quartiles of repeated chair stand times were determined, those in the best performing quartile were awarded 4 points, down to 1 point for those in the poorest performing quartile. Individuals that were unable to complete 5 cycles scored 0. Average gait speed results were also divided into quartiles, 4 points were awarded to the quartile with the fastest average time, down to 1 point for the quartile with the slowest gait speed. Participants unable to complete a 6m walk scored 0. Balance was assessed using a narrow walk test and an ordinal scale; those able to complete the test with three or fewer deviations scored 4 points, those

completing the walk but with more than 3 deviations scored 2 points, and those not able to complete the test scored 0 points.

2.2.6.6 Frailty assessment

Frailty was defined using criteria from the Fried phenotype model (table 11). The five elements of this are; slow gait speed, exhaustion, low physical activity, unintentional weight loss and poor grip strength. Frailty is associated with the presence of 3 or more of these, those with 1 or 2 elements present are considered pre-frail or vulnerable.

Table 11: Definition used for frailty

Frailty criteria	Definition used
Weight loss	Unintentional weight loss of >5% or >4.5kg in the past year
Handgrip strength	Adjusted by BMI in males BMI $\leq 24\text{kg/m}^2$: $\leq 29\text{kg}$ BMI $24\text{-}28\text{kg/m}^2$: $\leq 30\text{kg}$ BMI $>28\text{kg/m}^2$: $\leq 32\text{kg}$
Slowness	6m walk test, gait speed $<0.8\text{metres/second}$
Exhaustion	Self-reported using center for epidemiologic studies depression scale (CES-D)
Low physical activity	Self-reported, using SF-36 questions. Answers of 'limited a lot' considered as low activity.

2.2.7 ANTELOPE bone imaging procedure

2.2.7.1 DXA

Image acquisition and quality control

All study participants underwent DXA at the lumbar spine, total hip and whole body (using a postero-anterior projection) using the Hologic densitometer at the NGH Clinical Research Facility. This scanner uses a switched-pulse dual-energy (low 100kVp / high 140kVp) x-ray system with a maximum current of 10mA and has a multi-element detector array. The estimated dose of radiation associated with this procedure is 31uSv. The principles of DXA have been described previously. All scans were performed by two highly trained operators with standardised protocols for acquisition and analysis. The DXA scanner underwent daily quality using Hologic device-specific phantoms to ensure precision and stability. A weekly calibration scan of a step phantom (this contains 6 fields of acrylic and aluminium of different thicknesses and known absorptive properties) was undertaken to ensure accurate soft tissue assessment during the whole body DXA. A European spine phantom (QRM—quality assurance in radiology and medicine, Moehrendorf, Germany) was scanned weekly. The Hologic scanner automatically informs the operator if there are abnormalities related to quality control.

Study procedure

Representative images are shown in figure 12. The whole body DXA scan was undertaken with the participant in a supine position, with their head at the top of the table, their arms by their sides and their legs slightly separated. The scan operator ensured that the anterior superior iliac spines were equidistant from the table top to avoid rotation at the pelvis and feet. The operator also ensured that the participant was positioned within the scan line limits, and the sub-region defining lines were positioned in accordance with HologicQDR User Guide instructions.

The DXA procedure for the hip scan required each participant to lie in a central and supine position with their head in the head positioner and feet either side of the hip positioner. Both arms were folded across the chest away from the scan field. The scan operator ensured that the proximal femur was within the scan line limits, the hip was internally rotated by approximately 25 degrees and the leg abducted. An express scan ensured that positioning and the scan field were correct, and that the femoral shaft was straight. The array mode was used for the definitive scan which extended for at least 3cm below the greater trochanter up to the pelvis above the femoral head. The image was analysed, the global region of interest was positioned manually and the bone map was identified. The midline was placed on the central axis of the hip, the neck box close to the greater trochanter and the trochanteric line below the curve of the greater trochanter, with equal amounts of

soft tissue included on either side of the femoral neck. The Ward's triangle box was positioned automatically by the scan software.

Lumbar spine DXA was undertaken with the participant in a supine, straight and central position and their legs elevated over the spine positioning block (to reduce lumbar lordosis). The operator ensured that the lumbar spine was within the scan line limits on the table and that there was no rotation. An express scan confirmed correct positioning. The array mode was used to scan from the L5 vertebra down to mid-T12 level to ensure that the complete L1-L4 region was included. The image was analysed; the global region of interest was positioned with the top and bottom borders at the T12-L1 and L4-L5 intervertebral spaces respectively, and angled to accommodate the shape of the vertebrae. The lateral borders were not altered. The bone map was identified, and vertebral lines were placed within the lumbar intervertebral spaces. The decision to exclude vertebrae from the region of interest for BMD analysis was done in accordance with recommendations from the Royal Osteoporosis Society⁶³⁷. Vertebra with obvious abnormalities such as fracture or bone metastasis were excluded. A T-score difference of more than 1 standard deviation between adjacent vertebrae was also indicative that the BMD was likely to be inaccurate. A minimum of two evaluable vertebrae were required for analysis. One participant in group B had extensive lumbar vertebral metastases at baseline, and was excluded from further participation. The compare facility was used for follow-up scans, to identify comparable regions of interest.

Image analysis

The bone area (cm²), BMC (g) and mean areal BMD (g/cm²) were determined for the lumbar spine, whole body and total hip, and whole body and regional fat and lean mass were derived using Hologic Apex software (version 3.4.2). The T scores were calculated in accordance with recommendations by the International Committee for Standards in Bone Measurement⁶³⁸. DXA images and T score results were reviewed before the end of each baseline visit; participants found to have abnormal results were to the metabolic bone unit for further assessment and excluded from further participation.

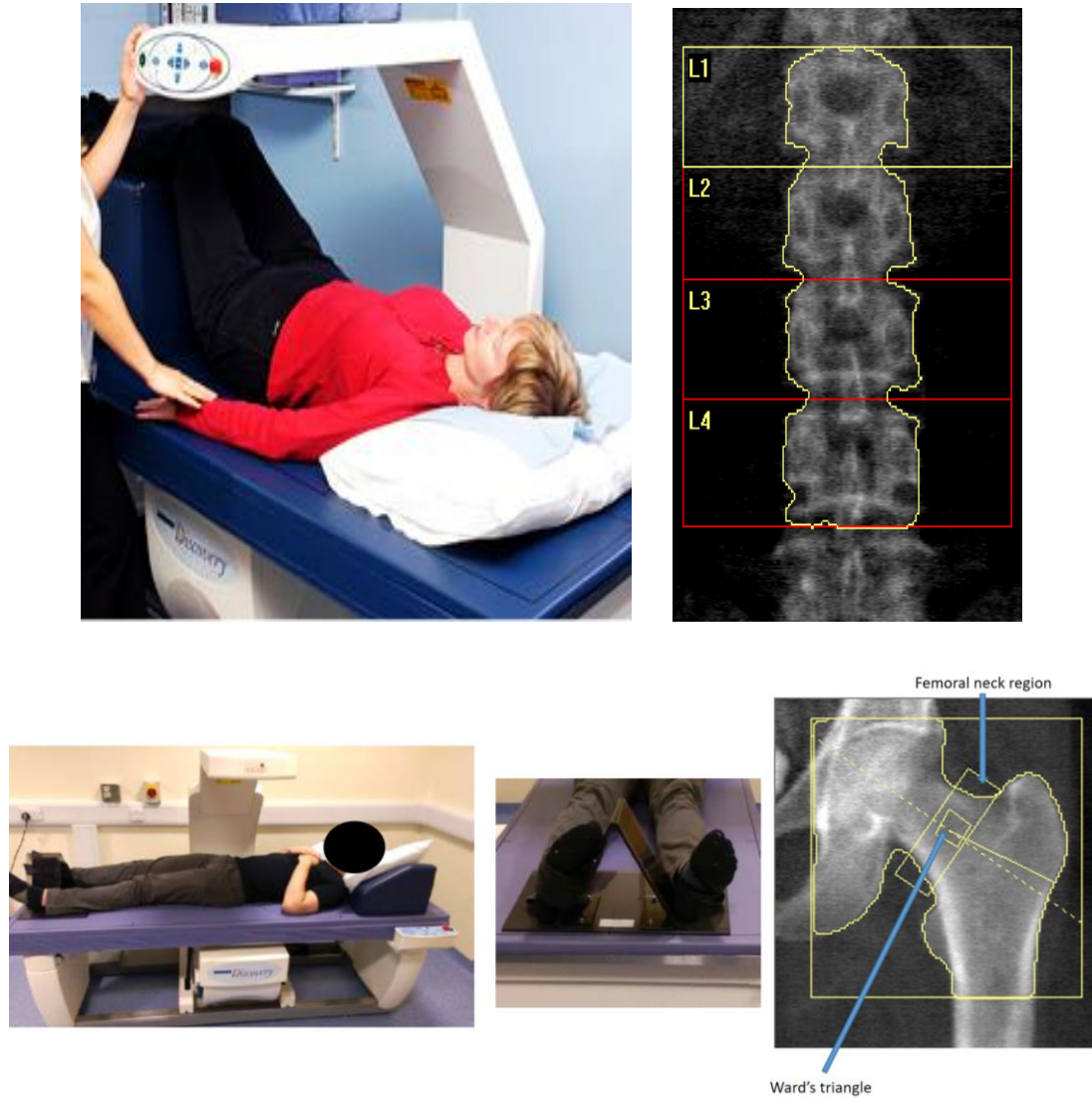


Figure 12: Patient positioning for DXA and example images.

Lumbar spine (top row images) and hip/ neck of femur (second row images). For the lumbar spine, participants were scanned in a supine position, with legs elevated over the spine positioning block, with an upper leg/table angle of approximately 45 degrees. An example of the region of interest is shown in the top right hand side image; including the L1-L4 vertebrae. Positioning for the femur/hip scan involves internal rotation of the proximal femur by 25 degrees with the leg abducted (lower left image). Application of the bone map/ global region of interest to a hip/femur DXA image is shown in the lower right image, with Ward's triangle and the femoral neck region shown by the blue arrows.

2.2.7.2 High resolution peripheral quantitative computed tomography

Image acquisition and quality control

Bone density and microstructure were assessed at the distal non-dominant radius in all participants at baseline. A high resolution peripheral quantitative computed tomography (HR-pQCT) scan was undertaken, using the Xtreme CT scanner (Scanco Medical AG, Bassersdorf, Switzerland) at the NGH Clinical Research Facility. This scanner has a 2-dimensional detector array and a 0.08mm point-focus x-ray tube. The standard operational settings were used; an x-ray tube potential of 60 kVp, an x-ray tube current of 95 mA, and an integration time of 100 ms, with an average scan duration of 2.8 minutes. A stack of parallel CT slices (110 slices) are acquired over a 150mm scan length and diameter, which produces 3-dimensional high resolution images with a voxel size of 82 μ m.

Quality control (QC) of the HR-pQCT measurements was ensured by daily calibration using the manufacturer device-specific phantom (Scanco Medical AG, Zurich, Switzerland). This has a soft tissue density (0mg/HAc³) and hydroxyapatite rods at 100, 200, 400 and 800 mg 0mg/HAc³ embedded in resin. In comparison to the standard QC procedure which recommends that the error for the highest density rod error is within 1%, the error for the highest HA density rod was towards the lower limit for the duration of the study period. All scans were performed by two highly trained operators who followed standard operating procedures.

Study procedure

For each scan, participants were seated, and the operator placed their hand and lower forearm into a carbon cast which was secured with straps and an arm pad provided stability (figure 13). The operator ensured that the arm was in line with the opening of the scanner gantry. Participants were asked to remain as still as possible during the scan to minimise motion artefact. A scout view scan prior to the main scan identified anatomical landmarks and determined the region of interest. A reference line was placed on the endplate of the distal radius to indicate the position of the first measurement slice (9.5mm from the reference line, shown in figure 13).

Upon completion of the scan, the carbon cast was removed and the scan quality was evaluated by the operator. Image slices were visually inspected and graded; grade 1 (no movement, clear image), grade 2 (slight movement, small streaking), grade 3 (moderate movement, large streaking particularly near the cortex) or grade 4 (significant movement, unacceptable image with discontinuity at the cortex) ⁶³⁹. Examples of grade 1-4 movement are shown in figure 14. One repeat scan was permitted if the grade was 2-4 and movement artefact affected the quality of the first scan. Any participant who had unacceptable movement artefact (grade 4

images after 2 scan attempts) had their scan excluded from analysis, and did not have a scan at the follow-up study visit.

Image reconstruction and analysis

Images were reconstructed using the standard protocol provided by the manufacturer. This includes a beam hardening correction to mitigate artefacts caused by preferential attenuation of low energy beams, which is commonly associated with polychromatic x ray sources. The corrected reconstructed attenuations were mapped onto a blank matrix to yield an isotropic voxel size of 82µm.

Images were analysed with the manufacturer's standard software for bone microarchitecture (Scanco Medical AG, version 6.0), and the extended analyses for cortical porosity and FE estimation of bone strength (summarised in table 12). Images were segmented by a skilled operator, who drew a contour around the periosteal boundary on the first image. The automated contouring detection algorithm was run through the slice stack, and was stopped and checked at 10-20 slice intervals to check the quality of the edge detection. Where this was not satisfactory, the boundary was manually adjusted, and slices were reconstructed into a three-dimensional image. A validated auto-segmentation method was used to separate cortical from trabecular bone, and images were then analysed using the 'Evaluation 3D' option to produce estimates of vBMD as well as trabecular and cortical parameters. Measurements of trabecular bone microstructure are computed, rather than measured directly, due to the closeness of the physical dimensions of individual trabeculae (approximately 200µm) to the spatial resolution (120-150µm).

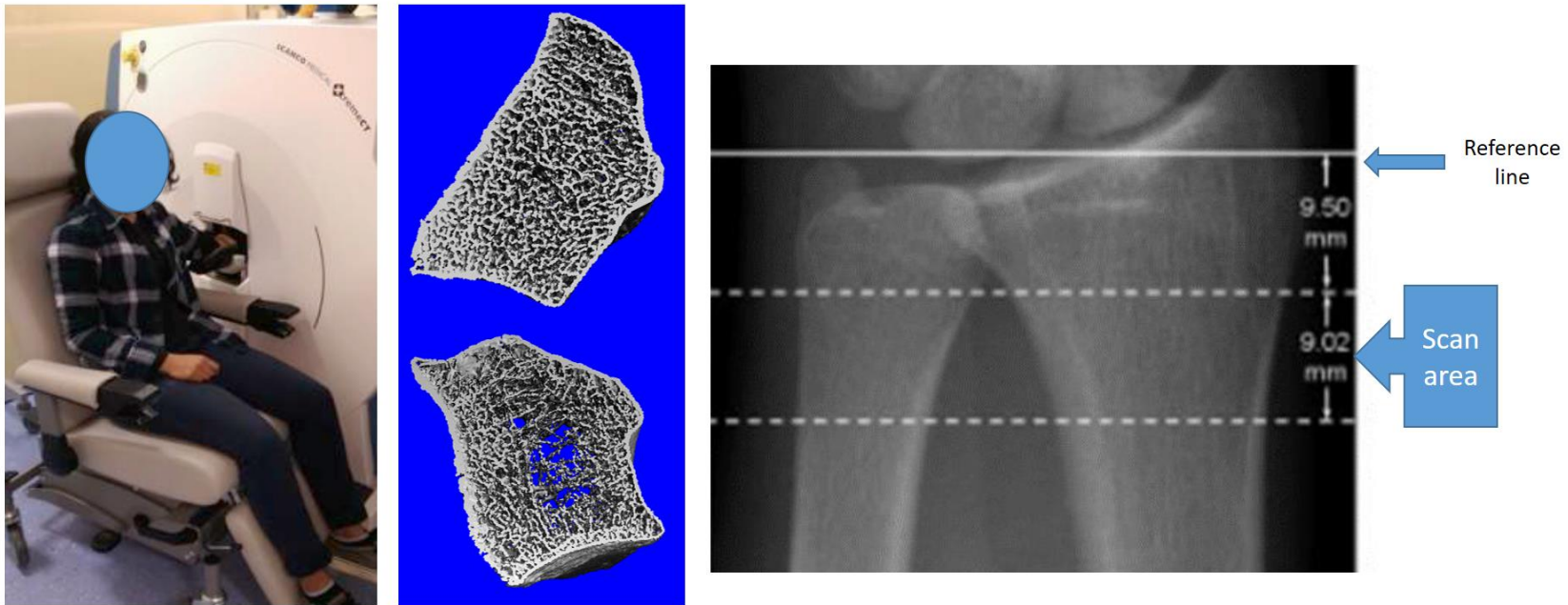
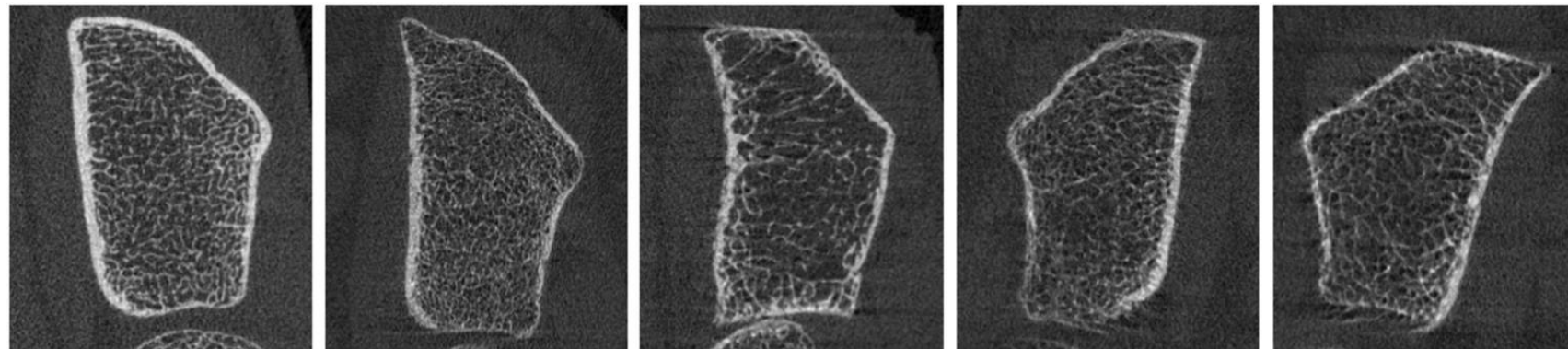


Figure 13: Patient positioning for DXA and example images.

HR-pQCT participant positioning with left radius in Xtreme CT scanner gantry (left), example three dimensional re-constructed radius images (centre) and scan region of interest (right).



1

No visible motion artifacts.

2

Very slight artifacts. Horizontal streaks at the upper and lower ends are visible.

3

Some artifacts. Horizontal streaks are visible, but cortex is intact.

4

Large horizontal streaks are visible. Cortex continuity is moderately disrupted at places and trabeculae are smeared.

5

Major horizontal streaks are visible. Complete disruption of continuity of the cortex and trabecular structure.

Figure 14: Motion artefact grading used for HR-pQCT scan analysis.

Grading system for HR-pQCT image quality and motion artefact⁶⁴⁰. Where possible, images are required to be grade 1 for analysis. Image taken from Whittier et al⁶⁴⁰ with permission from publisher.

Table 12: ANTELOPE outcomes of interest from HR-pQCT

Outcome (units of measurement)	Abbreviation	Description
Bone area		
Total bone area (mm ²)	Tot.Ar	Mean surface area of the cortical and trabecular compartments
Cortical area (mm ²)	Ct.Ar	Mean surface area of the cortical compartment
Trabecular area (mm ²)	Tb.Ar	Mean surface area of the trabecular compartment
Bone density		
Total volumetric bone mineral density (mgHA/cm ³)	Tot.vBMD	Total mineral mass divided by the total bone volume
Cortical volumetric bone mineral density (mgHA/cm ³)	Ct.vBMD	Cortical mineral mass divided by the cortical volume
Trabecular volumetric bone mineral density (mgHA/cm ³)	Tb.vBMD	Trabecular mineral mass divided by the volume inside the cortical bone
Cortical parameters		
Cortical thickness (mm)	Ct.Th	Mean thickness between the periosteal and endosteal surfaces
Cortical porosity (%)	Ct.Po	Percentage of cortical area occupied by pores
Cortical perimeter (mm)	Ct.Pm	Distance covered by the perimeter of the periosteal surface
Trabecular parameters		
Trabecular number (mm ⁻¹)	Tb.N	Mean number of trabeculae per mm within the trabecular compartment
Trabecular thickness (mm)	Tb.Th	Mean thickness of trabeculae within the trabecular compartment
Trabecular spacing/separation (mm)	Tb.Sp	Mean distance between trabeculae within the trabecular compartment

Trabecular bone volume fraction (%)	App.BV/TV	Division of Tb. vBMD by an assumed 100% mineralisation of 1200mg/HA/cm
Finite element analysis		
Bone stiffness (kN/mm)	-	Resistance to deformation when applying a load; total reaction force divided by displacement
Estimated ultimate failure load (kN)	Est.Fail.Load	The maximal load that a bone can bear before fracture.
Mean trabecular von Mises stress (MPa)	Tb.VM	Indicates whether combined stresses in the x, y and z directions in the trabeculae will cause failure
Mean cortical von Mises stress (MPa)	Ct.VM	Indicates whether combined stresses in the x, y and z directions in the cortex will cause failure
Proximal trabecular/ cortical load (%)	-	The distribution of the load between the proximal cortical and trabecular compartments
Distal trabecular/ cortical load (%)	-	The distribution of the load between the distal cortical and trabecular compartments

2.2.7.3 HR-CT T12 vertebra

Participants in Groups A and C underwent HR-CT of the T12 vertebra. Those in group B were expected to have a high frequency of spinal bone metastases (which would preclude analysis) and did not undergo this assessment. Images were obtained using the GE Healthcare LightSpeed 64VC CT scanner (General Electric Healthcare, Buckinghamshire, UK) in the medical imaging department at the Northern General Hospital, Sheffield. With 64 detector elements and a scintillation detector array system, this scanner converts the incident x ray beams into light energies that are detected by a photo diode and used to generate an image. Quality assurance was performed once per month using a Mindways phantom (Mindways Software, Inc., Austin, TX, USA). All scans were performed in the anteroposterior position, using the same noise index. The HR-CT protocol included a single scan from the superior edge of the T12 vertebra to the T12/L1 margin. The tube voltage was 120kV and the mean tube current was set at 360mAs to produce reconstructed images with a voxel size of 187 μ m and slice thickness of 300-500 μ m. Three dimensional reconstruction of the HR-CT scans was performed using the Mindways QCT Pro™ software version 5.0.3 (Mindways Software, Inc., Austin, TX, USA).

2.2.8 Study data management

All ANTELOPE data were secured in accordance with the 1998 Data Protection Act. Anonymised study data were entered into a study database held on a secure server at the Cancer Clinical Trials Centre (CCTC) at Weston Park Hospital. Paper case report forms were stored securely in locked offices, initially at the NGH Clinical Research Facility during the study and have been subsequently transferred to and stored at the CCTC at Weston Park Hospital.

2.2.9 Outcomes of interest

The primary and secondary outcomes of ANTELOPE are summarised in figure 15. The overall aim of the study was to characterise the 12 month change in bone density and structure in men receiving ADT (groups A and B) compared with healthy controls (group C). The primary outcome was the 12 month change in volumetric bone mineral density (vBMD) measured using HR-pQCT at the distal radius. Secondary aims were to determine the 12 month change in bone microstructural parameters, bone stiffness and bone strength at the radius, the change in areal BMD (by DXA) at the lumbar spine, total hip, neck of femur and whole body, and the change in vBMD at the T12 vertebra (by HR-CT). Additional measurements included the 12 month change in serum BTM and sex hormones, changes in body composition (DXA), grip strength and changes in physical and muscle function (SPPB score) over 12 months. The baseline ANTELOPE visit was also used to identify men that would meet criteria for frailty, and also determine their 10 year risk of fracture using FRAX.

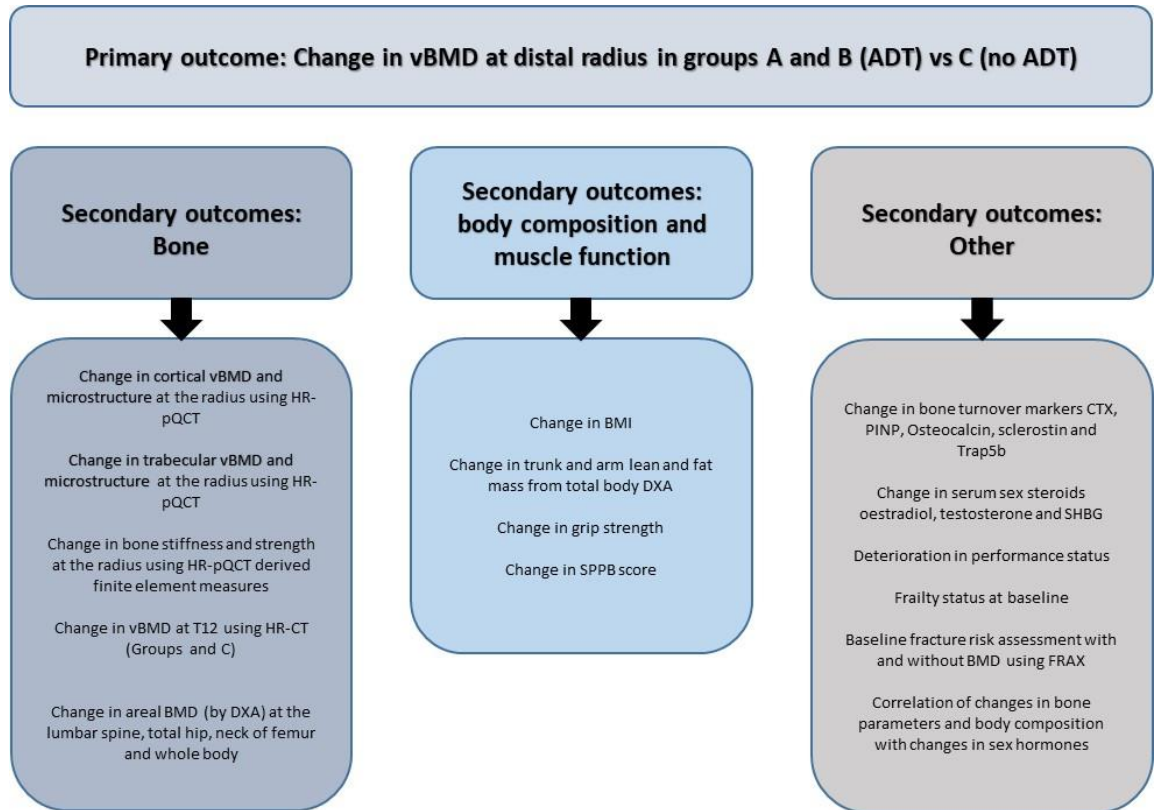


Figure 15: ANTELOPE primary and secondary outcomes.

The primary outcome was the 12 month change in vBMD at the distal radius in group A compared to group C. Secondary outcomes related to bone endpoints, changes in body composition and muscle function, strength, frailty and changes in sex hormones and biomarkers of bone turnover.

2.2.10 ANTELOPE statistical analysis

Statistical analysis was carried out using SPSS. Summary statistics (mean, standard deviation, median, interquartile range, and range) were calculated for all measurement both overall and within groups. Independent sample t tests were used to compare fracture risk between groups. BMD, microarchitecture, FEA and body composition measurements were then compared between the ADT and control groups using independent samples t-tests. The serum biomarker and hormone measurements were skewed, so comparisons were made using Mann-Whitney U tests.

There were two approaches to the analysis. The first investigated the change from baseline. For the bone density, microstructure and body composition measurements, the changes from baseline were approximately normally distributed, and the mean change and 95% confidence interval were calculated within each group. Changes in measurements were then compared between the ADT and control groups using repeated measures ANOVA. The interaction between group and time were tested to see if the change from baseline differed between groups. Serum biomarker and hormone data changes from baseline were more skewed, and the Hodges-Lehmann median difference and 95% confidence interval were calculated.

The second approach to analysis used analysis of covariance (ANCOVA) to compare measurements between the ADT and control groups. Each model included the 12-month measurement as the dependent variable, a fixed factor for group, and the baseline measurement as a covariate. An additional model was also tested, adjusting for age and BMI. For the bone density, microstructure and body composition measurements, the assumptions of the model were met and the difference in means was presented along with a 95% confidence interval. For the serum biomarker and hormone data the residuals from the ANCOVA models were skewed and there was some evidence of hetroskedasticity so the measurements were log transformed. The difference between groups was then presented as the ratio of geometric means along with a 95% confidence interval.

Chapter 3: ANTELOPE results (I) the effect of androgen deprivation on mobility, muscle mass and function and bone biomarkers

This chapter will present the ANTELOPE study results from the screening and recruitment process. It will also describe participant demographic details and PC details for the ADT groups. Data regarding bone health risk factors and fracture risk, frailty, changes in physical function and body composition will be presented, along with results of hormone measurements and biomarkers of bone turnover. Data regarding the effect of ADT on bone density, microarchitecture and finite element estimation of bone strength will be presented in chapter four.

3.1 Screening and recruitment

A total of 151 potentially eligible participants were screened between December 2016 and November 2018. Fifty two men (34.4%) did not subsequently participate in the study (figure 16). A total of 99 potentially eligible participants underwent a baseline study assessment.

A summary of study recruitment and screening for all participants is shown in figure 16 (all participants) and table 13 (by group). Thirty eight men with newly diagnosed localised or locally advanced PC were recruited to group A (ADT group) from urological oncology clinics at the Royal Hallamshire Hospital. These men all consented to study participation and attended the clinical research facility for their first study visit. The baseline assessment excluded seven individuals in this group from further participation. Three men were found to have a BMI greater than $35\text{kg}/\text{m}^2$. Based on DXA images, four men were found to have an undiagnosed metabolic bone disorder and these individuals were referred to the metabolic bone unit for further assessment. Of the 31 participants in group A that remained on study, two individuals chose not to attend their 12- month follow-up visit, therefore 29 group A participants completed all study assessments.

Thirty potentially eligible participants with newly diagnosed hormone sensitive metastatic PC were recruited to group B (chemotherapy with docetaxel/ prednisolone and ADT) from medical oncology outpatient clinics at Weston Park Hospital. Five of these were excluded at the baseline visit; of these one individual had a BMI greater than $35\text{kg}/\text{m}^2$; and two were found to have osteoporosis and were referred appropriately. One participant became unwell during the baseline visit due to an acute coronary syndrome, and required emergency medical treatment. One participant had extensive metastatic bone involvement of the spine that precluded accurate estimation of bone density and microstructural parameters, and was excluded. Of the 25 men on study after the baseline visit, seven were lost to follow-up; five died, one was too unwell due to spinal cord compression, and one chose not to attend for the second visit. One participant had

his second study visit brought forwards (as per protocol) due to progressive disease and the need to start bone targeted treatment. A total of 18 men in group B completed all study assessments.

A total of 31 healthy participants were recruited to Group C. These included men that responded to advertisements as well as volunteers from an existing database. Group C participants were matched to group A by age (± 5 years), height (± 5 cm) and BMI (± 5 kg/m²), this was achieved for 26 of the 29 men in group A. One participant had a BMD diagnostic of osteoporosis and was excluded from further participation and referred to the metabolic bone unit. Of the 30 participants on study after baseline assessment, two were lost to follow-up and 28 group C participants completed all study assessments.

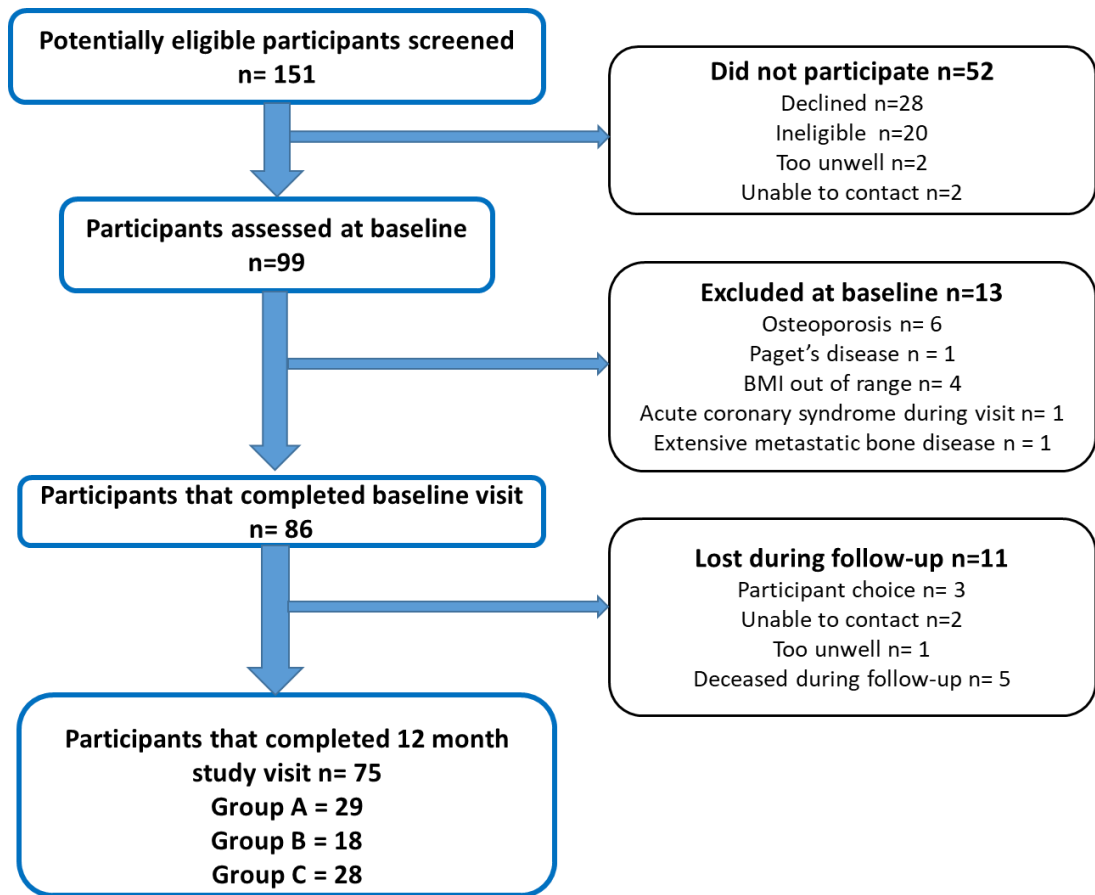


Figure 16: Summary of ANTELOPE screening, recruitment and retention

The total number of participants screened, assessed and completing the study assessments are shown on the left side, with the reasons for exclusion or losses to follow-up on the right side. A summary by group is shown in table 13.

Table 13: Summary of screening and recruitment by study group

Group	Number assessed at baseline	Exclusion at baseline		Lost to follow-up	Total completed
		Number	Reasons		
A (ADT)	38	7	High BMI (3) Paget's (1) Osteoporosis (3)	Participant choice (2)	29
B (ADT/chemo/ glucocorticoids)	30	5	High BMI (1) Osteoporosis (2) Spinal bone metastases (1) Unwell at study visit (1)	Died (5) Participant choice (1) Too unwell (1)	18
C (controls)	31	1	Osteoporosis (1)	Unable to contact (2)	28
Total number	99	13		11	75

3.1.1 Baseline assessment

3.1.1.1 Participant demographics

At baseline, the average age of participants in all study groups was 72 years and the majority (97%) were white British (table 14). Average height, weight and BMI were similar between study groups. The majority of participants (92%) had a WHO performance status of 0 and 20% of group B had a performance status of 1.

Polypharmacy (5 or more prescribed medications) was present in one third of all participants, and was more common in group A and B than in group C. For all study participants, the mean number of prescribed medications was 4.26 (SD 2.55).

3.1.1.2 Bone health and fracture risk

Risk factors for fracture were determined from the bone health questionnaire and anthropometric measurements (table 15). The majority of participants (95%) were non-smokers at the time of the baseline assessment. The average number of units of alcohol consumed per week was 9.4 (SD 11.10). Total alcohol consumption was greatest in group B (mean 12.46 units per week), but this was not significantly more than groups A and C. There were no significant differences between groups with regards to dietary calcium intake and sunlight exposure. Only 5 and 14 (5% and 16%) of all study participants reported taking vitamin D and calcium supplements, respectively.

FRAX was used to estimate the 10-year risk of hip fracture and major osteoporotic fracture (MOF) in all participants at baseline. The risk was calculated both with, and without BMD data (table 14), and did not include ADT as a risk factor for secondary osteoporosis.

There was no difference in the risk of hip fracture between study groups. In group A, the risk was 1.62% with BMD and was 2.74% without, compared to a risk in the control group of 1.61% with BMD ($p=0.98$) and 2.47% without BMD ($p=0.06$). The hip fracture risk in group B was 2.17% with, and 2.61% without BMD (p values of 0.41 and 0.79 respectively compared to the control group).

The 10-year risk of MOF was 5.22% in group A, which increased to 6.60% without BMD, and there was no difference in MOF risk between groups A and C ($p=0.06$ with BMD and 0.39 without). In group B, the risk of MOF was similar to group C without BMD ($p=0.99$) but when BMD was included there was a significantly increased risk of MOF in group B compared to group C ($p=0.004$).

We used UK National Osteoporosis Guideline intervention thresholds, which are age-dependent and based on the fracture risk in a woman with a previous fracture, in whom BMD is not known⁴⁴⁷. In our study population, more than three quarters

of all study participants were classified as above the intervention threshold for bone targeted treatment. The proportion of participants that required intervention was not higher in the ADT groups compared with the control group.

3.1.1.3 Prostate cancer details

Details of PC diagnosis and staging were obtained from clinical records for participants in groups A and B and are summarised in table 16. Those in group A had a median PSA of 27.4ng/ml at diagnosis, two thirds had a Gleason score of 8 or 9, and the majority had T3 disease. Four participants in this group had loco-regional lymph node involvement (N1). A total of twenty seven participants in group A received radical radiotherapy to prostate or prostate and pelvis during the study period.

Group B participants had a median PSA of 98.6ng/ml at diagnosis, all had metastatic disease and 21 participants had bone involvement. Of those who had a biopsy, 90% had a Gleason score of 9 or more. All participants received chemotherapy as planned, although 3 participants received fewer than 5 cycles due to disease progression or unacceptable toxicity. The median dose of prednisolone (or equivalent glucocorticoid) that was given to participants during the period of chemotherapy treatment was 2460mg (range 820mg-2460mg).

3.1.1.4 ADT administration and timing

All group A participants had started continuous ADT with an expected duration of at least 3 years, and the median duration of ADT before the baseline visit was 20 days (range 2-32 days). The majority of participants were treated with a LHRH agonist and initial anti-androgen. Group B participants were mostly treated with degarelix, and had initiated this a median of 57 days (range 0-82 days) prior to the baseline study visit.

Table 14: Participant demographics at baseline

	Group A n=31	Group B n=25	Group C n=30	Difference between groups (ANOVA)
Median age (range)	73 (64-82)	71 (56-78)	73 (53-82)	p=0.8
Height in cm (median, range)	173.9 (160.7-191.1)	172.1 (163.1-190.4)	175.1 (159.8-192.3)	p=0.69
Weight in kg (median, range)	81 (60.3-119)	81.3 (56.7-103)	81 (58-116.2)	p=0.73
BMI (kg/m ²) (median, range)	26.9 (21.9-34.4)	26.8 (19.8-32.5)	26.3 (20.4- 34.9)	p=0.59
Prescribed medications (mean, SD)	5 (3.2)	4.2 (1.9)	3.5 (2.1)	p=0.078
Polypharmacy	15 (48.4%)	11 (44%)	9 (30%)	p=0.03
Performance status				
0	29	20	30	
1	2	5	0	

Table 15: Baseline risk factors for fracture, and risk calculation

Fracture risk factor	All (n=86)	Group A (n=31)	Group B (n=25)	Group C (n=30)
History of major fracture	9	0	3	6
Parental history of hip fracture	16	5	6	5
Smoking status				
Current	6	2	2	2
Ex-smoker <5 years	4	0	2	2
Ex- smoker >5 years	43	15	10	10
Never	36	14	11	11
Alcohol consumption				
Mean number of units per week	9.42	8.06	12.46	8.40
More than 21 units per week (%)	12 (14)	3 (10)	5 (20)	4 (13)
FRAX 10-year risk *				
MOF risk without BMD	7.02 (3.06)	6.60 (2.62)	7.24 (3.43)	7.25 (3.22)
MOF risk with BMD	5.99 (3.12)	5.22 (2.5)	6.69 (3.92) [#]	3.92 (2.89) [#]
Hip fracture risk without BMD	2.60 (2.20)	2.74 (2.64)	2.61 (2.48)	2.47 (1.34)
Hip fracture risk with BMD	1.78 (2.36)	1.62 (2.13)	2.17 (3.42)	1.61 (1.33)
NOGG intervention thresholds				
Number (%) with risk above intervention threshold	67 (78)	20 (64.5)	21 (84)	26 (86.7)
Risk profile without BMD				
Number with 10 year risk of MOF ≥20%	1	0	0	1
Number with 10 year risk of MOF 10-20%	12	5	4	3
Number with 10 year hip fracture risk ≥5%	9	4	3	2

*Results are mean values and standard deviation, unless otherwise specified

[#] p<0.05 between the two values, from independent sample t test

Table 16: Prostate cancer staging and treatment in group A and B participants

		Group A	Group B
PSA at diagnosis	Median (range)	27.4 (2.3-222.3)	98.6 (4.0-2547)
Cancer stage at diagnosis	T2N0M0	3	-
	T3N0M0	24	-
	T3N1M0	4	-
	T3N0M1	-	4
	T3N1M1	-	12
	T4N0M1	-	2
	T4N1M1	-	5
	T4N2M1	-	1
Gleason score at diagnosis	Score available	29 (94%)	20 (80%)
	Total score 10	-	1
	Total score 9	17	17
	Total score 8	4	1
	Total score ≤7	8	1
Sites of metastatic disease	Bone		21
	Distant lymph nodes		5
Type of ADT	LHRH antagonist	1	17
	LHRH + antiandrogen	30	8
Duration of ADT at baseline	Median (range, days)	20 (2-32)	57 (0-82)
Radiotherapy	None	4	25
	Prostate	2	-
	Prostate and pelvis	25	-
Chemotherapy	None	31	0
	1-4 cycles	-	3
	5 cycles	-	1
	6 cycles	-	20
	Unknown		1
Dose of prednisolone given during chemotherapy	Median (range)	-	2460mg (820-2460mg)

3.1.1.5 Mobility, falls and frailty

Only one participant in group A used a walking aid at baseline. At the 12-month study visit, 2 participants in group A and 4 in group B reported using a stick most or all of the time. At baseline, 12 participants had fallen at least once in the preceding 6 months.

At baseline, frailty was present in 32% and 10% of group B and C respectively, and no participants in group A met the criteria for frailty (table 17). At 12 months, the prevalence of frailty increased substantially in groups A and B from baseline, and almost all participants were either frail or pre-frail (figure 17). In group C, there was a slight increase in the number of participants who were pre-frail or frail (15 at baseline and 17 at 12 months).

Table 17: Prevalence of frailty at baseline and at 12 months

	Group A baseline	Group A 12 months	Group B baseline	Group B 12 months	Group C baseline	Group C 12 months
Number assessed	31	29	25	18	30	28
Frail (%)	0	13 (44.8%)	8 (32%)	7 (38.9%)	3 (10%)	2 (7.1%)
Pre-frail / Vulnerable (%)	2 (6.5%)	15 (51.7%)	9 (36%)	10 (55.6%)	12 (40%)	15 (54%)
Fit (%)	29 (93.5%)	1 (3.4%)	8 (32%)	1 (5.6%)	15 (50%)	11 (39%)

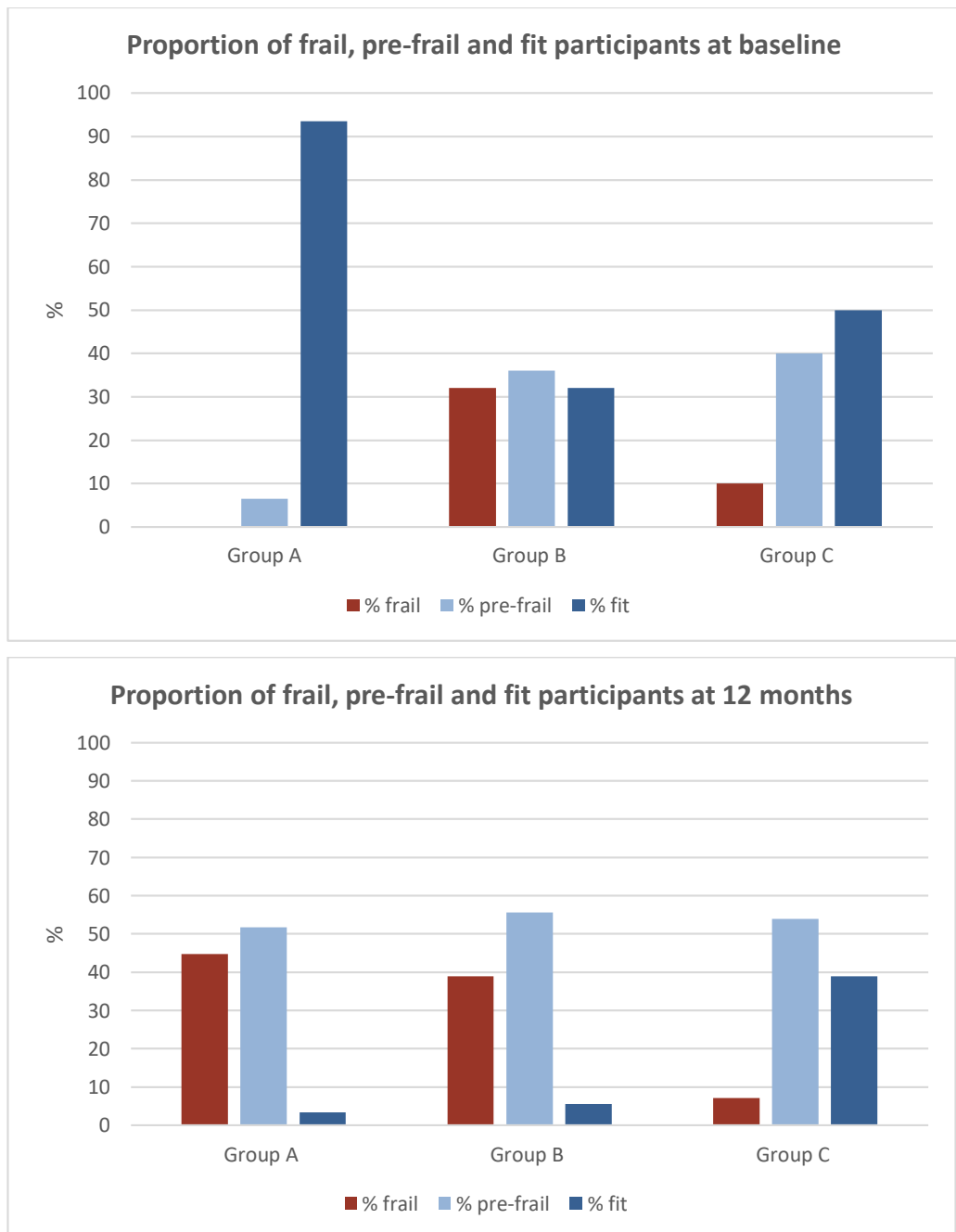


Figure 17: The prevalence of frailty.

The proportion of participants identified as **frail** (red), **pre-frail** (light blue) and **fit** (darker blue), shown by study group at baseline and at 12 months. The proportion of frail patients increased, most notably in groups A and B from baseline to 12 months.

3.1.2 Assessment of muscle function and strength

An overall summary of the results from the assessment of maximal grip strength and the SPPB is shown in tables 18 and 19, and figure 18.

At baseline, the maximal grip strength was similar between study groups. Over 12 months, grip strength deteriorated in all groups. Loss of grip strength was greatest in groups A and B (mean losses were 4.3kg and 3.2kg respectively) and the average loss was 0.4kg in Group C. Comparison of the 12-month change in groups A and C using an ANCOVA model to adjust for baseline grip, age, and BMI found that those in group A experienced significantly greater loss of grip strength, with a mean difference of -4.9Kg (95% CI -7.3 to -2.5kg, $p < 0.001$). Group B were not compared to group C using the ANCOVA model, as some of the biochemistry and microstructure data differed significantly from group A, and the number of group B participants that completed the study was lower than the recruitment target.

All participants scored a maximum of 4 points for the balance component of the short physical performance battery (SPPB). Therefore, the longitudinal change in the total SPPB score resulted from differences in the chair stand test and walk test between baseline and 12 months.

The overall scores (maximum of 12 points) are shown in table 18, and the scores were similar between groups at baseline. The mean score deteriorated slightly in group A (-0.55 points), increased slightly in Group B (+0.22 points) and increased by 0.36 points in group C participants. The mean difference between groups A and C was -1.3 points (95% CI -2.1 to -0.5 points, $p = 0.001$), and group A experienced a significantly greater reduction in SPPB score than group A, adjusting for baseline SPPB score, age, and BMI.

Table 18: 12-month change in grip strength and SPPB score

Outcome	Group A	Group B	Group C	p value
	n=29	n=18	n= 28	A Vs C
Maximal grip strength at baseline (kg)	31.5 (7.42)	31.9 (7.21)	34.0 (7.13)	0.27*
Maximal grip strength at 12 months (kg)	27.7 (4.54)	29.8 (6.81)	33.7 (7.14)	
Mean change in grip strength (kg)	-4.3 (6.28)	-3.2 (4.99)	-0.4 (4.38)	0.01#
SPPB score at baseline	8.68 (1.96)	8.56 (2.04)	9.63 (1.87)	0.15*
SPPB score at 12 months	8.24 (1.99)	8.89 (2.17)	9.89 (1.64)	
Mean change in SPPB score	-0.55 (2.05)	+0.22 (2.21)	+0.36 (1.52)	0.063#

Data are mean values and standard deviations. * P-Value from independent samples t-test comparing group A and C. # p value from repeated measures ANOVA model testing for an interaction between time and group

Table 19: Comparison of groups A and C for change in grip strength and SPPB

Outcome	Mean difference between group A Vs C	p value*
Mean change in grip strength (kg)	-4.9 (95% CI -7.3 to -2.5)	<0.001
Mean change in SPPB score	-1.3 (95% CI -2.1, -0.5)	0.001

* Derived from ANCOVA with the 12-month measurement set as the dependent variable, with a fixed factor for group, and the covariates of age, BMI and baseline measurement

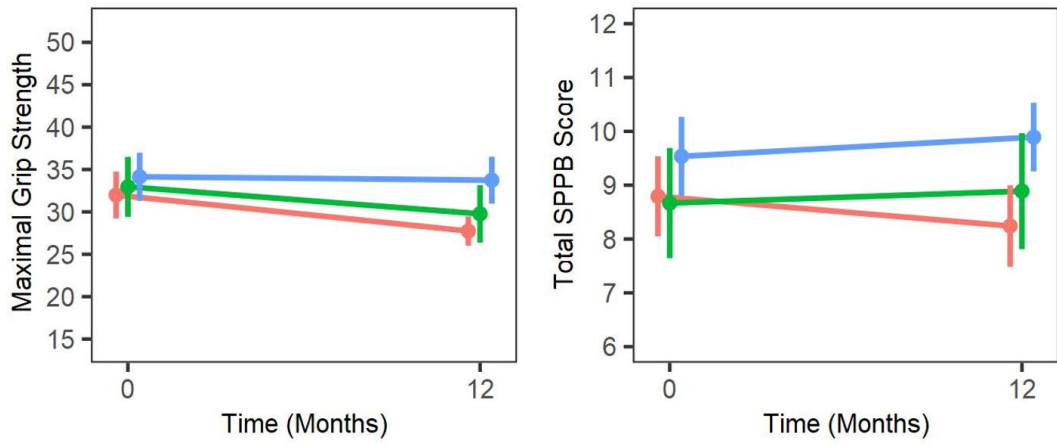


Figure 18: 12-month change in maximal grip strength and total SPPB score.

The red line represents group A, the green line represents group B and the blue line represents group C. The error bars show the 95% confidence intervals.

3.1.3 Changes in body composition

An overall summary of the results from the assessment of body composition using DXA is shown in tables 20 and 21, and figures 19 and 20.

The average BMI at baseline measured by DXA was 26.9 (kg/m²), and was similar between study groups (27.3, 26.3 and 29.9kg/m²), with no difference between groups A and C. Participants in groups A and B gained BMI over 12 months (average increases of 0.9kg/m² in group A and 1.1kg/m² in group B), whereas group C participants had a small reduction of -0.1kg/m². The mean change in BMI over 12 months was significantly different between groups A and C (p=0.002), and once baseline measurement and age had been adjusted for, the mean difference was 1.1kg/m² (95% CI 0.4 to 1.7, p=0.001).

Total fat mass and body fat percentage at baseline was not significantly different between groups. Over 12 months, groups A and B gained fat mass and body fat percentage whereas group C lost fat mass and body fat percentage. Group A gained an average 3286g fat mass (2.8% body fat), whereas group C lost 410g (0.1% body fat), p<0.001 for both. When adjusting for age and baseline fat mass, the mean difference in fat mass between groups A and C was 3822g (95% CI 2425g and 5220g, p<0.001) and the difference in body fat percentage was 3.1% (95% CI 2.1% to 4.1%, p<0.001).

Over 12 months, groups A and C lost lean mass and group B experienced a small gain. The difference between groups A and C was not significant.

Longitudinal analysis of trunk composition found that group A gained trunk fat mass in group A (+1169g) compared to group C (-296g). The mean difference between groups A and C adjusted for baseline value and for age was 1530g (95% CI 648g to 2413g, p=0.001). The greatest gain in trunk fat mass was observed in group B (1466g). Group B also gained lean mass (190g), whereas groups A and C lost similar small amounts of lean mass over the study period.

Group A lost lean mass (mean -254g) in upper limbs, and gained fat mass (mean +587g), whereas changes in group C participants were significantly smaller. The 12 month change in upper limb composition was significantly different between groups A and C (mean difference -264g for lean mass, 95% CI -423g to -105g, p=0.002 and 627g for fat mass, 95% CI 453g to 803g, p<0.001). Group B also gained upper limb fat mass (457g), but the lean mass did not change.

Table 20: Baseline and 12 month measures of body composition in all participants

Outcome measure obtained from DXA	All n=75	Group A n=29	Group B n=18	Group C n= 28	p value A Vs C*
<i>Whole body composition</i>					
Body mass index at baseline	26.9 (3.3)	27.3 (3.2)	26.3 (3.5)	26.9 (3.5)	0.68
Body mass index at 12 months	27.5 (3.3)	28.2 (3.1)	27.4 (3.5)	26.8 (3.3)	-
Mean change in body mass index	0.6	0.9	1.1	-0.1	0.002
(95% CI)	(0.3,0.9)	(0.5, 1.3)	(0.6,1.7)	(-0.6, 0.3)	
Total fat mass at baseline (g)	25,666 (6554)	26,546 (6298)	25,333 (6630)	24,840 (6857)	0.33
Total fat mass at 12 months (g)	27,566 (7183)	29,832 (6557)	28,792 (7521)	24,430 (6566)	
Mean change in total fat mass (g)	1900	3286	3259	-410	<0.001
(95% CI)	(1183, 2616)	(2383, 4189)	(2016, 4503)	(-1503, 684)	
Total % body fat at baseline	30.6 (4.6)	31.5 (4.1)	30.7 (5.1)	29.5 (4.7)	0.09
Total % body fat at 12 months	32.2 (5.0)	34.3 (3.9)	33.2 (5.3)	29.4 (4.7)	
Mean change in total % body fat	1.6	2.8	2.5	-0.1	<0.001
(95% CI)	(1.1, 2.1)	(2.2, 3.4)	(1.6, 3.3)	(-0.0, -0.7)	
Total lean mass at baseline (g)	57,222 (8287)	57,083 (7459)	56,698 (7880)	58,505 (9474)	0.53
Total lean mass at 12 months (g)	57,132 (8085)	56,597 (7352)	56,836 (7310)	57,876 (9408)	
Mean change in total lean mass (g)	-390	-486	138	-629	0.74
(95% CI)	(-759, -21)	(-1184, 212)	(-667, 942)	(-1128, -129)	

Trunk body composition					
Trunk fat mass at baseline (g)	13,319 (4080)	13,693 (4272)	13,118 (3911)	13,061 (4102)	0.57
Trunk fat mass 12 months (g)	14,012 (4174)	14,862 (4145)	14,584 (4194)	12,765 (4032)	
Mean change in trunk fat mass (g)	693	1169	1466	-296	0.002
(95% CI)	(287, 1110)	(617, 1721)	(675, 2257)	(-1030, 437)	
Mean trunk lean mass at baseline (g)	28,995 (4492)	28,553 (4211)	28,280 (4363)	29,657 (4937)	0.41
Mean trunk lean mass 12 months (g)	28,789 (4293)	28,344 (3932)	29,010 (3783)	29,109 (5011)	
Mean change in trunk lean mass	-206	-209	190	-458	0.30
(95% CI)	(-422, 10)	(-587, 169)	(-280, 661)	(-770, -145)	
Upper limb composition					
Mean lean mass in arms baseline (g)	6860 (1107)	6896 (1081)	6467 (934)	7076 (1201)	0.55
Mean arm lean mass in arms 12 months (g)	6768 (1123)	6643 (1056)	6480 (999)	7084 (1222)	
Mean change in lean mass of arms	-92	-254	13	7	0.002
(95% CI)	(-171, -14)	(-400, -108)	(-161, 188)	(-71, 85)	
Mean fat mass at baseline (g)	3139 (777)	3274 (733)	3096 (806)	3028 (809)	0.23
Mean fat mass in arms at 12 months (g)	3459 (949)	3861 (913)	3553 (932)	2981 (803)	
Mean change in fat mass of arms	319	587	457	-46	<0.001
(95% CI)	(221, 417)	(450, 724)	(308, 605)	(-155, 63)	

Data presented are means and standard deviations.

* p values for baseline comparison between group A and C were obtained by independent samples t tests, comparing mean from A and C. p value for the mean 12-month change was obtained from repeated measures ANOVA, testing for an interaction between time and group

Table 21: Comparison of the mean change in body composition between groups A and C

Outcome of interest for 12-month change	Mean difference between groups A and C (95% CI)	p-value*
Body mass index	1.1 (0.4, 1.7)	0.001
Total fat mass	3822 (2425, 5220)	<0.001
Total % body fat	3.1 (2.1, 4.1)	<0.001
Total lean mass	104 (-751, 958)	0.809
Trunk fat mass	1530 (648, 2413)	0.001
Trunk lean mass	210 (-274, 694)	0.388
Upper limbs fat mass	627 (453, 803)	<0.001
Upper limbs lean mass	-264 (-423, 105)	0.002

*p value obtained from ANCOVA model with 12-month measurement as dependent variable, including a fixed factor for group and baseline measurement and age as covariates.

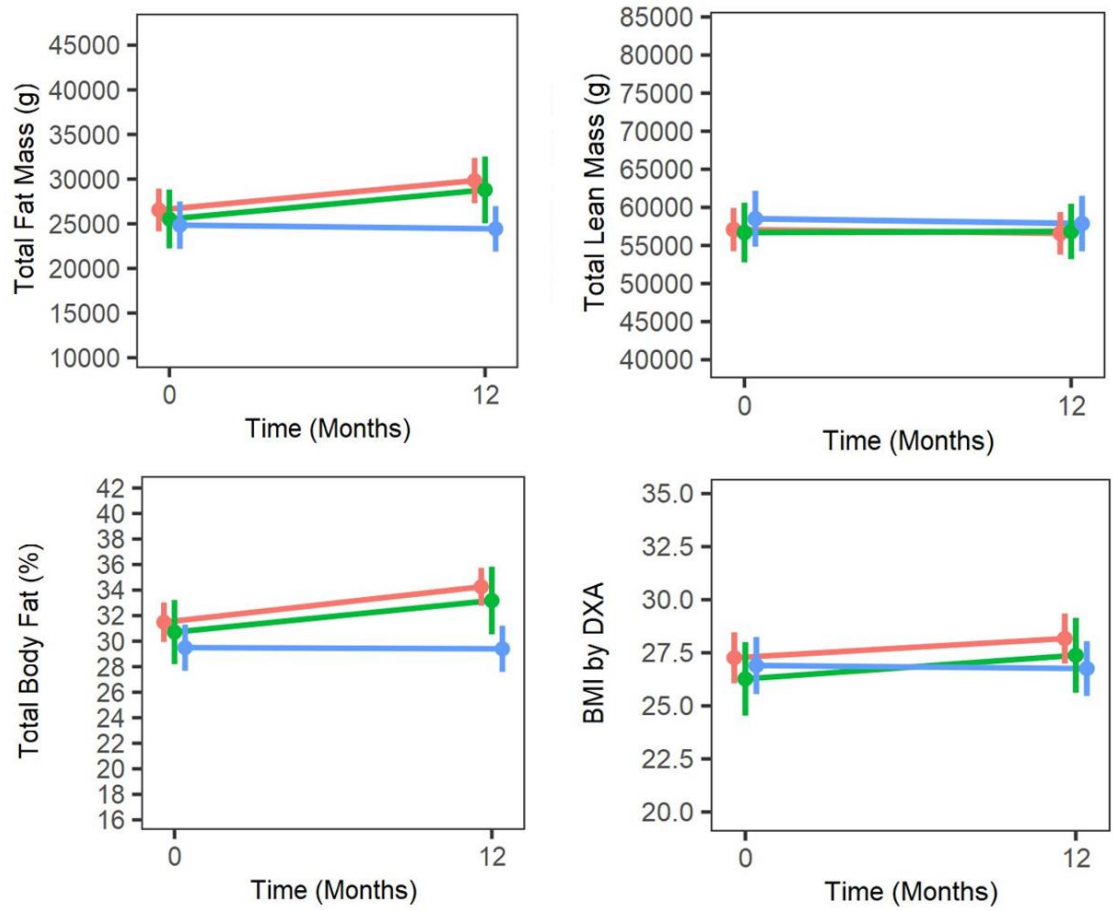


Figure 19: 12-month change in lean mass and fat mass, and BMI by DXA.

The red line represents group A, the green line represents group B and the blue line represents group C. The error bars show the 95% confidence intervals.

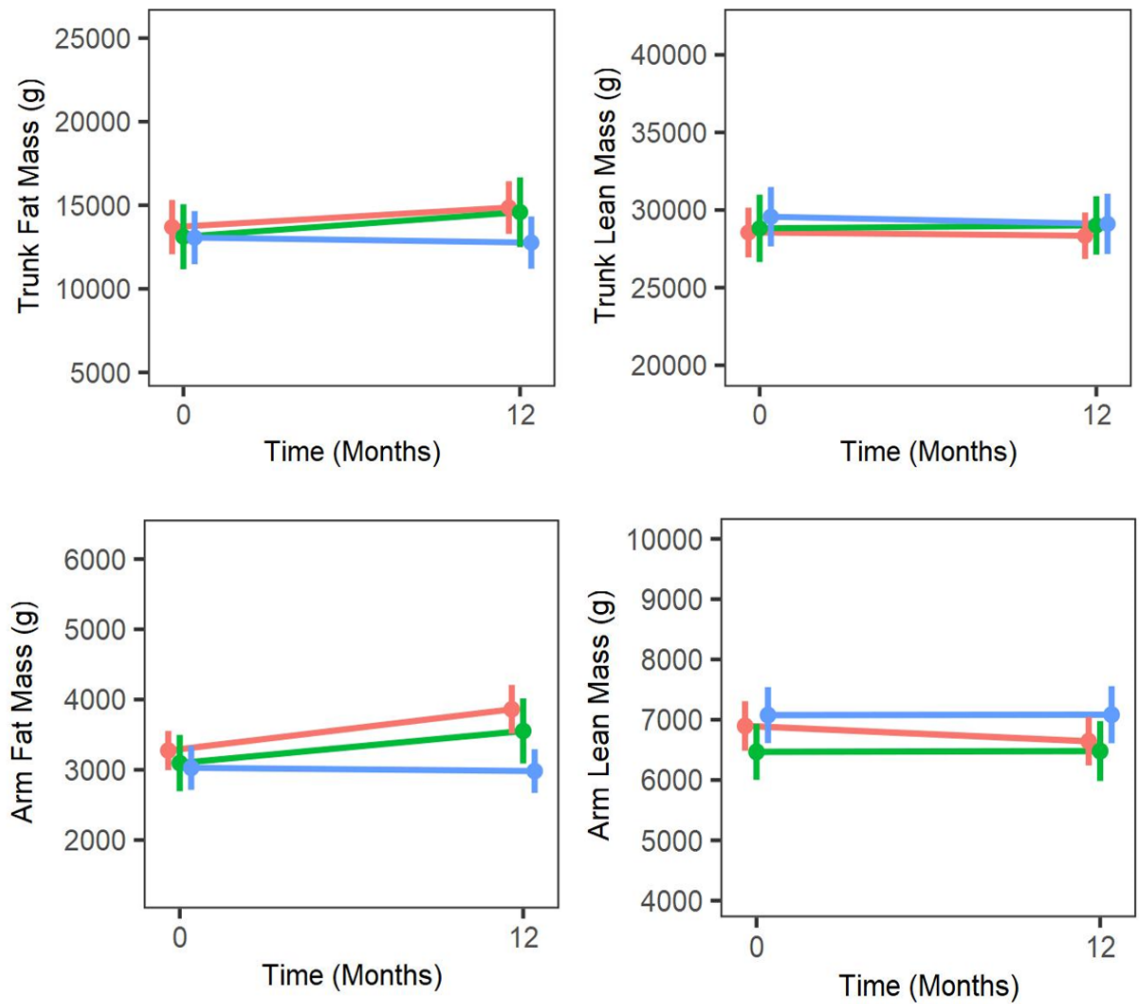


Figure 20: 12-month change in trunk and upper limb lean mass and fat mass by DXA.

The red line represents group A, the green line represents group B and the blue line represents group C. The error bars show the 95% confidence intervals.

3.1.4 Results of serum tests

3.1.4.1 Vitamin D status

The UK NICE guidelines for Vitamin D deficiency in adults define deficiency as a serum vitamin D level below 25nmol/L, this is equivalent to <10ng/ml. Levels between 25-50nmol/L (10-20ng/ml) are indicative of vitamin D insufficiency. The median serum total (OH)²⁵ Vitamin D levels in all 75 study participants was 24.7ng/ml (61.8nmol/L) at baseline. The median values were 27.6, 18.5 and 23.6ng/mL for groups A, B and C, respectively. The lowest levels in group B are equivalent to 46.25nmol/L. Comparison of the baseline values between group A and C showed that groups were similar (p=0.95, Mann Whitney U test).

After 12 months, vitamin D levels decreased most in group A (median difference - 2.7ng/ml, 95% CI -4.5 to -0.8) and the difference was -0.2ng/ml (95% CI -1.4 to 1.0) in group C participants. The 12-month reduction in serum vitamin D concentration was significantly greater in group A compared to group C (p=0.027).

3.1.4.2 Measurement of sex hormones

As previously described, group A had started ADT 20 days before the baseline visit. Serum testosterone at baseline reflected this, in group A the median concentration was 2.0nmol/L and 38% of participants had castration levels (table 22). By 12 months, 97% of group A had castration levels of testosterone, and the median result was below the lower limit of detection (<0.04nmol/L)

There was an average of 57 days from ADT initiation to baseline visit for group B participants, when the majority (89%) of group B had castration testosterone levels. By 12 months, all of the group B participants decreased to this level. The average group B testosterone level was below the limit of detection (<0.04nmol/L) at both baseline and 12 months. Participants in group C had normal testosterone levels, and none were in the castration range at baseline or at 12 months.

SHBG levels decreased slightly in group A, from a median value of 56.0nmol/L to 54.9nmol/L, and in group B from 57.3nmol/L to 54.1nmol/L (table 22) There was a small increase of 0.2nmol/L in group C. All results were within the normal SGBG reference range in all groups.

Serum oestradiol levels were below the limit of assay detection (<91.8pmol/L) in 23 (79%) of group A participants at baseline and in 28 (97%) after 12 months. They were below the limit of detection for all group B participants at both time points. Oestradiol levels remained stable in group C participants, and were within normal limits for healthy men.

Table 22: Change in serum sex hormones

Hormone	Group A (n=29)	Group B (n=18)	Group C (n=28)
Testosterone			
Median testosterone at baseline (nmol/L)	2.0	<0.4	15.7
(range)	(<0.4 to 42.6)	(<0.4 to 10.2)	(4.8 to 30.2)
Median testosterone at 12 months (nmol/L)	<0.4	<0.4	15.4
(range)	(<0.4 to 12.1)	(<0.4 to 1.3)	(3.2 to 30.7)
Number with baseline testosterone at castration level <1.7 nmol/L	11 (38%)	16 (89%)	0 (0%)
Number with 12-month testosterone at castration level <1.7 nmol/L	28 (97%)	18 (100%)	0 (0%)
SHBG			
Median SHBG at baseline (nmol/L)	56	57.3	50.1
(IQR)	(33.7 to 64.9)	(43.6 to 62.1)	(41.8-60.0)
Median SHBG at 12 months (nmol/L)	54.9	54.1	50.3
(IQR)	(28.4-66.1)	(41.0 to 67.5)	(38.4-60.7)
Oestradiol			
Median oestradiol at baseline (pmol/L)	<91.8	All values	96
(range)	(<91.8 to 161)	<91.8	(<91.8 to 235)
Median oestradiol at 12 months (pmol/L)	<91.8	All values	109
(range)	(<91.8 to 106)	<91.8	(<91.8 to 221)

3.1.4.3 Biomarkers and regulators of bone turnover

All BTM data is shown in table 23, with the mean differences between groups A and C from the ANCOVA model shown in table 24. At baseline, median serum PINP levels were highest in group B (127.5ng/ml), and were similar in groups A and C (p=0.9). The change in PINP over 12 months varied between group, with an increase in serum PINP in group A (+51.7ng/ml), decreased levels in group B (-54.9ng/ml), and levels in group C remained very similar. There was a significant difference in the 12-month change in PINP between groups A and C (mean difference 2.20, 95% CI 1.93 to 2.51, p<0.001), adjusting for age and baseline PINP.

Serum osteocalcin levels were similar at baseline between groups. At 12 months, osteocalcin increased the most in group A (+13ng/mL), with smaller increases in group B (+3.4ng/mL) and group C (+2.6ng/ml). There was a significantly greater increase in serum osteocalcin in group A compared to group C (mean difference 1.43ng/ml, 95% CI 1.16 to 1.75, p=0.001).

Baseline CTX levels in group B were almost double those measured in group C (0.42ng/ml in group B and 0.22ng/ml in C). Levels of serum CTX at baseline were similar between groups A and C (p=0.82). After 12 months, CTX levels increased by 0.36ng/L and 0.14ng/L in groups A and B respectively, with a small increase of 0.09ng/mL in group C. The change in CTX did not differ significantly between study groups A and C.

TRAP5b levels at baseline were highest in group B, and were significantly higher in group C than in group A (1.85U/L Vs 0.97U/L, p=0.04). After 12 months, the greatest change in serum levels was observed in group A, where there was a 1.36U/L increase, compared to an increase of 0.74U/L and 0.47U/L in groups B and C, respectively, though compared to group C the change in Group A was not significant (p=0.97).

Over 12 months, we observed a two- fold greater increase in serum sclerostin level in group A compared with group C. However, this did not reach statistical significance when adjusting for baseline value, age and BMI (mean difference 1.06g/ml, 95% CI 0.04 to 1.19, p=0.35). The increase in sclerostin was slightly higher in group B than group C.

Table 23: 12 month change in biomarkers and regulators of bone turnover

Serum marker	All (n=75)	Group A (n=29)	Group B (n=18)	Group C (n=28)	Difference A vs C (p value)
Median PINP at baseline (ng/mL)	41.9	39.8	127.5	40.7	0.9
(IQR)	(31.2 to 52.0)	(29.8 to 50.7)	(36.7 to 282.1)	(31.3 to 46.9)	
Median PINP at 12 month (ng/ml)	69.1	91.4	106.9	40.5	
(IQR)	(42.1 to 110)	(69.7 to 111.1)	(72.5 to 138.2)	(33.0 to 48.3)	
Change in PINP (ng/mL)	22.1	51.7	-54.9	0.4	<0.001
(95% CI)	(11.8, 32.7)	(40.6, 62.3)	(-211.9, 45.1)	(-2.8, 4.2)	
CTX at baseline (ng/mL)	0.26	0.28	0.42	0.22	0.82
(IQR)	(0.13 to 0.48)	(0.13 to 0.42)	(0.16 to 0.7)	(0.11 to 0.46)	
CTX at 12 months (ng/mL)	0.49	0.59	0.68	0.37	
(IQR)	(0.29 to 0.78)	(0.26 to 0.99)	(0.34 to 0.88)	(0.25 to 0.55)	
Change in CTX (ng/mL)	0.19	0.36	0.14	0.09	0.14
(95% CI)	(0.1, 0.28)	(0.2, 0.54)	(-0.27, 0.43)	(0.02, 0.17)	
TRAP5b at baseline (U/L)	1.39	0.97	2.21	1.85	0.04

	(IQR)	(0.77 to 2.65)	(0.56 to 2.16)	(1.03 to 3.62)	(0.96 to 2.97)	
TRAP5b months (U/L)		2.73	2.44	2.97	2.6	
	(IQR)	(1.33 to 3.85)	(1.27 to 3.97)	(1.06 to 4.26)	(1.74 to 3.69)	
Change in TRAP5b (U/L)		0.94	1.36	0.47	0.74	0.21
	(95% CI)	(0.54, 1.39)	(0.71, 1.98)	(-0.86, 2.01)	(0.25, 1.32)	
Osteocalcin at baseline (ng/mL)		14.5	13.3	14.5	15.5	0.18
	(IQR)	(9.6 to 21.5)	(9.0 to 17.8)	(9.4 to 48.1)	(10.6 to 22.1)	
Osteocalcin at 12 months (ng/mL)		22.4	26.4	26.5	17.8	
	(IQR)	(15.8 to 31.3)	(19.0 to 36.7)	(16.2 to 42.8)	(15.2 to 23.0)	
Change in osteocalcin		7.2	13.0	3.4	2.6	<0.001
	(95% CI)	(4.4, 10.2)	(9.0, 36.7)	(-19.9, 16.0)	(0.5, 4.5)	
Sclerostin at baseline (ng/mL)		40.2	42.7	35.9	42.0	0.482
	(IQR)	(31.0 to 56.7)	(29.8 to 57.1)	(29.8 to 57.1)	(31.7 to 66.6)	
Sclerostin at 12 months (ng/mL)		43.4	43.4	40.8	49.1	
	(IQR)	(35.9, 60.6)	(38.4 to 69.6)	(35.1, 50.7)	(37.7, 62.8)	
Change in sclerostin		3.8	5.2	3.0	2.6	0.146
	(95% CI)	(1.5, 6.3)	(2.1, 9.9)	(-3.5, 8.6)	(-1.8, 6.8)	

Data presented are median and interquartile range. *p values for baseline comparison between group A and C were obtained using a Mann-Whitney U test. p value for the mean 12-month change was obtained from repeated measures ANOVA, testing for an interaction between time and group (baseline and 12-month measurement log transformed prior to analysis)

Table 24: Comparison of the 12 month change in serum biomarkers and regulators of bone turnover between groups A and C

Serum biomarker	Mean difference	p value*
	between group A Vs C (95% CI)	
PINP	2.20 (1.93, 2.51)	<0.001
CTX	1.43 (0.99, 2.08)	0.059
TRAP5b	0.99 (0.65, 1.52)	0.973
Osteocalcin	1.43 (1.16, 1.75)	0.001
Sclerostin	1.06 (0.94, 1.19)	0.348

*derived from ANCOVA model with 12-month measurement as dependent variable, including a fixed factor for group and baseline measurement, age and BMI as covariates. The biomarker outcomes have been log transformed so difference between groups is expressed as the ratio of geometric means

3.2 Summary of key findings from this chapter

The ANTELOPE study has demonstrated that recruitment and retention of men with advanced PC in a longitudinal study is challenging due to their underlying diagnosis.

Fracture risk in men starting ADT for PC appears to be similar to the risk in healthy age matched men. The 10-year risk of hip fracture is between 1.62 and 2.74% and risk of major fracture is 3.92 to 7.24%. Fracture risk is higher when clinical risk factors are used without BMD in the FRAX algorithm. More than three quarters of men starting ADT have a fracture risk above the threshold for treatment.

ADT is associated with an increase in frailty and pre-frailty during the first year of treatment. Men with metastatic PC are more likely to be frail than men with localised disease at diagnosis and after 12 months. ADT is also associated with a significant reduction in grip strength and SPPB score, although did not affect balance in our study.

ADT causes sarcopenic obesity, with a gain in BMI and fat mass, and a loss of lean mass. When analysed by region, the change relates to a significant gain in trunk fat mass, and there is also loss of lean mass in the upper limbs.

ADT increases bone turnover, which was measured by the biomarkers PINP, CTX, osteocalcin. Trap5b and sclerostin were not significantly affected by ADT. Interpretation of bone biomarkers is challenging in men with metastatic bone disease who receive systemic treatments, as it is unclear which changes relate to ADT, use of GCs and which relate to a response to chemotherapy in bone.

Chapter 4: ANTELOPE results (II) the effect of androgen deprivation therapy on bone density and microarchitecture

This chapter will present ANTELOPE data for the 12-month change in areal BMD at the lumbar spine, hip and total body. This data is from all 75 study participants who had a DXA scan at baseline and 12 months (there were 29, 18 and 28 participants in groups A, B and C, respectively). It will also present data from HR-pQCT measurement of volumetric BMD and estimates of bone strength at the distal radius, which are available for 56 participants.

4.1 Results

4.1.1 Change in in lumbar spine and hip bone mineral density and bone mineral content by DXA

The mean areal BMD was similar between study groups A and C at baseline, at all sites that were measured. The baseline and 12-month BMD data are shown in table 25, along with the change in BMD. A comparison of the mean baseline BMD values and the 12-month change between groups A and C is also presented. Table 26 presents the mean difference between groups A and C for each BMD outcome of interest, using ANCOVA and after adjustment for baseline value, age and BMI. Figures 21 and 22 show plots of the changes over 12 months.

Over the 12-month study period, participants in groups A and B experienced loss of BMD at all skeletal sites. The site that experienced the greatest loss of BMD was the lumbar spine (LS); group A lost an average of 0.045g/cm² (3.9%) and loss in group B was 0.07g/cm² (5.9%). There was a small gain in LS BMD of 0.024 g/cm² (2.2%) in Group C. The 12-month change in LS BMD was significant when group A and group C were compared (mean difference -0.072 g/cm², 95% CI -0.092 to -0.052, p<0.001) adjusting for baseline value, age and BMI (table 26). Group B were not compared to group C due to the small number of participants, and differences in the data between group A and B.

BMD loss at the femoral neck (FN) and total hip (TH) was greatest in group A, where the changes over 12 months were -0.031 g/cm² (3.8%) at FN and -0.035 g/cm² (3.3%) at TH. Group B lost 0.029g/cm² (3.5%) at FN and 0.029g/cm² (2.8%) at TH. BMD at FN and TH was similar at baseline and 12 months in group C participants. When compared to group C, group A lost significantly more BMD at both the FN (mean difference -0.034g/cm², 95% CI -0.048 g/cm² to -0.019 g/cm², p<0.001) and TH (-0.036 g/cm², 95%CI -0.048 g/cm² to -0.025g/cm², p<0.001, table 26).

There was a reduction in total body BMD over 12 months in both group A (-0.038g/cm², 3.1%) and group B (-0.039g/cm² 3.2%). Group C had a small gain of 0.008g/cm² (0.7%) which was significantly different to the change observed in

group A (mean difference -0.044g/cm^2 , 95% CI -0.061g/cm^2 to -0.028g/cm^2 , $p < 0.001$, table 26, figure 22).

There was a similar reduction in bone mineral content (BMC) over the 12-month study period in groups A and B, who lost 94.3g and 92.2g (3.3% and 3.5%), respectively. There was a slight increase in the mean BMC in group C, and the 12-month change in BMC was significantly different between group A and C (mean difference -110.5g , 95% CI -147.6g to -73.5g , $p < 0.001$, table 26, figure 22).

Table 25: 12-month change in areal BMD

DXA outcome measure		All participants n=75	Group A n=29	Group B n=18	Group C n= 28	Difference A Vs C*
Mean femoral neck BMD (g/cm ²)						
	Baseline	0.810 (0.136)	0.826 (0.133)	0.828 (0.140)	0.781 (0.135)	p=0.21
	12 months	0.793 (0.125)	0.795 (0.121)	0.799 (0.118)	0.786 (0.137)	
Change in femoral neck BMD (g/cm ²)		-0.017	-0.031	-0.029	0.005	p<0.001
	(95% CI)	(-0.027, 0.008)	(-0.043, -0.02)	(-0.059, 0.001)	(-0.003, 0.014)	
% change from baseline		2.1	3.8	3.5	0.6	
Mean total hip BMD (g/cm ²)						
	Baseline	1.033 (0.145)	1.058 (0.127)	1.020 (0.162)	1.014 (0.153)	p=0.25
	12 months	1.012 (0.139)	1.022 (0.129)	0.992 (0.140)	1.016 (0.152)	
Change in total hip BMD (g/cm ²)		-0.020	-0.035	-0.029	0.001	p<0.001
	(95% CI)	(-0.028, -0.013)	(-0.044, -0.026)	(-0.052,-0.006)	(-0.005, 0.008)	
% change from baseline		1.9	3.3	2.8	0.1	
Mean lumbar spine BMD (g/cm ²)						
	Baseline	1.130 (0.189)	1.141 (0.168)	1.186 (0.219)	1.081 (0.184)	p=0.21
	12 months	1.104 (0.183)	1.095 (0.174)	1.116 (0.189)	1.105 (0.194)	
Change in lumbar spine BMD (g/cm ²)		-0.026	-0.045	-0.070	0.024	p<0.001
	(95% CI)	(-0.042, -0.010)	(-0.061, -0.029)	(-0.119,-0.021)	(0.012, 0.035)	
% change from baseline		2.3	3.9	5.9	2.2	

Mean total body BMD (g/cm ²)					
Baseline	1.215 (0.124)	1.228 (0.133)	1.213 (0.110)	1.203 (0.125)	P=0.47
12 months	1.194 (0.122)	1.190 (0.117)	1.173 (0.108)	1.211 (0.135)	
Change in total body BMD (g/cm ²)	-0.021	-0.038	-0.039	0.008	p<0.001
(95% CI)	(-0.030,-0.013)	(-0.050,-0.026)	(-0.054,-0.024)	(-0.004,0.019)	
% change from baseline	1.7	3.1	3.2	0.7	
Mean bone mineral content (g)					
Baseline	2812.7 (412.9)	2849.2 (377.5)	2803.9 (396.0)	2780.4 (467.1)	p=0.54
12 months	2760.2 (410.3)	2754.9 (362.4)	2711.8 (382.5)	2796.8 (479.6)	
Change in bone mineral content (g)	-52.5	-94.3	-92.2	16.4	p<0.001
(95% CI)	(-72.7, -32.3)	(-120.9,-67.7)	(-127.1, -57.3)	(-11.4, 44.2)	
% change from baseline	1.9	3.3	3.5	0.6	

*Baseline comparison p-value from independent samples t-test comparing group A and C. p value for 12-month change is from repeated measures ANOVA model testing for an interaction between time and group.

Table 26: Comparison of mean change in BMD and BMC between groups A and C

DXA outcome measure	Mean difference between group A Vs C (95% CI)	p value*
Femoral neck BMD (g/cm ²)	-0.034 (-0.048 to -0.019)	<0.001
Total hip BMD (g/cm ²)	-0.036 (-0.048 to -0.025)	<0.001
Total hip BMD (g/cm ²)	-0.036 (-0.048 to -0.025)	<0.001
Lumbar spine BMD (g/cm ²)	-0.072 (-0.092 to -0.052)	<0.001
Total body BMD (g/cm ²)	-0.044 (-0.061 to -0.028)	<0.001
Whole body BMC (g)	-110.5 (-147.6 to -73.5)	<0.001

*Derived from ANCOVA with the 12-month measurement set as the dependent variable, with a fixed factor for group, and the covariates of age, BMI and baseline measurement

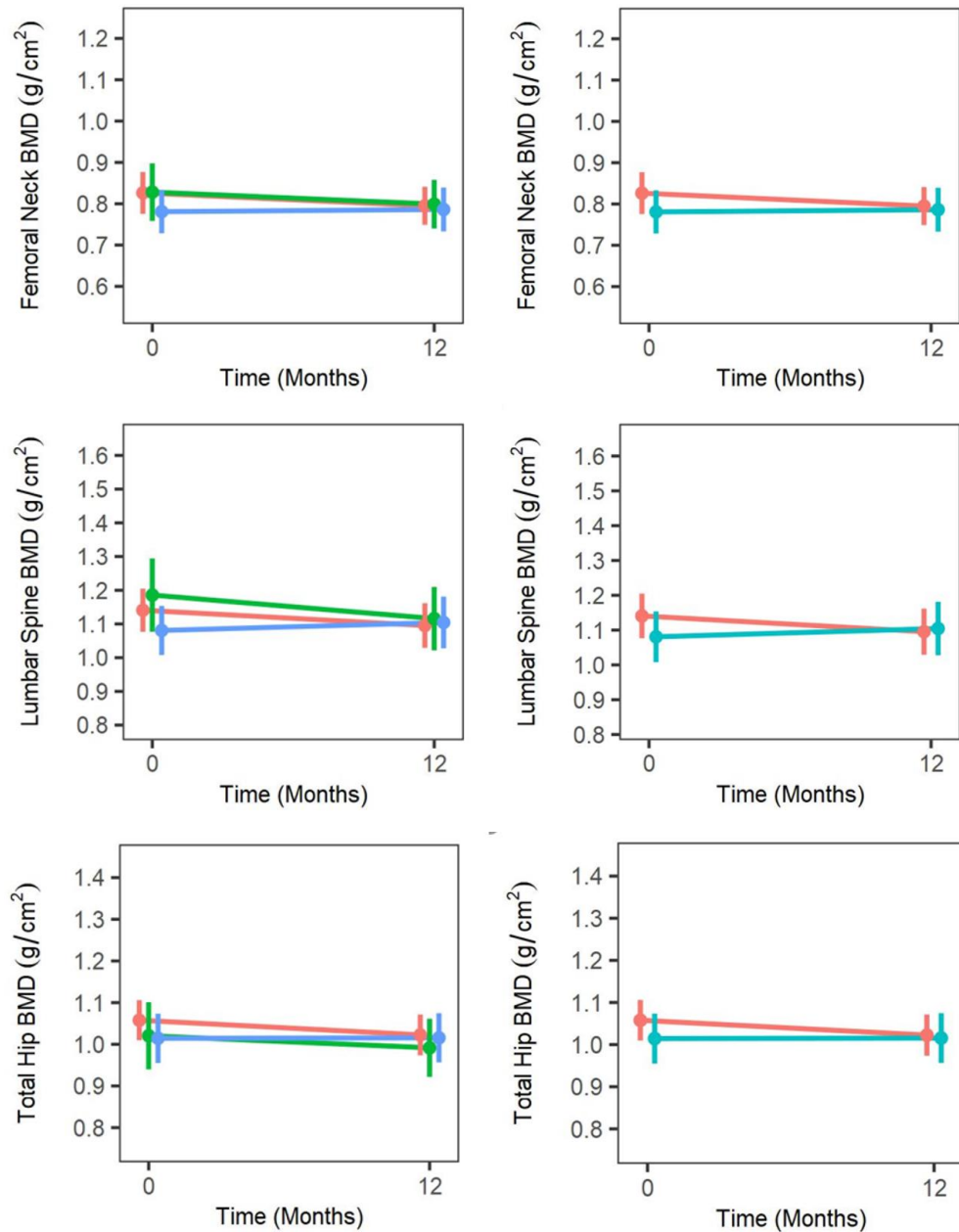


Figure 21: 12-month change in hip and lumbar spine BMD.

Plots of the change in hip and lumbar spine BMD for groups A, B and C are show on the left side column of the figure. The red line represents group A, the green line represents group B and the blue line represents group C. The error bars show the 95% confidence intervals. The right-hand plots show groups A and C only.

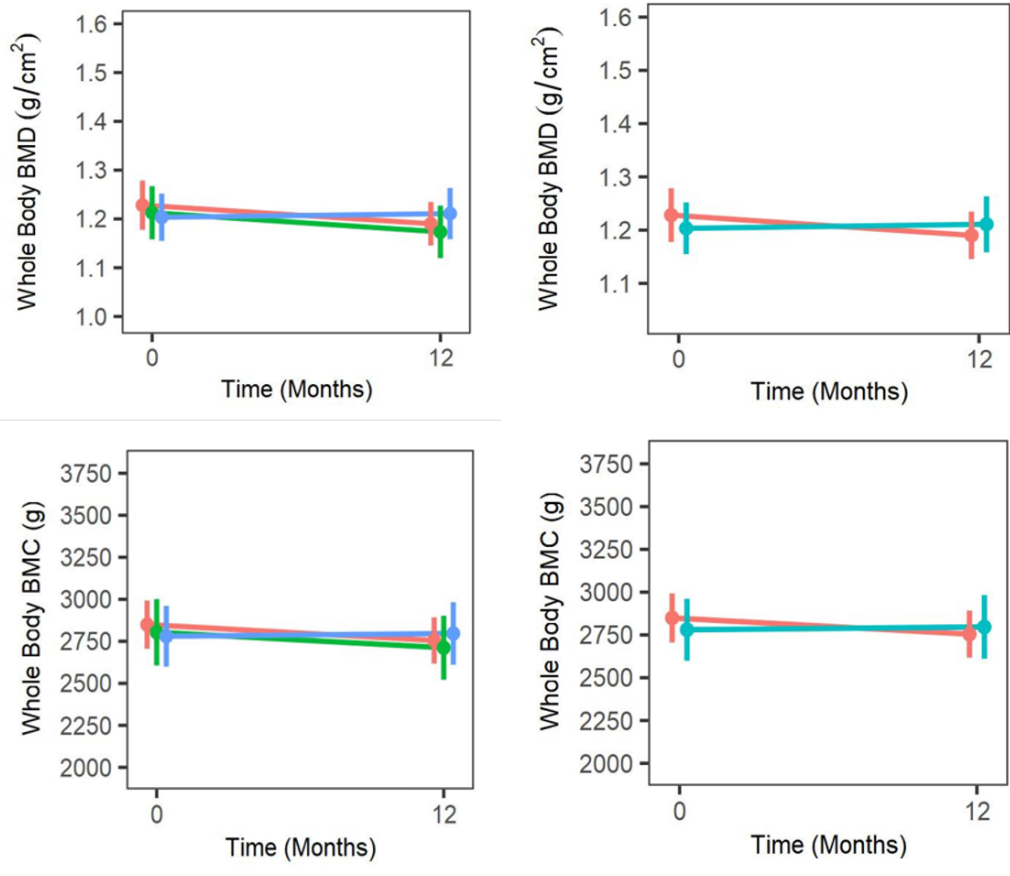


Figure 22: 12-month change in total body BMD and BMC measurements.

Plots of the change in total body BMD and BMC for groups A, B and C are show on the left side column of the figure. The right-hand plots show groups A and C only.

The red line represents group A, the green line represents group B and the blue line represents group C. The error bars show the 95% confidence intervals.

4.1.2 Change in radius volumetric density and microarchitecture by HR-pQCT

Data from baseline and 12-month HR-pQCT scans of the distal radius were available for 56 participants (75%). Two participants could not be scanned at baseline; one due to a scanner machine fault and another had an unusually large hand that would not fit into the scanner gantry. One participant did not receive a follow-up scan at 12 months due to wrist swelling. The remaining participants with missing data had movement artefact that prevented image analysis.

HR-pQCT results for change in microarchitecture are shown in table 27. Data are presented for baseline and 12 months, in addition to the mean change for each outcome of interest. Table 28 presents the results of ANCOVA comparison between groups A and C, with a fixed factor for group, and the covariates of age, BMI and baseline HR-pQCT measurement.

At baseline, there was no difference between groups A and C in any of the microarchitectural outcomes of interest. The primary outcome of the study was the change in vBMD at the distal radius between groups A and C; after 12 months, vBMD loss was greatest in groups A and B where the losses were 13.7mgHA/cm³ (4.1%) and 13.5mgHA/cm³ (4.3%) respectively, and the loss was 1.3mg HA/cm³ (0.4%) in group C. There was significantly greater loss in group A compared with group C (mean difference -11.111mgHA/cm³, 95% CI -17,515mgHA/cm³ and -4,707mgHA/cm³, p=0.001, table 28). The 12-month change in vBMD is shown in the plot in figure 23.

There was a general 12-month decline in cortical bone microarchitecture in groups A and B, and changes were observed in all cortical measures compared to baseline (table 27, figure 24). The mean loss of cortical vBMD was greatest in group B, who lost 31.8mg HA/cm³, compared with 27.1 mg HA/cm³ loss in group A and 7.5mg HA/cm³ loss in group C. The loss of cortical vBMD in group A was significantly greater than in group C (p<0.001, table 28). The overall cortical area decreased by a similar amount in group A (-5.9mm³) and group B (-6.6mm³), and by a significantly smaller amount (-1.6mm³) in group C compared to A (p<0.001). There was loss of cortical thickness in both groups A and B (0.07mm), and the mean loss was 0.002mm in group C (mean difference A Vs C was -0.05mm, 95% CI -0.07mm to -0.02mm, p=0.001). Cortical porosity increased the most over 12 months in group A (0.008), with a slightly smaller increase of 0.006 in group B and was 0.001 in group C. The increased porosity in group A was significantly greater than group C once adjusted for the baseline cortical porosity, age and BMI. (mean difference 0.007, 95% CI 0.003 to 0.011, p=0.002, table 28).

The 12-month changes in trabecular bone parameters are shown in table 27 and figure 25. There was loss of trabecular vBMD in groups A and B; group A lost an average of 2.2mg HA/cm³ and group B lost 2.5 mg HA/cm over 12 months. Group C did not lose trabecular vBMD, and the 12-month change between groups A and C

was significant (mean difference 2.6mgHA/cm³ 95% CI -4.8 to -0.5, p=0.016, table 28). All groups experienced a gain in trabecular area, which was greatest in group A and significantly greater than in group C (mean difference 2.7mm², 95% CI 0.4 to 4.9, p=0.02). There was no difference in the change in trabecular thickness or number between groups A and C. Trabecular separation increased and the bone to tissue volume ratio decreased, whereas the opposite occurred in group C, and the difference between groups A and C was significant for both measures (mean difference for trabecular separation 0.02, 95% CI -0.01 to 0.05, p=0.06, mean difference for BV/TV -0.02, 95% CI -0.04 to -0.002, p=0.03, table 28). Group B experienced small losses of trabecular thickness, separation and also BV/TV over 12 months.

Table 27: Change in volumetric bone mineral density and bone microarchitecture

Outcome measure	All (n=56)	Group A (n=18)	Group B (n=15)	Group C (n=23)	Difference between A and C *
Total vBMD (mg HA/cm ³) baseline	319.8 (51.8)	336.8 (42.9)	317.6 (59.5)	307.9 (51.6)	p=0.06
Total vBMD (mg HA/cm ³) 12 months	311.2 (49.9)	323.1 (41.9)	304.1 (58.7)	306.6 (49.9)	
12 month change in vBMD	-8.6	-13.7	-13.5	-1.3	p<0.001
(95% CI)	(-11.6, 11.5)	(-17.8, -9.6)	(-21.6, -5.4)	(-4.3, 1.7)	
% change	2.7	4.1	4.3	0.4	
Cortical parameters					
Cortical vBMD (mg HA/cm ³) baseline	834.9 (58.3)	855.9 (51.5)	824.6 (66.3)	825.1 (55.7)	p=0.08
Cortical vBMD (mg HA/cm ³) 12 months	814.6 (60.9)	828.8 (55.9)	792.8 (73.2)	817.6 (54.6)	
12 month change in cortical vBMD	-20.3	-27.1	-31.8	-7.5	p<0.001
(95% CI)	(-25.7, -14.9)	(-33.2 -21.0)	(-46.8, -16.8)	(-12.7, -2.4)	
Cortical area (mm ²) baseline	70.0 (14.5)	75.0 (14.2)	69.4 (17.6)	66.6 (11.7)	p=0.044
Cortical area (mm ²) 12 months	65.7 (14.4)	69.1 (14.9)	62.8 (18.4)	65.0 (10.9)	
12 month change in cortical area	-4.3	-5.9	-6.6	-1.6	p<0.001
(95% CI)	(-5.6,-3.0)	(-7.5, -4.3)	(-10.1-3.1)	(-2.9-0.3)	
Cortical thickness (mm) baseline	0.79 (0.19)	0.85 (0.19)	0.76 (0.21)	0.75 (0.17)	p=0.06
Cortical thickness (mm) 12 months	0.74 (0.19)	0.79 (0.19)	0.69 (0.22)	0.73 (0.16)	

12 month change in cortical thickness	-0.05	-0.07	-0.07	-0.02	p<0.001
(95% CI)	(-0.64, -0.03)	(-0.09,-0.05)	(-0.11, -0.03)	(-0.03,0.004)	
Cortical perimeter (mm) baseline	90.4 (9.3)	88.7 (8.6)	92.1 (9.6)	90.5 (9.9)	p=0.53
Cortical perimeter (mm) 12 months	90.5 (9.3)	88.8 (8.5)	92.3 (9.4)	90.7 (9.9)	
12 month change in cortical perimeter	0.2	0.1	0.2	0.2	p=0.80
(95% CI)	(-0.02, 0.4)	(-0.2, 0.4)	(-0.2, 0.7)	(-0.1, 0.5)	
Cortical porosity baseline	0.040 (0.017)	0.038 (0.013)	0.038 (0.017)	0.043 (0.020)	p=0.32
Cortical porosity 12 months	0.045 (0.016)	0.046 (0.013)	0.045 (0.016)	0.045 (0.019)	
12 month change in cortical porosity	0.005	0.008	0.006	0.001	p=0.002
(95% CI)	(0.003, 0.007)	(0.005, 0.012)	(0.001, 0.012)	(-0.002,0.004)	
Trabecular parameters					
Trabecular vBMD (mg HA/cm ³) baseline	191.3 (34.9)	195.9 (38.3)	193.7 (37.1)	186.3 31.3)	p=0.39
Trabecular vBMD (mg HA/cm ³) 12-months	190.1 (34.4)	193.7 (38.4)	191.2 (36.2)	186.7 (30.9)	
12 month change in trabecular vBMD	-1.2	-2.2	-2.5	0.4	p=0.017
(95% CI)	(-2.4, -0.1)	(-4.2, -0.3)	(-5.7, 0.7)	(-0.8, 1.5)	
Trabecular area (mm ²) baseline	333.7 (77.5)	320.3 (64.7)	338.6 (78.6)	341.0 (87.0)	p=0.41
Trabecular area (mm ²) 12 months	335.8 (76.4)	323.9 (64.4)	340.8 (74.3)	341.9 (87.7)	
12 month change in trabecular area	2.1	3.6	2.2	0.9	p=0.014
(95% CI)	(0.7, 3.5)	(2.0, 5.2)	(-2.3, 6.8)	(-0.6, 2.4)	

Trabecular number baseline	2.16 (0.28)	2.20 (0.28)	2.20 (0.22)	2.10 (0.32)	p=0.34
Trabecular number 12 months	2.19 (0.30)	2.15 (0.31)	2.27 (0.28)	2.16 (0.31)	
12 month change in trabecular number	0.03	-0.05	0.07	0.06	p=0.07
(95% CI)	(-0.03, 0.08)	(-0.12, 0.02)	(-0.06, 0.20)	(-0.04, 0.16)	
Trabecular thickness baseline	0.074 (0.012)	0.074 (0.012)	0.074 (0.014)	0.074 (0.012)	p=0.97
Trabecular thickness 12 months	0.073 (0.012)	0.074 (0.012)	0.070 (0.010)	0.072 (0.011)	
12 month change in trabecular thickness	-0.001	0.001	-0.004	-0.002	p=0.145
(95% CI)	(-0.003, 0.001)	(-0.001, 0.004)	(-0.008, 0.001)	(-0.006, 0.001)	
Trabecular separation baseline	0.398 (0.066)	0.389 (0.070)	0.386 (0.044)	0.412 (0.073)	p=0.31
Trabecular separation 12 months	0.394 (0.069)	0.401 (0.081)	0.377 (0.058)	0.399 (0.068)	
12 month change in trabecular separation	-0.003	0.012	-0.008	-0.013	p=0.039
(95% CI)	(-0.014, 0.007)	(-0.003, 0.027)	(-0.032, 0.016)	(-0.030, 0.005)	
Trabecular BV/TV baseline	0.160 (0.029)	0.163 (0.032)	0.161 (0.031)	0.155 (0.026)	p=0.39
Trabecular BV/TV 12 months	0.158 (0.029)	0.161 (0.032)	0.159 (0.030)	0.156 (0.026)	
12 month change in trabecular BV/TV	0.001	-0.002	-0.002	0.0002	p=0.029
(95% CI)	(-0.002, -0.0001)	(-0.003, -0.0001)	(-0.005, 0.001)	(-0.001, 0.001)	

* Baseline comparison P-Value is from an independent samples t-test comparing group A and C. The p-value for 12-month change is from a repeated measures ANOVA model testing for an interaction between time and group

Table 28: Comparison of microarchitecture change between groups A and C

Outcome of interest	Mean difference between group A and C (95% CI)	p-value*
Total vBMD (mg HA/cm ³)	-11.7 (-16.7, -6.7)	<0.001
Cortical parameters		
Cortical vBMD (mg HA/cm ³)	-20.5 (-28.7, -12.3)	<0.001
Cortical area (mm ²)	-4.0 (-6.1, -1.9)	<0.001
Cortical thickness (mm)	-0.05 (-0.07, -0.02)	0.001
Cortical perimeter (mm)	-0.02 (-0.46, 0.41)	0.911
Cortical porosity	0.007 (0.003, 0.011)	0.002
Trabecular parameters		
Trabecular vBMD (mg HA/cm ³)	-2.6 (-4.8, -0.5)	0.016
Trabecular area (mm ²)	2.7 (0.4, 4.9)	0.02
Trabecular number	-0.09 (-0.22, 0.03)	0.13
Trabecular thickness (mm)	0.003 (-0.001, 0.007)	0.18
Trabecular separation	0.02 (-0.001, 0.05)	0.06
Trabecular BV/TV	-0.002 (-0.004, -0.0002)	0.03

*Derived from ANCOVA with the 12-month measurement set as the dependent variable, with a fixed factor for group, and the covariates of age, BMI and baseline measurement

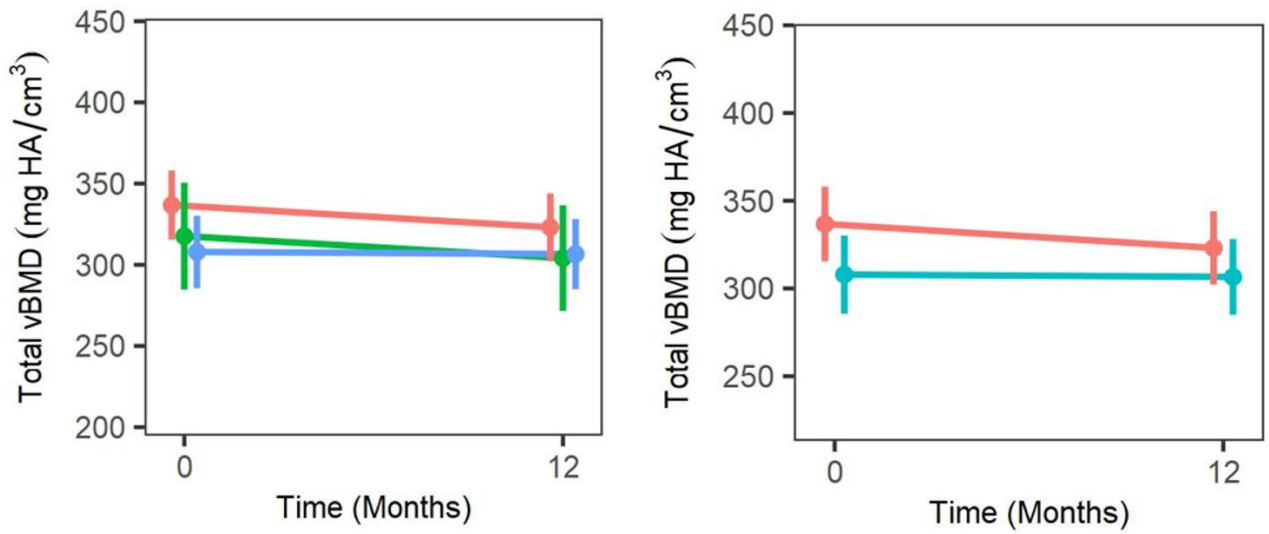


Figure 23: 12-month change in vBMD by HR-pQCT at the distal radius.

The red line represents group A, the green line represents group B and the blue line represents group C. The error bars show the 95% confidence intervals. This was the primary outcome of the ANTELOPE study.

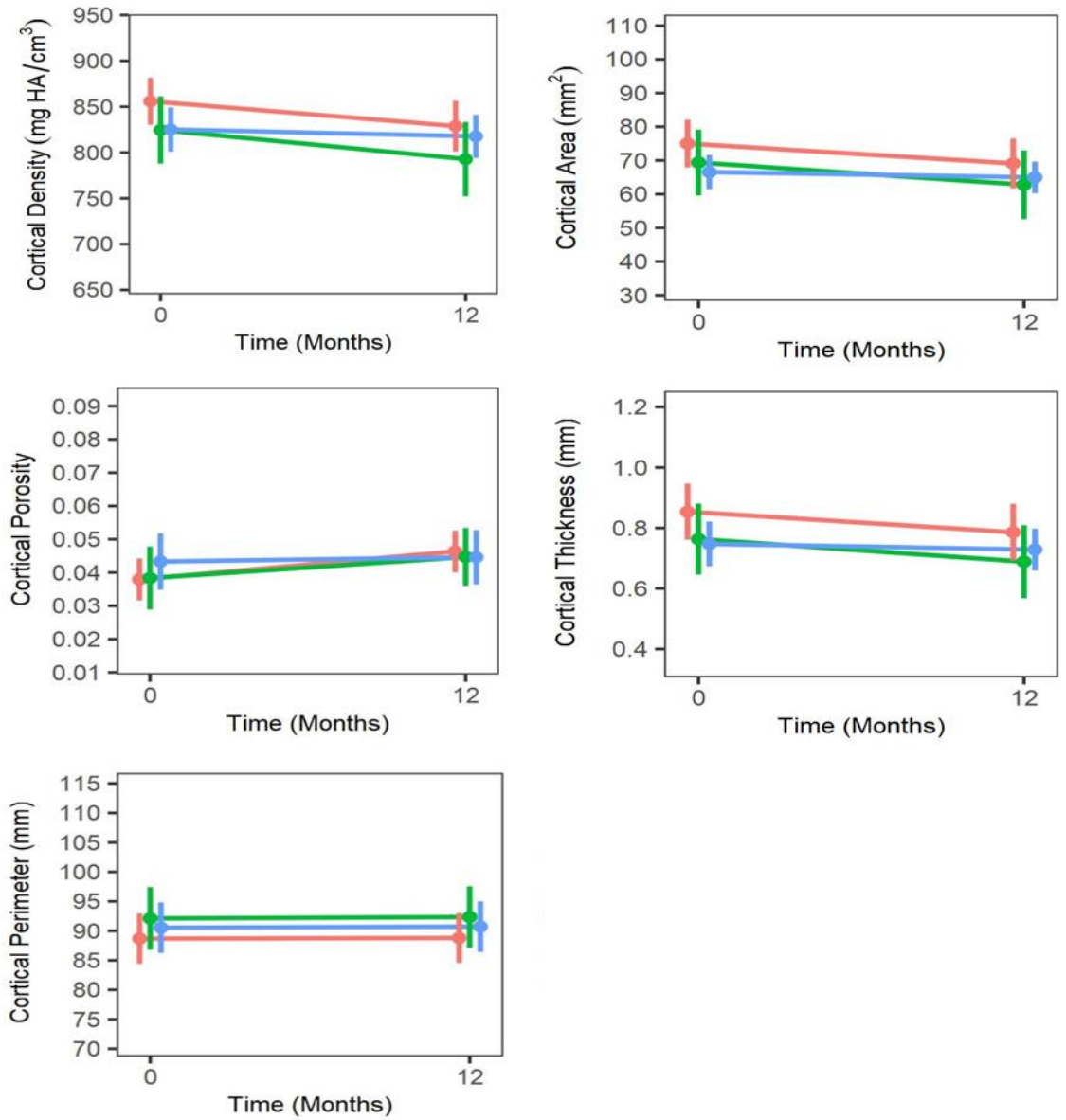


Figure 24: Plots of the 12-month change in cortical microarchitecture at the distal radius by HR-pQCT.

The red line represents group A, the green line represents group B and the blue line represents group C. The error bars show the 95% confidence intervals.

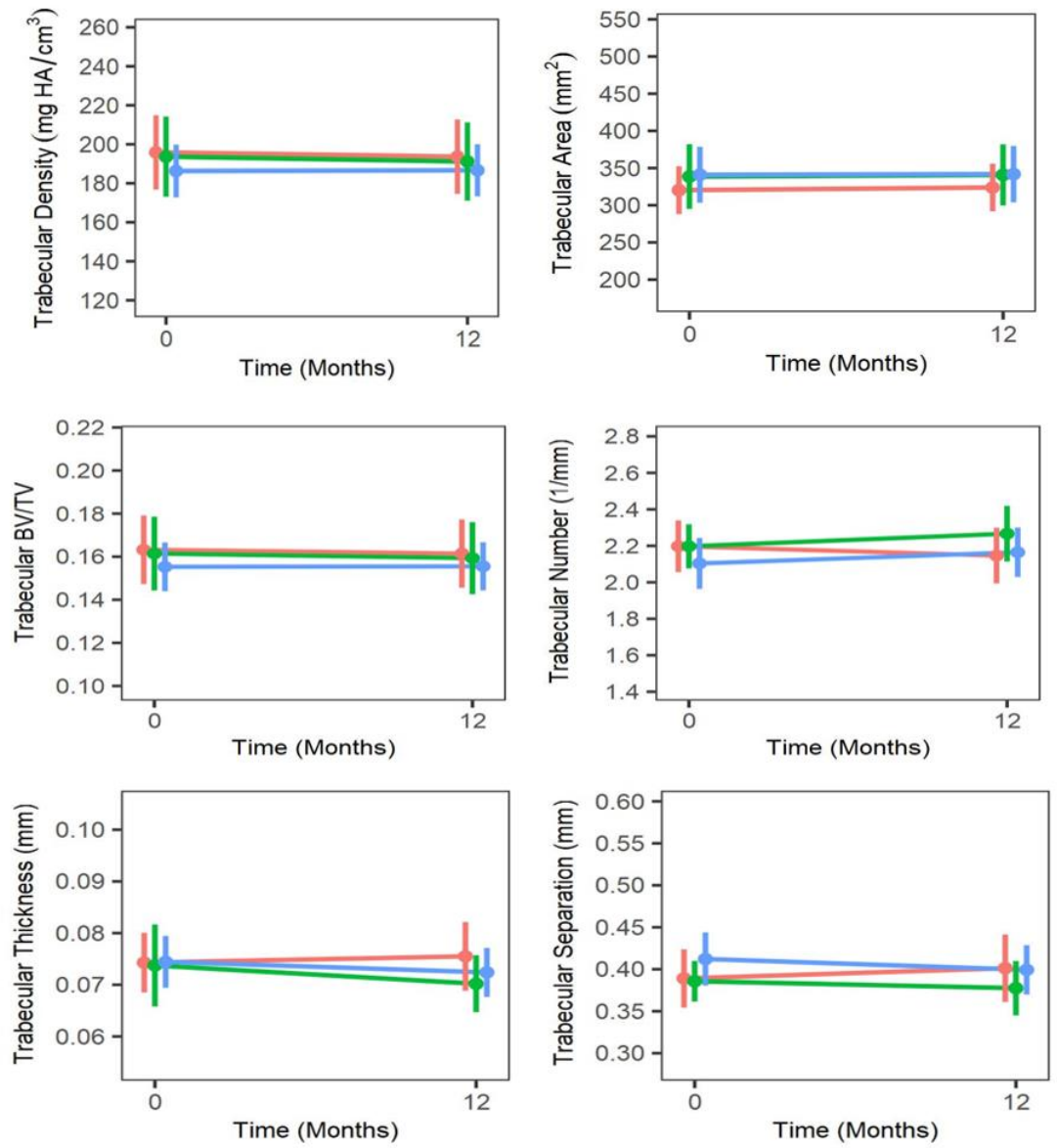


Figure 25: 12-month change in trabecular microarchitecture at the distal radius by HR-pQCT.

The red line represents group A, the green line represents group B and the blue line represents group C. The error bars show the 95% confidence intervals.

4.1.3 Finite element analysis

FE analysis was undertaken for all 56 participants with a baseline and 12-month HR-pQCT scan, and the results are shown in tables 29 and 30, and figure 26. At baseline, there were no differences between groups A and C in any of the finite element outcomes of interest.

Bone stiffness decreased from baseline in all three study groups after 12 months. The greatest change occurred in group B, in whom the mean loss was 8.0kN/mm, compared to 4.4kN/mm in group A and 2.4 kN/mm in group C. When adjustment was made for baseline stiffness, age and BMI, there was no difference in the 12-month change between groups A and C ($p=0.24$, table 30). There was also a reduction in ultimate failure load observed in all groups, and group B experienced the largest reduction (-0.37kN). The mean loss in group A was more than twice the loss in group C, which was significant (mean difference -0.14kN, 95% CI -0.26 to -0.01kN, $p=0.032$, table 30).

There was no difference between study groups A and C in the change in von Mises stresses in cortical and trabecular bone over 12 months. The greatest change in von Mises stresses were seen in group B, where the 12-month change was -0.13 and -0.17 for cortical and trabecular bone, respectively. There was also no difference observed between study groups at baseline or 12 months in the ratio of the load taken by the trabeculae in relation to the total load (proximal or distal).

Table 29: Finite element analysis outcomes from HR-pQCT at the distal radius

Mean FEA measure	All (n=56)	Group A (n=18)	Group B (n=15)	Group C (n=23)	Difference between A and C*
Stiffness (kN/mm) at baseline	109.9 (22.7)	115.9 (24.0)	109.3 (28.2)	105.7 (16.9)	P=0.12
Stiffness (kN/mm) at 12 months	105.4 (21.3)	111.5 (24.4)	101.3 (24.8)	103.3 (15.5)	
12 month change in stiffness (kN/mm)	-4.6	-4.4	-8.0	-2.4	p=0.22
(95% CI)	(-6.3, -2.8)	(-6.1, -2.7)	(-12.9, -3.1)	(-5.0, 0.1)	
Ultimate failure load (kN) at baseline	5.58 (1.12)	5.86 (1.18)	5.53 (1.38)	5.39 (0.85)	p=0.14
Ultimate failure load (kN) at 12 months	5.36 (1.05)	5.62 (1.19)	5.16 (1.22)	5.29 (0.78)	
12 month change in ultimate failure load (kN)	-0.22	-0.24	-0.37	-0.10	p=0.037
(95% CI)	(-0.30, -0.14)	(-0.32, -0.17)	(-0.60, -0.14)	(-0.21, 0.01)	
Trabecular von Mises stress at baseline	5.36 (0.64)	5.42 (0.56)	5.32 (0.79)	5.35 (0.62)	p=0.70
Trabecular von Mises stress at 12 months	5.31 (0.61)	5.52 (0.64)	5.15 (0.60)	5.26 (0.58)	
12 month change in trabecular von Mises stress	-0.05	0.10	-0.17	-0.09	p=0.14
(95% CI)	(-0.15, 0.06)	(-0.03, 0.23)	(-0.38, 0.05)	(0.10, -0.29)	
Cortical von Mises stress at baseline	7.56 (0.50)	7.71 (0.52)	7.40 (0.51)	7.55 (0.47)	p=0.30
Cortical von Mises stress at 12 months	7.47 (0.47)	7.65 (0.43)	7.26 (0.41)	7.46 (0.49)	
12 month change in cortical von Mises stress	-0.09	-0.06	-0.13	-0.09	p=0.73
(95% CI)	(-0.16, -0.02)	(-0.17, 0.05)	(-0.29, 0.02)	(-0.22, 0.04)	

Trabecular load at distal radius at baseline	65.3 (7.2)	63.1 (9.7)	66.6 (6.8)	66.2 (4.4)	p=0.18
Trabecular load at distal radius at 12 months	67.1 (7.2)	64.9 (8.9)	68.5 (6.4)	68.0 (6.0)	
12 month change in trabecular load at distal radius	1.8	1.9	1.9	1.8	p=0.98
(95% CI)	(0.7, 3.0)	(-0.1, 3.8)	(-1.0, 4.7)	(-0.04, 3.7)	
Trabecular load at proximal radius at baseline	28.8 (7.8)	28.2 (10.1)	28.3 (7.4)	29.5 (6.2)	P=0.62
Trabecular load at proximal radius 12 months	29.5 (7.8)	29.2 (9.7)	29.4 (6.8)	29.8 (7.0)	
12 month change in trabecular load at proximal radius	0.7	0.9	1.1	0.2	p=0.43
(95% CI)	(-0.1, 1.5)	(-0.1, 1.9)	(-0.9, 3.2)	(-1.1, 1.6)	

* Results for baseline and 12 months are means (SD). Baseline p values are derived from ANOVA between groups. For the mean 12-month change, p values are from repeated measures ANOVA testing for an interaction between group and time .

Table 30: Comparison of finite element outcomes between groups A and C

Finite element outcome of interest	Mean difference between group A and C (95% CI)	p-value*
Stiffness (kN/mm)	-1.8 (-4.8, 1.2)	0.24
Ultimate failure load (kN)	-0.14 (-0.26, -0.01)	0.032
Trabecular von Misen's stress	0.17 (-0.06, 0.41)	0.15
Cortical Von Misen's stress	0.04 (-0.13, 0.21)	0.62
Trabecular loading at distal radius	-0.49 (-3.20, 2.22)	0.72
Trabecular loading at proximal radius	0.52 (-1.25, 2.29)	0.56

*Derived from ANCOVA with the 12-month measurement set as the dependent variable, with a fixed factor for group, and the covariates of age, BMI and baseline measurement

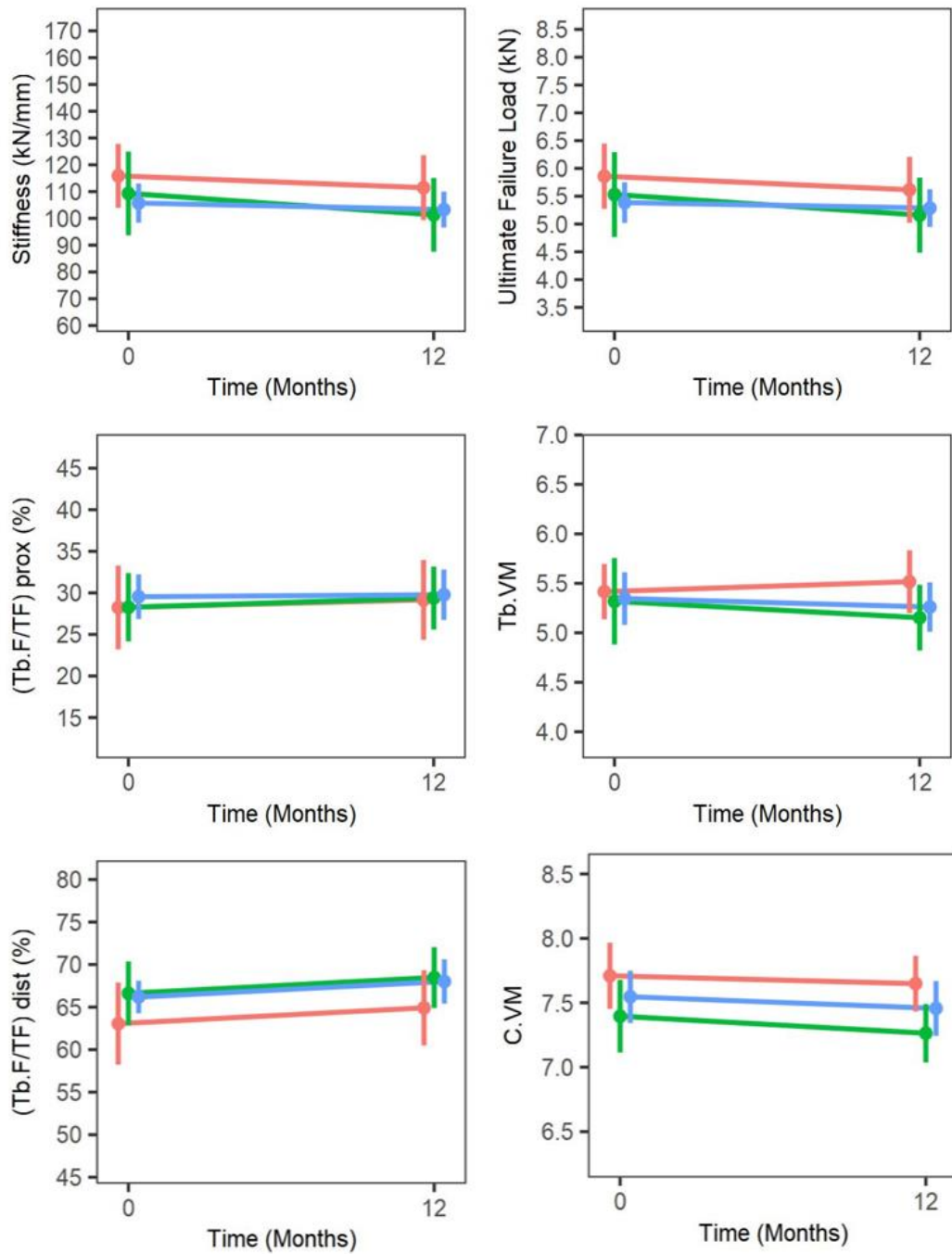


Figure 26: 12-month change in estimates of bone strength and stiffness at the distal radius by HR-pQCT.

The red line represents group A, the green line represents group B and the blue line represents group C. The error bars show the 95% confidence intervals.

4.2 Summary of key findings from this chapter

ADT is associated with significant loss of areal BMD in the first year of therapy, which is most marked at the lumbar spine, but also affects the hip and total body. There is a corresponding reduction in bone mineral content.

ADT causes a significant reduction in vBMD at the distal radius over 12 months, and affects both cortical and trabecular vBMD. Cortical vBMD loss may be increased further when chemotherapy and glucocorticoids are used in addition to ADT in men with metastatic PC. ADT also causes important microarchitectural changes at the distal radius; there was significant loss of cortical area and thickness, and an increase in cortical porosity. Trabecular architecture at the distal radius is also affected by ADT. There is a reduction in the number of trabeculae, increased trabecular separation, gain in trabecular area, and loss of BV/TV.

The first year of ADT is associated with a reduction in stiffness and strength at the distal radius, which may be exacerbated by the use of glucocorticoids and chemotherapy.

Chapter 5: ANTELOPE: Overall discussion

This chapter will summarise and discuss the key ANTELOPE study findings from chapters three and four.

5.1 Study recruitment and retention

A total of 151 potentially eligible participants were screened, and 28 individuals that chose not to participate either did not want additional hospital visits, lived too far away, or did not want to attend an early morning appointment where they were required to have fasted overnight. Another 20 potential participants had either commenced ADT before the window permitted by study inclusion criteria, or other study exclusion criteria were present. There were 2 patients who were unwell to attend their baseline visit, and another 2 individuals could not be contacted to arrange a study visit.

The total number of participants assessed at baseline exceeded the initial target of 90, however another 13 were excluded after the baseline visit. A further 11 participants were lost to follow-up, 7 of whom were in group B, and the overall rate of loss was higher than the 10% that had been accounted for in the study design.

Group A were recruited from urology oncology clinics, and therefore most men in this group had locally advanced PC and were due to undergo radiotherapy in addition to ADT. The number of participants required (30 for group A), and the permitted one-month window between ADT initiation and baseline study visit made recruitment of men with localised PC from general urology clinics difficult. The choice of one month was pragmatic, in order to meet the recruitment target but also to capture the rapid change in serum sex hormones (which can occur within 2-4 weeks of ADT initiation) and the greatest decline in BMD in the first year of ADT. The median time from ADT initiation to baseline visit in group A was 20 days; this was because most had started ADT when they were approached and screened, and there was also a limitation in the availability of study visit appointments. At baseline, the median testosterone level in this group was not at castration level, whereas the 12-month measurement was below the lower limit of detection, suggesting that compliance with ADT over 12 months was acceptable, and that important sex hormone changes occurred as a result of ADT.

Group B were recruited from oncology clinics, and all participants in this group were due to start chemotherapy for metastatic disease. As expected, this group had higher Gleason scores and higher serum PSA than those in group A. Participants in group B were established on ADT, and the protocol had been designed to reflect standard clinical timelines and allowed 3 months between ADT initiation and study participation. The median duration of ADT at the time of the

baseline visit was approximately 2 months. The longer duration of ADT in group B was confirmed by the average baseline testosterone levels, which were below the lower limit of detection. Group B experienced the greatest loss of participants between baseline and 12-month visits. This was due to the advanced nature of their underlying cancer; five participants died from their disease during the study period, and one developed metastatic spinal cord compression and was unable to attend the 12-month study visit.

Group C were recruited from volunteer databases and from advertising. Participants were selected to ensure that baseline age height, weight and BMI did not vary between study groups A and C, in order to ensure that these factors did not for any of the observed changes.

5.2 Changes in sex hormones

Serum testosterone and oestrogen levels were within normal limits for the control group, ensuring that any observed change in our study outcomes were related to the effects of ADT. Serum testosterone levels in group A and B were low at baseline, and the majority of participants had levels equivalent to castration at follow-up. This reflects the duration of ADT at baseline in both groups, and confirms compliance with therapy. Serum testosterone and oestrogen levels decrease rapidly and significantly after just 2-4 weeks of ADT. Ideally, study assessments would have been undertaken at the same time as ADT initiation to maximise accuracy, however in practice this was not possible due to practicalities and logistics. The lower limits of the testosterone and oestrogen laboratory assay precluded analysis of this data as continuous data; the majority of true values lay below the limit of normal detection.

5.3 Bone health

Key determinants of bone health and fracture risk factor data were obtained from questionnaire completion by participants. Data are therefore reliant upon accurate completion and subject to recall bias. At baseline, a very small proportion of all participants were smokers, and most had stopped smoking more than 5 years before baseline study visit or had never smoked. Similar levels of alcohol consumption, dairy intake, calcium and vitamin D supplementation and sunlight exposure were observed between groups, ensuring that the observed changes were not affected by these factors.

Vitamin D deficiency and insufficiency are common in older adults, and also highly prevalent in men with PC ^{342,503,641}. We found that the average serum vitamin D concentration was similar between all study groups, and not indicative of deficiency at baseline. Interestingly, only 14 participants reported taking

supplements of vitamin D in the bone health questionnaire. Over 12 months, vitamin D levels decreased the most in the groups that received ADT, and the reduction in group A was significantly greater than group C. Importantly, the median concentration at 12 months was still above the threshold for insufficiency. The larger reduction associated with ADT may reflect a period of feeling less well, requiring additional hospital visits, feeling unwell with poor oral intake, and an increased likelihood of spending time indoors.

In healthy adults, calcium and vitamin D supplementation reduces fracture risk^{642,643}. Calcium and vitamin D supplementation have formed the control arm in studies of bone targeted agents in men receiving ADT, however daily doses of 200-500IU vitamin D and 1000-1500mg calcium did not prevent bone loss³⁴⁸. No trial has compared the effects of calcium or vitamin D with no supplementation on bone density in men undergoing ADT. There is no clear consensus on the optimal doses required which has been acknowledged by recently published guidelines for the assessment of bone health in men with PC^{345,644,645,646}. Based on current evidence, serum vitamin D should be measured in all men starting ADT, and supplementation offered to those found to be deficient under the guidance of a clinician (up to 4000/IU per day has been reported as safe)^{345,647}. In men who are vitamin D replete, a maintenance dose of 800-1000 units vitamin D per day is recommended³⁴².

5.4 Fracture risk

We did not include ADT and GC as a secondary cause of osteoporosis in the FRAX calculation. ADT had just been initiated in group A and B participants, and group B had not received GC at the time of the first study visit. At baseline, the risks of fracture were broadly similar in study groups, with the exception of an increased risk of MOF in group B compared with controls. We did not expect differences between groups at baseline, as the prevalence of fracture risk factors such as smoking, alcohol intake and parental hip fracture history were similar.

The estimated risk of hip fracture in our study is similar to published data from large studies in male populations^{648,649}. It is also similar to previous data in men with PC, where the risk of hip fracture was between 1- 3%^{458,460,461,467}. The largest study to have addressed this before was undertaken in more than 6000 men participating in the STAMPEDE clinical trial. The risk of hip fracture in men with hormone sensitive PC starting ADT was 3.06% and the risk of MOF was 8.7%, when clinical risk factors were used without BMD⁴⁶⁵.

Reliance on FRAX clinical risk factors without BMD has been shown to produce a higher estimate of fracture risk than FRAX with BMD data.^{458,461} Without BMD, the FRAX algorithm preferentially selects for a low BMD⁶⁵⁰. Our results support this premise, and are likely to reflect the average age of our study population, as FRAX

without BMD is strongly influenced by increasing age⁴⁴⁶. It also emphasises the importance of consideration of non-BMD fracture risk factors, it has been well described that many fractures occur in individuals with normal BMD⁴⁴⁰.

More than three quarters of our study participants had a fracture risk above the threshold for treatment. This is very similar to results from a study in 363 men receiving ADT, where 76.6% of those aged between 70-79 years met the criteria for treatment, and where age had a significant impact on the recommendations for treatment (median age was 72, and half of these warranted treatment, in those aged over 80 years the proportion was 98.8%).

Our results suggest that men starting ADT for PC are at relatively high risk of fracture; over a 10-year period three participants would be expected to experience a hip fracture, and over 8 would have a MOF. As our risk assessment was undertaken before the effects of ADT and GC use were considered, it is likely that we may have under-estimated the ongoing risk in the ADT treated men. One study found that inclusion of ADT as a risk factor for secondary osteoporosis increased the risk of hip fracture from 1.8% to 3.1% in men with PC, and the proportion requiring treatment based on intervention thresholds increased from a third to just over half⁴⁵⁸. In general, there is a lack of prospective and robust data in large, multi-ethnic cohorts, and future studies should seek to correlate FRAX with fracture end points, compare FRAX in ADT and non-ADT treated men, and explore the relationship between fracture risk and duration of ADT.

5.5 Prevalence of frailty

Frailty is an important clinical syndrome, which predicts falls, disability, loss of independence and mortality in older patients. The established methods for frailty identification are the Fried phenotype model³⁵³, the cumulative deficit model⁵⁴⁹ and comprehensive geriatric assessment (CGA)⁵⁵⁰. CGA is a multi-disciplinary and multi-dimensional assessment which is time consuming and not routinely part of oncology clinical practice. Screening tools may predict those likely to benefit from CGA (such as G8, VES) but there is a lack of consensus as to which tool should be used. The phenotype method was used in this study, as frailty was a secondary outcome and the data for the components were collected as part of the planned study assessments.

We found that the prevalence of frailty at baseline was highest in group B, where the duration of ADT was longest. More than two thirds of group B participants were either frail or pre-frail. After 12 months, pre-frailty and frailty increased in both ADT groups (A and B), with the greatest change from baseline in group A.

Our results suggest that ADT may accelerate the development of frailty in men with PC. This is to be expected, given the overlap between the components of the phenotype model and the known adverse effects of ADT (such as fatigue). In

general, frailty is a dynamic process, and transition to a level of worse frailty is more common than improvement ⁵⁴⁷.

In addition to ADT, the underlying physiological changes present in men with PC (such as chronic inflammation and alterations in metabolism), the effects of cancer treatment and comorbid conditions are also likely to have contributed to our study findings. A recent study in 146 men with PC receiving ADT found that 29% and 10% were pre-frail and frail, which increased to 47% and 15% when the adapted obese frailty phenotype model was used (this substitutes weight loss for BMI >30kg/m², to account for sarcopenic obesity that is associated with ADT) ⁶⁵¹. In men with PC, ADT use increases the likelihood of men being classified as frail or pre-frail, and also predict falls ^{553,652}. A recent case control study reported that the prevalence of frailty increased over 12 months, and was related to reduction in grip strength ⁶⁵³.

Frailty is common in all cancer patients; a systematic review reported the prevalence of frailty and pre-frailty as being 42% and 43% respectively ⁵⁴⁸. It has also been associated with increased mortality and poor tolerance to treatment. Given the association of frailty with important clinical outcomes such as hospitalization and death, this potential consequence of ADT should be considered carefully when initiating ADT in older men with PC. Guidelines have been developed which specifically recommend assessment of frailty status in older patients ⁶⁵⁴. However, implementation into clinical practice requires increased awareness amongst and education of clinicians, and the availability of resources in clinical settings. Further studies should seek to identify risk factors for frailty in men receiving ADT, and seek to explore effective interventions that can halt the ADT-associated decline in frailty status.

5. 6 Tests of physical function

We found that ADT was associated with a decline in grip strength over 12 months. The greatest loss of grip strength was in group A who had recently started ADT. Group A lost 4.3kg, compared with a small loss of -0.4kg. A related finding that will be discussed later was a significant loss of lean mass in the upper extremities of group A, compared with C.

Our results support published cross-sectional data that have demonstrated that ADT is associated with an overall decline in upper body strength ^{294,655}. A longitudinal study in 109 patients with PC compared grip strength over 12 months ⁶⁵⁶. In those receiving ADT, there was a significant decline in grip strength after 12 months compared to baseline (p=0.04). This was significantly greater those that did not receive ADT (p=0.01). Radiotherapy treatment, Gleason score and co-morbidities were not predictive of changes grip strength in this study.

Another longitudinal study compared grip strength in men with PC receiving ADT, men with PC not receiving ADT and healthy controls. Grip strength significantly

declined after 3 months in the ADT group, and between 3 and 12 months, grip strength in the ADT group remained stable. There was no change in grip observed in the other study groups. Similarly, our study findings that group A lost more grip strength than group B (group A had received ADT for longer) which suggests that the most rapid decline in grip strength may occur shortly after ADT initiation. It is possible that upper body strength is more susceptible to the effects of ADT, as lower body muscle is more subject to daily usage and intensity, for example walking, climbing stairs and standing up from a seated position. Prospective longitudinal studies are required to determine the true rate of grip strength loss during the first year of ADT, and should also correlate loss of strength with functional impairment and impact on quality of life. Many studies have sought to develop exercise intervention programmes to mitigate loss of muscle strength associated with ADT. Related to our findings, a recent study reported that early targeted exercise intervention at the onset of ADT may not only preserve, but also improve muscle strength and physical function ⁶⁵⁷.

The SPPB score was calculated out of 12 points, and the changes were minimal over 12 months. This was possibly due to the fact that all participants in all groups scored the maximum of 4 points for the assessment of balance, and variations in the total score were due to changes in gait speed and chair stand test. Group A lost a mean of 0.55 points, whereas group C gained 0.36 points. This was a significant difference ($p=0.001$), and could be explained by loss of lean mass and gain of fat mass that are associated with ADT. Another explanation may involve reduced physical activity levels in group A (related to ADT-associated fatigue or effects of radiotherapy treatment). The improvement observed in group C may also reflect practice effects, whereby positive changes in performance are due to familiarity with the task.

A previous study in men receiving ADT reported a decline in SPPB score over 3 months, and an increased risk of falls ⁶⁵⁸. A cross sectional study comparing men with PC on no ADT, short term and long term ADT and healthy controls found that long-term ADT was associated with significantly slower gait speed, and lower SPPB scores than controls ⁵⁹². A lower SPPB score has also been associated with impairment in daily activities (IADL) in older men with PC ⁶⁵⁸.

Group B had a small increase in SPPB score, which was not expected. This group were receiving ADT and chemotherapy and steroids, the effects of which would usually be loss of proximal and skeletal muscle. A possible explanation could be that those able to complete the study assessments were by definition, relatively physically fit compared to those who had progressive disease and/or were lost to follow-up. The number of participants in group B that completed the study was low, and repeating the SPPB assessment in a similar group over 12 months would help to improve the accuracy of our initial results in this group.

The advantages of the SPPB score are its ease, lack of equipment and space required and high reliability and validity⁶⁵⁹. Its minimally clinically important difference (MCID) has been established; a one-point change leads to a meaningful difference to an individual in the risk of future mortality and morbidity and loss of independence^{590 660}. However, the SPPB is limited in its ability to distinguish performance in high functioning individuals, and there is a ceiling effect when used in active and independent study participants⁶⁶¹. This was also demonstrated by our results, all participants scored a maximum of 4 points for the assessment of balance. A 400m walk test may be a more robust method of assessing physical performance, however is limited by the space and time available.

5.7 Changes in body composition

Compared to the control group, ADT was associated with an increase in BMI, total fat mass and total percentage of body fat over 12 months. There was a large increase in trunk fat mass in both ADT groups, whereas the control group lost fat mass at this site. Further analysis of upper limbs was undertaken to explore a possible relationship with of grip strength. Group A lost upper limb lean mass and gained fat mass, Group B also gained fat mass but there was only a very small difference in lean mass over 12months. The control group did not experience much change in upper limb composition over the study period.

In healthy men, androgen levels decline with increasing age. This is due to a combination of both primary testicular failure (loss of number of leydig cells and decreased responsiveness to gonadotrophins) and the secondary disruption of the hypothalamic-pituitary axis (decreased GnRH production or increased suppression)^{662,663}. There is also an age-related increase in SHBG levels. Low levels of circulating androgens increase fat mass and decrease lean mass⁶⁶⁴. Replacement of testosterone in men with acquired hypogonadism can reverse the changes on body composition, however this is clearly not possible in men receiving ADT for PC.

Several studies have demonstrated accelerated loss of lean body mass and gain in body fat in men during the first 12 months of ADT. This condition is termed sarcopenic obesity, and predisposes men to frailty, falls and fractures⁶⁶⁵. Infiltration of muscle by adipose tissue impairs its strength and function⁶⁶⁶, and the pro-inflammatory state that is associated with obesity (and with malignancy) exacerbates sarcopenia further⁶⁶⁷. Meta-analysis has suggested an average 7.7% increase in fat mass during the first year of ADT, although there was considerable variation in study design and methodology²⁶³. One study investigated the 3-month change in body composition after ADT initiation, and reported a mean increase of 1.7kg in total fat mass, suggesting that the effects of ADT on adiposity may occur rapidly after the onset of ADT²⁸⁴.

Our results show an increase in trunk fat mass associated with ADT. Prior studies have also reported that ADT seems to increase abdominal subcutaneous fat (rather than intra-abdominal fat), with reported gains of 1.4-1.9% in waist circumference after 6-12 months of ADT^{668,669}. Low circulating testosterone levels may increase abdominal fat via loss of the inhibitory effect of testosterone on triglyceride uptake and lipoprotein lipase activity in abdominal, but not in peripheral subcutaneous fat⁶⁷⁰. It may also promote stem cell differentiation into adipocytes, and has motivational effects that lead to decreased physical activity⁶⁷¹. Testosterone also stimulates lipolysis and reduces intracellular fat storage⁶⁷². Abdominal adiposity is a risk factor for several important cardiometabolic sequelae such as insulin resistance, hyperglycaemia, dyslipidaemia, hypertension and cardiovascular disease, and is independent of BMI^{673,674}. The effects of ADT are compounded by a relatively high incidence of obesity, hypertension, hyperlipidaemia and cardiovascular disease in men diagnosed with PC, before ADT is even initiated⁶⁷⁵. Increased fat mass and increased BMI are associated with other negative outcomes in men with PC; they are predictive of skeletal related events and may also increase the risk of death⁶⁷⁶⁶⁷⁷. A meta-analysis of prospective cohort studies found that PC-specific mortality increased by 15% per 5kg/m² increase in BMI⁶⁷⁸.

In our study, lean mass (total, and trunk) reduced in group A and C over 12 months, but did not decrease in group B. It is difficult to explain these findings. It was expected that Group B would experience the greatest loss in skeletal muscle; this group had the longest exposure to ADT and also had metastatic cancer with its associated catabolic state. Group B participants also underwent chemotherapy during the study and would be more likely to have low physical activity levels. Importantly, this group also received a moderate dose of glucocorticoids, which cause muscle atrophy via increased protein degradation (by the ubiquitin-proteasome and autophagy lysosome systems), decreased production of anabolic factors such as IGF-1, and impaired protein synthesis⁶⁷⁹. It is possible that the group B participants able to complete all study assessments were exceptionally fit for their age, or modified their lifestyles to aim to maintain good health in the context of an incurable malignancy. The number of participants in this group was relatively low, and investigation in a larger group would be helpful to improve the accuracy of our findings.

The loss of skeletal muscle mass that was observed in group A was similar to previously published data in men receiving ADT. In general, ADT has been associated with a larger gain in fat mass than the loss of lean mass (and an overall gain in BMI), which occurred in group A. The loss of lean mass was 0.9%, 0.7% and 3.7% in the whole body, trunk and upper limbs, respectively. However, once adjustment had been made for age, BMI and baseline value, only the loss of skeletal muscle in the upper limbs was significantly more than the control group.

Previous studies have found that ADT is associated with between 2- 4% loss of total lean mass over 12 months ^{202,680,289,290,681}, and a recent meta-analysis reported an average loss of 2.82% (95%CI -3.64 to -2.01%) over the same period ²⁶³. This occurs on a background of 1-2% annual age-related loss of lean mass in healthy men ⁶⁸². One study identified 1.4% loss of skeletal muscle after only 3 months of ADT ²⁸⁵. Other authors have also identified that the most rapid loss of lean mass occurs during the early phase (first 6-9 months) of ADT ^{290,680,262}. In addition, men aged over 70 years who receive ADT are at increased risk of sarcopenia compared to younger men ²⁶², and ageing (and related changes) is clearly an important contributor. The majority of published studies included patients receiving GnRH agonists as the standard method of ADT. The BLADE study has published the first results of the effect of GnRH antagonists on body composition (these are increasingly used in men with metastatic PC) ^{683,201}. The results suggest that lean mass may be relatively preserved by GnRH antagonists, however larger prospective studies are required to explore this further ⁶⁸³.

We observed a notable loss of lean mass in the upper arms in group A, who lost significantly more than the control group over 12 months. This was associated with a reduction in grip strength in group A as described above. Our findings are similar to published data, which suggest that upper extremity strength is significantly reduced after only 3 months of ADT and gradually declines over the course of the first year ^{274,656}. Upper limb musculature may be more susceptible to ADT-induced hypogonadism and loss of the anabolic effect of circulating sex steroids. Upper extremities are also usually less subject to daily use (walking, standing) than lower limbs. Upper limb strength has been improved or maintained when exercise interventions have been compared to usual care in men receiving ADT ⁶⁸⁴.

Sarcopenia is multi-factorial, and in men with PC receiving ADT it affects physical function, notably lower limb muscle strength ⁵⁴¹. Men receiving ADT are at increased risk of falls and associated injuries and fractures; one study found that around one quarter of current and past ADT users were recurrent fallers, compared to 5% of those that did not receive ADT ⁶⁵².

Guidelines are available for the management of ADT-related effects on body composition. Suggested interventions may also have a beneficial effect on the adverse metabolic consequences of ADT, and generally involve increasing awareness amongst clinicians, risk identification, lifestyle interventions and/or pharmacotherapy ^{645,153,685}. However, published guidance varies in content, by region and also by the composition of the expert group providing recommendations. The optimal strategy to prevent or reverse ADT-associated changes in body composition is not yet clear.

Exercise has an important role in reducing the burden of the undesirable consequences of ADT. Progressive resistance training can prevent and to reverse

muscle loss in non-cancer populations of older individuals⁶⁸⁶. In men receiving ADT, it can maintain lean mass, reduce fat mass and percentage body fat, and improve arm strength^{687,688,689,690,691}. Exercise can also improve cancer-specific fatigue, quality of life, physical fitness and function in men receiving ADT for PC³⁴⁹. However, there is no consensus as to the most effective exercise programme in terms of frequency, type and duration of exercise in order to achieve these outcomes. Current UK NICE guidelines for PC recommend a 12 week supervised programme of exercise for men starting ADT¹⁵³, however this is not yet standardised or embedded in cancer care. Despite support and engagement from patients, less than 20% of NHS trusts currently have provision for this³⁵⁶. Concerns have also been raised regarding the sustainability of exercise after a period of intervention, which are not maintained after supervision is withdrawn⁶⁹². Ongoing trials aim to explore the efficacy and cost effectiveness of long term exercise interventions in men with PC, and also explore the role of technology^{693 358}.

5. 8 Changes in biomarkers of bone turnover

5.8.1 Resorption and formation markers in non-metastatic prostate cancer

Our study findings suggest that ADT increases bone turnover in men with non-metastatic PC. Compared to the control group, there was an increase in formation (PINP and OC) and resorption (CTX) markers in group A.

Our results are consistent with most other studies in which men treated with ADT for non-metastatic PC had elevated biomarkers of bone turnover when compared with former ADT users, men treated with antiandrogens, PC controls and healthy controls^{231,294,233,290,694,695}. A 12-month prospective study compared men with PC who had received ADT for less than 6 months (acute ADT), more than 6 months (chronic), no ADT, and age-matched healthy controls²⁹⁰. After 12 months, the formation markers PINP, CTX and BALP were significantly elevated in the acute ADT group compared to all other groups (all $p < 0.05$). The resorption marker NTX was elevated in all men treated with ADT compared with men not on ADT. Those with the highest level of bone turnover markers experienced the greatest loss of BMD at multiple skeletal sites over 12 months. The combination of accelerated bone turnover and loss of BMD increases the fracture risk in this population, and could be used in the future to identify a subgroup of men at high risk of bone loss and fracture after ADT is initiated.

A small study compared 12 month change in bone turnover markers in men starting GnRH agonist therapy, compared with age-matched healthy controls⁶⁹⁶. After 12 months, ADT was associated with a significant increase in the resorption marker NTX, compared with controls. The formation markers bone sialoprotein and OC did not differ between groups. A recent study compared men that used ADT with former ADT users and healthy controls²³⁴. Cross sectional analysis at baseline

found that PINP and CTX were higher in men who had ongoing ADT. However longitudinal analysis did not find a difference between groups in the change in PINP or CTX over 6 months. The authors acknowledged that the study was limited by small numbers and lack of statistical power to detect differences between groups.

Another study sought to investigate the relationship between ADT, markers of bone turnover and sex steroids in men with PC treated with and without ADT. The authors observed higher CTX and bone sialoprotein levels in patients receiving ADT compared with patients with no ADT, after adjustment for age. There was no relationship between circulating androgens and bone turnover, however oestrogen levels were inversely correlated with OC, BALP and TRAP5b. These findings highlight the importance of oestrogen in bone turnover in males. It is an important determinant of peak bone mass⁶⁹⁷, and exogenous oestrogen has been found to improve BMD and reduce bone turnover in men with aromatase deficiency⁶⁹⁸. In elderly men treated with both a GnRH agonist and an aromatase inhibitor, oestrogen (but not testosterone) prevented an increase in bone resorption⁴²⁹. Oestradiol therapy has also been associated with reduced bone turnover in men with PC receiving ADT⁶⁹⁹.

Bisphosphonates may be used to reduce bone turnover that is associated with secondary hypogonadism due to ADT. A comparison between ADT and ADT and pamidronate found that ADT alone led to a significant increase in BALP, OC and NTX over the 48-week study period²⁰⁵. In the pamidronate group, markers generally decreased and returned to baseline levels.

5.8.2 Resorption and formation markers in metastatic prostate cancer

Bone metastases in men with PC are usually osteoblastic, with an increase in both bone formation and resorption. We found high levels of baseline PINP and CTX in this group, indicative of a high bone turnover state. The baseline serum PINP concentration in group B was four times greater than the value for groups A and C, and CTX was twice as high in group B as groups A and C. These baseline measurements are expected, and reflect the high prevalence of metastatic bone disease in group B, which is associated with increased markers of bone turnover in previous studies. Complex interactions between PC cells and the bone microenvironment involve the upregulation of osteoblast stimulatory factors by PC cells (such as PDGF, FGF, IGF-1, BMPs and Wnt) and release of factors that facilitate bone formation such as VEGF and endothelin 1^{327,328,329}. PINP is produced as a result of type 1 collagen formation.

Over 12 months, PINP levels fell considerably in group B. This is most likely as a consequence of docetaxel chemotherapy which was used in this group, and reflects a response to treatment in the bone metastases. The cytotoxic effects of docetaxel are exerted by its ability to stabilise microtubule assembly and prevent microtubule

depolymerisation. This prevents mitotic cell division and leads to accumulation of microtubules and causes apoptosis. In men with metastatic PC, docetaxel is effective in both the hormone-sensitive and castration resistant settings⁷⁰⁰⁻⁷⁰².

CTX levels were high at baseline in group B and increased slightly over 12 months. The change in group B was more than we observed in group C but much less than group A. The use of chemotherapy and glucocorticoids seems to have limited the increase in bone turnover that is associated with ADT, possibly due to a reduction in burden and activity of the metastatic bone disease.

Osteocalcin (OC) is a marker of osteoblast function, and is increased in association with high bone turnover. Serum OC levels increased over 12 months in group B, but to a lesser extent than was observed in group A. This difference is likely to be explained by the use of glucocorticoids, which were given alongside docetaxel based chemotherapy in group B participants. It has been shown in previous clinical studies that glucocorticoids reduce serum OC levels in a dose-dependent manner^{703,704} via modification of the OC gene itself, and also its promoter sites^{705,706,707}.

In general, we observed changes in bone turnover that occurred as a result of three therapeutic agents (ADT, glucocorticoids and docetaxel) that were used in group B participants. The overall picture is complex, and it is difficult to distinguish between the effects of the treatments on bone turnover, and changes related to underlying metastatic bone disease.

5.9 ADT and osteoclast activity

TRAP5b is a sensitive marker of osteoclast number and bone resorption, and the greatest increase was in group A. A previous study in men with PC has reported similar results in men treated with ADT, compared with PC controls, and also found inverse correlation between TRAP5b levels and serum total testosterone ($r=-0.33$, $p=0.009$) and oestradiol ($r=-0.28$, $p=0.003$)⁷⁰⁸. Osteoclast activity measured by TRAP5b levels can be modified by bone targeted agents such as denosumab, and those with highest TRAP5b levels may benefit the most^{281,709}. However, denosumab is not currently approved in the UK for routine use to suppress bone loss that is associated with ADT¹⁵³.

Although TRAP5b results increased the most in group A, group B had the highest average serum measurement at baseline and at 12 months. The baseline result reflects the autocatalytic vicious cycle of bone metastasis propagation, where cancer cells release substances that mediate the upregulation of RANKL and inhibit OPG and osteoclast activity. The 12 month TRAP5b change in group B was smaller than groups A and C, which may reflect a high level of baseline osteoclast number and activity related to the presence of bone metastases.

Over the 12-month study period there was no significant difference between groups A and C in the change in TRAP5b, and our findings suggest that may not be a useful marker of ADT-associated changes in bone turnover. However additional data are required to explore this further in larger studies.

5.10 ADT and osteocyte activity

Sclerostin is encoded by the SOST gene, and is one of the main secreted products of osteocytes⁸⁶. It is considered to be a major negative regulator of bone formation via the inhibition of Wnt signalling and promotion of osteoclast activity. Levels increase with age and are higher in men⁷¹⁰. Over 12 months, we observed a two-fold greater increase in serum sclerostin in group A compared with group C. However, this did not reach statistical significance when adjusting for baseline value, age and BMI.

Increased serum sclerostin in group A is an expected finding, as ADT increases bone turnover. Overexpression of the SOST gene is associated with osteopenia, and sclerostin has also been positively correlated with both BMD and T score^{711,712}, and is associated with reduced risk of fracture in older men⁷¹³. Oestrogen deficiency increases sclerostin and is associated with bone loss; this can be prevented by oestrogen replacement in postmenopausal women⁷¹⁴. A study in elderly men used GnRH to induce sex steroid deficiency, and found that oestrogen (not testosterone) prevented an increase in sclerostin⁷¹⁴. The interaction between oestrogen and sclerostin may be due to the effects of oestrogen on the Wnt/ β -catenin signalling pathway; oestrogen binds to its receptor via factors involved in this pathway such as prostaglandin E2^{715,716}.

Only a few studies have investigated sclerostin in the PC setting. A cross sectional study found that sclerostin levels were higher in men with non-metastatic PC than in healthy controls⁶⁹⁵. They are also higher in men with PC on ADT, compared with PC controls that did not have ADT⁶⁹⁵. In addition to the relationship between oestrogen and sclerostin described above, there was an inverse relationship between serum sclerostin and circulating testosterone in men with PC on ADT. Both sex steroids therefore appear to have important roles in the regulation of bone metabolism; which is in agreement with studies that have investigated other biomarkers of bone turnover in older men. In general, oestrogen appears to be the dominant sex steroid that regulates bone resorption, whereas both oestrogen and testosterone are important in maintaining bone formation^{429,714}.

Our study results found a small increase in serum sclerostin in group B over 12 months, and this was less than group A and only slightly more than in the control group. Importantly, there is differential expression of sclerostin in the circulation, and in bone⁷¹⁰. In animal models, high sclerostin levels reduced PC invasion and the development of bone metastases^{717,718}. Therefore, evaluation of sclerostin at

tissue level is required to accurately determine its contribution to metastatic bone disease ⁷¹⁹. Previous PC studies have found high levels of sclerostin associated with bone metastases ^{695,720}, which may be related to PC cell production of cytokines such as BMP-6 ⁷²¹. High sclerostin levels inhibit Wnt signalling that is required for the initiation and progression of metastasis ^{722,723}. However, the underlying mechanism that leads to increased sclerostin at sites of predominantly osteoblastic bone metastases remains to be determined; a possible explanation is that it may be a compensatory response to increased osteoblast activity.

There may be a future role for anti-sclerostin antibodies in the management of metastatic bone disease. Evidence for their efficacy has been established in osteoporosis ⁷²⁴, and they may promote bone formation, prevent cancer-induced bone loss, and reduce the rate of progression of bone metastasis in cancer populations ^{725,726,727}. Although initial results are encouraging, much work remains to be done to understand the exact contribution of sclerostin to each of the stages of cancer metastasis, and to cancers other than breast and myeloma, in which the majority of data to date have been published.

The observed increase in sclerostin in group B may also have been affected by the use of glucocorticoids. The literature regarding the effects of glucocorticoid use and sclerostin levels is contradictory. In mouse models, glucocorticoids increase SOST gene expression ⁷²⁸, and sclerostin deficiency or inhibition maintains bone mass and integrity in conditions of glucocorticoid excess ³⁹¹. Glucocorticoids have also been associated with increased osteocyte apoptosis ⁷²⁹. In human studies, results have been mixed. One study found that 12 months of glucocorticoid treatment significantly increased serum sclerostin ⁷³⁰, whereas other studies have reported the opposite ^{731,732,733}. In general, data are scarce, and limited by poor study design (non-blinded or randomised) different assays used, heterogeneity of study populations, doses and forms of glucocorticoids and duration of follow up.

5.11 Conclusion: the effects of ADT on biomarkers of bone turnover

ADT was associated with an increase in the rate of turnover compared to the control group, based upon significantly increased levels of PINP and osteocalcin in group A, and also a trend towards a greater increase in CTX. We can be confident that our findings are accurate, as the groups were well matched by size and age, the groups were similar at baseline, and adjustment was made for age, baseline value and BMI when the 12 month changes were compared. Similar values for CTX, PINP and osteocalcin at baseline suggest that important ADT-related changes in these markers had not occurred at the time of the baseline study visit. In group B, the combination of ADT, chemotherapy and glucocorticoids caused PINP levels to fall over 12 months, and there were slight increases in CTX and osteocalcin, that were greater than in the control group, but that had been attenuated by the likely

response of the bone metastases to systemic therapies. Despite a reduction in PINP and smaller increases in CTX and osteocalcin than group A, the average 12 month values for these markers in group B was still higher than in group A, indicative of an underlying high bone turnover state.

Trap5b levels increased the most in group A, however the change was not significantly greater than in group C, and the highest levels of Trap5b were observed in group B. Sclerostin levels increased the most in group A, but there was no difference between groups over 12 months. We have confirmed that ADT is associated with a disruption in bone homeostasis, and that non-invasive measurement of markers of bone turnover is feasible and can detect important changes. Whether these changes are related to important density and microstructural changes is not clear, and future work should seek to investigate this further, in addition to their relationship with fracture outcomes in men treated with ADT.

5.12 Changes in areal bone mineral density

Between 1-2% loss of BMD is lost on an annual basis, in healthy men. Men with PC appear to lack knowledge about the risk of treatment-associated bone loss and the role of lifestyle modifications, which is not always considered by clinicians^{734,735,346}. It is also evident that a low proportion of men starting ADT currently undergo routine BMD testing⁷³⁶, despite evidence that it is a cost-effective intervention⁷³⁷ and recommended by guidance^{345,346,153,738,145}. This is in contrast to breast cancer, where guidelines are well established for the assessment and management of bone loss related to cancer treatment, and consideration of bone health is standard practice⁷³⁹⁻⁷⁴¹.

Our study excluded men found to have osteoporosis at baseline, as abnormal baseline values would have affected our findings, and allowed the affected individuals to seek appropriate and timely treatment. We excluded 6 men found to have osteoporosis at baseline; five of these were in the ADT groups and only one was a healthy control. Our findings at baseline support previous data that osteoporosis (and osteopenia) are more common in men with PC than healthy men, and are also more common in men with PC receiving ADT, than PC controls⁷⁴².

Between 3.9% and 37.8% of hormone naïve men with PC were found to have osteoporosis by a recent meta-analysis, this was lower than in men with PC receiving ADT (prevalence 9-53%) but greater than in healthy older men (6-10%)²¹¹. Another study reported an incidence of osteoporosis of 42% in men with PC compared with 27% of age matched healthy men ($p=0.022$)⁷⁴². Evidence also suggests that less than one in five men with PC due to start ADT have normal BMD²⁰⁹, and data from prospective studies has shown that BMD is lower at the lumbar

spine, hip and forearm in men starting ADT for PC, compared with age-matched healthy controls^{243,743}. Q-CT may also increase the diagnostic yield of osteoporosis when compared more established DXA techniques⁷⁴⁴. The increased prevalence of osteoporosis in men with PC is likely to be multifactorial; related to age, co-morbid conditions and other fracture risk factors. However, data from our study and from published literature suggest that PC itself may be a risk factor for osteoporosis, independent of ADT or age. In those with metastatic disease this could relate to increased bone resorption, and in those with localised or locally advanced disease could relate to PC cell production of PTHrP or other similar factors that act to disrupt the bone remodelling equilibrium³²⁸.

Once individuals with osteoporosis had been excluded from ongoing study participation, baseline BMD and BMC were similar between study groups at all skeletal sites. This suggests that important ADT-related changes had not occurred before study participation (the median time from ADT initiation to baseline visit was 20 days in group A and 57 days in group B). The study exclusion criteria ensured that observed differences between groups were related to ADT rather than other influences on bone. In addition, we excluded men with metastatic bone disease affecting the spine from group B, in order to improve the accuracy of our DXA spine results.

We found that ADT was associated with significant loss of areal BMD at the LS, FN, TH and TB and loss of BMC over 12 months ($p < 0.001$ for all comparisons). The skeletal site that experienced the greatest reduction in areal BMD was the LS, where losses were 3.94% and 5.9% in groups A and B, respectively. Loss of BMD at TH, FN and TB were between 2.8% and 3.8% in groups A and B, and there was a small gain in BMD at all sites in group C.

ADT has previously been associated with loss of areal BMD. However, the magnitude of change has varied by the skeletal site(s) measured, methodology and number of participants. Only a few longitudinal studies have investigated change in BMD in the period following ADT initiation. A comparison of 62 men starting ADT for PC and age-matched PC controls not receiving ADT found that ADT was associated with significant BMD loss over the first 12 months²³⁸. The mean losses in the ADT group were 4.8% at LS, 2.99% at FN and 3.76% at TH. A similar study in 185 men with hormone naïve PC and healthy controls reported that BMD decreased the most at the LS and TH in the ADT group, and significantly more than in the control group ($p = 0.004$ for LS and < 0.001 at TH)⁷⁴³. After 12 months, the prevalence of osteoporosis at the LS was 18% in men receiving ADT (4% of these had vertebral fractures identified) and 4.8% in the control group. Both of the above studies included an additional year of follow-up between 12 and 24 months after ADT initiation. BMD loss continued at a significantly greater rate than the control groups, but it was less than the change observed over the first 12 months of ADT^{238,743}.

Another study found a significant decrease in LS and TH BMD over 12 months following ADT initiation ⁶⁸¹. BMD loss was greater than 2% at the LS and TH in 54% and 43% of participants, respectively, with a parallel reduction in BMC. Another study compared BMD in men with PC due to commence ADT with age matched healthy controls over 12 months. BMD loss was greatest at TH (-3.3%) and ultra-distal radius (-5.3%) in the ADT group, with no change in the control group ⁶⁹⁶. ADT was associated with decreased BMD at all other sites measured (2.3-2.8%) but these were not significant when compared to baseline, likely due to a lack of power due to a small number of participants.

BMD change at TH was over 12 months was investigated along with body composition in men receiving ADT ²³⁶. The authors reported a 1.9% reduction in TH BMD over 12 months, which was a smaller change than we observed at TH (3.3% and 2.8% in groups A and B, respectively). However, the duration of ADT and age of participants varied from our study; one third had been on ADT prior to study entry, and the average age was only 66 years, which may account for the difference.

A recent cross sectional study included a group of men on ADT, with a median duration of ADT of 12 months. In comparison to healthy controls and PC controls (no ADT), the ADT group had 7.2% lower BMD at LS than PC controls ($p=0.037$) and 7.8% lower BMD than healthy controls ($p=0.01$) ²¹⁵.

In addition to longitudinal changes in BMD, some investigators have explored the temporal relationship between ADT and BMD. A 12-month prospective study compared men receiving acute ADT (less than 6 months), chronic ADT (more than 6 months), no ADT, and healthy controls ²⁹⁰. Compared to baseline, acute ADT was associated with a significant reduction in BMD at TH (-2.5%), trochanter (-2.4%), radius (-2.6%), total body (-3.3%) and the greatest loss of -4.0% was observed at the LS (all p values <0.05). Chronic ADT was associated with loss of BMD at the radius, with no difference in the no ADT or control group. Another comparison of similar groups (acute and chronic ADT, healthy controls) also included a group of former ADT users ²³⁴. Chronic ADT was associated with reduced TB BMD compared with all other groups in cross sectional analysis ²³⁴. After 6 months, there was significant loss of BMD at the distal forearm (4.08% and 2.7%, $P=0.012$ and 0.026 , respectively) in acute and chronic ADT groups, with smaller but non-significant loss of FN BMD (-1.52%, $p=0.42$ in acute ADT group; -1.4%, $p=0.16$ in chronic ADT). Former ADT users experienced a significant gain in BMD at LS (+2.84%, $p=0.0076$) and FN (+1.59%, $p=0.002$). These findings suggest that it is possible to recover TB BMD after ADT discontinuation, and support previous observations that ADT causes loss of BMD that is most marked during the first 6-12 months of treatment.

Compared to most other skeletal sites, the LS has a high proportion of trabecular bone (approximately two thirds), which is more metabolically active than cortical bone and may be more susceptible to ADT-related changes

pQCT at the distal radius in men with PC reported a similar rate of scan exclusion due to movement (19%)⁶⁸⁰. Motion artefact is a well described shortcoming of HR-pQCT, and occurs as a result of tiny movements (as small as 50µm) over the scan acquisition period of up to three minutes. It is extremely difficult to prevent all movement, even when peripheral skeletal sites are immobilised in a cast, the risk is slightly less when HR-pQCT is used at the tibia⁶³⁹. Motion artefact ultimately leads to poor image quality and can introduce error into measurements, especially microarchitectural parameters⁶⁴⁰. Although grading systems have been developed^{639,752}, motion scoring is a subjective assessment with poor agreement between assessors⁶⁴⁰. To ensure accuracy of our data, our radiation protection assessment allowed for one repeat scan if there was significant movement during the first scan. Study participants with significant motion at baseline did not have a follow-up scan, and both baseline and follow-up scans were excluded when motion was problematic at follow-up.

Using HR-pQCT, we found that ADT was associated with a significant reduction in vBMD, with a mean difference of -11.7mg HA/cm³ (p<0.001) between group A and the control group. The loss of vBMD was very similar in groups A and B (-13.7 and -13.5 mg HA/cm³, 4.1% and 4.3% respectively). Loss of cortical vBMD accounted for the majority of the decline in total vBMD; group A lost 3.2% of cortical BMD, with a 1.12% reduction in trabecular BMD. The annual loss of vBMD in healthy older men is between 0.5% and 1.0%⁴¹⁶, which is similar to our findings in the study control group (0.42% total vBMD loss). Our results demonstrate that ADT is associated with accelerated loss of total BMD, and affects both cortical and trabecular bone.

Only a few studies to date have used HR-pQCT to assess vBMD in men with PC receiving ADT. Our findings correspond with those from a prospective observational study of 26 men with non-metastatic PC starting ADT, with a similar mean age (70.6 years) and BMI (27.6kg/m²) to our study cohort. vBMD was measured at the distal radius at baseline, 6 and 12 months⁶⁸⁰. Over 12 months, vBMD decreased by 5.2%, mostly due to a 3.4% reduction in cortical vBMD, with a 1.1% loss of trabecular vBMD.

A cross sectional study included 70 men with PC on ADT (median duration of 12 months), 52 PC controls (o ADT) and 70 age matched healthy controls²¹⁵. At the distal radius, total vBMD was significantly lower in the ADT group than in the PC and healthy controls (14.4% and 12.2%, respectively, p=0.001 for both). Trabecular vBMD was also significantly lower than PC controls (14.8%, p=0.003) and healthy controls (10.7%, p=0.029). Cortical vBMD was not reported, and there were no differences in vBMD between groups at the proximal radius.

A feasibility study in 22 men who had recently started ADT for PC used HR-pQCT techniques at the radius and tibia⁶³⁵. Trabecular vBMD at the radius was negatively correlated with the duration of ADT and positively correlated with

serum testosterone. However, the small number of study participants, cross sectional design, median age (64.5 years) and lack of published methodology are clear limitations.

A randomised placebo controlled trial in men with non-metastatic PC starting ADT compared microarchitecture using HR-pQCT in a group given one dose of zoledronate and a placebo group⁶³⁴. Total vBMD at the radius decreased over 12 months in both groups, with a greater reduction in cortical vBMD than trabecular vBMD. Interestingly, a single dose of bisphosphonate did not prevent loss of total vBMD at the radius or tibia over 12 or 24 months. The only effect on volumetric BMD was a modest benefit in preventing loss of cortical vBMD at the radius after 12 months. In support of other published data, zoledronate was associated with improvement in DXA areal density outcomes.

Together with published data, our results indicate that ADT affects both cortical and trabecular bone density at the distal radius, and it appears that loss of cortical density contributes more to loss of total vBMD.

5.14 Changes in bone microarchitecture

In addition to reduced cortical vBMD, we found that ADT was also associated with a significant loss of cortical area (7.9% in group A) and thickness (8.2%), and increased cortical porosity compared to the control group. The results for cortical microarchitecture in group B were similar to group A and followed the same trend. In mouse models, orchietomy decreases cortical density and thickness, and androgen receptor knockout increases bone turnover and resorption with loss of cortical bone area and volume^{753,754}. Our results correspond with those from a previous longitudinal study, which reported that ADT led to a 5.1% reduction in cortical area after 6 months, which increased to 11.5% at 12 months⁶⁸⁰. The derived measure of cortical thickness decreased significantly by 11.3% over 12 months. A subset of men receiving ADT in a prospective cohort study experienced significant and rapid declines in total and cortical BMD, cortical area and thickness⁶³⁶. In older healthy men, those with the lowest levels of serum testosterone experienced the most rapid decrease in cortical area at the distal radius⁶³⁶.

We also observed important changes in trabecular microarchitecture. Trabecular area and BV/TV increased significantly in group A compared with the control group, and there was a trend towards increased trabecular separation. In general, data regarding microarchitectural changes in men with PC are scarce. Both the BV/TV ratio and duration of ADT have previously been correlated with total BMD at the ultradistal radius. Increased trabecular area has also been associated with ADT^{636,680}, along with a decrease in trabecular number; which did not quite reach significance in our study. In addition to CT techniques, high resolution MRI has been used in men with PC. This technique classifies each image voxel as belonging

to a surface or curve junction and quantifies the degree to which trabecular plates (surfaces) have deteriorated to become rods (curves). The bone/tissue volume was lower, surface density was lower and erosion index was higher (indicative of worse trabecular structure) in men receiving ADT and who had moderate to severe vertebral fractures²¹⁷. Another study used magnetic resonance imaging to investigate bone density and trabecular architecture in hypogonadal men⁷⁵⁵. There was no difference in bone density between hypogonadal men and age matched men, but trabecular architecture (using surface/curve ratio, bone volume fraction and erosion index) deteriorated significantly in the hypogonadal group.

The changes in trabecular architecture in group B were mixed, and did not follow the same pattern as group A. There was a gain in trabecular area and a reduction in BV/TV, along with corresponding loss of trabecular vBMD, which were also observed in the group A and reported in previous studies. However, we found that there was there a gain in trabecular number and a reduction in thickness and separation, which were opposing findings to group A. The difference between groups was the use of GCs in group B. Studies that have assessed microarchitectural change associated with GC use have reported increased trabecular separation, reduced number and thickness at the radius^{510,756}. It is possible that there has been an error in image analysis, although highly trained scan technicians and standard software would make this unlikely. An increase in trabecular number and loss of separation in group B may result from the combination of ADT and GC causing rapid loss of cortical bone, and trabecularisation of cortical bone. The small number of group B participants that completed both HR-pQCT scans limits the ability to draw firm conclusions, and further investigation is needed.

5.15 Changes in bone strength

We found that ADT was associated with reduced bone stiffness and ultimate failure load, although only the latter reached significance when compared with group C. To our knowledge, there are no published data regarding FEA outcomes for bone strength in men receiving ADT. One recent study applied a bone strength index (BSI)⁷⁵⁷ and calculated the polar moment of inertia²⁷ in HR-pQCT scans undertaken in ADT and non-ADT treated men²¹⁵. BSI at the distal radius was reduced by between 23.6% and 27.5% in men treated with ADT when compared to healthy men and PC controls ($p < 0.001$). There was no difference between groups in the polar moment of inertia at the proximal radius. BSI is a less sophisticated measure than FEA, and may be affected by loss of total and trabecular vBMD.

We observed the greatest reduction in distal radius stiffness and strength in group B, likely as a consequence of the ADT and glucocorticoid combination. Central HR-pQCT FEA evaluation of vertebra in men with GC induced osteoporosis found that

bone strength showed the most significant association with vertebral fracture ⁷⁵⁸. This study also confirmed the superiority of high resolution techniques over DXA. Limited evidence in men with GC induced osteoporosis suggests that bone strength and stiffness may be improved by anti-resorptive treatment ⁷⁵⁹.

FEA data from eight HR-pQCT studies were combined and used to explore the relationship between HR-pQCT outcomes, aBMD and fracture incidence in over 7,000 individuals ⁷⁶⁰. The majority of participants had normal aBMD. Failure load was most strongly predictive of future fracture, and at the radius the HR for fracture was 2.13, (95% CI 1.77-2.56) per SD decrease in failure load. Other important microarchitectural predictors of fracture included cortical vBMD, density, trabecular number, and thickness at the distal radius. Reduced failure load may contribute to risk of fracture independently of BMD and FRAX. Additional data are required in men with PC to more accurately determine the magnitude of ADT related changes in bone strength, and the effect of anti-resorptive therapies. There may be a future role for assessment of volumetric density, microstructure and strength in selected individuals, however high resolution techniques are not yet widely available.

5.16 Strengths of study

This is the first study that has used a combination of established and novel techniques to investigate longitudinal changes in bone turnover, density, structure and strength in ADT-treated men with PC. It is the first investigation of changes in bone turnover, density and structure in men with metastatic hormone sensitive PC who are treated with chemotherapy and GCs.

A key strength of ANTELOPE is the prospective study design, and inclusion of a longitudinal control group that were well matched by age and BMI to group A. This increases the likelihood that observed changes are related to the effects of therapy. The study inclusion and exclusion criteria were selected to exclude important conditions that would affect bone, but also allow for the study to recruit to target. An initial power calculation identified a minimum of 26 participants required in each group to detect important differences.

All study assessments were completed on the same day. Additional logistical strengths included the use of the same DXA and Xtreme (HRpQCT) scanner machines, and the undertaking of all scans by the same two highly trained operators, using established standard operating procedures. These same two individuals carried out scan image analysis. Tests of muscle function and strength were assessed using the same equipment and standard protocol. Serum testing was standardised by ensuring that all samples were fasted and taken at the start of the day, as several of the biomarkers exhibit postprandial and circadian variation.

Analysis of biomarkers was undertaken simultaneously in batch analysis at the end of the study.

Statistical strengths included adjustment for skewed data, the use of both repeated measures ANOVA model testing for an interaction between time and group, and ANCOVA, which adjusted 12 month changes for age, BMI and baseline value.

5.17 Study limitations

Whilst the study design sought to minimise bias, recruitment of the control group was done by advertising and approach of previous volunteers. Volunteer bias may have led to the recruitment of a healthier or more health conscious control group, who may not fully represent the general population.

We recruited a total of 99 participants who underwent baseline study assessment. Although this was greater than the initial recruitment target, the final number of study participants was lower than expected. We allowed for 10% of participants to be excluded or lost to follow-up in the study design. In reality, a greater proportion (13%) required exclusion at baseline, and a further 13% were lost to follow-up over the study period. Group B experienced the greatest loss to follow-up. Of 25 participants that completed the baseline visit, 7 (28%) did not complete the study, a reflection of their underlying condition, age, and complications associated with treatment. Although men with metastatic hormone sensitive PC have a median survival of 4-8 years^{167,702}, some individuals have aggressive and rapidly progressive disease. In the primary comparison between groups A and C, for the majority of study outcomes, the number of participants in these groups was sufficient, based on the initial power calculation.

The ANTELOPE exclusion criteria included those participants found to have osteoporosis at their baseline visit. Whilst this was ethically and clinically sound, it may have underestimated the magnitude of bone loss that occurred in groups A and B; those with lower BMD related to age, genetic and lifestyle factors may have experienced the greatest BMD loss related to ADT, chemotherapy and GCs.

An additional challenge to the final sample size arose from motion artefact on HR-pQCT scans. This was most problematic in group A, where only 18 participants had acceptable scan images at baseline and 12 months. Whilst the incidence of motion artefact was similar to results from previous studies, it is possible that our study was underpowered to detect between group changes in HR-pQCT outcomes. We could have undertaken additional HR-pQCT scans at the distal tibia, however this would have added significant cost, radiation exposure, and still has the risk of motion artefact. We chose to assess microarchitecture at the radius due to several factors; published data suggest it is highly susceptible to the effects of ADT; bone metastases in PC rarely affect the radius; and because radius BMD has been shown to predict fractures in men.

The timing of recruitment in relation to ADT initiation required scientific accuracy of the results to be balanced with feasibility of recruitment. Ideally, participants would have their baseline study assessment undertaken before ADT initiation, in order to fully capture ADT-related changes. However, for ethical, logistical and practical reasons, this was not possible. We did not collect data regarding compliance with ADT, however our results for serum testosterone and oestradiol levels in group A and B suggest that compliance was excellent. Study data regarding medications, supplements, falls, frailty and FRAX risk factors were collected from questionnaire data, and therefore subject to re-call bias.

Participants in groups A and C underwent high resolution CT scans of T12 as described in chapter 2, section 2.2.7.3. Image analysis from these scans has been delayed due to covid-19 pandemic factors. It would be useful to have this data regarding central skeletal microarchitecture in addition to the peripheral HR-pQCT measurements. Notably, the greatest loss in aBMD in ANTELOPE participants occurred at the lumbar spine. It is hoped that HR-CTR data from T12 would confirm ANTELOPE study findings at the distal radius, and determine the pattern of bone loss and cortical and trabecular deterioration in greater detail, and also help to select the best bone targeted therapy for this group.

5.2 ANTELOPE: Main conclusions and future work

ANTELOPE is the first study that has investigated ADT and chemotherapy-associated changes in aBMD, vBMD, microarchitecture, estimates of bone strength and body composition. The ANTELOPE study results are in agreement with existing data, but have also added significantly to our knowledge and understanding of the effects of ADT and chemotherapy on bone, body composition, frailty and physical performance (table 31).

We found that recruitment and retention of men receiving treatment for PC (including those with metastatic disease) is feasible, but that there are logistical challenges in undertaking additional assessments before ADT is initiated. Longitudinal study of those with advanced disease is difficult due to a combination of their underlying condition and treatment-related adverse effects.

Our results have identified that frailty is an important clinical problem in men with PC who start ADT. Although there is an increasing focus on geriatric assessment in clinical oncology practice, many studies to date are retrospective, have small numbers of participants and only a few have been undertaken in men with PC. We found that frailty is more prevalent in men diagnosed with PC than healthy age matched men, and the prevalence appears to increase after ADT is initiated. This may relate to factors other than ADT, such as co-morbid conditions and the effects of cancer treatments such as fatigue. Nevertheless, frailty is an important clinical syndrome, which is related to reduced mobility and falls, the latter of some

concern in an older male population with PC, likely to have reduced BMD due to age and ADT.

Recent efforts have sought to increase awareness and understanding of frailty in oncology patients, and guidelines are available for the identification of frailty and other geriatric syndromes. In geriatric medicine, CGA is the gold standard for frailty diagnosis, however this is time consuming and requires a multi-disciplinary team. Frailty screening tools may predict which individuals are likely to benefit from CGA, however there is no consensus as to which tool is best to use in the oncology setting. A significant concern related to frailty assessment is a lack of published intervention studies; these are only just beginning to emerge in the literature, and no study to date has reported data in participants with cancer.

There is an urgent need for further studies; both epidemiological studies that robustly assess the prevalence of frailty in men with PC, in addition to well-designed frailty intervention studies that include cancer-specific outcomes and include health economic aspects (figure 27). Alongside these initiatives, the importance of frailty and methods used to identify the condition needs to be highlighted in the education, training and professional development of clinicians across the multidisciplinary PC team.

Table 31: Contribution of ANTELOPE data to our current understanding of the effects of ADT on bone, body composition, frailty and physical performance

What was previously known (and has been confirmed by ANTELOPE)	Additional information provided by ANTELOPE
<ul style="list-style-type: none"> • ADT is associated with a rapid and significant reduction in circulating sex hormones • ADT causes increased bone turnover • ADT causes aBMD loss at TH, LS, FN and TB (Chapter 1 table 4 and 5) • ADT is associated with gain in BMI, fat mass and loss of lean mass (sarcopenic obesity, Chapter 1 table 6) • Men with PC are at increased risk of fracture compared with the general population • A significant number of men with PC have a fracture risk above the intervention threshold for treatment (limited data, Chapter 1 table 7) • Frailty and pre-frailty are common in cancer patients 	<ul style="list-style-type: none"> • Longitudinal assessment of men with advanced cancer is difficult and losses to follow-up are significant • ADT causes increased bone turnover, with important increases in the biomarkers PINP, osteocalcin and CTX • Interpretation of biomarker changes in men with metastatic bone disease treated with ADT and chemotherapy is challenging due to multiple mechanisms responsible for change • 12 months of ADT causes loss of aBMD at all skeletal sites, and affects LS the most • HR-pQCT measurement at the distal radius is limited by motion artefact • ADT is associated with significant loss of vBMD at the distal radius, due to loss of both cortical and trabecular vBMD. • ADT increases cortical porosity, and is associated with loss of cortical area and thickness and deterioration in trabecular architecture • ADT compromises bone strength and stiffness • The majority of all older men have a fracture risk above the intervention threshold for treatment • 12 months of ADT (with or without chemotherapy) is associated with deterioration in frailty status • ADT lead to gains in BMI, fat mass and % body fat, especially trunk fat mass • ADT significantly affects upper limb body composition, there is increased fat mass and loss of lean mass • ADT is associated with a significant reduction in grip strength and worse physical performance over 12 months

Risk factors for hip and major osteoporotic fracture are prevalent in both men starting treatment for PC and also in healthy age-matched men. The most frequent risks include increased age, raised BMI, parental history of hip fracture and alcohol intake in excess of recommended limits. A very small proportion of men appear to regularly use calcium and vitamin D supplements.

Using FRAX, the risk of fracture is greater when clinical risk factors are used without BMD, which relates to a conservative estimate of fracture probability when BMD is unknown⁶⁵⁰. Three quarters of men in our study were at sufficient risk of fracture to warrant intervention based on NOGG thresholds. Over ten years and without bone targeted treatment, as many as eight of our study participants would be likely to experience a significant fracture. The economic and social burden of hip and major osteoporotic fractures cannot be underestimated, in terms of the cost to health and social care services related to loss of independence, hospitalisation, surgical interventions and need for long term medications and care. Fractures are also associated with deterioration in quality of life, and in men with PC, lead to increased mortality. This must be balanced against the relatively low cost of most anti-resorptive therapies.

Our findings highlight the importance of routine assessment of fracture risk in clinical practice. This should be considered in all older men, and especially in those starting ADT. Our risk estimates were undertaken without inclusion of ADT and GC use as a secondary cause of osteoporosis; in which case the risk would be even greater, and bone targeted treatments would be indicated in a larger proportion. However, compared to the female population, assessment of bone health in male patients is less frequently considered. In women receiving hormone based treatment (such as aromatase inhibitors) for breast cancer, assessment of fracture risk is standard practice, yet this is not yet the case in PC care. Current guidance for assessment of fracture risk in ADT-treated men varies by country, composition of the expert group of authors, health service design and availability of BMD testing. In general, fracture risk assessment is recommended in all men due to commence ADT (NICE clinical guideline 131)¹⁵³, but in practice, this is often not done. In the UK, it is not clear where the responsibility lies for consideration and optimisation of bone health, as the management of men with PC involves urology and oncology services in addition to primary care. Clarification of this by national guidance, in addition to appropriate service design, commissioning and design of clinical pathways for bone health assessment in men starting ADT is urgently required.

Treatment with ADT is associated with important physical changes during the first year of therapy. The reduction in grip strength may be related to loss of upper limb lean mass and increased fat mass. Few studies have reported regional body composition changes related to ADT, and it is not yet clear whether this would relate to functional impairment. ADT has consistently been associated with sarcopenic obesity, with significant gains in BMI, trunk fat mass and loss of lean

mass. Together with metabolic changes associated with ADT, this has potentially serious consequences in terms of cardiovascular risk. Exercise interventions have an important role in mitigating the effects of ADT, and supervised exercise programmes are recommended by current PC guidelines. However, it is unclear whether the benefits are sustained when the period of supervision ends, and current studies aim to evaluate the efficacy and cost effectiveness of long term exercise interventions (figure 27).

ADT increases bone turnover, evident in measurement of biomarkers of bone resorption and formation. TRAP5b and sclerostin are novel markers, which may have a role in non-invasive assessment of the activity of BM and response to ADT in bone, however require further investigation in a larger number of men. Biomarker interpretation is challenging in men with metastatic bone disease, it is difficult to distinguish between changes related to response to systemic treatment by BM, and the effects of ADT.

ADT is strongly associated with loss of areal BMD, most significant at the LS, with effects at the TH, FN and TB, with a corresponding reduction in BMC. Loss of vBMD at the distal radius over 12 months is approximately four times greater in association with ADT than would be expected from increased age, and occurs as a consequence of both cortical and trabecular vBMD loss. ADT-associated microarchitectural changes include loss of cortical area and thickness, as well as increased porosity. Trabecular microarchitecture deterioration occurs with ADT, and is manifested by an increase in trabecular area, separation and BV/TV. ADT also compromises bone strength, represented by a significant reduction in failure load, and a possible reduction in stiffness, and the addition of GC and chemotherapy appears to accelerate this effect.

Ongoing analysis of the HR CT scans carried out in ANTELOPE Group A and C participants (delayed by Covid-19) will provide information regarding vertebral microarchitecture, and FE estimates of bone strength. Given that the loss of aBMD was greatest at the LS using DXA, it is anticipated that this site will experience an even greater deterioration in vBMD, microarchitecture and strength. Based upon these findings, future studies should aim to determine which anti-resorptive therapies are the most effective in the prevention of bone loss and in maintaining microstructure and strength (figure 27).

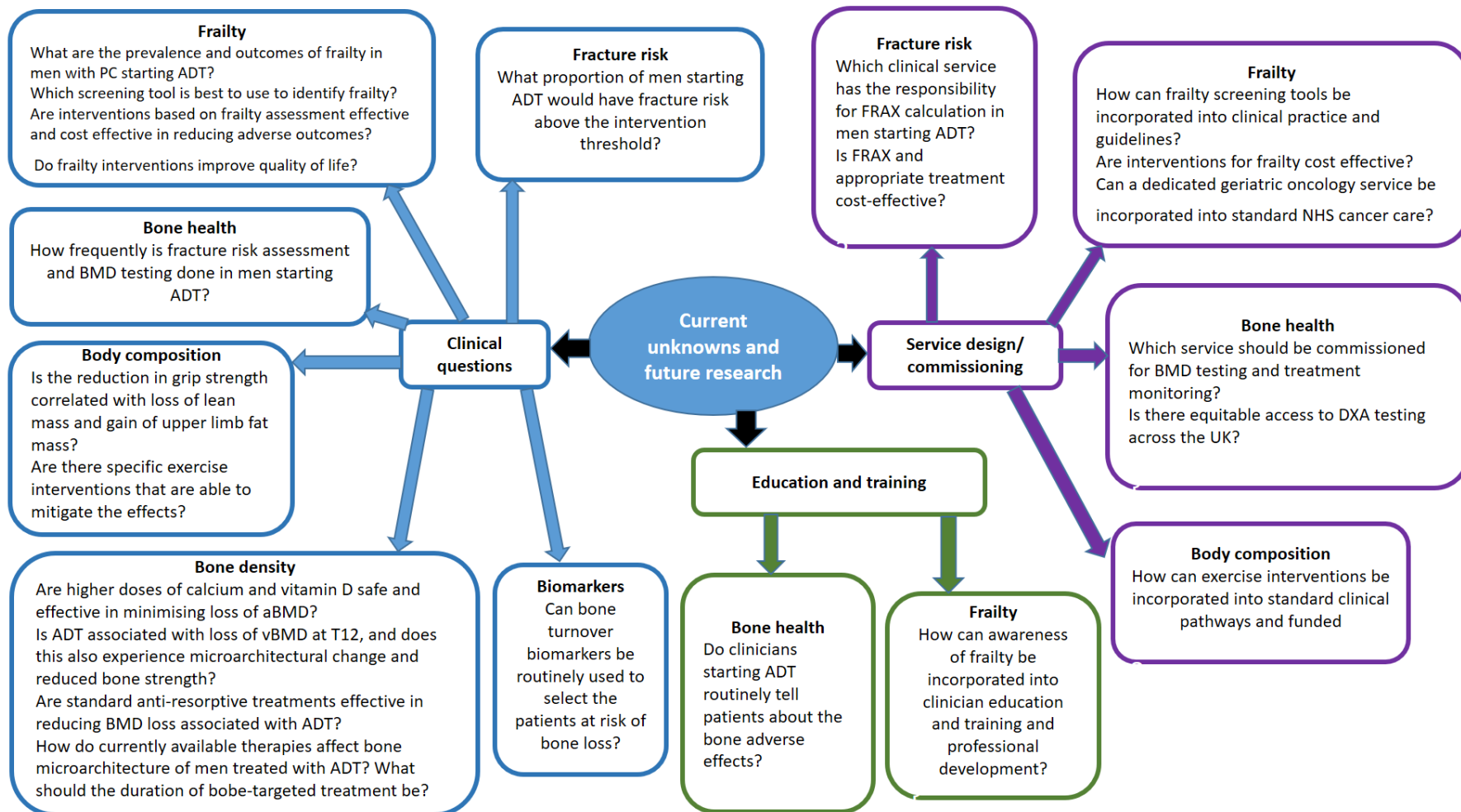


Figure 27: Summary of important future research questions in ADT-treated men with PC

5.3 Overall conclusion

PC is increasing in both incidence and survival, and consideration of the long term consequences of PC treatments are of increasing importance. The adverse effects of PC treatment have the potential to significantly impact quality of life, function and independence.

ADT is the cornerstone of treatment for PC, and is associated with improved overall survival in appropriately selected patients. ADT affects aBMD, and the greatest reduction has been observed during the first 12 months of therapy. The ANTELOPE study has confirmed that ADT is associated with significant loss of aBMD at all sites over 12 months, with the LS affected the most. This is of significance, as vertebral fractures are frequently associated with skeletal fragility, are often difficult to detect, and are associated with significant morbidity and adverse health outcomes.

ANTELOPE also identified significant vBMD loss at the distal radius as a result of ADT, and that this may be accelerated in men treated with chemotherapy and GCs in addition. Both cortical and trabecular vBMD loss contributed to the overall loss of vBMD. ADT appears to cause a reduction in cortical area and thickness, increased porosity and loss of trabecular area. ANTELOPE is the first study to identify this pattern of microarchitectural deterioration over 12 months of ADT, and has also identified a corresponding reduction in bone stiffness and strength using FE methods.

ADT is also associated with; a sarcopenic obesity phenotype; loss of upper limb lean mass and gain in fat mass; accelerated bone turnover, and compromise of both bone density and structure which are key determinants of whole-bone strength. These effects are super-imposed upon a population of older men who are already likely to be at increased risk of fracture due to their age, co-morbid conditions and frailty.

Assessment of bone health is an unmet need in ADT-treated men. Education of patients and clinicians is poor, fracture assessment is not standard practice, DXA estimates of aBMD underestimate the risk of fracture, and it is not clear how ADT treated men are best selected for intervention. Without the introduction of strategies to risk stratify men, select appropriate individuals for intervention, and clarify who has responsibility for bone health optimisation, men treated with ADT are more likely to experience avoidable fractures which have considerable economic, social and personal cost. There is also a need to implement and evaluate evidence supporting the use of lifestyle interventions and optimal therapeutic strategies to ameliorate and manage the adverse effects of ADT (figure 27). Increased awareness of the challenge to, and the importance of skeletal health in men with PC treated with ADT is essential, in order to minimise treatment associated morbidity and mortality.

Chapter 6: Potential biomarkers of metastatic bone disease in prostate cancer

6.1 Overview

Chapters two, three four and five have explored the effect of ADT, chemotherapy and GCs on bone loss, microarchitecture, body composition and serum hormones and biomarkers in men with PC. This chapter will investigate metastatic bone disease, which is another potential skeletal complication of PC and its treatment. Chapter one provided a thorough overview of PC and metastatic bone disease, and included the classification, pathophysiology and sequelae of bone metastases (BM).

This chapter will present the methods and results of a laboratory based project, where both established and novel proteomic techniques were applied to PC cell lines. This project sought to determine whether biomarkers may be used to predict the development of future BM in PC.

6.2 Introduction

Between 10-20% of men with prostate cancer (PC) have bone metastases (BM) at diagnosis, and more than 90% of those with metastatic disease have skeletal involvement^{157,296}. More than 80% of those with PC will ultimately develop metastatic spread to bone. BM are associated with significantly increased morbidity and mortality due their propensity to cause skeletal related events (SREs)³⁰³. As described in chapter one of this thesis, SREs include bone fractures, spinal cord compression, hypercalcaemia and the need for radiation to bone³⁰³. BM are usually identified radiologically by using either X rays, isotope bone scans (scintigraphy), computed tomography (CT) or magnetic resonance imaging (MRI). Plain radiography detects increased blood flow and reactive bone formation at sites of BM, but has low sensitivity and specificity. Bone must demineralise by at least 50% before a lesion is detected by X-ray, and this method identifies lesions more than 18 months later than bone scintigraphy⁷⁶¹. Although scintigraphy is more sensitive than X-ray, it lacks specificity. MRI and CT are both sensitive methods for the detection of bone lesions. MRI is preferred for spinal imaging, and CT can readily distinguish between osteolytic, osteoblastic and soft tissue lesions.

Osteotropism refers to the process by which cells from cancers (including those arising from breast, prostate, lung and kidney) acquire characteristics that allow them to detach from a primary tumour, travel into and through vasculature and lymphatic channels, and adapt to the micro-environment within the bone-homing niche eventually developing macro-metastases⁷⁶². The seed and soil hypothesis (explained in chapter one) describes this process, which requires the presence of a highly vascular bone marrow, production of a diverse array of cytokines and growth

factors by cancer cells and tumour-adjacent stromal cells and cancer and cell interactions with the bone microenvironment, the combination of which creates favourable conditions for BM³²⁴. Disseminated cancer cells may remain dormant for a latent period of time (this can be many years), either as solitary cells that do not divide, or as pre-angiogenic micrometastases that lack the ability to become vascularised^{763,762}.

Significant progress has been made in the treatment of PC, and individuals may live for many years with metastatic bone disease. Relatively few studies have explored the use of diagnostic biomarkers for BM in men with PC, or sought to identify factors that could predict risk of BM development. Early identification of those at high risk of BM could allow for early intervention to prevent or to delay BM, and reduce the associated morbidity.

Prostate specific antigen (PSA) is a serine protease that is secreted from the prostatic epithelium, and it is widely used as a diagnostic, prognostic and predictive biomarker in PC^{145,764}. However, PSA has important limitations with regard to metastatic bone disease; it does not predict the development of BM, does not correlate with the extent of bone involvement, and its levels may not accurately reflect the bone-specific benefits of newer systemic anticancer therapies^{765,766}

6.2.1 Use of bone biomarkers in men with PC and metastatic bone disease

Biomarkers of bone turnover (BTM) have been introduced in chapter 1 of this thesis. They are measured in serum and urine, at relatively low cost, and may be used for diagnostic, prognostic and predictive purposes, as well as for monitoring the effects of bone targeted therapies. There have been relatively few studies that have investigated the role of BTM in metastatic bone disease.

6.2.1.1 Diagnosis and prognostication

In men with PC, the serum BTMs BALP, PINP and PICP and urinary CTX correlated with the presence and extent of BM in a retrospective analysis^{300,767,768}. In men with PC, serum PINP was significantly greater in men with BM than in men with non-metastatic PC or with only lymph node metastases⁷⁶⁹. CTX may be used as a sensitive marker of accelerated bone resorption in BM³⁰⁹. However, published studies are limited by their retrospective nature, lack of validation and correlation with clinical outcomes.

Elevated levels of biomarkers including PINP, BALP, OPG, NTX, TRACPb5, and CTX have been found to predict worse overall survival in men with CRPC^{770,771}. Raised urinary NTX and BALP have been associated with an increased risk of developing SREs and reduced overall survival (OS) in men with metastatic CRPC^{772,773,774}.

6.2.2 Biomarkers predictive of response to therapy

Biomarkers may be useful to predict and monitor the response to bone targeted treatments. In a subset of men with castration-resistant prostate cancer (CRPC), zoledronic acid normalised urinary NTX after 3 months of treatment, and this was also associated with improved OS and reduced SRE incidence ⁷⁷⁵. In men with CRPC, a decrease in BAP, PINP, NTX, ICTP, CTX, and PSA after administration of zoledronic acid was also associated with fewer SREs ^{776,777}. In addition, high baseline NTX levels have been demonstrated to predict the rate of bone progression in PC BM patients ⁷⁷².

The limitations of BTM within cancer treatment have been discussed previously, including their diurnal and postprandial variation, and their changes with exercise, diet and with season. Although current evidence suggests that they may have the potential for clinical use, they require prospective validation and are yet to be incorporated into routine practice.

Currently, no biomarker can predict the risk of BM development in men with PC or identify early skeletal involvement, and novel approaches are required to address this.

6.2.3 Novel approaches to biomarker discovery in PC bone metastases

6.2.3.1 Circulating tumour cells, tumour DNA and micro RNA

Circulating tumour cells (CTCs) are shed from either the primary tumour or metastases, and can be readily measured in serum. Individuals with PC and BM have higher serum CTC numbers than those with soft-tissue metastases ⁷⁷⁸. CTCs may have prognostic implications in PC and be an early predictor of BM potential, and their levels may also reflect the metastatic burden ^{779,780}. In addition to CTC number, the molecular phenotype of CTCs can reveal important information about the genetic alterations within the primary tumour and its potential for response to treatment ⁷⁸¹.

Circulating tumour DNA (ctDNA) is shed from primary tumours and can be an important source of information about tumour-specific genetic and epigenetic alterations ⁷⁸². In addition, levels of ctDNA may predict BM ^{783,784}.

Micro RNAs are small, stable, non-coding RNAs that have a role in regulating diverse events within BM including escape from the primary tumour (extravasation), survival in the bloodstream, intravasation into the bone microenvironment and eventual development of macro-metastases and bone remodelling ⁷⁸⁵. In PC, the micro-RNA miR-466 inhibits Runx2 activity in xenograft models and prevents BM formation ⁷⁸³. In PC tissue, miR-466 predicted

biochemical relapse⁷⁸³. Since Runx2 is an important regulator of BM, serum detection of Runx2-targeting microRNAs could be useful to monitor BM progression. Exosomal microRNAs are also of interest; these are released by cancer cells in small vesicles (up to 100 nm in diameter) and facilitate PC cancer cell invasion and progression⁷⁸⁶. In pre-clinical studies they appear to have a role in BM regulation⁷⁸⁷; high levels of specific miRNAs have been found in the exosomes of osteotropic PC cells⁷⁸⁸.

6.2.3.2 Proteomics

A proteomics approach uses medium to high throughput protein sequencing and quantification to identify potential biomarkers of disease. Typical steps of a proteomics workflow involve protein separation, enzymatic protein digestion into peptides (using proteases including trypsin), peptide-separation using reverse liquid chromatographic separation, and analysis by mass spectrometry. The peptide fragments generated within tandem mass-spectrometry can be analysed and compared to theoretically predicted peptide fragments from initiatives such as genomic sequencing, to generate a list of the proteins present within a sample and their levels⁷⁸⁹.

Using proteomic techniques, a panel of proteins was identified which were expressed at levels which displayed a statistically significant association with PC relapse, and also with poorer survival⁷⁹⁰. In a separate study, a group of amyloid proteins was also observed to be highly expressed within the serum of men with PC and BM⁷⁹¹. A recent analysis of the PC BM proteome identified two distinct BM phenotypes that were related to prognosis⁷⁹². Further studies must validate these pre-clinical findings and correlate them with clinical outcomes in elected patient populations. Despite these challenges, there is hope that proteomics could aid the development of future personalised therapies.

Using proteomic techniques, several studies have identified proteins in primary solid tumours that may predict the development of BM (table 32).

Table 32: Studies of the protein expression of a primary tumour as a biomarker of BM

Author (year)	Potential biomarker	Tumour type	Predictive role in bone metastasis
Westbrook (2016) ⁷⁹³	Macrophage-capping protein (CAPG)	Breast	Increased expression of both CAPG and GIPC. In primary BC tissue from a large RCT, CAPG and GIPC predicted skeletal disease free survival and overall survival. Those with high expression were more likely to respond to adjuvant zoledronic acid.
	GIPC PDZ domain-containing protein (GIPC1)		
Li (2015) ⁷⁹⁴	Integrin beta-like 1 (ITGBL1)	Breast	ITGBL1 was co-expressed with genes related to osteomimicry in primary BC tissue, and also correlated with the presence of BM
Nutter (2014) ⁷⁹⁵ and Hohen (2016) ⁷⁹⁶	Interleukin -1 β (Interleukin (IL)-1 β)	Breast	Interleukin (IL)-1 β was upregulated in a bone-seeking model of BC cells. There was correlation between IL-1 β and the onset of BM in tissue from primary BC biopsies. IL-1 β inhibitors skeletal events in murine models
Westbrook (2019) ⁷⁹⁷	Dedicator of cytokinesis protein 4 (DOCK4)	Breast	High levels of DOCK4 was prognostic for bone recurrence in a TMA in those who had not been treated with zoledronic acid
Li (2019) ⁷⁹⁸	Nuclear p21-activated kinase 4 (nPAK4)	Breast	nPAK4 expression was associated with BM development in those with oestrogen receptor +positive breast cancer
Tiedemann (2019) ⁷⁹⁹	Peroxiredoxin-4 (PRDX4) and L-plastin (LPC1)	Breast, prostate renal	PRDX4 and LPC1 were, responsible for tumour bone colonization in osteotropic tumours
Sutherland (2016) ⁸⁰⁰ Tikk (2014) ⁸⁰¹	Prolactin (PRL) and its receptor (PRLR)	Breast	High expression of PRLR gene in primary breast tumours correlated with shorter time to BM

6.2.4 Potential protein biomarkers of cancer metastasis to bone

As described in chapter 1 of this thesis, cancer cell metastasis relies on several key steps, including: separation from the primary tumour; invasion through the extracellular membrane (including penetration of the basement membrane) and extravasation into vasculature and the lymphatic system. Subsequent entry into a distant organ and interactions with the local microenvironment is, followed by angiogenesis and formation of a new macro-metastasis. All of the above steps are critical for successful metastasis, and differentially expressed molecules within metastasis may promote any one of these stages (or several of these stages). We sought to investigate proteins that have been identified as potential biomarkers of breast cancer metastases to bone, and explore their expression in PC.

6.2.4.1 Macrophage capping protein (CAPG)

Gene name: CAPG, Protein Name: Macrophage-capping protein, Uniprot: P40121).

Structural features and mechanism of action

Also known as membrane capping protein, gelsolin-like actin-capping protein, and gelsolin-related actin-binding protein, macrophage capping protein (CAPG) is a regulator of actin-based cellular motility. In this role, CAPG represents a plausible candidate regulator of cancer cell migration and invasion.

CAPG is a calcium responsive protein with a MW of approximately 38KDa. CAPG is part of the gelsolin family of proteins⁸⁰², however, it differs to other gelsolin family members in lacking a nuclear export sequence, and is therefore located in both the nucleus and cytoplasm⁸⁰³. CAPG binds to and blocks (but does not sever) the barbed ends of actin filaments and together with other actin binding proteins (such as formin tensin and tropomodulin), CAPG acts to control actin filament length, thus regulating cell motility, morphology and polarity, transcription regulation and RNA transport^{804,805,806}. Nuclear export of CAPG appears required for its ability to promote cancer cell invasion⁸⁰³. Despite these studies, the role of CAPG within cancer metastasis is still incompletely understood.

Role in cancer biology

In breast cancer, high CAPG expression within a bone homing variant of breast cancer cells was observed to be predictive of BM and worse OS⁷⁹³. These findings have been confirmed within other studies of BC metastatic variants⁸⁰⁷.

Furthermore reduced invasiveness of breast cancer cells was observed following CAPG knockdown⁸⁰⁸, as well as alterations in the nuclear export of CAPG⁸⁰⁸. Gene expression profiling techniques have also confirmed the upregulation of CAPG in breast tumours⁸⁰⁹.

In lung adenocarcinoma, CAPG is overexpressed compared to adjacent normal lung tissue, and expression is increased further under hypoxic conditions⁸¹⁰. CAPG knockdown in lung tissue reduces cancer cell migration and invasiveness and correlates with time to recurrence⁸¹¹. Furthermore, CAPG expression levels as assessed by IHC within non-small cell lung cancer found high expression correlated with increased mortality (HR 2.79, 95% CI 1.27-6.17, n = 121 patients, p= 0.011)⁸¹². In addition to lung cancer, CAPG is also overexpressed in a range of other solid malignancies which include; colorectal^{813,814}, pancreatic⁸¹⁵, ovarian^{809,816} and oral tumours⁸¹⁷.

CAPG in prostate cancer

A small number of studies have investigated the role CAPG in PC cell lines and tissues. Genome Wide Association Studies in PC cells identified a single nucleotide polymorphism (SNP) within the CAPG locus which resulted in altered gene expression via epigenetic regulation⁸¹⁸ SiRNA-mediated gene silencing of CAPG within DU145 cells reduced their proliferative rate and decreased their migration and invasive ability⁸¹⁹. These effects of CAPG upon PC cell-line proliferation and apoptosis were primarily regulated via alterations in the activity of the Caspase 6/9 pathway⁸²⁰. The role of CAPG in PC metastasis was confirmed in a subsequent TMA-based study⁸²⁰.

CAPG and cancer metastasis

The role of CAPG in bone metastasis of breast cancer was further elucidated by the discovery that CAPG acts as an epigenetic enhancer for the gene expression of stanniocalcin-I (STC-I), a pro-metastatic gene implicated in breast cancer spread⁸²¹. STC-I is associated with poorer survival in breast cancer; and its knockdown inhibits primary tumour formation and metastasis within murine models⁸²². The discovery that CAPG acts as an epigenetic regulator suggests that it may have a role in metastasis outside of its role as a regulator of the actin-cytoskeleton.

6.2.4.2 GAIP interacting protein C terminus member 1 (GIPC1)

Gene Name: GIPC1, Protein Name: PDZ-domain containing protein GIPC1, Uniprot: O14908).

Structural features and mechanism of action

The GAIP interacting protein C terminus members 1 (GIPC1), 2 (GIPC2) and 3 (GIPC3) are PDZ domain proteins that constitute the GIPC family⁸²³. Their physiological roles include; trafficking of transmembrane proteins, regulation of cellular proliferation, cell-polarity, cytokinesis and cellular migration⁸²³. The majority of the downstream effects involve the central PDZ domain, which interacts with receptors and cytokines involved in G protein signalling. Most PDZ

ligands for GIPC1 are transmembrane proteins, with only few cytosolic signalling regulators.

GIPC1 has a molecular weight of approximately 36KDa. The GH2-domain at the C-terminus of GIPC1 interacts with MYO6, a member of the myosin family that facilitates the trafficking of endosomes, and promotes cytokinesis and migration (figure 28) ⁸²⁴. GIPC1 dimerizes via its N-terminal GH1 domain assembling into cargoes for MYO6-containing endosomes ^{825, 826}. GIPC1 interacts with cell surface transmembrane receptors, most importantly integrins, which act as mechano-sensory receptors regulating actin dynamism ⁸²⁷. GIPC1 is required for the trafficking of internalized integrins during cell migration, angiogenesis and cytokinesis ^{828,829}. GIPC1 also regulates receptor tyrosine kinase signalling binding to IGFR1 and NTRK1 resulting in the activation of the PI3K–AKT, phospholipase and other signalling cascades ^{830,831,832}. In addition, GIPC1 also interacts with IGF1 and TGFβ receptor type III, the latter resulting in increased cell surface expression of TGFβ and therefore enhanced responsiveness ⁸³³. It has been suggested that down-regulation of GIPC1 may promote cellular proliferation through TGFβ signalling interference ⁸³⁴. GIPC1 is also involved with cell adhesion via E-cadherin ⁸³⁵, and cell migration via interaction with the 5T4 protein ⁸³⁶.

Role in cancer biology

Studies to date have reported upregulation of GIPC1 in a range of human tumours including breast, ovarian and pancreatic cancer ^{834,837,838,839,840}. GIPC1 stabilises IGFR1 and promotes cell proliferation and survival in pancreatic and breast cancer cells ^{841,837,840}. Conversely, knockdown of GIPC1 inhibits cancer-cell proliferation and promotes apoptosis, leads to G2 cell cycle arrest and decreases motility in cancer cells ^{842,843}, confirming the involvement of GIPC1 in both cytokinesis and cell migration ⁸²⁸. In cervical cancer associated with human papilloma virus 18 infection, GIPC1 is downregulated via E6 oncoprotein production and activity ⁸⁴⁴. As GIPC1 enhances cell surface expression of TGFβ receptor III ⁸³³, the poly-ubiquitination and proteasomal degradation of GIPC1 decreases cancer cell responsiveness to cytostatic signalling via TGFβ.

Role as a biomarker

Proteomic analysis identified GIPC1 as being upregulated within bone homing variants (BM1 and BM2) of the breast cancer cell line MDA-MB-231, compared with parental cells ⁷⁹³. Clinical validation was undertaken using immunohistochemical (IHC) analysis of tumour tissue microarrays (TMAs) from a large randomised trial of adjuvant bisphosphonate ⁸⁴⁵. In the control arm, high GIPC expression was predictive of distant BM, and this risk was greatest when expression of both GIPC and CAPG were high. In the bisphosphonate arm this association was not observed, suggesting a protective effect for treatment. The effect persisted when data from a training and validation set were combined to include 571 patients; the HR for

developing a skeletal event was 2.92 (95% CI = 1.51 to 5.65, $P = 0.001$) for those with high GIPC scores, and 4.54 (95% CI = 2.11 to 9.78, $P < 0.001$) when CAPG and GIPC expression were both high ⁷⁹³. Therefore, GIPC alone, and also the composite biomarker CAPG/GIPC, may have prognostic significance for the subsequent development of BM in BC patients, and has potential to inform the decision to use bisphosphonate treatment for breast cancer.

In addition, high GIPC/CAPG expression was associated with significantly shorter OS in those that did not receive bisphosphonate (5-year survival 76.2% vs 85.9% in those with normal CAPG/GIPC, HR 1.81, 95% CI 1.01-3.24, $p=0.045$) ⁷⁹³. This effect was not observed in the treatment group. Further study of these biomarkers in clinical samples from a range of tumours where bone involvement is frequent would be useful.

Studies in prostate cancer

There is little published data with regards to GIPC and PC. In a small subset from a study of multiple tumour types, GIPC1 was downregulated in primary PC tumours ⁸³⁴. Another study aimed to use biopsy samples to determine the role of GIPC in predicting the radio-resistance of PC cells, and correlate this with clinical outcomes in men undergoing radical radiotherapy ⁸⁴⁶. Depletion of GIPC1 did not affect radiosensitivity, nor did it correlate with clinical endpoints (OS or biochemical recurrence-free survival).

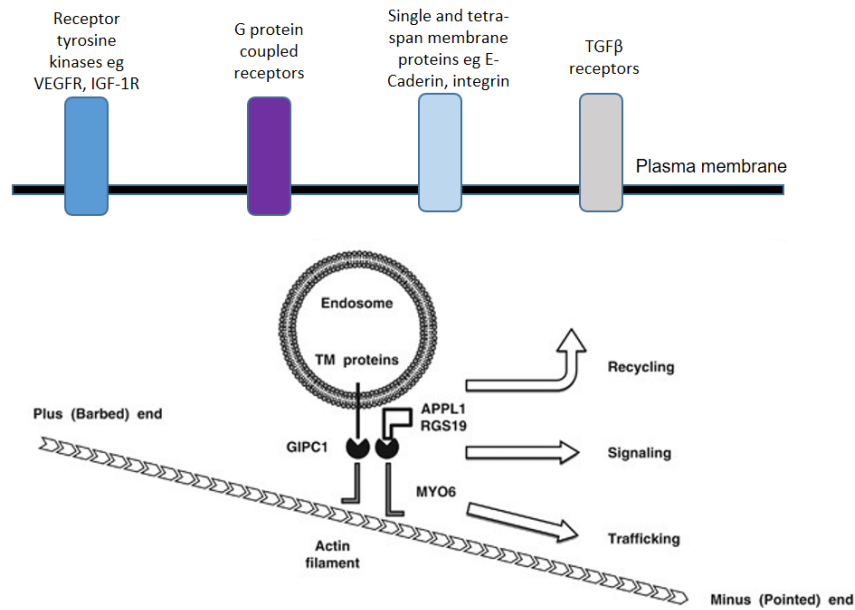


Figure 28: Activity of GIPC1.

Both GIPC and MYO6 act as a protein complex involved in the trafficking of endocytic vesicles. GIPC1 acts as an adaptor protein interacting with trafficking cargoes, while MYO6 is a motor protein that can move along actin filaments from the barbed end (closest to the plasma membrane) to the pointed end in the cytoplasm. Cargoes trafficked by the GIPC1–MYO6 complex include receptor tyrosine kinases, G protein-coupled receptors, transmembrane proteins and cytosolic signalling regulators. The GIPC1–MYO6 complex is also indirectly involved in the recycling of its cargoes. Figure adapted from Katoh et al.⁸²⁴

6.2.4.3 Deducator of cytokinesis protein 4 (DOCK4)

Gene Name: DOCK4, Protein Name: Deducator of cytokinesis protein 4, Uniprot: Q8N1IO).

Structural features and mechanism of action

Deducator of cytokinesis protein 4 (DOCK4) is a member of the DOCK subfamily of guanine nucleotide exchange factors (GEFs). It has a molecular weight of approximately 225KDa. DOCK4 has a Src-binding site at the proline-rich C terminus, a DHR1 (Docker1) domain which binds phosphatidylinositol (3,4,5)-triphosphate, the latter being required for recruitment to the plasma membranes; and a DHR2 (Docker 2) domain which is highly conserved among all DOCK family proteins and mediates their GEF-dependent functions^{847,848}. The adapter protein ELMO is key to the action of DOCK proteins, relieving the autoinhibitory domain of the protein⁸⁴⁹. Binding to ELMO causes a conformational change and enables the G proteins to access the DHR2 domain (figure 29)⁸⁴⁹.

DOCK4 is an important regulator of cell migration, a key process within cancer cell metastasis. Metastasis requires cell polarisation, extension of protrusions in the direction of migration, and detachment at the rear side of the cell, and these are all tightly regulated processes^{850,851}. GEFs such as DOCK4 activate small GTPases, which act as molecular switches (they cycle between an inactive GDP-bound state and an active GTP-bound state) as shown in figure 30. Once activated, they bind to downstream effectors that mediate a variety of biological functions. DOCK4 activates small-GTPases of the Rho family (such as Rac1, Cdc42) and also Rap1^{852,853,854}. DOCK4-mediated Rac1 activation at the leading edge of motile cells induces the formation of lamellipodia protrusions, which act as a key focus and driver of cell migration⁸⁵⁵. Rac1 also has a central role in the generation of endothelial cell filopodial protrusions necessary for blood vessel morphogenesis within tumour angiogenesis⁸⁵⁶.

Rac1 activation also influences Wnt/ β -catenin signalling⁸⁵⁷, thus regulating diverse processes including stem cell renewal, cellular proliferation and differentiation as well as apoptosis⁸⁵⁸. Activation of β -catenin-mediated transcriptional activity is key in this pathway, as outlined in chapter 1 of this thesis. The cytoplasmic level of β -catenin is tightly regulated by a degradation complex (consisting of the proteins adenomatous polyposis coli, axin and glycogen synthase kinase 3b)⁸⁵⁹. Aberrant regulation of Wnt/ β -catenin signalling is associated with accelerated cell growth and neoplasia. DOCK4 is an important scaffold protein in the β -catenin degradation complex, and is important in maintaining β -catenin stability⁸⁶⁰.

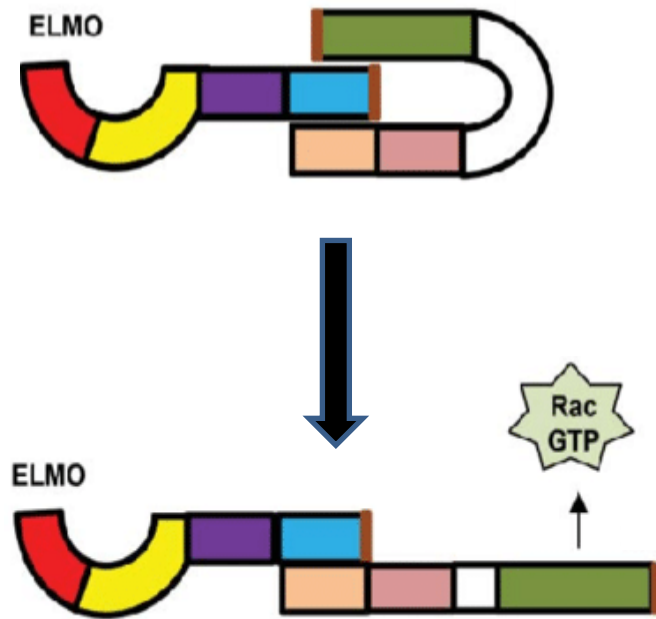


Figure 29: Regulation of DOCK proteins by ELMO.

In the inactive state, the GEF activity of DOCK4 is inhibited. When ELMO binds to DOCK4 at its N terminal, a conformational change allows GEF proteins to gain access to the DHR2 domain. ELMO also recruits the RhoG protein which recruits the Elmo-DOCK4 complex to areas of high substrate availability (such as the plasma membrane). The C terminus of DOCK4 interacts with the Crk adapter protein. Figure adapted from Jin et al ⁸⁶¹.

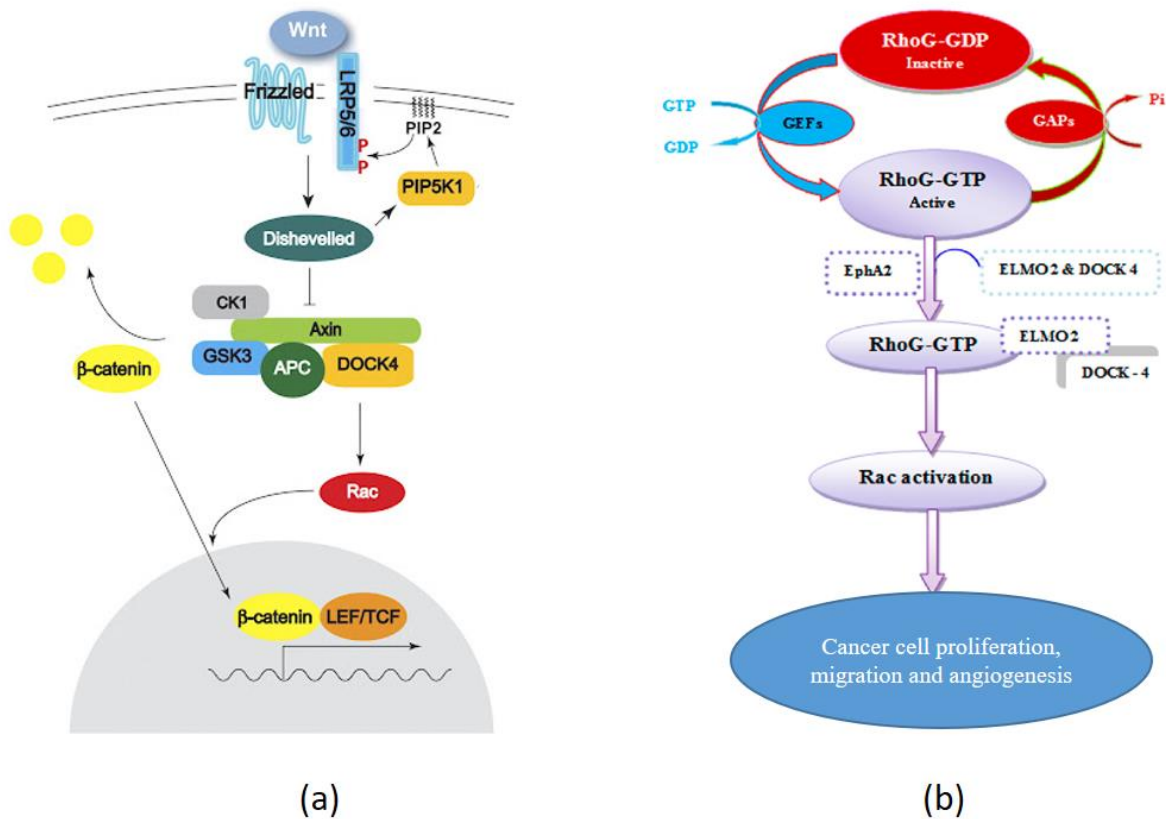


Figure 30: DOCK4 mechanisms of action.

Figure 30 (a): Role of DOCK4 in Wnt signalling. In the unstimulated state of the cell β catenin is bound to a multi-protein degradation complex which inhibits β -catenin. Upon Wnt-action, this is phosphorylated (by GSK β), poly-ubiquitinated and degraded by the 21S proteasome. Release from the degradation complex allows β catenin to accumulate in the cytoplasm from which it is translocated to the nucleus and stimulates gene expression in complex with the T-cell-factor transcription factor. DOCK4 is also required for activation of Rac, a small GTPase that is also a regulator of the actin cytoskeleton. Image 30(a) adapted from Tolwinski et al ⁸⁶². **Figure 30(b): Dock family of GEFs activate Rho family GTPases.** DOCK4 activates GTPases such as Rac1, Cdc42 and also Rap1. Rac1 activation has multiple downstream effects including formation of cellular lamellipodia protrusions for migration, a role in angiogenesis and also controlling cellular morphology, transcriptional activation, and apoptosis. Figure 30(b) from Dasari et al ⁸⁶³.

DOCK family proteins and cancer biology

Previous studies have identified that members of the DOCK class of proteins are required for cancer cell proliferation and metastasis, through a range of protein-protein interactions. In melanoma cells, DOCK10 increased cell migration and invasion⁸⁶⁴ and DOCK3 has been identified as a driver of mesenchymal cell migration through a complex containing NEDD9 (a known melanoma metastasis gene)⁸⁶⁵. In HER2 positive breast cancer, DOCK1 promotes cancer progression to metastasis⁸⁶⁶ and in glioblastoma multiforme cells, EGFR-induced phosphorylation of DOCK180 increases both cell survival and migration⁸⁶⁷. DOCK4 regulates the activity of the small GTPase protein Rac1 (a feature it shares with the other DOCK family members), however, unlike the other DOCK proteins, DOCK4 also regulates the activity of the small GTPase Rap1. The ability of DOCK4 to regulate Rap1, suggests that DOCK4 could potentially play a role in the regulation of integrin mediated cell-cell contacts, alter signalling via B-Raf / Raf-1 or regulate intracellular vesicle trafficking⁸⁶⁸

DOCK4 and tumorigenesis

An important interaction has been identified between DOCK4 and the cytokine transforming growth factor beta (TGF β)⁸⁶⁹. TGF β has numerous diverse roles in metastasis, initially TGF β acts as a tumour suppressor, however in later stages of tumorigenesis (when it is produced from both tumour and stromal cells) TGF β is a highly potent driver of local motility, tumour cell invasion, intra- and extravasation, and tumour cell survival at distant sites, all of which are fundamental to cancer cell invasion and metastasis⁸⁷⁰. DOCK4 expression (but not that of other DOCK family members) is induced by TGF β via the Smad pathway in lung adenocarcinoma cells, a key step in TGF β exerting its pro-metastatic effect⁸⁶⁹.

DOCK4 expression also correlates with expression of the transcription factor c-MAF in primary breast tumours. c-MAF has been identified as a key regulator of BM in breast cancer and expression of this transcription factor has been demonstrated to be induced by TGF β ^{871,797}. DOCK4 may be one of several proteins that alter in response to elevated c-MAF expression within metastatic bone homing breast cancer cells⁷⁹⁷.

DOCK4 as a clinical biomarker

DOCK4 has recently been identified as a potential biomarker for risk of BM development in patients with early breast cancer. Using well established proteomic methods, DOCK4 was upregulated in bone homing variants (BM1) of a parental breast cell line (MDA-MB-231) compared with parental non-bone homing cells⁷⁹⁷.

The clinical significance of DOCK4 levels for prediction of BM outcomes was determined by IHC staining of a training breast tumour tissue microarray (TMA), where high DOCK4 expression was associated with high grade histology⁷⁹⁷.

Subsequent TMA analysis within > 700 patients enrolled in the AZURE breast cancer trial found that high DOCK4 expression was prognostic for cancer recurrence in bone in the control arm (no adjuvant bisphosphonate, HR 2.13, 95% CI 1.06-4.30, $p=0.034$), an association not observed in the treatment arm⁸⁴⁵. These findings suggest that high DOCK4 levels predict risk of metastasis to bone and that measuring DOCK4 levels within BC could have potential to inform patient treatment decisions.

Studies of DOCK in prostate cancer

Very few studies have investigated the role of other DOCK family members in PC. DOCK2 may contribute to PC cell proliferation in hormone resistant cells, and in these cell lines was required for chemokine (CXCL13)- induced cell proliferation through the activation of JNK⁸⁷². No studies to date have specifically sought to explore the role of DOCK4 in PC progression.

6.2.5 Prostate cell lines and in vitro models

Cell and tissue models have been developed in order to improve our understanding of the molecular pathogenesis of PC. Cell lines are derived from patient biopsies, and advances in murine models have allowed the investigation of tumourigenic and metastatic processes. Murine models in particular enable the study of metastasis in a well-defined biological context, and within a timeframe which is amenable to scientific research.

There are many prostate cell lines available which have been derived from different prostate cell types and which include benign and malignant forms. Malignant prostate cell lines are available that originate from both hormone-sensitive and hormone resistant tumours. Cellular expression of androgen receptors, PSA, p53, PTEN varies between the cell lines, as does their growth rate and optimal culture conditions.

Human PC cell lines may also be transplanted into mice, and the three main xenograft models that are used are subcutaneous, orthotopic (the introduction of cancerous prostatic tissue into the mouse prostate) and subrenal capsule implantation, each has different advantages, costs and limitations.

Murine metastatic models of PC are also available. Intratibial injection involves the direct injection of prostate cancer cells (often labelled with a fluorescent dye for tracking) in suspension into genetically manipulated or wild type mice, whereas other models use tail vein or intracardiac injection. In vivo imaging techniques (including bioluminescence) are used to track the growth of lesions. However, these models all have their limitations and there is currently no single murine model that accurately and reliably seeds tumour cells from prostate to bone. This is in contrast to breast cancer, where the depth and breadth of molecular characterisation has been far more extensive. Well established breast cancer cell

lines represent the whole spectrum of disease and include bone homing variants (and isogenic parental cell-lines). Results obtained using murine cell-models obviously require clinical validation before they can influence patient treatment decisions.

6.2.5.1 Prostate cancer cell lines

A summary of the PC cell lines used in this chapter is shown in table 33.

LNCaP

The LNCaP cell line is derived from a needle aspiration biopsy of a supraclavicular lymph node lesion in a 50 year-old Caucasian male in 1977⁸⁷³. This patient had rapidly progressing PC that failed to respond to hormone deprivation therapy (medical and subsequently surgical) and chemotherapy (estramustine and methyl-CCNU).

LNCaP are androgen-sensitive adenocarcinoma cells, which grow readily in vitro (up to 8×10^5 cells/cm²; doubling time approximately 60hrs) as both aggregates and single cells. They show an aneuploid human male karyotype (the chromosome number ranges from 76-91), are of luminal epithelial origin (cytokeratin 8 and 18 positive) and express wild type p53, PSA mRNA and PCA3. They also have a point mutation in the ligand binding domain of the androgen receptor, which affects their steroid binding characteristics and contributes to androgen-independent tumour growth⁸⁷⁴. Cytogenetic analysis of LNCaP cells has demonstrated deletion of the tumour suppressor gene PTEN⁸⁷⁵ and over-expression of the ETS transcription factor ETV1. ETV1 promotes the development of a neoplastic phenotype in mouse models⁸⁷⁶, and may be associated with advanced disease in the clinical setting⁸⁷⁷.

Subcutaneous injection of LNCaP cells into athymic nude mice leads to the development of rapidly growing, highly vascular and poorly differentiated tumours at the injection site⁸⁷⁸. The tumour take rate is enhanced by testosterone supplementation, and significantly reduced in castrated nude mice. Development of metastatic lesions is rare following subcutaneous injection of LNCaP.

Orthotopic inoculation of LNCaP cells into the dorsal prostate of athymic mice results in tumour formation in more than 50% of cases, and in SCID mice this increases to 90%⁸⁷⁸. Ultimately, orthotopic xenograft in athymic nude mice results in 50-60% developing regional lymph node, lung and liver metastases. Following the same procedure, all SCID mice develop regional lymph node metastases, and 40% develop pulmonary lesions⁸⁷⁸, most likely due to a greater degree of immunocompromise (both B and T cell deficiency relative to athymic mice) and significantly greater serum testosterone concentrations that may facilitate metastatic tumour growth. Tumour incidence can be increased further with testosterone supplementation, or use of a scaffold matrix (such as Matrigel™)

which is mixed with inoculated cells to prevent leakage from the prostate capsule⁸⁷⁹.

Metastatic bone involvement from LNCaP cell administration is rare, and thus these models therefore do not fully replicate human disease. Both primary and metastatic lesions arising from LNCaP are poorly differentiated, express androgen receptors and secrete PSA. Castration suppresses tumour formation, and a PSA response is detectable after 1 week⁸⁷⁸.

C4, C5 and C4-2 cell lines

The C4 and C5 cell lines were derived from LNCaP cells, after subcutaneous co-inoculation with human bone stromal cells into athymic nude mice⁸⁸⁰. Tumours formed between 4-5 weeks. In order to replicate androgen insensitivity, mice were castrated (mid scrotal incision) 8 weeks following injection. Tumours were maintained for 4 weeks (C4) and 5 weeks (C5) before harvesting. The C4 cells were then co-injected with human fibroblasts into a castrated host to generate the C4-2 subline.

The C4-2 subline follows the metastatic patterns of CRPC, as both lymph node and BM develop following subcutaneous or orthotopic injection into either hormonally intact or castrated mice^{880,881}. Osseous lesions arise in 10-25% of athymic nude mice following orthotopic injection, and are phenotypically similar to human BMs, primarily osteoblastic with some evidence of osteolysis, and decreased bone volume and BMD. C4-2 cells form highly vascularised tumours which are AR positive and stain positively for PSA. They are independent from both androgens and inductive fibroblasts; cell growth is unresponsive to androgens *in vitro*, and it is the only cell line that is able to produce tumours without co-injection of MS bone stromal cells into castrated mice. Based upon the propensity of C4-2 tumours to develop PSA secreting BM, orthotopic xenografts have been widely used as a preclinical model to study PC cancer progression and metastasis.

The C4-2B and C4-2B4 cell lines

The C4-2B cell line was developed following orthotopic injection of C4-2 cells into castrated mice, and primary tumours developed in the prostate, regional lymph nodes and bone. Several rounds of sub-culturing of C4-2 cells led to the development of the pure BM-derived lines C4-2B, which has enhanced our understanding of the *in vivo* behaviour of BM⁸⁸². Cells express PSA, and have been shown to express higher levels of osteoprotegerin, osteocalcin, bone alkaline phosphatase, bone sialoprotein, RANK ligand than LNCaP cells (all indicate increased osteoblastic activity)⁸⁸³. C4-2B2 cells derive from a lesion in an intact host, C4-2B3 and C4-2B5 from a castrated host, and C4-2B4 from a castrated orthotopic tumour⁸⁸².

PC3 and PC3M cell lines

The PC3 cell line originates from a vertebral metastasis of human prostatic adenocarcinoma in 1979⁸⁸⁴. PC3 cells are aneuploid, with an average of 58 chromosomes and doubling time of approximately 33hrs. Electron microscopic studies have confirmed that cells retain features common to neoplastic cells of epithelial origin, including numerous microvilli, junctional complexes, abnormal nuclei and nucleoli, abnormal mitochondria and lipoidal bodies⁸⁸⁴. PC3 cells are androgen independent, and there is no expression of androgen receptors or production of PSA mRNA or protein. Cells highly express both TGF α and the EGR-R (which allows autonomous growth and may also facilitate metastatic bone involvement)⁸⁸⁵, and have aberrant expression of p53 and PTEN deficiency⁸⁸⁶. It has been suggested that some features of PC3 cells may be more characteristic of a small cell variant of PC than the more common adenocarcinoma⁸⁸⁷.

In xenograft mouse models, both intravenous injection and orthotopic implantation of PC3 cells leads to the development of lymph node metastases^{888,889}. Harvesting of intra-prostatic mouse tumours and re-injection into the prostate (cycle repeated several times) has led to the creation of PC3 sublines such as PC-3M with increased metastatic ability⁸⁸⁸. Intravenous or intra-cardiac injection with PC-3M cells produces a high incidence of lung and bone metastasis respectively⁸⁸⁸.

6.2.6 Hypothesis and aims

Previous research undertaken within the bone-biomarkers group at Sheffield, utilized proteomic methods and an isogenic bone homing cell-line to identify novel biomarker proteins within triple negative breast cancer^{793,797}. This protein panel, comprising CAPG, GIPC1 and DOCK4 was identified by quantitative proteomic profiling of parental and bone-homing MDA-MB-231 cells. The ability of this protein panel to predict the risk of subsequent development of cancer spread to bone within patients, was validated by immunohistochemical (IHC) analysis of primary breast tumour sections derived from a large clinical trial that compared treatment with and without bisphosphonate^{792,797}.

This study aimed to build upon the previous work in breast cancer, and investigate the role of CAPG, GIPC1 and DOCK4 as predictive markers in PC. Both prostate and breast cancer frequently metastasise to bone, however as previously described, once within bone they develop different types of metastatic lesions. However, there is evidence suggests that CAPG, GIPC1 and DOCK4 may have a key role in PC progression. It has also been demonstrated that although solid tumours may be associated with different BM phenotypes (osteoblastic Vs osteolytic), there is overlap in signalling pathways and mechanisms of metastasis⁸⁹⁰.

We aimed to quantify the expression of the proteins DOCK4, CAPG and GIPC across a panel of selected PC cell lines, using an antibody based approach (western blotting and immunohistochemistry (IHC)). A series of well-established PC cell-lines with differing degrees of bone homing were utilized together with well-validated commercial antibodies towards the three protein targets.

The selected PC cell lines (shown in table 33) represent various stages of the PC continuum, and we hypothesised that the cell lines strongly associated with or derived from xenograft BM (PC3M and C4-2B) would potentially have a higher expression of the target biomarkers (figure 31). However, this panel has not been used to identify potential biomarkers of PC bone metastasis before, and is therefore exploratory. Any differences identified may be applicable to human PC BM, although would require further validation. Overall, the results of this pre-clinical study, if successful, would provide a useful precursor to further validation of the proteins within patient derived PC samples.

Table 33: Prostate cancer cell lines used

Panel	Cell line	Derivation	Hormone status	Key features	Predicted bone homing ability
1	LNCaP	Supraclavicular lymph node metastasis in male with PC	Sensitive	High incidence of lymph node and liver metastases Poor tumourigenicity in athymic nude mice	Low
	C4-2	Derived from injection of from LNCaP cells with human bone stromal cells into athymic castrated nude mice, tumours harvested from bone at 4 weeks	Resistant	Readily forms tumours in intact hosts Osteoblastic phenotype of bone metastases Androgen independent	Moderate
	C4-2B	From C4-2 injection into castrated mouse, samples taken from osseous tumour	Resistant	High propensity to metastasise to bone Osteoblastic phenotype of bone lesions	High
2	PC3	Vertebral metastasis in male with PC	Resistant	Androgen independent Expression of multiple growth factors Osteolytic metastases	Moderate/ high
	PC3M	Harvesting and orthotopic re-injection of PC3 cells into mouse	Resistant	Metastatic variant of PC3 cells High incidence of lung and osteolytic bone metastases	High

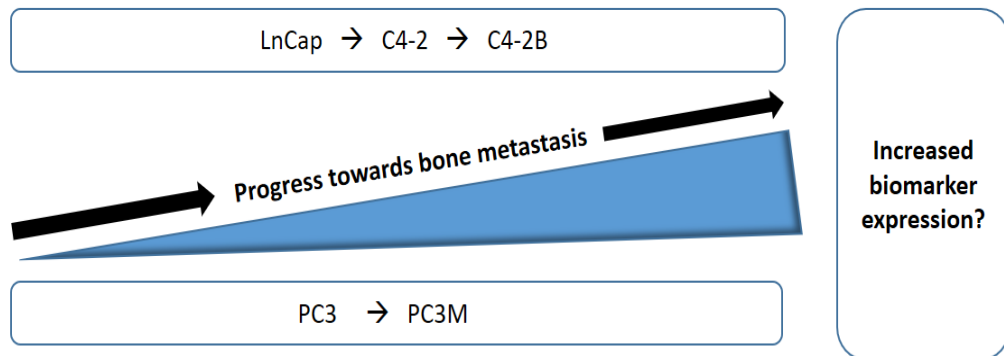


Figure 31: Hypothesis for the relationship between the prostate cancer cell lines and expression of potential biomarkers of BM.

This is based upon the cell line derivation and behaviour in xenograft models, and expression of the target biomarkers in breast cancer lines.

6.3 Materials and methods

6.3.1 Cell culture

Prostate cancer cell lines (LNCaP, C4-2, C4-2B and PC3) were obtained from the American Type Culture Collection (ATCC, Gaithersburg, USA). PC-3M cells were kindly gifted from Dr Ning Wang (University of Sheffield). All cell lines were cultured in Dulbecco's Modified Eagle's Medium (DMEM) and 4.5 g/L glucose with ultraglutamine (Lonza, Verviers, Belgium) supplemented with 10% foetal bovine serum (FBS) (Life Technologies, Brazil) at 37°C in 5% CO₂. Cells were cultured in flasks of increasing size (T2, T75 and T175) and split with trypsin upon >90% confluency.

6.3.2 Preparation of cell lysate

Once the cells reached > 90% confluency, DMEM + FCS was removed and the flasks were rinsed three times with 10-20ml of sterile phosphate buffered saline (PBS) each time. Cells from each flask were then lysed into 2ml of 2X Laemmli Sample Buffer (LSB) (Sigma, Cat No: S3401-10VL). A rubber scraper was used to detach the cells into LSB. Subsequent repeat passage of the cells through a narrow gauge (0.22 µm) needle with five to ten repeats was performed to shear genomic DNA in the samples. The sample were the centrifuged at 14,000 rpm (insert g) for 10 minutes, and the supernatant was removed, transferred into aliquots and stored at -20°C as the final Total Cell Lysate (TCL) samples.

6.3.3 Protein assay

The protein content of the cell lysate was quantified using a Bio-Rad detergent-resistant RC-DC™ assay (Cat No: 5000121). The recommended additional wash was undertaken to minimise transfer of any residual SDS into the protein assay thus minimising contaminant interference.

6.3.4 Western blotting

Target protein expression levels (for DOCK4, GIPC and CAPG) within TCL samples was determined western blotting (WB) following protein separation by one-dimensional sodium dodecyl-sulfate polyacrylamide gel electrophoresis (1D-SDS-PAGE). Immunoprobng was performed in cell lysates from LNCaP, C4-2, C4-2B, PC3 and PC3M cell lines (figure 32). 30ug total protein from each TCL sample was loaded into the lanes of a 10% Mini-PROTEAN® TGX™ precast gel (Bio-Rad TGX precast gels), and proteins were separated using a Bio Rad MiniPROTEAN® electrophoresis system. SDS-PAGE gels were run (using a Glycine-SDS buffer system) at 120V for approximately 1 hour until the dye front was at the bottom of the gel. Band MW was determined using dual colour precision plus protein™ standards markers (Bio-Rad).

Blots were transferred onto nitrocellulose membranes (GE-Healthcare Life Science) using Bio-Rad Mini Trans-Blot electrophoretic transfer cell (Cat. No: 170-3930) at 100V constant voltage for 1-hour, in 1X 20% (v/v) methanol, Tris-Glycine-SDS WB transfer buffer. Ice was used to surround the cell to prevent heat build-up and avoid running abnormalities and band deformations, bubbles and bubble expansion. Blots were blocked in blocking buffer (5% (w/v) milk-powder in PBS) overnight at 4°C before probing.

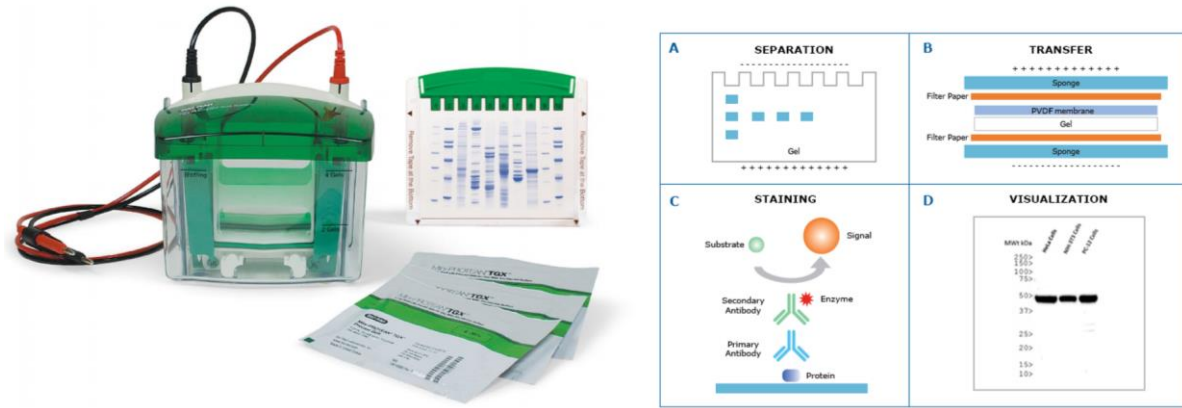
Western blots underwent immunoprobings with primary antibodies, including; Abcam ab123653 (GIPC1), Abcam ab85723 (DOCK4) and Sigma prestige HOA019080 (CAPG). Details and dilutions are shown in table 34. Blots were incubated with primary antibodies for 1 hour at room temperature. Blots were then washed (4 washes of 5 minutes each) with PBS-0.05% (v/v) Tween-20. HRP-labelled goat anti-rabbit or HRP-labelled goat anti-mouse IgG were used for secondary antibody incubation (table 34) again for 1 hour at room temperature, followed by 4 further PBS 0.05% (v/v) Tween-20 washes. β tubulin was used as a loading control for all samples.

Immunoreactivity was visualized using an enhanced chemiluminescence substrate (ECL; Promega). ECL immunoreactivity was visualized by blot exposure using x-ray film and cassette (Hyperfilm, Amersham). Exposure times were optimized according to target, with subsequent manual film development using Kodak developer and fixer. Digital images were acquired using the ChemiDoc imaging system and ImageLab software (BioRad). ImageLab was used for band quantification.

6.3.5 Optimisation

Optimisation of the primary antibody dilutions and X ray exposure times was required. The initial dilution of primary antibodies used was the manufacturer-specified dilution. X-ray exposure time varied between antibodies, and films were exposed at intervals ranging from 30 secs up to 60 minutes in order to obtain optimal band intensities.

For each biomarker under investigation, western blots were repeated five times once the antibody conditions had been optimised. The mean band intensity was used for analysis with normalization to the β -tubulin loading control.



1	2	3	4	5	6	7	8	9	10
Marker	LNCap with CAPG/GIPC antibody	C4-2 with CAPG/GIPC antibody	C4-2B with CAPG/GIPC antibody	-	Marker	LNCap with Tubulin antibody	C4-2 with Tubulin antibody	C4-2B with Tubulin antibody	-

1	2	3	4	5	6	7	8	9	10
Marker	PC3 with CAPG/GIPC antibody	PC-3M with CAPG/GIPC antibody	-	-	Marker	PC3 with Tubulin antibody	PC-3M with Tubulin antibody	-	-

1	2	3	4	5	6	7	8	9	10
Marker	LNCap with DOCK4 and tubulin	C4-2 with DOCK4 and tubulin	C4-2B with DOCK4 and tubulin		Marker	PC3 with DOCK4 and tubulin	PC-3M with DOCK4 and tubulin		

Figure 32: Western blot analysis for biomarker validation.

The BioRad mini-gel system was used to perform one dimensional gel electrophoresis (1D-SDS-PAGE). Proteins were loaded (30 µg / lane) into 10 lane gels as shown in the figure. CAPG and GIPC1 were run simultaneously as their predicted molecular weights were similar to the tubulin control. DOCK4 was analysed using one gel. Cell lysates underwent separation by electrophoresis before transfer onto nitrocellulose membranes. The blots were blocked in milk buffer overnight before undergoing immunoprobeing with primary and secondary antibodies. The addition of a chemiluminescent substrate allowed visualisation using standard X ray techniques.

Table 34: Primary and secondary antibodies used for immunoprobng, dilutions and optimal conditions used for film development (all cell lines)

Target	Supplier, number and concentration of primary antibody	Primary antibody dilution	Secondary antibody and dilution	Optimal film exposure time
GIPC1	Abcam (Rb) ab123653, 0.1ml/ml	1/250	Goat anti-rabbit, Invitrogen A16096, 0.1mg/ml 1/2500	30 min
DOCK4	Abcam (Rb) ab85723, 0.2mg/ml	1/2000	Goat anti-rabbit, Invitrogen A16096, 0.1mg/ml 1/2500	60 min
CAPG	Sigma Prestige (Rb) HOA019080, 0.1 mg/ml	1/1000	Goat anti-rabbit, Invitrogen A16096, 0.1mg/ml 1/2500	30 min
β -Tubulin (control)	Abcam (Ms) ab7792-100, 1mg/ml	1/1000	Invitrogen 0.1ml/ml A16066, 1/2500	1 min
	Origene (Rb) TA309059, 1mg/ml	1/1000	Goat anti-rabbit, Invitrogen A16096, 0.1mg/ml 1/2500	5 min

6.3.6 Immunohistochemistry

Immunohistochemistry (IHC) was done to validate the results of WB, and to replicate the detection of protein expression using formalin fixed paraffin embedded (FFPE) sections, typical of the procedures used with clinical samples, such as TMAs. Preservation in 10% neutral buffered formalin (NBF) is one of the most commonly used fixatives in histopathology; it leads to the formation of methylene cross-links which prevents protein degradation. Tumour biopsies may then be stored for subsequent diagnostic or prognostic analysis and are stable for years.

6.3.6.1 Preparation of slides

Use of FFPE cell pellets mimics the expression of target proteins within clinical IHC analysis, as the protein modifications and storage methods used are similar. FFPE-cell pellet analysis is a semi-improvised, interim step that guides the development of optimal staining conditions for use with patient-derived tissue-microarrays (TMAs). In addition, FFPE pellets from cell-lines allows a combination of this procedure with targeted gene knockdown (using methods such as short hairpin - shRNA or CRISPR-gene editing).

FFPE TMA slides were prepared using cell pellets from LNCaP, C4-2, C4-2B, PC3 and PC-3M cell lines. 100 µl molten (1% w/v) agarose was transferred into 1.5ml Eppendorfs and allowed to set overnight at 4°C to form a base. Cell pellets (trypsinized from confluent T175 flasks) were fixed in 10% Neutral Buffered Formalin for 48 hours at room temperature, and then suspended in 300µL molten (1% w/v) agarose (1% w/v). This cell-suspension in molten agarose was immediately pipetted on top of the previously-prepared agarose bases and left to solidify overnight at 4°C. The agar cell pellets were removed and placed into plastic cassettes for serial dehydration with graded ethanol followed by xylene. The histology lab (Medical school, University of Sheffield) processed these samples and sectioning of the 5µm sections was done by a trained operator.

6.3.6.2 Verification of target proteins

A citrate buffer heat antigen retrieval method was used, and the key steps are shown in figure 33. Protein cross-linking caused by FFPE fixation obscures protein epitopes, so the heat-induced antigen retrieval method (citrate buffer pH 6.0 at 100°C for four minutes within a microwave) improves staining. FFPE slides prepared from cell pellets of each of the biomarkers investigated were de-waxed by two 5-minute xylene washes, then dehydrated in 100% ethanol (5minutes), 100% ethanol (5minutes) and 95% ethanol (5 minutes). Endogenous peroxidase activity was blocked by incubation of the slides in 0.1% (v/v) hydrogen peroxide/methanol. Three 5-minute PBS washes were then carried out.

Sections were blocked using 10% (v/v) normal goat serum (NGS) (Cat no S-1000, Vector Laboratories) at room temperature for 30 minutes. This was followed by primary antibody incubation in 2% (v/v) NGS in PBS. The antibodies that were used for the IHC were; DOCK4 Abcam (Rb) ab85723 (0.2mg/ml) and GIPC1 Abcam (Rb) ab123655 (details in table 35). All primary antibody incubations were performed overnight at 4°C. Control slides without primary antibody were also prepared to test for staining specificity, and a bone homing breast cell line was used (P7) for comparison. An example of a standard run is shown in figure 34.

The following day, slides underwent secondary antibody incubation (details in table 35) with antibody diluted 1/200 in 2% NGS, for 1hr at room temperature. Three five-minute PBS washes were then done, before staining.

Staining was developed using Vectastain Elite ABC kit (Cat No PK-6100 Vector Laboratories) followed by three further 5-minute PBS washes. A DAB substrate Kit (Cat No: SK-4100 Vector Laboratories) was applied to the slides for 5 minutes, and slides were imaged at 40X magnification using a Leica DM1000 LED microscope (images captured using Leica LCSLite software). Slides were washed in water and a DAB counterstain was applied using Gills haematoxylin for 1 minute. A final 2-minute wash preceded sample dehydration using graded ethanol concentrations (3 minutes each at 70%, 90%, 95%, 100% and 100% v/v). All slides were then immersed in xylene (for 6 minutes in total) before they were mounted using DPX (distrene, plasticizer and xylene). Slides were then labelled and left to dry overnight.

Slides were scanned using a Panoramic 250 Flash III Slide Scanner (3DHISTECH, Budapest, Hungary). The intensity of DAB staining was determined using QuPath software. For each slide, five areas containing between 5000-6000 cells/area were selected at random, and the average percentage of positive cells was measured. All cells on each slide were used to determine the mean DAB intensity.

6.3.7 Statistical analysis

Analysis of western blot data was performed using ImageLab software (BioRad) which provides quantification of band densitometry, following background selection. β -normalized band intensity was compared between the cell lines using SPSS-software and the student's two-sample two tailed t-test, with a significance level of $p < 0.05$. For IHC analysis, DAB protein staining within slides was quantified using a colour deconvolution tool within the Fiji software (<http://Fiji.sc/>). The relative intensity value was calculated as the absorbance value divided by the total cell area. The process was set to binary using the "particle analyser" function.

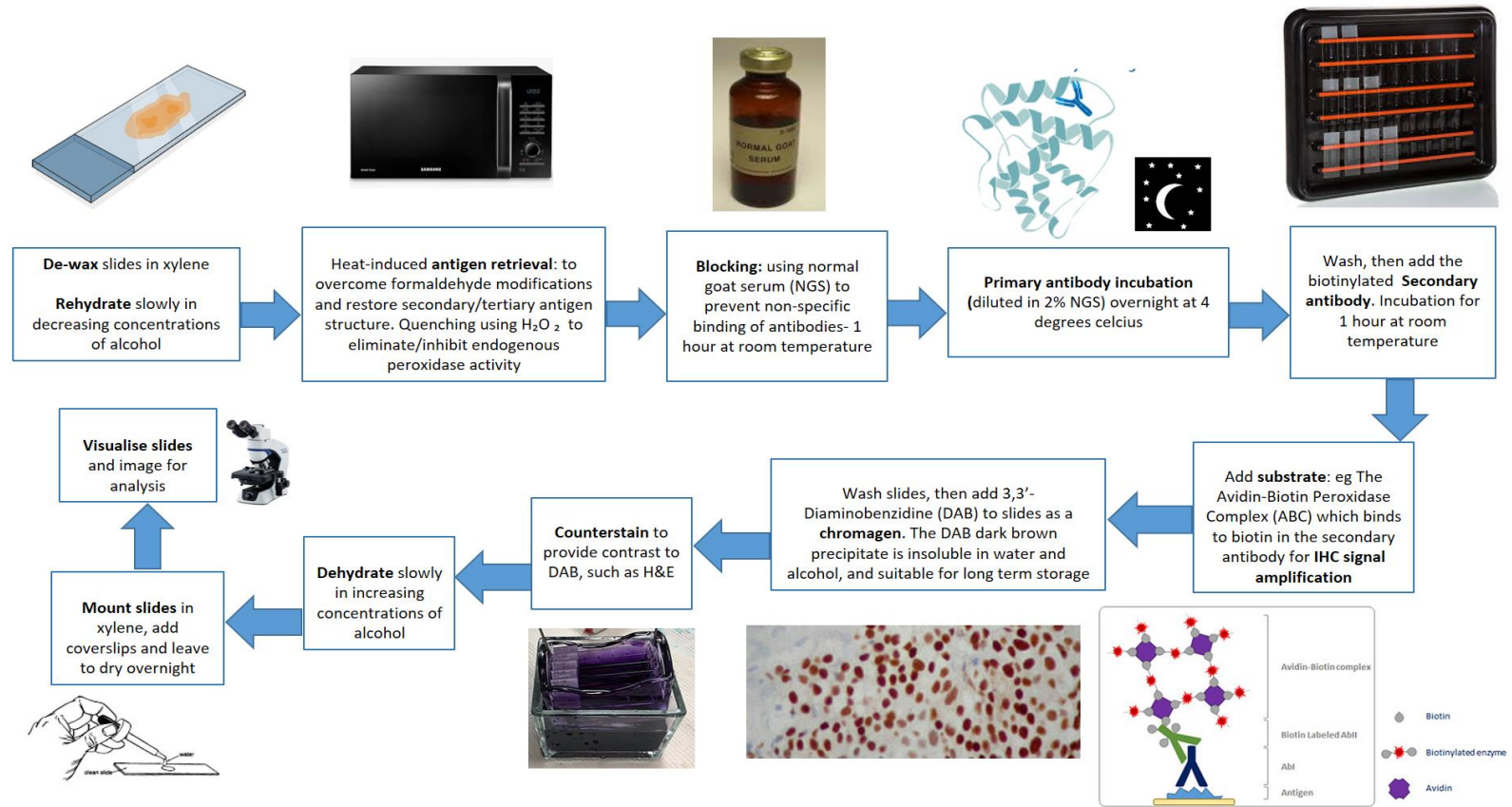


Figure 33: Immunohistochemistry using heat antigen retrieval.

The key steps are outlined, along with representative images.

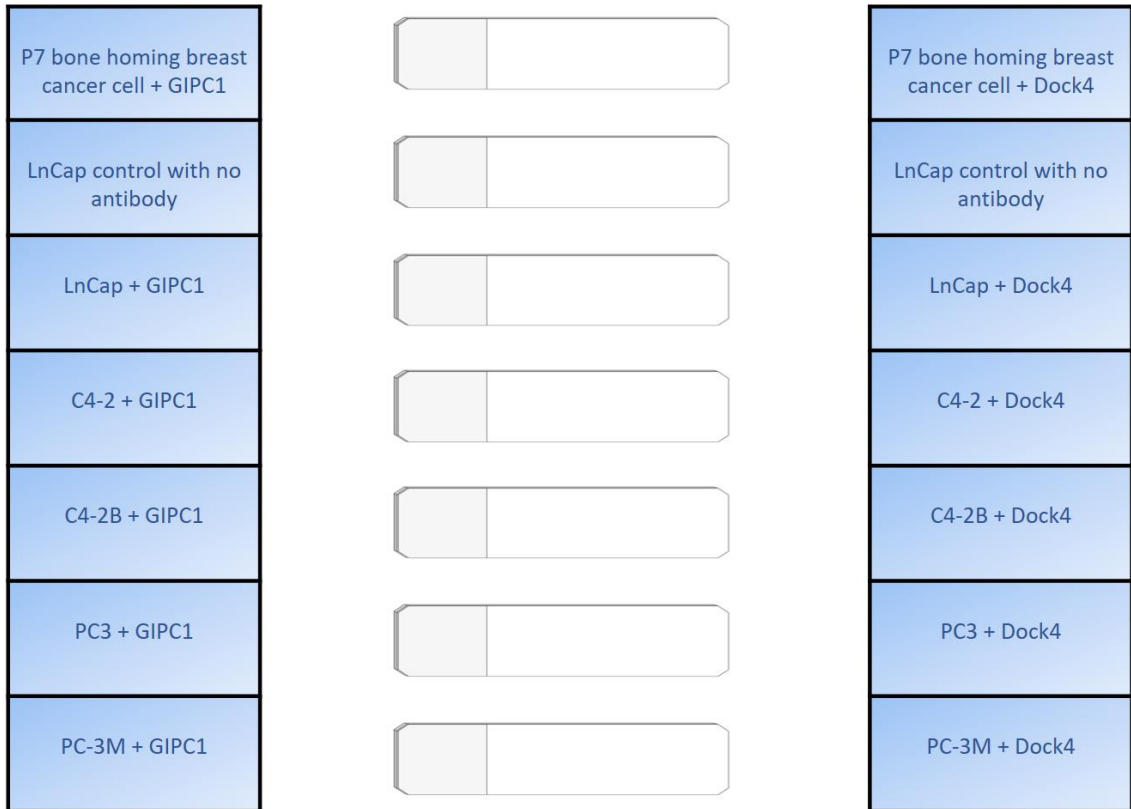


Figure 34: A standard IHC run with DOCK4 and GIPC.

Each run included each of the five prostate cancer lines as well as a control (no primary antibody) and a fully-bone homing breast cancer cell-line (P7). A total of four runs were done for each of the targets.

Table 35: Primary and secondary antibodies used for immunohistochemistry

Target	Supplier, number and concentration of primary antibody	Primary antibody dilution	Secondary antibody and dilution	Optimal DAB time
GIPC	Abcam (Rb) ab123653, 0.1ml/ml	1/50	1/200	10 min
DOCK4	Bethyl (Rb) 800-338-9579, 0.2mg/ml	1/100	Vector lab BA1000 Goat anti-rabbit IgG	10 min

6.4 Results

6.4.1 CAPG

6.4.1.1 Verification by western blot

The predicted molecular weight of CAPG is 38KDa, and a 30 min exposure time produced a blot with acceptable band intensity for CAPG, although the β tubulin exposure time was much shorter (1-5 minutes). An example is shown in figure 35, along with the reference MW markers used. The average band intensities for Cap G were normalised to β tubulin for each of the repeated experiments, and this data is outlined in table 36.

The blots showed a clear band at the correct molecular weight with differential expression across all five cell lines. The mean band intensity in the LNCaP cell line was 0.43 (range 0.19-0.68), and was 0.24 (range 0.11-0.49) for C4-2 and 0.39 (range 0.12-0.97) for C4-2B cells. Although there was a reduction in band intensity from LNCaP to C4-2 and a further decrease between C4-2 and C4-2B, the difference was not statistically significantly different between them.

The mean band intensities for the PC3 and PC-3M cell lines were 0.62 and 0.47 respectively (range 0.29-1.0 for PC3 and 0.05-1.28 for PC-3M). The decrease in intensity between PC3 cells and the derived cell line PC-3M was not statistically significant. Based upon these results, CAPG was not taken forward into immunohistochemistry.

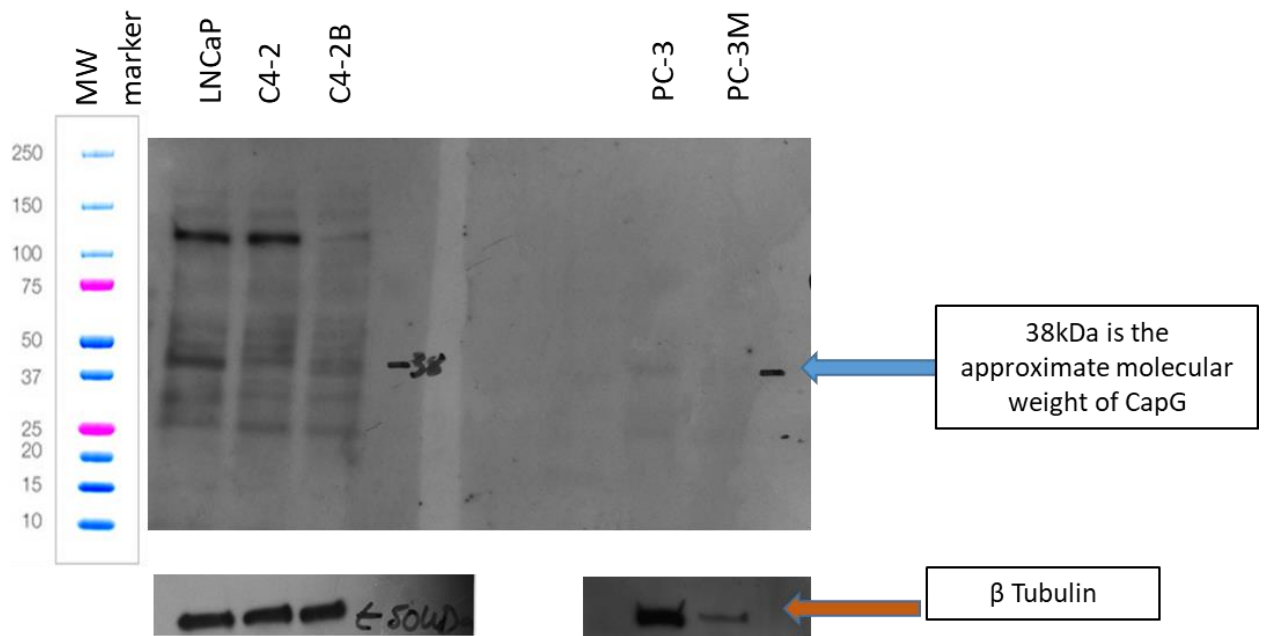


Figure 35: CAPG protein quantified by western blot.

A representative blot of the detection of CAPG at 38KDa (blue arrow) with corresponding β -tubulin loading control (orange arrow) blot shown below, for all five cell lines. 30 μ g of each total lysate sample was added per lane. Images were taken and analysed using Image Lab software.

Table 36: Quantification of CAPG identified by western blot

Ratio of CAPG to beta tubulin

Cell line	Gel 1	Gel 2	Gel 3	Gel 4	Gel 5	Mean ratio	p value*
LNCaP	0.30	0.68	0.19	0.33	0.64	0.43	LNCaP Vs C4-2 p=0.12
C4-2	0.23	0.15	0.22	0.11	0.49	0.24	
C4-2B	0.97	0.25	0.55	0.09	0.12	0.39	C4-2 Vs C4 2B p=0.19
PC3	0.67	0.69	1.0	0.29	0.46	0.62	PC3 Vs PC3M p=0.6
PC-3M	0.21	1.28	0.05	0.71	0.13	0.47	

*comparison of means using independent samples t test

6.4.2 GIPC1

6.4.2.1 Verification by western blot

The predicted molecular weight of GIPC1 is 36KDa. Using the Abcam ab123653 antibody, a 30 min film exposure time produced the optimal band intensity (table 34). An example blot is shown in figure 36. The average band intensities were normalised to Tubulin for all of the repeated experiments, and data are shown in table 37. One repeat was not included as there was an error with the immunoprobng.

Across four experiments, the mean band intensity of GIPC1 in LNCaP cells was 0.99 (range 0.93-1.08), and was 0.75 (range 0.54-0.88) for C4-2 and was 0.57 (range 0.35-0.88) for C4-2B cells. The mean band intensities for the PC3 and PC-3M cell lines were 4.51 and 1.88 respectively (range 0.65-14.63 for PC3 and 0.11-6.05 for PC-3M). There was a significantly lower band intensity in C4-2 and C4-2B cell lines than in LNCaP ($p=0.03$ and 0.01 respectively). Although the band intensity was lower in PC-3M cells compared to PC3, this difference in expression did not reach statistical significance.

Table 37: Quantification of GIPC1 identified by western blot

Ratio of GIPC1 to beta tubulin						
Cell line	Gel 1	Gel 2	Gel 3	Gel 4	Mean ratio	p value *
LNCaP	1.08	0.96	0.98	0.93	0.99	LNCaP Vs C4-2 p=0.03*
C4-2	0.54	0.88	0.73	0.83	0.75	LNCaP vs C4-2B p=0.01*
C4-2B	0.55	0.88	0.49	0.35	0.57	C4-2 Vs C4-2B p=0.25
PC3	14.63	1.54	1.22	0.65	4.51	PC3 Vs PC3M p=0.5
PC-3M	6.05	0.98	0.37	0.11	1.88	

*comparison of means using independent samples t test

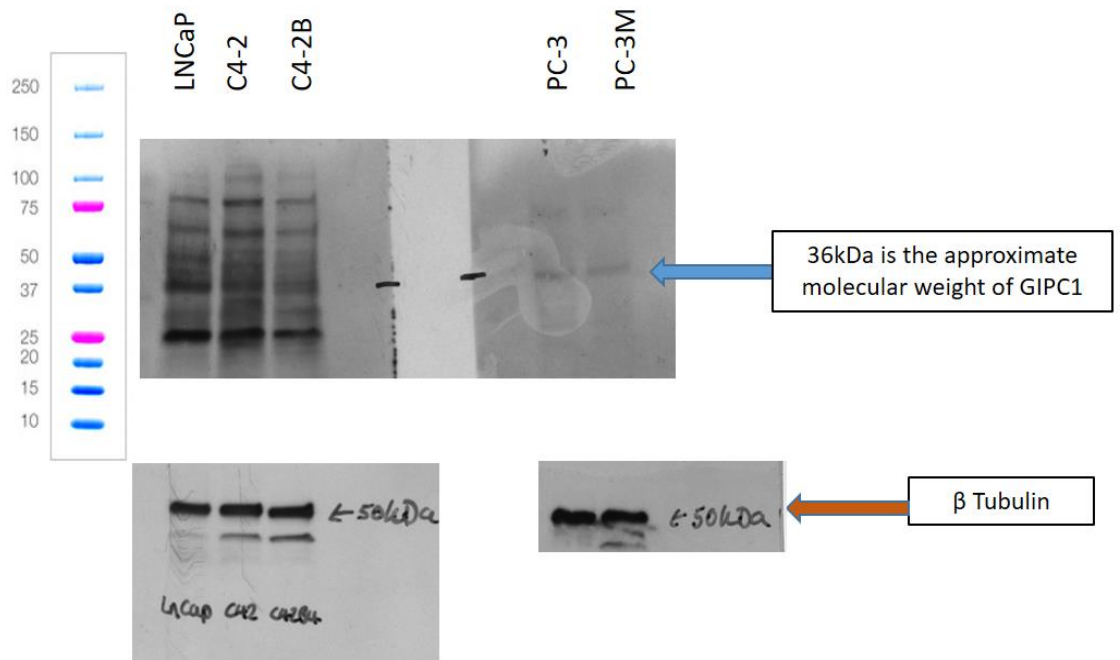


Figure 36: GIPC1 protein identified by western blot.

A representative blot of the detection of GIPC1 at 36kDa (blue arrow) with corresponding β -tubulin loading control (orange arrow) blot shown below, for all five cell lines. 30 μ g of each total lysate sample was loaded per lane. The x ray film was exposed for 30mins to produce the above images. Images were taken and analysed using Image Lab software.

6.4.2.2 Verification by immunohistochemistry

In order to verify the results from western blots, IHC was used for FFPE-embedded cell pellets from all 5 PC cell lines. Quantification of the average number of DAB positive cells and the mean DAB optical density (OD) is shown in table 38. Representative images of the GIPC1 IHC results are shown in figure 37. A very small proportion of control LNCaP cells were positive (0.05%), with a DAB intensity of 0.02. This was used as a baseline, and all other DAB intensity values were adjusted accordingly. The bone homing breast cell line did express GIPC at a high level, which demonstrated the accuracy of the IHC methodology. The average DAB intensities and number of DAB-positive cells for each run are shown in tables 39 and 40. GIPC1 expression (measured by the DAB intensity and proportion of DAB positive cells) was greatest in LNCaP cells and was lower in the more bone-homing cell lines C4-2 and C4-2B. The differences between the LNCaP and C4-2 cell lines followed the pattern that was observed in the western blots; in that there was a decrease in the expression of GIPC1 between LNCaP and C4-2 cells ($p=0.07$) based on the DAB intensities. This was also reflected in the average proportion of DAB positive cells that were detected; 67.9% vs 54.6% for LNCaP and C4-2 cells respectively ($p = 0.03$). There was no measured difference in DAB intensity or number of DAB positive cells between the C4-2 and C4-2B cells.

In the PC3 and PC3M cell lines, there was a slight reduction in DAB intensity (0.27 Vs 0.23) and a reduction in the percentage of DAB-positive cells (43.8% vs 40.8%) in the PC3M cell line compared to PC3 cells, however the difference was not statistically significant.

Table 38: Verification of GIPC1 using IHC

Cell line	Mean number of cells per slide (n=4)	Mean % of DAB positive cells (n=4)	Mean DAB intensity overall (n=4)	Mean DAB intensity adjusted for control (n=4)
P7 breast cell	111,871	39.3	0.23	0.21
LNCaP (control)	52,159	0.05	0.02	N/A
LNCaP	89,324	67.9	0.43	0.41
C4-2	58,258	54.6	0.29	0.27
C4-2B	46,194	56.6	0.29	0.27
PC3	75,022	43.8	0.27	0.25
PC-3M	69,988	40.8	0.23	0.21

Table 39: Average GIPC1 DAB intensity across cell lines

Cell line and antibody	DAB intensity				Mean (SD)
	Run 1	Run 2	Run 3	Run 4	
P7 controls + GIPC1	0.18	0.2	0.2	0.31	0.23 (0.06)
LNCaP controls	0.033	0.008	0.025	0.011	0.02 (0.01)
LNCaP + GIPC1	0.034	0.039	0.039	0.062	0.43 (0.24)
C4-2 + GIPC1	0.29	0.25	0.25	0.36	0.29 (0.05)
C4-2B + GIPC1	0.28	0.33	0.3	0.23	0.29 (0.04)
PC3 + GIPC1	0.19	0.32	0.29	0.28	0.27 (0.06)
PC3M + GIPC1	0.16	0.31	0.24	0.21	0.23 (0.07)

Independent samples t-test

LNCaP controls vs LNCaP + GIPC p=0.00006*

LNCaP Vs C4-2 p=0.07

LNCaP Vs C4-2B p=0.06

C4-2 Vs C4-2B p=0.94

PC3 Vs PC3M p=0.38

Table 40: Average GIPC1 DAB positive cells across cell lines

Cell line and antibody	Proportion of positive cells				Mean (SD)
	Run 1	Run 2	Run 3	Run 4	
P7 controls + GIPC1	32.0	35.3	35.0	55.1	39.3 (10.6)
LNCaP controls	0.07	0.01	0.1	0.03	0.05 (0.04)
LNCaP + GIPC1	60	64.5	66.4	80.8	67.9 (9.0)
C4-2 + GIPC1	54.7	51.7	52.5	59.3	54.6 (3.4)
C4-2B + GIPC1	55.1	56.2	59	56	56.6 (1.69)
PC3 + GIPC1	25.4	57.5	44.8	48	43.8 (13.5)
PC3M + GIPC1	34.2	51.5	41.1	36.4	40.8 (7.7)

Independent samples t-test

LNCaP controls vs LNCaP + GIPC $p < 0.001^*$

LNCaP Vs C4-2 $p = 0.032$

LNCaP Vs C4-2B $p = 0.047$

C4-2 Vs C4-2B $p = 0.33$

PC3 Vs PC3M $p = 0.7$

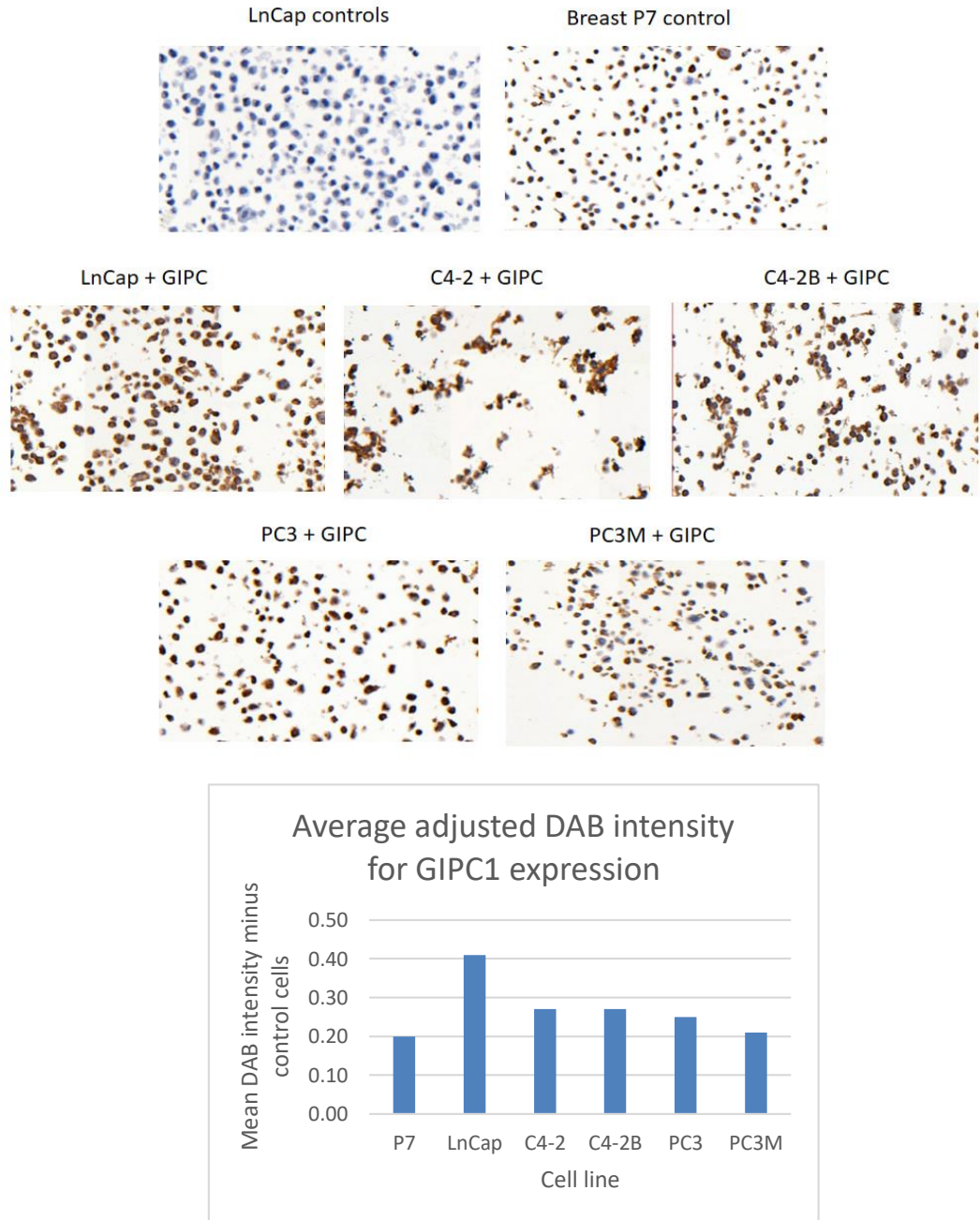


Figure 37: IHC images for GIPC1 and DAB intensity.

Representative images from each of the cell lines, and mean adjusted DAB intensity values for GIPC1 in each cell line

6.4.3 DOCK4

6.4.3.1 Verification by western blot

The predicted molecular weight of DOCK4 is 225KDa, and it required a slightly longer western blot exposure time than for CAPG and GIPC1 in order to obtain satisfactory band intensity for analysis. An example blot is shown in figure 38, along with the reference MW markers and β -tubulin loading controls (average band intensities were normalised to β -tubulin for each of the experiments). Band densitometry data are shown in table 41. The mean intensity of DOCK4 in the LNCaP cell line was 0.47 (range 0.25-1.15) and was 0.45 (range 0.17-1.12) for C4-2 and 0.19 (range 0.13-0.28) for C4-2B cells. Although there was a reduction in the DOCK4 band intensity from LNCaP to C4-2 and a further decrease between C4-2 and C4-2B, the difference was not statistically significantly different between them.

The mean band intensities for the PC3 and PC3 cell lines were 0.75 and 0.4 respectively (range 0.48-0.89 for PC3 and 0.11-0.53 for PC-3M), and there was a statistically significant decrease in DOCK4 intensity between the PC3 and the PC-3M cell lines.

Table 41: Quantification of DOCK4 identified by western blot

Ratio of DOCK4 to β tubulin							
Cell line	Gel 1	Gel 2	Gel 3	Gel 4	Gel 5	Mean ratio	p value *
LNCaP	1.15	0.29	0.30	0.25	0.33	0.47	LNCaP Vs C4-2 p=0.98
C4-2	1.12	0.59	0.16	0.17	0.21	0.45	
C4-2B	0.28	0.24	0.13	0.13	0.18	0.19	C4-2 Vs C4-2B p=0.21
PC3	0.86	0.75	0.48	0.79	0.89	0.75	PC3 Vs PC3M p=0.01
PC-3M	0.53	0.53	0.11	0.38	0.48	0.40	

*comparison of means using independent samples t test

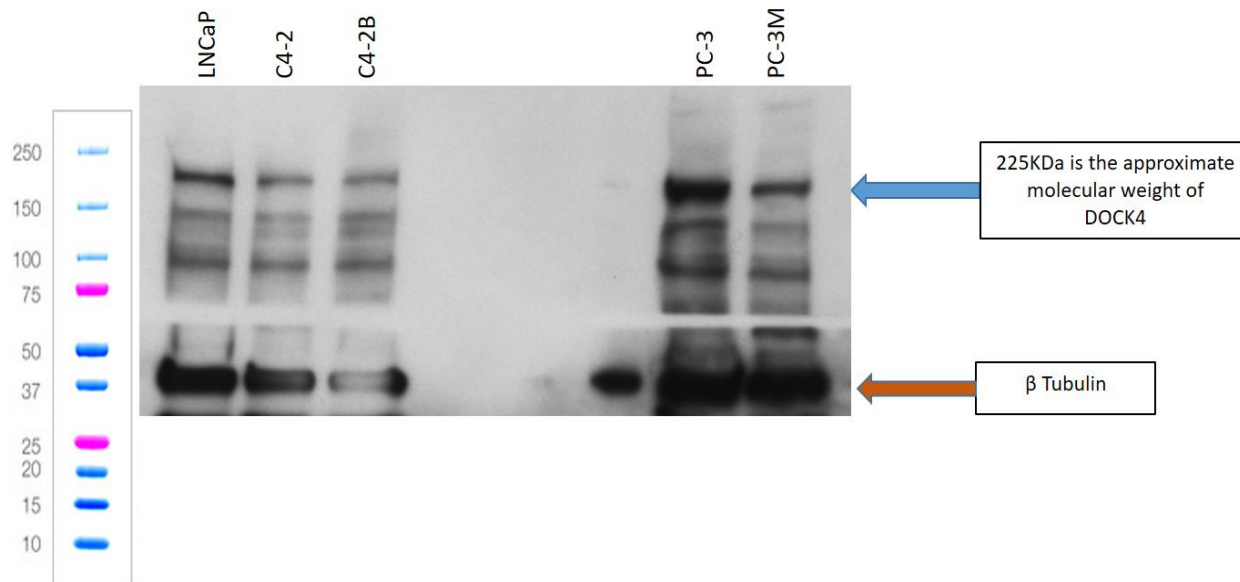


Figure 38: DOCK4 quantification by western blotting.

A representative blot of the detection of DOCK4 at 225KDa (blue arrow) with corresponding β -tubulin loading control (orange arrow) blot shown below, for all five cell lines. 30 μ g of each total lysate sample was loaded per lane. The x ray film was exposed for 30mins to produce the above images. Images were taken and analysed using Image Lab software.

6.4.3.2 Verification by immunohistochemistry

Representative images of the DOCK4 IHC analysis are shown in figure 39. The control cell line contained only a few positive cells with a mean DAB intensity of 0.2. The DAB intensities for other cell lines were adjusted by this amount (table 42). DAB intensities and the number of positive cells are shown in tables 43 and 44.

LNCaP cells expressed very low levels of DOCK4, with a mean DAB intensity of 0.018 (0 when adjusted for control intensity) and few (0.26%) positive cells. The values were consistent across all repeat runs (DAB intensities for the 4 runs were 0.017, 0.017, 0.021 and 0.018). The more bone-homing, derived cell lines C4-2 and C4-2B had significantly higher mean DAB intensities than LNCaP (0.39 and 0.45 respectively) and 64% of the C4-2 cells and 64.8% of C4-2B cells were identified as DAB positive by the analysis software. There was no statistically significant difference in the expression of DOCK4 between C4-2 and C4-2B ($p < 0.0001$ for both) cells. DOCK4 expression was lower in PC-3M cells compared to PC3 cells (DAB intensities of 0.26 for PC-3M and 0.37 for PC3) and there were fewer DAB-positive cells. The difference between these cell lines was found to be significant in the DOCK4 western blot analysis, but did not reach significance in IHC ($p = 0.11$ for mean DAB intensity and 0.19 for the mean % of positive cells).

Table 42: Verification of DOCK4 using IHC

Cell line	Mean number of cells per slide (n=4)	Mean % of DAB positive cells (n=4)	Mean DAB intensity (n=4)	Mean DAB intensity adjusted for control (n=4)
P7 breast cell	101,931	45.2	0.27	0.25
LNCaP (control)	58,266	0.8	0.02	-
LNCaP	36,463	0.3	0.018	0
C4-2	58,841	64	0.42	0.40
C4-2B	40,615	64.8	0.47	0.45
PC3	110,622	58.5	0.37	0.35
PC-3M	57,181	44.7	0.26	0.24

Table 43: Average DOCK4 DAB intensity across cell lines

Cell line and antibody	Mean DAB intensity				Mean (SD)
	Run 1	Run 2	Run 3	Run 4	
P7 controls + DOCK4	0.17	0.31	0.33	-	0.27 (0.08)
LNCaP controls	0.036	0.01 4	0.01 9	0.01 2	0.02 (0.01)
LNCaP + DOCK4	0.017	0.01 7	0.02 1	0.01 8	0.018 (0.002)
C4-2 + DOCK4	0.38	0.45	0.33	0.42	0.42 (0.07)
C4-2B + DOCK4	0.55	0.31	0.54	0.48	0.47 (0.11)
PC3 + DOCK4	0.52	0.24	0.34	0.39	0.37 (0.11)
PC3M + DOCK4	0.35	0.23	0.21	0.23	0.26 (0.06)

Independent samples t test

LNCaP Vs C4-2 p<0.0002

LNCaP C4-2B p<0.0001

C4-2 vs C4-2B p=0.88

PC3 Vs PC3M p=0.012

Table 44: Average DOCK4 DAB positive cells across cell lines

Proportion of DOCK4 DAB positive cells					
Cell line and antibody	Run 1	Run 2	Run 3	Run 4	Mean (SD)
P7 controls + DOCK4	26.5	54	55.1	-	45.2 (14.3)
LNCaP controls	0.69	0.47	1.89	0.1	0.79 (0.77)
LNCaP +DOCK4	0.27	0.3	0.2	0.26	0.26 (0.04)
C4-2 + DOCK4	69.2	58.6	60.1	67.9	64 (5.37)
C4-2B + DOCK4	72.8	52.2	65	69	64.8 (8.95)
PC3 + DOCK4	77.7	44	52.2	60.2	58.5 (14.3)
PC3M + DOCK4	61.7	42.9	35.4	38.7	44.7 (11.75)

Independent samples t test

LNCaP Vs C4-2 $p < 0.0001$

LNCaP Vs C4-2B $p < 0.0001$

C4-2 vs C4-2B $p = 0.88$

PC3 Vs PC3M $p = 0.019$

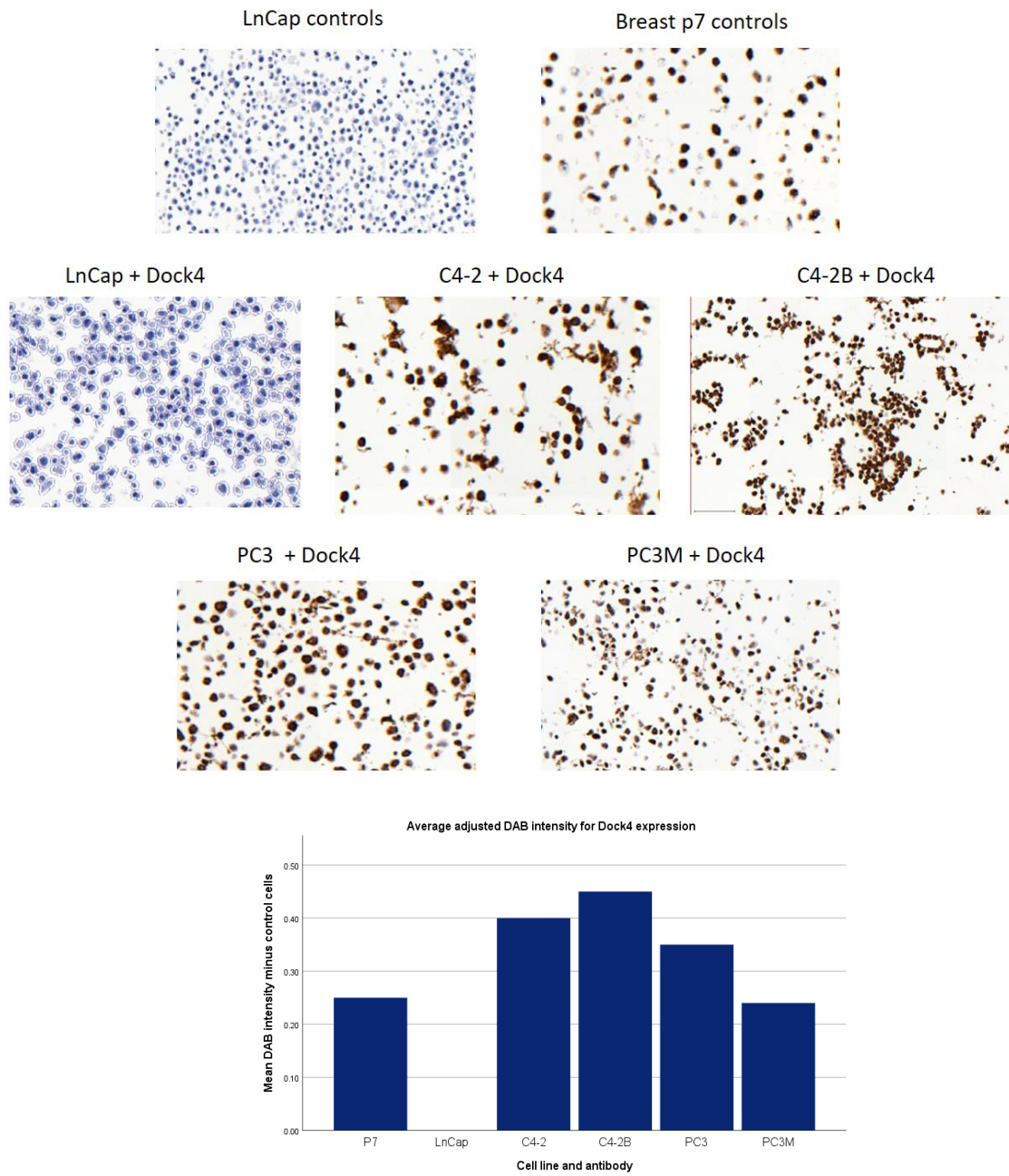


Figure 39: IHC images for DOCK4 and DAB intensity.

Representative images from each of the cell lines, and mean adjusted DAB intensity values for GIPC1 in each cell line

6.4.4 Overall summary of analysis

The mean western blot band intensity ratios and DAB IHC results for CAPG, GIPC1 and DOCK4 are summarised in table 45. There was differential expression of all biomarkers across the five cell lines, in both total cell lysate analysis (by western blot) and IHC (FFPE embedded cell pellets).

CAPG was investigated in cell lysate only. Within the LN-CAP and bone-homing derived cells, expression was greatest in LNCaP cells, but was not significantly different in the C4-2 or C4-2B cells. The band intensity was slightly higher in PC3 cells compared to PC-3M.

The expression of GIPC1 in cell lysates was greatest in the LNCaP cell line, and was significantly less within C4-2 cells. A further statistically non-significant reduction was observed between C4-2 and C4-2B cells. A reduction in GIPC1 expression between LNCaP and C4-2 was also observed by IHC analysis, with a significant reduction in both the mean DAB intensity and the percentage of DAB-positive cells. This result was further confirmed by the results for C4-2 and C4-2B using IHC. GIPC1 expression was greater within PC3 cells compared to PC-3M cells in both western blotting and IHC analysis, however the difference was not statistically significant.

DOCK4 expression was significantly reduced within the PC-3M cell line compared to PC3 cells. This trend was also apparent within IHC analysis of cell-pellets, however this difference did not reach statistical significance. DOCK4 expression was similar in the LNCaP, C4-2 and C4-2B cell lysates, however analysis using IHC found very low levels of expression in LNCaP cell pellets. This was similar to levels in the negative controls, and was also significantly less than in C4 and C4-2B.

Table 45: Overall summary of biomarker results

Cell line	Western blot band ratios			Adjusted DAB intensity		% of DAB positive cells	
	CAPG	GIPC1	DOCK4	GIPC1	DOCK4	GIPC1	DOCK4
LNCaP	0.43	0.99*	0.47	0.41*	0*	67.9 *	0.26*
C4-2	0.24	0.75*	0.45	0.27*	0.40*	54.6 *	64 .0*
C4-2B	0.39	0.57	0.19	0.27	0.45	56.6	64.8
PC3	0.62	4.51	0.75*	0.25	0.35	43.8	58.5
PC-3M	0.47	1.88	0.40*	0.21	0.24	40.8	44.7

*Denotes p<0.05 between the two measurements

6.5 Discussion

This project aimed to investigate the differential expression of the protein biomarkers CAPG, GIPC1 and DOCK4 within a panel of PC cell lines. The proteins being investigated have all been discovered by proteomic analysis experiments to increase in expression as triple negative breast cancer cells develop bone homing ability within murine models of breast cancer bone metastasis. A prostate cancer cell-line panel was chosen to mimic the natural development of PC towards androgen-independent growth and eventual spread to bone ^{793,797}.

Although there are clear differences between breast and prostate malignancies, they are both hormone sensitive and share a propensity to metastasise to bone; on this basis it was felt to be reasonable, and certainly an interesting comparative, approach in PC cell lines. The expression of CAPG, GIPC1 and DOCK4 was quantified first by western blotting in five selected cell lines, and based upon the results of these, GIPC1 and DOCK4 were then taken forwards for additional pre-clinical validation using IHC. The derivation of the cell lines that were used, and the phenotypic appearance of the resulting bone metastases in xenograft models (osteoblastic lesions in LNCaP derived cell lines and osteolytic lesions in PC3 derived cells) required separate analysis which was performed prior to the work within this chapter. Due to derivation from different PC patients, and also characteristics of the cells, LNCaP, C4-2 and C4-2B formed a natural first series, and PC3 and PC-3M were considered separately. In this way, comparisons of protein expression were conducted within cells which shared a common precursor – this approach is as equivalent as possible to the original comparison of parental and fully bone homing breast cancer cells (which are isogenic in this comparison).

6.5.1 CAPG

Due to the similar molecular weights of the tubulin control and CAPG, the LNCaP /C4-2 and C4-2B panel and the PC3/PC-3M were analysed in parallel on two gels in the same tank (under the same conditions). Blots can be stripped and re-probed with 2 different antibodies sequentially, however to avoid any concerns about possible antigen loss, separate gels were run. The exact nature of CAPG's mechanistic role in bone metastasis is still the subject of active research, however roles of CAPG have been identified within the regulator of actin filament length and cell motility and cell polarity, the epigenetic regulation of transcription of key pro-metastatic genes as well as roles in nuclear export ^{804,816,891}.

Commercially available antibodies previously used within published studies in breast cancer were used to measure the expression of GIPC1 in the selected cell lines. In the LNCaP panel, the expression of CAPG was greatest in LNCaP

cells, and was lower in the more bone-homing, derived cells C4-2 and C4-2B. LNCaP cells originate from a human lymph node metastasis, whereas C4-2 cells originated from a subcutaneous (castrated) xenograft tumour, and C4-2B cells were obtained from osseous tumours that developed in the same xenograft models. Based upon the western blot results, CAPG levels appear to be highest within the LNCaP-cells and to decrease in expression as the cells develop towards more distant metastasis including bone. It is possible that CAPG may be required for the early stages of metastasis and for entry into the lymphatic system, whereas it is less likely to be required for bone homing and interaction with the bone microenvironment. A previous study using the DU-145 prostate cell line found that CAPG suppression slowed cellular proliferation, and decreased migration and invasive ability⁸¹⁹ so CAPG may play a role in the extravasation of PC cells from the primary tumour and their migration towards blood vessels and the lymphatic system.

PC3 cells are derived from a human BM, and the subsequent orthotopic injection of PC3 cells into xenograft mouse models lead to the development of lymph node metastases^{884,889}. PC-3M cells were initially obtained from repeated cycles of orthotopic injection of PC3 cells and the harvesting of tumours⁸⁸⁸. PC-3M cells produce a high frequency of lung and bone metastases, depending on the model used⁸⁸⁸. We initially anticipated that PC3-M cells would have a higher expression of CAPG than PC3; this was based both on their origin and expected potential to cause BM and the previously published observation that CAPG levels were higher within bone homing breast cancer cells than parental, primary tumour cells. However, we found that within the PC3-prostate cancer cells the opposite appeared to be true; that the expression of CAPG was greater in PC3 cells than in PC-3M. This was in agreement with the results from the LNCaP panel, namely that the increased CAPG expression in PC3 vs PC3M cells suggests that CAPG may be required for the initial, early stages of metastasis into the lymphatic system, rather than in later stages of spreading to distant organ sites including bone.

CAPG was significantly up-regulated specifically within bone metastatic breast cancer cells compared with non-metastatic cells and cells which are metastatic to lung, and these findings were further validated within tissue microarrays derived from breast cancer patients within the large phase III, AZURE trial⁷⁹³. CAPG is also upregulated in several other tumour types, and there is published evidence associating CAPG-expression with adverse clinical outcomes in several cancer types^{810,817}.

Our results in this pilot study, did not suggest that measuring CAPG levels within PC would predict risk of spread to bone, however several important limitations must be considered. For logistical reasons we were unable to obtain a cell-line which mimicked the primary tumour or benign prostate tissue, so we

do not know if the level of expression of CAPG is elevated (or not) within all PC cells compared to benign prostate tissue, or within lymph-node metastases compared to prostate primary tumours. Furthermore, as with all protein expression based studies we are trying to infer the mechanism of a protein from its level of expression; the inherent assumption is that, a greater level of the protein in the cell at a stage of metastasis, implies that the protein is required for that stage. As proteins can both inhibit and activate signalling pathways the opposite may well be true. In order to fully determine the role of CAPG within PC metastasis, further mechanistic studies are required with engineered knock-down (or over-expression) of the proteins of interest and *in vivo* studies within murine model systems.

6.5.2 GIPC1

As the estimated molecular weight of GIPC1 is similar to both tubulin and CAPG, we used parallel analysis of the five cell lines using two gels (one for the marker western blot and one for the tubulin loading control). We found that previously used commercially available antibodies used for equivalent studies within breast cancer cell lines were suitable for use within the PC cell-line panels. GIPC1 expression decreased significantly from LNCaP cells to C4-2 and to C4-2B cell lysates, and this result was also further confirmed using IHC within FFPE cells. There was no statistically significant difference in expression between the C4-2 and C4-2B cell-lines. As was observed in the CAPG results in the same cell lines, GIPC1 expression was lower in PC3M cells than within PC3-M cells in both western blotting within total cell lysates and IHC, although the differences in expression were not statistically significant.

GIPC1 is a cell-signalling scaffold protein which plays a role in numerous cellular-processes. GIPC1 is involved in endosomal trafficking during cell migration and angiogenesis⁸²³ and it also has a role within the expression of cell surface receptors and adhesion molecules. In addition, GIPC1 plays a key role within tyrosine kinase signalling and is a key-interactor with the TGF β receptor^{823,824,834}. The role of GIPC1 within metastasis is still an area of active research and its exact role in carcinogenesis and metastasis is not yet fully understood. GIPC1 is upregulated in many tumour types⁸³⁴, and its role in bone metastasis was suggested by significantly increased expression within bone homing breast cancer cell lines compared to non-bone homing lines⁷⁹³. This was validated by IHC staining within primary breast tumours from the large, phase-III AZURE trial⁷⁹⁵. In breast cancer cells, GIPC1 knockout has also been shown to inhibit cell proliferation and promotes apoptosis⁸⁴².

Our pilot findings are that GIPC1 expression was greatest within cell lines derived from lymph node metastasis (LNCaP) and also may be greater in human-derived cell lines (PC3 and LNCaP) than cells that originate from

xenograft models (PC3M, C4-2 and C4-2B). The extrapolation of results from xenograft models to humans is not always straight forwards and it is by no means certain that results obtained in xenograft model systems will translate into the human (patient) setting⁸⁹². Thus we cannot be certain that our results would be further validated if pursued within primary tissue samples. Having initially obtained our results in cell lysates and validated them in IHC, we have optimised the IHC antibodies for future use with prostate cancer TMAs. Clearly, further repeats would be useful, and if the results are replicated, future work should seek to investigate GIPC1 expression in human tissue microarrays using IHC. It may also be useful to investigate GIPC1 in cell migration and invasion assays in the cell lines that we used, as there is no published literature that has explored this.

An ongoing area of research within the bone biomarkers group is the generation of cell-lines over-expressing (and cell-lines with selective knockdown) of proteins of interest. Targeted over-expression as well as knockdown of proteins both provides suitable material for use in antibody specificity studies as well as appropriately engineered cells for use in mechanistic in vivo studies within animal models. Generation of these cell lines is currently under way in Sheffield, however they were not available for the current study due the large number of potential metastasis regulatory proteins being pursued and the time involved to generate each engineered cell line. The potential clinical role of GIPC1 would be dependent on these results; it has potential as a biomarker of metastasis, but our results do not suggest that it may be specific to bone metastasis.

6.5.3 DOCK4

DOCK4 (MW 225kDa) and β tubulin (MW = 37kDa) were analysed simultaneously within one western blot. DOCK4 expression was significantly reduced within the PC-3M cell lysates compared to PC3 cells as measured by western blot. On the basis of this difference, DOCK4 was taken forwards into IHC-validation, which confirmed the decrease in DOCK4 expression within PC-3M compared to PC3, although this did not reach statistical significance. Given that PC3 cells originate from both bone and produce lymph node metastases, and PC-3M cells produce a high frequency of BM the results suggest that high DOCK4-expression may be more required within the earlier stages of metastasis.

The results from western blots for DOCK4 within the LNCaP-cell-line panel (including C4-2 and C4-2B cells) were less conclusive. However, the results for LNCaP from IHC were surprising as very-low to no DOCK4 expression was observed within the LNCaP line (staining was observed within other cell-line pellets in the same staining run, and this result was observed in 5 experimental

repeats). This was reflected in both the measured DAB intensity and in the proportion of DAB-positive cells, and was found in all repeat runs (where the results of the breast p7 controls and the LNCaP controls were as expected). Recent data suggests that DOCK4 levels are responsive to changes in the extracellular matrix (ECM) and, in particular, to the adaptation of cancer cells to growth on mechanically resistant matrices such as bone. Cell derived from a lymph node metastasis may have different ECM-interactions that result in a reduced expression level of DOCK4.

DOCK4 has an important role within cell migration via the activation of G protein-mediated signalling and within angiogenesis via the activation of Rac1, as well as in Wnt/ β -catenin signalling (part of the β -catenin degradation complex). Furthermore, DOCK4 is also a key protein within the action of TGF β to drive cancer cell proliferation and invasion. These multiple, pleiotropic actions of DOCK4 increase the likelihood of DOCK4 having a role in PC metastasis, however no studies to date have investigated the role of DOCK4 in PC cell proliferation or progression. In breast cancer, DOCK4 was upregulated in bone homing TNBC cells compared to parental cells and its knockout resulted in reduced invasive ability of cells ⁷⁹⁷. Within breast cancer TMAs from the large international phase III AZURE trial, high DOCK4 expression levels correlated with a reduced time to development of BM ⁷⁹⁷. Our results show differential expression across the cell lines, but as this is the first study to have used the combination of cell lines reported here for assessment of DOCK4 expression and further repeats, combined with mechanistic studies are required to elucidate the role of DOCK4 within the metastatic spread of prostate cancer.

6.5.4 Strengths of this study

No previous studies have investigated such a diverse panel of PC cell lines based upon novel biomarkers of PC metastasis discovered by cutting-edge proteomic analysis. We have used very well established techniques and protocols to pursue the two complementary approaches reported here. Western blotting is one of the most frequently employed methods for quantification of protein expression levels within biological samples. The great advantage of western blotting is that it provides information regarding the MW of quantified proteins, thus providing reassurance regarding antibody specificity. We normalised all of the western blots to a loading control (β tubulin) to ensure that any changes observed in the target protein abundance represented actual differences and this use of a 'housekeeping protein' is a standard procedure within WB analysis. Each gel was repeated five times, and an average band ratio was used for the final comparison in order to improve accuracy. Significant results in western blot analysis were taken forward for IHC to provide a second method of verification. This has allowed optimisation of

the antibodies, antigen retrieval and processing steps, which may be used in future clinical validation using TMAs or patient-derived samples as well as providing a validation of the results of WB by using a complementary method.

6.5.5 Study limitations

As described earlier in this thesis chapter, established breast cancer cell lines are known to be bone-homing and have been used in models of metastasis. In addition, isogenic cell-lines (derived by techniques such as repeated intra-cardiac injection) have resulted in state-of-the-art cell-line pairs derived from identical genetic backgrounds for use in techniques such as genetic sequencing and proteomic analysis. Unfortunately, equivalent models are not so readily available for PC, and selection of the cell lines was based upon availability which was a factor in the experimental design. We acknowledge that the heterogeneity of PC makes it probable that any future biomarker of PC metastasis would be likely to form part of a wider biomarker panel.

LNCaP and PC3 cell lines are patient-derived cell-lines, with C4-2, C4-2B and PC-3M cell-lines originating from within xenograft models. The different origins of the LNCaP and PC3 series (from different patients), and the different approaches used within cell-line derivation may go some way towards explaining instances where differing results were obtained in the two cell-line panels. It must be noted in this regard that proteomic studies have identified distinct molecular subtypes within prostate cancer previously ⁷⁹². In order to fully assess the potential of these proteins as markers of PC metastasis a considerable series of further experiments would have to be performed (see “further work” section below).

The methods used within this study do have some inherent limitations; most notably that to some extent western blotting is a semi-quantitative method. Concerns of assay linearity and sensitivity are even more pronounced for the IHC method where the colloidal nature of DAB staining means that its linear range of accumulation and measurement is even more limited. Both western blotting and IHC are also heavily dependent upon antibody availability and the properties (affinity and specificity) of commercially available antibodies.

6.6 Conclusions and recommendations for future work

The main conclusion from the current study appears to be that the intracellular levels of GIPC1 and DOCK4 within the PC cell-lines used alter most significantly within the earliest stages of metastasis (escape from the primary tumour and into the lymph nodes), but these markers do not appear to predict the risk of subsequent development of metastatic spread to bone. No statistically significant correlation was observed for CAPG for either primary tumour spread to lymph nodes or bone.

The results were obtained within a cell-culture model and could not be further validated within patient derived material owing to sample availability issues. Proteins such as GIPC1 and DOCK4, which may predict the escape of tumour cells from the primary tumour and entry into the bloodstream and lymphatic system could potentially be validated by measurement within circulating tumour cells (CTCs). Recent published data has demonstrated the feasibility of measuring protein expression within CTCs derived from PC ⁸⁹³, and in this regard the measurement of the expression of pro-metastatic genes (including CAPG and GIPC1) has recently been reported within CTCs from breast cancer. CTCs have also provided a source of biological material useful for sequencing the genetic mutations which are correlated within metastatic PC.

Previous studies within breast cancer using tissue micro-arrays (TMAs) derived from the large, phase-3 AZURE trial, have used IHC-methods to identify novel proteins which correlated with lymph node involvement. An equivalent study within PC primary tumour tissue samples would further validate the predictive potential of the protein panel within PC metastasis. Using patient-derived samples, a further development of the work outlined here would be to measure the circulating level of these proteins within serum or plasma samples from individuals with PC using either ELISA or targeted mass-spectrometry (e.g. selected reaction monitoring – SRM) ⁸⁹⁴.

One final limitation of the current study, and as a consequence therefore a potential future development of this biomarker work, concerns the spatial distribution of biomarker proteins within tumour sections and cells. Metastasis is by definition a spatial process in which cells have a “leading edge” and tumours have an invasive front. The IHC-based cell staining presented here, as well as the western blotting procedures used, all either disrupt the cell structure, or remove PC cells from their biological context of being part of a primary tumour or distant metastatic site. Recently developed digital spatial Profiling (DSP) techniques have begun to illuminate the role of proteins within the spatially defined regions within metastatic PC samples, providing considerable insight into both the inter-patient heterogeneity and the spatially distinct pattern of protein expression within a tumour ⁸⁹⁵. The proteins which formed the basis of the panel assessed in the current study, may have specific roles in cellular locations such as the leading edge of metastatic PC cells. This may be particularly true for proteins such as GIPC1 which are known to bind to plasma membrane receptors. A spatially resolved analysis of the expression levels of the current protein panel may therefore further dissect the precise roles of these proteins within PC metastatic spread from the primary tumour to the lymph nodes and beyond to bone and other distant sites.

Overall summary of thesis

The incidence of PC continues to increase alongside the ageing population, and it is the commonest cancer in the UK. PC is most prevalent in men aged over 70 years, a population at risk of low BMD due to; age-related BMD decline; physiological changes that occur with ageing; and the presence of comorbid conditions. Ageing is also associated with frailty, changes in body composition, functional impairment and increased risk of falls, and the effects of PC treatment are super-imposed upon all of these. Consideration of the long term consequences of cancer treatments is of increasing importance; they have the potential to significantly impact morbidity, mortality, quality of life and function, all of which are associated with considerable economic cost.

Assessment and optimisation of bone health in men treated for PC is an unmet need, and risks avoidable harm. There is a disparity in the management of bone health in women treated for breast cancer and men with PC, despite the propensity of both tumours to metastasise to bone and for treatments to affect bone health. Results from ANTELOPE suggest that the majority of older men (with and without PC) are at significant risk of fracture and would benefit from intervention, even before ADT is initiated. However, fracture risk assessment is not currently incorporated into routine clinical practice, and BMD testing is under-used.

ANTELOPE found that ADT rapidly and profoundly reduces circulating sex steroid levels and accelerates bone turnover, manifested by a significant increase in BTM after 12 months. We also identified high bone turnover with predominant bone formation in men with metastatic PC. These men were subsequently treated with chemotherapy and GC, and interpretation of BTM after 12 months is challenging, as changes may reflect a response to systemic treatment and GC use in BM, in addition to ADT.

Over the first 12 months of ADT, there is net loss of areal BMD at all sites. Loss of aBMD is greatest at the lumbar spine which predisposes men to vertebral fractures. Analysis of HR-CT T12 scans from ANTELOPE is ongoing, and will provide greater detail regarding microarchitectural changes at this site. At the distal radius, ADT is associated with significant loss of volumetric BMD and the addition of GC and chemotherapy may exacerbate loss of cortical vBMD here. ADT appears to cause microarchitectural deterioration at the distal radius; there is loss of cortical area and thickness, increased cortical porosity, loss of trabeculae, increased separation and gain in trabecular area. This leads to

important reductions in bone stiffness and strength, and concomitant use of chemotherapy and GC may reduce this further.

In addition to a reduction in BMD, microarchitectural deterioration and strength, ANTELOPE has shown that 12 months of ADT is associated with important changes in body composition. The resulting phenotype is one of sarcopenic obesity, with notable increases in BMI, trunk and upper limb fat mass, loss of upper limb lean mass, impaired grip strength, worse physical performance and frailty.

ANTELOPE has demonstrated significant and clinically important changes in bone and body composition. These should not be underestimated, and in combination with frailty, sarcopenic obesity and changes in physical performance, leads to is a potentially vulnerable clinical state that would seem to increase the likelihood of falls and fractures, with their associated morbidity and mortality.

Current guidelines lack specific recommendations for bone health assessment, adherence to them is poor and there is no current consensus as to who has responsibility for bone health optimisation. Urgent clarification is required and specific recommendations should be incorporated into future guidelines and service design.

Future design of clinical PC services needs to address a number of issues; where the responsibility for fracture risk assessment lies, which services should be commissioned for BMD testing and treatment, whether access to BMD testing is equitable across the UK, how frailty screening can be incorporated into PC care, and whether interventions for frailty are effective in reducing adverse outcomes. Studies must also evaluate the cost effectiveness of interventions for frailty and fracture risk and include patient reported outcomes.

Future PC trials should aim to include bone-specific endpoints. They should seek to determine the efficacy of available bone-targeted therapies in mitigating the deterioration in bone microarchitecture and the reduction in bone density. Ongoing studies seek to determine the efficacy of exercise interventions in maintaining lean muscle mass in this population; supervised exercise programmes are currently recommended but after the initial period of supervision it appears that compliance is poor and the effects of interventions are short-lived.

In addition to the effects of PC treatment on bone, metastatic bone disease provides a separate challenge to skeletal integrity. Bone is the most frequent site of metastasis in PC, and the presence of BM increases the risk of SRE.

These impact quality of life, are associated with worse survival and have considerable cost implications. The risk of SREs can be reduced by the use of bone targeted therapies in men with PC. There are currently no biomarkers predictive of BM development in men with localised or locally advanced PC, which would allow earlier detection and prompt intervention.

Work presented in this thesis has shown that proteomic techniques can be useful in establishing the role of target proteins in the process of cancer metastasis. The selected PC cell lines exhibited differential expression of the biomarkers GIPC1 and DOCK4, that were previously found to be predictive of BM in breast cancer. Although GIPC1 and DOCK4 do not appear to predict development of BM in PC, they may predict the escape of tumour cells from the primary tumour. This work should be extended further by measurement of GIPC1 and DOCK4 expression in circulating tumour cells and in patient derived tissue samples.

Bibliography

1. Clarke, B. Normal bone anatomy and physiology. *Clinical journal of the American Society of Nephrology : CJASN* **3 Suppl 3**, S131 (2008).
2. Erikson EF, Axelrod DW, M. F. *Bone histomorphometry*. New York. Raven Press (1994).
3. Nordin M, F. V. Biomechanics of bone. in *Basic biomechanics of the musculoskeletal system* 472 (Lippincott Williams and Wilkins, 2012).
4. Osterhoff G, Morgan EF, Shefelbinec SJ, et al. Bone mechanical properties and changes with osteoporosis. *Injury* **47 (Supp2)**, S11–S20 (2016).
5. Seeman, E. & Delmas, P. D. Mechanisms of Disease Bone Quality-The Material and Structural Basis of Bone Strength and Fragility. *N Engl J Med.* **25**, 2250-61 (2006)
6. Boskey, A. L. & Coleman, R. Critical reviews in oral biology & medicine: Aging and bone. *J. Dent. Res.* **89**, 1333–1348 (2010).
7. Keaveny TM, H. W. A 20-Year Perspective on the Mechanical Properties of Trabecular Bone. *J. Biomech. Eng.* **115**, 534–542 (1993).
8. Carter DR, H. W. Compact bone fatigue damage: a microscopic examination. *Clin. orthotopic Relat. Res.* **127**, 265–274 (1977).
9. Cooper, D. M. L., Kawalilak, C. E., Harrison, K., Johnston, B. D. & Johnston, J. D. Cortical Bone Porosity: What Is It, Why Is It Important, and How Can We Detect It? *Current Osteoporosis Reports* **14**, 187–198 (2016).
10. Cooper, D. M. L. et al. Age-dependent change in the 3D structure of cortical porosity at the human femoral midshaft. *Bone* **40**, 957–965 (2007).
11. Fonseca, H., Moreira-Gonçalves, D., Coriolano, H. J. A. & Duarte, J. A. Bone quality: The determinants of bone strength and fragility. *Sport. Med.* **44**, 37–53 (2014).
12. Dong, X. N. & Guo, X. E. The dependence of transversely isotropic elasticity of human femoral cortical bone on porosity. *J. Biomech.* **37**, 1281–1287 (2004).
13. Nicks KM, Amin S, Atkinson EJ, et al. Relationship of Age to Bone Microstructure Independent of Areal Bone Mineral Density. *J. Bone Miner. Res.* **27**, 637–644 (2012).
14. Morgan, E. F., Unnikrisnan, G. U. & Hussein, A. I. Bone Mechanical Properties in Healthy and Diseased States. *Annu. Rev. Biomed. Eng.* **20**, 119–143 (2018).
15. Dempster WT, L. R. Compact bone as a non-isotropic material. *Am. J. Anat.* **91**, 331–362 (1952).
16. Feng, X. Chemical and Biochemical Basis of Cell-Bone Matrix Interaction in Health and Disease. *Curr. Chem. Biol.* **3**, 189–196 (2012).
17. Morgan EF, Barnes GF, E. T. The bone organ system: form and function. In *Osteoporosis* (ed. Marcus R, Dempster D, Cauley J, F. D.) p3–20 (Elsevier, 2013).
18. Fratzl, P., Gupta, H. S., Paschalis, E. P. & Roschger, P. Structure and mechanical quality of the collagen-mineral nano-composite in bone. *J. Mater. Chem.* **14**, 2115–2123 (2004).
19. Martin, E. & Shapiro, J. R. Osteogenesis imperfecta: Epidemiology and pathophysiology. *Curr. Osteoporos. Rep.* **5**, 91–97 (2007).
20. Pinnell SR. Regulation of collagen biosynthesis by ascoric acid: a review. *Yale J. Biol. Med.* **58**, 553–559 (1985).
21. Viguier-Carrin, S., Garnero, P. & Delmas, P. D. The role of collagen in bone strength. *Osteoporos. Int.* **17**, 319–336 (2006).
22. Saito, M. & Marumo, K. Collagen cross-links as a determinant of bone quality: A possible explanation for bone fragility in aging, osteoporosis, and diabetes mellitus.

Osteoporos. Int. **21**, 195–214 (2010).

23. Boskey AL, G. P. The Composition of Bone. in *Primer on the Metabolic Bone Diseases and Disorders of Mineral Metabolism* (ed. .J. Rosen, R. Bouillon, J.E. Compston, V. R.) 49–59 (Wiley Blackwell, 2013).
24. Anderson, H. C. Matrix vesicles and calcification. *Curr. Rheumatol. Rep.* **5**, 222–226 (2003).
25. Hart, N. H. *et al.* Mechanical basis of bone strength: Influence of bone material, bone structure and muscle action. *J. Musculoskelet. Neuronal Interact.* **17**, 114–139 (2017).
26. Turner, C. H. Determinants of skeletal fragility and bone quality. *J. Musculoskelet. Neuronal Interact.* **2**, 527–528 (2002).
27. Turner, C. H. & Burr, D. B. Basic biomechanical measurements of bone: A tutorial. *Bone* **14**, 595–608 (1993).
28. Felsenberg, D. & Boonen, S. The bone quality framework: Determinants of bone strength and their interrelationships, and implications for osteoporosis management. *Clin. Ther.* **27**, 1–11 (2005).
29. Bouxsein, M. L. Bone quality: where do we go from here? *Osteoporos. Int.* **14 Suppl 5**, 118–127 (2003).
30. Currey, J. D. Bone strength: What are we trying to measure? *Calcif. Tissue Int.* **68**, 205–210 (2001).
31. Follet, H., Boivin, G., Rumelhart, C. & Meunier, P. J. The degree of mineralization is a determinant of bone strength: A study on human calcanei. *Bone* **34**, 783–789 (2004).
32. Allen, M. R. & Burr, D. B. Mineralization, microdamage, and matrix: How bisphosphonates influence material properties of bone. *BoneKEy-Osteovision* **4**, 49–60 (2007).
33. Sharir, A., Barak, M. M. & Shahar, R. Whole bone mechanics and mechanical testing. *Vet. J.* **177**, 8–17 (2008).
34. Ammann P, et al. Bone density and shape as determinants of bone strength in IGF-I and/or pamidronatetreated ovariectomized rats. *Osteoporos. Int.* **6**, 219–217 (1996).
35. Taes, Y. *et al.* Prevalent fractures are related to cortical bone geometry in young healthy men at age of peak bone mass. *J. Bone Miner. Res.* **25**, 1433–1440 (2010).
36. SeemanE. Periosteal bone formation—a neglected determinant of bone strength. *N. Engl. J. Med.* **349**, 320–323 (2003).
37. Russo CR, Lauretani F, Seeman E, et al. Structural adaptations to bone loss in aging men and women. *Bone* **38**, 112–118 (2006).
38. Parkkari, J. *et al.* Majority of hip fractures occur as a result of a fall and impact on the greater trochanter of the femur: A prospective controlled hip fracture study with 206 consecutive patients. *Calcif. Tissue Int.* **65**, 183–187 (1999).
39. Beck, T. J. Extending DXA beyond bone mineral density: Understanding hip structure analysis. *Curr. Osteoporos. Rep.* **5**, 49–55 (2007).
40. Dalle Carbonare, L. & Giannini, S. Bone microarchitecture as an important determinant of bone strength. *J. Endocrinol. Invest.* **27**, 99–105 (2004).
41. Ikeda, S. *et al.* Effect of trabecular bone contour on ultimate strength of lumbar vertebra after bilateral ovariectomy in rats. *Bone* **28**, 625–633 (2001).
42. Borah, B. *et al.* Risedronate preserves trabecular architecture and increases bone strength in vertebra of ovariectomized minipigs as measured by three-dimensional microcomputed tomography. *J. Bone Miner. Res.* **17**, 1139–1147 (2002).
43. Legrand, E. *et al.* Trabecular Bone Microarchitecture , Bone Mineral Density ,. **15**, 13–19 (2000).

44. Khosla S, Riggs BL, Atkinson EJ, et al. Effects of sex and age on bone microstructure at the ultradistal radius: a populationbased noninvasive in vivo assessment. *J. Bone Miner. Res.* **21**, 124–131 (2006).
45. Augat P, Reeb H, C. L. Prediction of fracture load at different skeletal sites by geometric properties of the cortical shell. *J. Bone Miner. Res.* **11**, 1356–1363 (1996).
46. Martin RB. Porosity and specific surface of bone. *Crit. Rev. Biomed. Eng.* **10**, 179–222 (1984).
47. Sroga, G. E. & Vashishth, D. Effects of bone matrix proteins on fracture and fragility in osteoporosis. *Curr. Osteoporos. Rep.* **10**, 141–150 (2012).
48. Bailey AJ, Paul RG, K. L. Mechanisms of maturation and ageing of collagen. **106**, 1–56 (1998).
49. Saito M, Fuki K, M. K. Degree of mineralization-related collagen crosslinking in the femoral neck cancellous bone in cases of hip fracture and controls. *Calcif. Tissue Int.* **79**, 160–168 (2006).
50. Garnero P. The contribution of collagen crosslinks to bone strength. *Bonekey Rep.* **1**, 182 (2012).
51. Wang, X., Shen, X., Li, X. & Mauli Agrawal, C. Age-related changes in the collagen network and toughness of bone. *Bone* **31**, 1–7 (2002).
52. Vashishth D, Gibson GJ, Khoury JI, et al. Influence of nonenzymatic glycation on biomechanical properties of cortical bone. *Bone* **28**, 195–201 (2001).
53. Wallace JM, Golcuk K, Morris MD, et al. Inbred strain-specific response to biglycan deficiency in the cortical bone of C57BL6/ 129 and C3H/He mice. *J. Bone Miner. Res.* **24**, 1002–1012 (2009).
54. Martin RB, I. J. The relative effects of collagen fiber orientation, porosity, density, and mineralization on bone strength. *J. Biomech.* **22**, 419–426 (1989).
55. Banse X, Sims TJ, B. A. Mechanical properties of adult vertebral cancellous bone: correlation with collagen intermolecular cross-links. *J. Bone Miner. Res.* **17**, 1621–1628 (2002).
56. Oxlund H, Barckman M, Ortoft G, et al. Reduced concentrations of collagen cross-links are associated with reduced strength of bone. *Bone* **17**, 365S–371S (1995).
57. Meunier PJ, B. G. Bone mineral density reflects bone mass but also the degree of mineralization of bone: Therapeutic implications. *Bone* **21**, 373–377 (1997).
58. Boivin G, M. P. Changes in bone remodeling rate influence the degree of mineralization of bone. *Connect. Tissue Res.* **43**, 535–537 (2002).
59. Lenart BA, Lorich DG, L. J. Atypical fractures of the femoral diaphysis in postmenopausal women taking alendronate. *N. Engl. J. Med.* **358**, 1304–1306 (2008).
60. Donnelly, E. et al. Reduced cortical bone compositional heterogeneity with bisphosphonate treatment in postmenopausal women with intertrochanteric and subtrochanteric fractures. *J. Bone Miner. Res.* **27**, 672–678 (2012).
61. Boskey, A. Bone mineral crystal size. *Osteoporos. Int.* **14 Suppl 5**, 16–21 (2003).
62. Yerramshetty JS, Lind C, A. O. The compositional and physicochemical homogeneity of male femoral cortex increases after the sixth decade. *Bone* **39**, 1236–1243 (2006).
63. Capulli, M., Paone, R. & Rucci, N. Osteoblast and osteocyte: Games without frontiers. *Arch. Biochem. Biophys.* **561**, 3–12 (2014).
64. Keith, A. Concerning the Origin and Nature of Osteoblasts. *J. R. Soc. Med.* **21**, 301–308 (1927).
65. Long, F. Building strong bones: Molecular regulation of the osteoblast lineage. *Nat. Rev. Mol. Cell Biol.* **13**, 27–38 (2012).

66. Downey, P. A. & Siegel, M. I. Bone biology and the clinical implications for osteoporosis. *Phys. Ther.* **86**, 77–91 (2006).
67. Grigoriadis, A. E., Heersche, J. N. M. & Aubin, J. E. Differentiation of muscle, fat, cartilage, and bone from progenitor cells present in a bone-derived clonal cell population: Effect of dexamethasone. *J. Cell Biol.* **106**, 2139–2151 (1988).
68. Stein, G. S. *et al.* Runx2 control of organization, assembly and activity of the regulatory machinery for skeletal gene expression. *Oncogene* **23**, 4315–4329 (2004).
69. Florencio-Silva F, Rodrigues da Silva G, Sasso-Cerri E, Simoes M, *et al.* Biology of Bone Tissue: Structure, Function, and Factors That Influence Bone Cells. *Biomedoccal Res. Int.* ID 421746, 1–17 (2015).
70. Wiesmann, H. P., Meyer, U., Plate, U. & Höhling, H. J. Aspects of collagen mineralization in hard tissue formation. *Int. Rev. Cytol.* **242**, 121–156 (2004).
71. Rutkovskiy, A., Stensløkken, K.-O. & Vaage, I. J. Osteoblast Differentiation at a Glance. *Med. Sci. Monit. Basic Res.* **22**, 95–106 (2016).
72. Chen, D. *et al.* Bone morphogenetic protein 2 (BMP-2) enhances BMP-3, BMP-4, and bone cell differentiation marker gene expression during the induction of mineralized bone matrix formation in cultures of fetal rat calvarial osteoblasts. *Calcif. Tissue Int.* **60**, 283–290 (1997).
73. Tam, C. S., Heersche, J. N. M., Murray, T. M. & Parsons, J. A. Parathyroid hormone stimulates the bone apposition rate independently of its resorptive action: Differential effects of intermittent and continuous administration. *Endocrinology* **110**, 506–512 (1982).
74. Jilka, R. L., Weinstein, R. S., Bellido, T., Parfitt, A. M. & Manolagas, S. C. Osteoblast programmed cell death (apoptosis): Modulation by growth factors and cytokines. *J. Bone Miner. Res.* **13**, 793–802 (1998).
75. Miller SC, de Saint Georges L, Bowman BM, *et al.* Bone lining cells: structure and function. *Scanning Microsc.* **3**, 953–960 (1989).
76. Andersen, T. L. *et al.* A physical mechanism for coupling bone resorption and formation in adult human bone. *Am. J. Pathol.* **174**, 239–247 (2009).
77. Currey, J. D. The many adaptations of bone. *J. Biomech.* **36**, 1487–1495 (2003).
78. Schaffler M, Cheung W, M. R. *et al.* Osteocytes: Master orchestrators of bone. *Calcif. Tissue Int.* **94**, 5–24 (2014).
79. Zhang, K. *et al.* E11/gp38 Selective Expression in Osteocytes: Regulation by Mechanical Strain and Role in Dendrite Elongation. *Mol. Cell. Biol.* **26**, 4539–4552 (2006).
80. Bonewald, L. F. Osteocyte mechanosensation and transduction. in *Mechanosensing Biology* (ed. Noda M) 141–155 (Springer Tokyo, 2011).
81. Burger, E. H. & Klein-Nulend, J. Mechanotransduction in bone-role of the lacuno-canalicular network. in *Mechanosensing Biology* **13**, S101–S112 (1999).
82. Bonewald, L. F. The amazing osteocyte. *J. Bone Miner. Res.* **26**, 229–238 (2011).
83. Kogianni, G., Mann, V. & Noble, B. S. Apoptotic bodies convey activity capable of initiating osteoclastogenesis and localized bone destruction. *J. Bone Miner. Res.* **23**, 915–927 (2008).
84. Kitase, Y. *et al.* Mechanical induction of PGE2 in osteocytes blocks glucocorticoid-induced apoptosis through both the β -catenin and PKA pathways. *J. Bone Miner. Res.* **25**, 2657–2668 (2010).
85. Kramer, I. *et al.* Osteocyte Wnt/ β -Catenin Signaling Is Required for Normal Bone Homeostasis. *Mol. Cell. Biol.* **30**, 3071–3085 (2010).
86. Li, X. *et al.* Sclerostin binds to LRP5/6 and antagonizes canonical Wnt signaling. *J. Biol.*

- Chem.* **280**, 19883–19887 (2005).
87. Poole, K. E. S. *et al.* Sclerostin is a delayed secreted product of osteocytes that inhibits bone formation. *FASEB J.* **19**, 1842–1844 (2005).
 88. Balemans, W. *et al.* Increased bone density in sclerosteosis is due to the deficiency of a novel secreted protein (SOST). *Hum. Mol. Genet.* **10**, 537–543 (2001).
 89. Robling, A. G. *et al.* Mechanical stimulation of bone in vivo reduces osteocyte expression of Sost/sclerostin. *J. Biol. Chem.* **283**, 5866–5875 (2008).
 90. Keller, H. & Kneissel, M. SOST is a target gene for PTH in bone. *Bone* **37**, 148–158 (2005).
 91. Boyle, W. J., Simonet, W. S. & Lacey, D. L. Osteoclast differentiation and activation. **423**, 337–342 (2003).
 92. Salo J, Lehenkari P, Mulari M, Metsikkö K, V. H. Removal of osteoclast bone resorption products by transcytosis. *Science (80-.)*. **276**, (1997).
 93. Charles JF, A. A. Osteoclasts: more than ‘bone eaters’. *Trends Mol. Med.* **20**, 449–459 (2014).
 94. Chabadel A, *etr al.* CD44 and Beta3 Integrin Organize Two Functionally Distinct Actin-based Domains in Osteoclast. *Mol. Biol. Cell* **18**, 4899–4910 (2007).
 95. Luxenburg, C. *et al.* The architecture of the adhesive apparatus of cultured osteoclasts: From podosome formation to sealing zone assembly. *PLoS One* **2**, e179 (2007).
 96. Li, Y. P., Chen, W., Liang, Y., Li, E. & Stashenko, P. Atp6i-deficient mice exhibit severe osteopetrosis due to loss of osteoclast-mediated extracellular acidification. *Nat. Genet.* **23**, 447–451 (1999).
 97. Teitelbaum, S. L. Osteoclasts: What do they do and how do they do it? *Am. J. Pathol.* **170**, 427–435 (2007).
 98. Fuller K, Owens JM, Jagger CJ, Wilson A, M. R. & TJ, C. Macrophage Colony-stimulating Factor Stimulates Survival and Chemotactic Behavior in Isolated Osteoclasts. *J. Exp. Med.* **178**, 1733–1744 (1993).
 99. Yasuda, H. *et al.* Osteoclast differentiation factor is a ligand for osteoprotegerin/osteoclastogenesis-inhibitory factor and is identical to TRANCE/RANKL. *Proc. Natl. Acad. Sci. U. S. A.* **95**, 3597–3602 (1998).
 100. Leibbrandt, A. & Penninger, J. M. RANK/RANKL: Regulators of immune responses and bone physiology. *Ann. N. Y. Acad. Sci.* **1143**, 123–150 (2008).
 101. Lacey, D. L. *et al.* Osteoprotegerin ligand is a cytokine that regulates osteoclast differentiation and activation. *Cell* **93**, 165–176 (1998).
 102. Roy, M. & Roux, S. Rab GTPases in Osteoclastic Bone Resorption and Autophagy. *Int. J. Mol. Sci.* **2020**, Vol. 21, Page 7655 **21**, 7655 (2020).
 103. Agerbæk, M. O., Eriksen, E. F., Kragstrup, J., Mosekilde, L. & Melsen, F. A reconstruction of the remodelling cycle in normal human cortical iliac bone. *Bone Miner.* **12**, 101–112 (1991).
 104. Raubenheimer, E., Miniggiò, H., Lemmer, L. & van Heerden, W. The Role of Bone Remodelling in Maintaining and Restoring Bone Health: an Overview. *Clin. Rev. Bone Miner. Metab.* **15**, 90–97 (2017).
 105. Hauge, E. M., Qvesel, D., Eriksen, E. F., Mosekilde, L. & Melsen, F. Cancellous bone remodeling occurs in specialized compartments lined by cells expressing osteoblastic markers. *J. Bone Miner. Res.* **16**, 1575–1582 (2001).
 106. Frost, H. M. Skeletal structural adaptations to mechanical usage (SATMU): 1. Redefining Wolff’s law: The bone modeling problem. *Anatomical Record* **226**, 403–413 (1990).
 107. Burr, D. B. Targeted and nontargeted remodeling. *Bone* **30**, 2–4 (2002).

108. Swarthout, J. T., D'Alonzo, R. C., Selvamurugan, N. & Partridge, N. C. Parathyroid hormone-dependent signaling pathways regulating genes in bone cells. *Gene* **282**, 1–17 (2002).
109. Li, X. *et al.* Parathyroid hormone stimulates osteoblastic expression of MCP-1 to recruit and increase the fusion of pre/osteoclasts. *J. Biol. Chem.* **282**, 33098–33106 (2007).
110. McHugh, K. P. *et al.* Mice lacking $\beta 3$ integrins are osteosclerotic because of dysfunctional osteoclasts. *J. Clin. Invest.* **105**, 433–440 (2000).
111. Everts, V. *et al.* The bone lining cell: Its role in cleaning Howship's lacunae and initiating bone formation. *J. Bone Miner. Res.* **17**, 77–90 (2002).
112. Zhou, H., Chernenky, R. & Davies, J. E. Deposition of cement at reversal lines in rat femoral bone. *J. Bone Miner. Res.* **9**, 367–374 (1994).
113. Sims, N. A. & Martin, T. J. Coupling the activities of bone formation and resorption: a multitude of signals within the basic multicellular unit. *Bonekey Rep.* **3**, 481 (2014).
114. Wheeler, G., Elshahaly, M., Tuck, S. P., Datta, H. K. & van Laar, J. M. The clinical utility of bone marker measurements in osteoporosis. *J. Transl. Med.* **11**, (2013).
115. Clowes, J. A. *et al.* Effect of feeding on bone turnover markers and its impact on biological variability of measurements. *Bone* **30**, 886–890 (2002).
116. Lorentzon, M. *et al.* Algorithm for the Use of Biochemical Markers of Bone Turnover in the Diagnosis, Assessment and Follow-Up of Treatment for Osteoporosis. *Adv. Ther.* **36**, 2811–2824 (2019).
117. Vasikaran, S. *et al.* Markers of bone turnover for the prediction of fracture risk and monitoring of osteoporosis treatment: A need for international reference standards. *Osteoporos. Int.* **22**, 391–420 (2011).
118. Kuo, T. R. & Chen, C. H. Bone biomarker for the clinical assessment of osteoporosis: Recent developments and future perspectives. *Biomark. Res.* **5**, 5–13 (2017).
119. Hannon, R. & Eastell, R. Preanalytical variability of biochemical markers of bone turnover. *Osteoporosis International* **11**, (2000).
120. Eastell, R. & Szulc, P. Use of bone turnover markers in postmenopausal osteoporosis. *The Lancet Diabetes and Endocrinology* **5**, 908–923 (2017).
121. Vasikaran, S. *et al.* International Osteoporosis Foundation and International Federation of Clinical Chemistry and Laboratory Medicine Position on bone marker standards in osteoporosis. *Clin. Chem. Lab. Med.* **49**, 1271–1274 (2011).
122. Cox, G., Einhorn, T. A., Tzioupis, C. & Giannoudis, P. V. Bone-turnover markers in fracture healing. *Journal of Bone and Joint Surgery - Series B* **92**, 329–334 (2010).
123. Anderson, D. M. *et al.* A homologue of the TNF receptor and its ligand enhance T-cell growth and dendritic-cell function. *Nature* **390**, 175–179 (1997).
124. Wong, B. R. *et al.* TRANCE is a novel ligand of the tumor necrosis factor receptor family that activates c-Jun N-terminal kinase in T cells. *J. Biol. Chem.* **272**, 25190–25194 (1997).
125. Yasuda, H. *et al.* Identity of Osteoclastogenesis Inhibitory Factor (OCIF) and Osteoprotegerin (OPG): A Mechanism by which OPG/OCIF Inhibits Osteoclastogenesis *in Vitro*¹. *Endocrinology* **139**, 1329–1337 (1998).
126. Simonet, W. S. *et al.* Osteoprotegerin: A novel secreted protein involved in the regulation of bone density. *Cell* **89**, 309–319 (1997).
127. Jones, D. H., Kong, Y. Y. & Penninger, J. M. Role of RANKL and RANK in bone loss and arthritis. *Ann. Rheum. Dis.* **61**, 32–39 (2002).
128. Pinzone, J. J. *et al.* The role of Dickkopf-1 in bone development, homeostasis, and disease. *Blood* **113**, 517–525 (2009).

129. Baron, R. & Rawadi, G. Minireview: Targeting the Wnt/ β -catenin pathway to regulate bone formation in the adult skeleton. *Endocrinology* **148**, 2635–2643 (2007).
130. Van Bezooijen, R. L. *et al.* Sclerostin Is an Osteocyte-expressed Negative Regulator of Bone Formation, But Not a Classical BMP Antagonist. *J. Exp. Med. J. Exp. Med.* **199**, 805–814 (2004).
131. CRUK. Cancer Research UK cancer statistics. (2020). Available at: <https://www.cancerresearchuk.org/health-professional/cancer-statistics/statistics-by-cancer-type/prostate-cancer>. Accessed 2nd November 2020.
132. Prostate cancer UK. Prostate Cancer UK facts and figures. Available at: <https://prostatecanceruk.org/prostate-information/about-prostate-cancer>. (Accessed: 2nd November 2020)
133. Hemminki, K. Familial risk and familial survival in prostate cancer. *World Journal of Urology* **30**, 143–148 (2012).
134. Ferlay, J. *et al.* Cancer incidence and mortality worldwide: Sources, methods and major patterns in GLOBOCAN 2012. *Int. J. Cancer* **136**, E359–E386 (2015).
135. Davies, N. M. *et al.* The effects of height and BMI on prostate cancer incidence and mortality: a Mendelian randomization study in 20,848 cases and 20,214 controls from the PRACTICAL consortium. *Cancer Causes Control* **26**, 1603–1616 (2015).
136. Office for National Statistics. *Cancer survival by stage at diagnosis*. (2019).
137. Gebauer, J., Higham, C., Langer, T., Denzer, C. & Brabant, G. Long-Term Endocrine and Metabolic Consequences of Cancer Treatment: A Systematic Review. *Endocr. Rev.* **40**, 711–767 (2019).
138. Loeb, S. Guideline of guidelines: Prostate cancer screening. *BJU Int.* **114**, 323–325 (2014).
139. Jahn, J. L., Giovannucci, E. L. & Stampfer, M. J. The high prevalence of undiagnosed prostate cancer at autopsy: Implications for epidemiology and treatment of prostate cancer in the Prostate-specific Antigen-era. *International Journal of Cancer* **137**, 2795–2802 (2015).
140. Bell, K. J. L., Del Mar, C., Wright, G., Dickinson, J. & Glasziou, P. Prevalence of incidental prostate cancer: A systematic review of autopsy studies. *Int. J. Cancer* **137**, 1749–1757 (2015).
141. Ilic, D. *et al.* Prostate cancer screening with prostate-specific antigen (PSA) test: A systematic review and meta-analysis. *BMJ* **362**, (2018).
142. Hayes, J. H. & Barry, M. J. Screening for prostate cancer with the prostate-specific antigen test: A review of current evidence. *JAMA - Journal of the American Medical Association* **311**, 1143–1149 (2014).
143. Nam, R. K. *et al.* Assessing individual risk for prostate cancer. *J. Clin. Oncol.* **25**, 3582–3588 (2007).
144. Thompson, I. M. *et al.* Assessing prostate cancer risk: Results from the Prostate Cancer Prevention Trial. *J. Natl. Cancer Inst.* **98**, 529–534 (2006).
145. Mottet, N. *et al.* EAU-ESUR-ESTRO-SIOG Guidelines on Prostate Cancer. *Eur. Assoc. Urol.* **2018** 1–145 (2018).
146. Stamey, T. A. *et al.* Prostate-Specific Antigen as a Serum Marker for Adenocarcinoma of the Prostate. *N. Engl. J. Med.* **317**, 909–916 (1987).
147. Ahmed, H. U. *et al.* Diagnostic accuracy of multi-parametric MRI and TRUS biopsy in prostate cancer (PROMIS): a paired validating confirmatory study. *Lancet* **389**, 815–822 (2017).
148. Kasivisvanathan, V. *et al.* MRI-Targeted or Standard Biopsy for Prostate-Cancer Diagnosis. *N. Engl. J. Med.* (2018). doi:10.1056/nejmoa1801993

149. Brierley JM, et al. *Union for international control (UICC) TNM classification of malignant tumors. 8th Ed.* (Wiley Blackwell, 2017).
150. Epstein, J. I. et al. The 2005 International Society of Urological Pathology (ISUP) consensus conference on Gleason grading of prostatic carcinoma. in *American Journal of Surgical Pathology* **29**, 1228–1242 (Am J Surg Pathol, 2005).
151. Epstein, J. I. et al. The 2014 international society of urological pathology (ISUP) consensus conference on gleason grading of prostatic carcinoma definition of grading patterns and proposal for a new grading system. *Am. J. Surg. Pathol.* **40**, 244–252 (2016).
152. Parker, C. et al. Prostate cancer: ESMO Clinical Practice Guidelines for diagnosis, treatment and follow-up. *Ann. Oncol.* **31**, 1119–1134 (2020).
153. National Institute for Health and Care Excellence (NICE). *Prostate cancer: diagnosis and management. Clinical guideline 131.* (2019). <https://www.nice.org.uk/guidance/ng131>.
154. Hofman, M. S. et al. Prostate-specific membrane antigen PET-CT in patients with high-risk prostate cancer before curative-intent surgery or radiotherapy (proPSMA): a prospective, randomised, multicentre study. *Lancet* **395**, 1208–1216 (2020).
155. Gandaglia, G. et al. Impact of the Site of Metastases on Survival in Patients with Metastatic Prostate Cancer. *Eur. Urol.* **68**, 325–334 (2015).
156. Gandaglia, G. et al. Distribution of metastatic sites in patients with prostate cancer: A population-based analysis. *Prostate* **74**, 210–216 (2014).
157. Bubendorf, L. et al. Metastatic patterns of prostate cancer: An autopsy study of 1,589 patients. *Hum. Pathol.* **31**, 578–583 (2000).
158. Albertsen, P. C. Observational studies and the natural history of screen-detected prostate cancer. *Current Opinion in Urology* **25**, 232–237 (2015).
159. Bruinsma, S. M. et al. Expert consensus document: Semantics in active surveillance for men with localized prostate cancer—results of a modified Delphi consensus procedure. *Nature Reviews Urology* **14**, 312–322 (2017).
160. Bill-Axelsson, A. et al. Radical Prostatectomy or Watchful Waiting in Prostate Cancer — 29-Year Follow-up. *N. Engl. J. Med.* **379**, 2319–2329 (2018).
161. Wilt TJ. Follow-up of prostatectomy versus observation for early prostate cancer. *NEJM* **377**, 132-142 (2017).
162. Zelefsky, M. J. et al. Incidence of Late Rectal and Urinary Toxicities After Three-Dimensional Conformal Radiotherapy and Intensity-Modulated Radiotherapy for Localized Prostate Cancer. *Int. J. Radiat. Oncol. Biol. Phys.* **70**, 1124–1129 (2008).
163. Matzinger, O. et al. Acute toxicity of curative radiotherapy for intermediate- and high-risk localised prostate cancer in the EORTC trial 22991. *Eur. J. Cancer* **45**, 2825–2834 (2009).
164. Pagliarulo, V. et al. Contemporary role of androgen deprivation therapy for prostate cancer. *European Urology* **61**, 11–25 (2012).
165. Akaza, H. et al. Combined androgen blockade with bicalutamide for advanced prostate cancer: Long-term follow-up of a phase 3, double-blind, randomized study for survival. *Cancer* **115**, 3437–3445 (2009).
166. Dalesio, O., Van Tinteren, H., Clarke, M., Peto, R. & Schroder, F. H. Maximum androgen blockade in advanced prostate cancer: An overview of the randomised trials. *Lancet* **355**, 1491–1498 (2000).
167. Sweeney, C. J. et al. Chemohormonal Therapy in Metastatic Hormone-Sensitive Prostate Cancer. *N. Engl. J. Med.* **373**, 737–746 (2015).
168. James, N. D. et al. Addition of docetaxel, zoledronic acid, or both to first-line long-term hormone therapy in prostate cancer (STAMPEDE): Survival results from an adaptive,

- multiarm, multistage, platform randomised controlled trial. *Lancet* **387**, 1163–1177 (2016).
169. Gravis, G. *et al.* Androgen-deprivation therapy alone or with docetaxel in non-castrate metastatic prostate cancer (GETUG-AFU 15): A randomised, Open-label, Phase 3 trial. *Lancet Oncol.* **14**, 149–158 (2013).
 170. Vale, C. L. *et al.* Addition of docetaxel or bisphosphonates to standard of care in men with localised or metastatic, hormone-sensitive prostate cancer: A systematic review and meta-analyses of aggregate data. *Lancet Oncol.* **17**, 243–256 (2016).
 171. Tucci, M. *et al.* Addition of docetaxel to androgen deprivation therapy for patients with hormone-sensitive metastatic prostate cancer: A systematic review and meta-analysis. *European Urology* **69**, 563–573 (2016).
 172. Cornford, P. *et al.* EAU-ESTRO-SIOG Guidelines on Prostate Cancer. Part II: Treatment of Relapsing, Metastatic, and Castration-Resistant Prostate Cancer. *Eur. Urol.* **71**, 630–642 (2017).
 173. Attard, G., Belldegrun, A. S. & De Bono, J. S. Selective blockade of androgenic steroid synthesis by novel lyase inhibitors as a therapeutic strategy for treating metastatic prostate cancer. *BJU International* **96**, 1241–1246 (2005).
 174. James, N. D. *et al.* Abiraterone for Prostate Cancer Not Previously Treated with Hormone Therapy. *N. Engl. J. Med.* **377**, 338–351 (2017).
 175. Fizazi, K. *et al.* LBA5 A phase III trial with a 2x2 factorial design in men with de novo metastatic castration-sensitive prostate cancer: Overall survival with abiraterone acetate plus prednisone in PEACE-1. *Ann. Oncol.* **32**, S1299 (2021).
 176. Attard, G. *et al.* LBA4 Abiraterone acetate plus prednisolone (AAP) with or without enzalutamide (ENZ) added to androgen deprivation therapy (ADT) compared to ADT alone for men with high-risk non-metastatic (M0) prostate cancer (PCa): Combined analysis from two comparisons in the STAMPEDE platform protocol. *Ann. Oncol.* **32**, S1298 (2021).
 177. Schalken, J. & Fitzpatrick, J. M. Enzalutamide: Targeting the androgen signalling pathway in metastatic castration-resistant prostate cancer. *BJU International* **117**, 215–225 (2016).
 178. Armstrong, A. J. *et al.* Arches: A randomized, phase III study of androgen deprivation therapy with enzalutamide or placebo in men with metastatic hormone-sensitive prostate cancer. *J. Clin. Oncol.* **37**, 2974–2986 (2019).
 179. Davis, I. D. *et al.* Enzalutamide with Standard First-Line Therapy in Metastatic Prostate Cancer. *N. Engl. J. Med.* **381**, 121–131 (2019).
 180. Rathkopf, D. E. & Scher, H. I. Apalutamide for the treatment of prostate cancer. *Expert Rev. Anticancer Ther.* **18**, 823–836 (2018).
 181. Taylor, C. D., Elson, P. & Trump, D. L. Importance of continued testicular suppression in hormone-refractory prostate cancer. *J. Clin. Oncol.* **11**, 2167–2172 (1993).
 182. Ryan, C. J. *et al.* Abiraterone acetate plus prednisone versus placebo plus prednisone in chemotherapy-naive men with metastatic castration-resistant prostate cancer (COU-AA-302): Final overall survival analysis of a randomised, double-blind, placebo-controlled phase 3 study. *Lancet Oncol.* **16**, 152–160 (2015).
 183. Beer, T. M. *et al.* Enzalutamide in Metastatic Prostate Cancer before Chemotherapy. *N. Engl. J. Med.* **371**, 424–433 (2014).
 184. Berthold, D. R. *et al.* Docetaxel plus prednisone or mitoxantrone plus prednisone for advanced prostate cancer: Updated survival in the TAX 327 study. *J. Clin. Oncol.* **26**, 242–245 (2008).
 185. Petrylak, D. P. *et al.* Docetaxel and Estramustine Compared with Mitoxantrone and

- Prednisone for Advanced Refractory Prostate Cancer. *N. Engl. J. Med.* **351**, 1513–1520 (2004).
186. De Bono, J. S. *et al.* Prednisone plus cabazitaxel or mitoxantrone for metastatic castration-resistant prostate cancer progressing after docetaxel treatment: A randomised open-label trial. *Lancet* **376**, 1147–1154 (2010).
 187. Parker, C. *et al.* Alpha Emitter Radium-223 and Survival in Metastatic Prostate Cancer. *N. Engl. J. Med.* **369**, 213–223 (2013).
 188. Smith, M. *et al.* Addition of radium-223 to abiraterone acetate and prednisone or prednisolone in patients with castration-resistant prostate cancer and bone metastases (ERA 223): a randomised, double-blind, placebo-controlled, phase 3 trial. *Lancet Oncol.* **20**, 408–419 (2019).
 189. Tombal, B. F. *et al.* Decreased fracture rate by mandating bone-protecting agents in the EORTC 1333/PEACE III trial comparing enzalutamide and Ra223 versus enzalutamide alone: An interim safety analysis. *J. Clin. Oncol.* **37**, 5007–5007 (2019).
 190. Huggins, C. & Hodges, C. V. Studies on prostatic cancer: I. The effect of castration, of estrogen and of androgen injection on serum phosphatases in metastatic carcinoma of the prostate. 1941. *J. Urol.* **168**, 9–12 (2002).
 191. Labrie, F. Adrenal androgens and intracrinology. *Seminars in Reproductive Medicine* **22**, 299–309 (2004).
 192. Imamoto, T. *et al.* The role of testosterone in the pathogenesis of prostate cancer. *International Journal of Urology* **15**, 472–480 (2008).
 193. Feldman, B., Feldman, D. The development of androgen-independent prostate cancer. *Nat. Rev. Cancer* **1**, 35–45 (2001).
 194. Gilbert, S. M., Kuo, Y. fang & Shahinian, V. B. Prevalent and incident use of androgen deprivation therapy among men with prostate cancer in the United States. *Urol. Oncol. Semin. Orig. Investig.* **29**, 647–653 (2011).
 195. Liede, A. *et al.* International survey of androgen deprivation therapy (ADT) for non-metastatic prostate cancer in 19 countries. *ESMO Open* **1**, 40 (2016).
 196. Morote, J. *et al.* Individual variations of serum testosterone in patients with prostate cancer receiving androgen deprivation therapy. *BJU Int.* **103**, 332–335 (2009).
 197. Harris, W. P., Mostaghel, E. A., Nelson, P. S. & Montgomery, B. Androgen deprivation therapy: Progress in understanding mechanisms of resistance and optimizing androgen depletion. *Nature Clinical Practice Urology* **6**, 76–85 (2009).
 198. Eisenhauer, E. A. *et al.* New response evaluation criteria in solid tumours: Revised RECIST guideline (version 1.1). *Eur. J. Cancer* **45**, 228–247 (2009).
 199. Feldman, B. J. & Feldman, D. The development of androgen-independent prostate cancer. *Nat. Rev. Cancer* **1**, 34–45 (2001).
 200. Bubley, G. J. Is the flare phenomenon clinically significant? in *Urology* **58**, 5–9 (Urology, 2001).
 201. National Institute for Health and Care Excellence (NICE). *Technology Appraisal 404: Degarelix for treating advanced hormone-dependent prostate cancer.* (2016). <https://www.nice.org.uk/guidance/ta404/documents/prostate-cancer-advanced-hormone-dependent-degarelix-depot-fad-document2#:~:text=1.1%20Degarelix%20is%20recommended%20as,symptoms%20of%20spinal%20cord%20compression.>
 202. Smith, M. R. *et al.* Bicalutamide monotherapy versus leuprolide monotherapy for prostate cancer: Effects on bone mineral density and body composition. *J. Clin. Oncol.* **22**, 2546–2553 (2004).
 203. Choo R, Lukka H, Cheung P, et al. Randomized, double-blinded, placebo-controlled,

- trial of risedronate for the prevention of bone mineral density loss in nonmetastatic prostate cancer patients receiving radiation therapy plus androgen deprivation therapy. *Int. J. Radiat. Oncol. Biol. Phys.* **85**, 1239–1245 (2013).
204. Diamond, T. H. *et al.* The antiosteoporotic efficacy of intravenous pamidronate in men with prostate carcinoma receiving combined androgen blockade: a double blind, randomized, placebo-controlled crossover study. *Cancer* **92**, 1444–50 (2001).
205. Smith, M. R. *et al.* Pamidronate to Prevent Bone Loss during Androgen-Deprivation Therapy for Prostate Cancer. *N. Engl. J. Med.* **345**, 948–955 (2001).
206. Satoh, T. *et al.* Single infusion of zoledronic acid to prevent androgen deprivation therapy-induced bone loss in men with hormone-naïve prostate carcinoma. *Cancer* **115**, 3468–3474 (2009).
207. Finkelstein, J. S. *et al.* Bone mineral density changes during the menopause transition in a multiethnic cohort of women. *J. Clin. Endocrinol. Metab.* **93**, 861–868 (2008).
208. Melton L. J. *et al.* Effects of Body Size and Skeletal Site on the Estimated Prevalence of Osteoporosis in Women and Men. *Osteoporosis Int* **11**, 977-983 (2000).
209. Morote, J. *et al.* Prevalence of Osteoporosis During Long-Term Androgen Deprivation Therapy in Patients with Prostate Cancer. *Urology* **69**, 500–504 (2007).
210. Lassemillante, A. C. M., Doi, S. A. R., Hooper, J. D., Prins, J. B. & Wright, O. R. L. Prevalence of osteoporosis in prostate cancer survivors: A meta-analysis. *Endocrine* **45**, 370–381 (2014).
211. Lassemillante, A. C. M., Doi, S. A. R., Hooper, J. D., Prins, J. B. & Wright, O. R. L. Prevalence of osteoporosis in prostate cancer survivors II: a meta-analysis of men not on androgen deprivation therapy. *Endocrine* **50**, 344–354 (2015).
212. Looker, A. C. *et al.* Prevalence of low femoral bone density in older U.S. adults from NHANES III. *J. Bone Miner. Res.* **12**, 1761–1768 (1997).
213. Nguyen, T. V., Center, J. R. & Eisman, J. A. Osteoporosis in elderly men and women: Effects of dietary calcium, physical activity, and body mass index. *J. Bone Miner. Res.* **15**, 322–331 (2000).
214. Bruder, J. M., Ma, J. Z., Basler, J. W. & Welch, M. D. Prevalence of osteopenia and osteoporosis by central and peripheral bone mineral density in men with prostate cancer during androgen-deprivation therapy. *Urology* **67**, 152–155 (2006).
215. Dalla Via, J. *et al.* Bone mineral density, structure, distribution and strength in men with prostate cancer treated with androgen deprivation therapy. *Bone* **127**, 367–375 (2019).
216. Gatti, D. *et al.* Effect of aging on trabecular and compact bone components of proximal and ultradistal radius. *Osteoporos. Int.* **6**, 355–360 (1996).
217. Greenspan, S. L. *et al.* Vertebral fractures and trabecular microstructure in men with prostate cancer on androgen deprivation therapy. *J. Bone Miner. Res.* **28**, 325–332 (2013).
218. Hamilton, E. J. *et al.* Structural decay of bone microarchitecture in men with prostate cancer treated with androgen deprivation therapy. *J. Clin. Endocrinol. Metab.* **95**, (2010).
219. Garcia-Cirera S, Casado E, Munoz J, *et al.* Effects of androgen deprivation therapy on bone quality in patients with prostate cancer. *Ann. Rheum. Dis.* **79**, 1191–1192 (2020).
220. Melton, L. J. *et al.* Fracture risk in men with prostate cancer: A population-based study. *J. Bone Miner. Res.* **26**, 1808–1815 (2011).
221. Shahinian, V. B., Kuo, Y.-F., Freeman, J. L. & Goodwin, J. S. Risk of Fracture after Androgen Deprivation for Prostate Cancer. *N. Engl. J. Med.* **352**, 154–164 (2005).
222. Daniell, H. W. Osteoporosis After Orchiectomy for Prostate Cancer. *J. Urol.* **157**, 439–

- 444 (1997).
223. Wallander, M., Axelsson, K. F., Lundh, D. & Lorentzon, M. Patients with prostate cancer and androgen deprivation therapy have increased risk of fractures—a study from the fractures and fall injuries in the elderly cohort (FRAILCO). *Osteoporos. Int.* **30**, 115–125 (2019).
 224. Abrahamsen, B. *et al.* Fracture risk in Danish men with prostate cancer: A nationwide register study. *BJU Int.* **100**, 749–754 (2007).
 225. MG, O., V, R., W, C. & MI, R. Skeletal fractures negatively correlate with overall survival in men with prostate cancer. *J. Urol.* **168**, 1005–1007 (2002).
 226. Van Hemelrijck, M. *et al.* Mortality following Hip Fracture in Men with Prostate Cancer. *PLoS One* **8**, e74492 (2013).
 227. Shao, Y. H. *et al.* Fracture after androgen deprivation therapy among men with a high baseline risk of skeletal complications. *BJU Int.* **111**, 745–752 (2013).
 228. Yuasa, T. *et al.* Relationship Between Bone Mineral Density and Androgen-deprivation Therapy in Japanese Prostate Cancer Patients. *Urology* **75**, 1131–1137 (2010).
 229. Kiratli, B. J., Srinivas, S., Perakash, I. & Terris, M. K. Progressive decrease in bone density over 10 years of androgen deprivation therapy in patients with prostate cancer. *Urology* **57**, 127–132 (2001).
 230. Galvão, D. A. *et al.* Reduced muscle strength and functional performance in men with prostate cancer undergoing androgen suppression: A comprehensive cross-sectional investigation. *Prostate Cancer Prostatic Dis.* **12**, 198–203 (2009).
 231. Stoch, S. A. *et al.* Bone Loss in Men with Prostate Cancer Treated with Gonadotropin-Releasing Hormone Agonists 1. *J. Clin. Endocrinol. Metab.* **86**, 2787–2791 (2001).
 232. Basaria, S. *et al.* Long-term effects of androgen deprivation therapy in prostate cancer patients. *Clin. Endocrinol. (Oxf)*. **56**, 779–786 (2002).
 233. Yamada, Y. *et al.* The effect of combined androgen blockade on bone turnover and bone mineral density in men with prostate cancer. *Osteoporos. Int.* **19**, 321–327 (2008).
 234. Wang, A. *et al.* Effect of Androgen Deprivation Therapy on Bone Mineral Density in a Prostate Cancer Cohort in New Zealand: A Pilot Study. *Clin. Med. Insights Oncol.* **11**, (2017).
 235. Galvão, D. A. *et al.* Changes in muscle, fat and bone mass after 36 weeks of maximal androgen blockade for prostate cancer. *BJU Int.* **102**, 44–47 (2008).
 236. Lee, H., McGovern, K., Finkelstein, J. S. & Smith, M. R. Changes in bone mineral density and body composition during initial and long-term gonadotropin-releasing hormone agonist treatment for prostate carcinoma. *Cancer* **104**, 1633–1637 (2005).
 237. Poulsen, M. H. *et al.* Osteoporosis and prostate cancer; a 24-month prospective observational study during androgen deprivation therapy. *Scand. J. Urol.* **53**, 34–39 (2019).
 238. Morote, J. *et al.* Bone Mineral Density Changes in Patients With Prostate Cancer During the First 2 Years of Androgen Suppression. *J. Urol.* **175**, 1679–1683 (2006).
 239. Preston, D. M. *et al.* Androgen deprivation in men with prostate cancer is associated with an increased rate of bone loss. *Prostate Cancer Prostatic Dis.* **5**, 304–310 (2002).
 240. Ziaran, S., Goncalves, F. M. & Sn, J. B. Complex metabolic and skeletal changes in men taking long-term androgen deprivation therapy. *Clin. Genitourin. Cancer* **11**, 33–38 (2013).
 241. Bergström, I., Gustafsson, H., Sjöberg, K. & Arver, S. Changes in bone mineral density differ between gonadotrophin-releasing hormone analogue-and surgically castrated men with prostate cancer. A prospective, controlled, parallel-group study. *Scandinavian Journal of Urology and Nephrology.* **38**, 148-152 (2004).

242. Daniell H, Dunn SR, Ferguson DW, Lomas G, N. Z. and S. P. Progressive osteoporosis during androgen deprivation for prostate cancer. *J. Urol.* **163**, 181–186 (2000).
243. Wadhwa, V. K., Weston, R., Mistry, R. & Parr, N. J. Long-term changes in bone mineral density and predicted fracture risk in patients receiving androgen-deprivation therapy for prostate cancer, with stratification of treatment based on presenting values. *BJU Int.* **104**, 800–805 (2009).
244. Israeli, R. S. *et al.* The effect of zoledronic acid on bone mineral density in patients undergoing androgen deprivation therapy. *Clin. Genitourin. Cancer* **5**, 271–277 (2007).
245. SMITH, M. R. *et al.* Randomized Controlled Trial of Zoledronic Acid to Prevent Bone Loss in Men Receiving Androgen Deprivation Therapy for Nonmetastatic Prostate Cancer. *J. Urol.* **169**, 2008–2012 (2003).
246. Ryan, C. W., Huo, D., Demers, L. M., Beer, T. M. & Lacerna, L. V. Zoledronic acid initiated during the first year of androgen deprivation therapy increases bone mineral density in patients with prostate cancer. *J. Urol.* **176**, 972–978; discussion 978 (2006).
247. Ryan, C. W. *et al.* Suppression of bone density loss and bone turnover in patients with hormone-sensitive prostate cancer and receiving zoledronic acid. *BJU Int.* **100**, 70–75 (2007).
248. Klotz, L. H., McNeill, I. Y., Kebedjian, M., Zhang, L. & Chin, J. L. A phase 3, double-blind, randomised, parallel-group, placebo-controlled study of oral weekly alendronate for the prevention of androgen deprivation bone loss in nonmetastatic prostate cancer: The cancer and osteoporosis research with alendronate and leupr. *Eur. Urol.* **63**, 927–935 (2013).
249. Bhoopalam, N. *et al.* Intravenous Zoledronic Acid to Prevent Osteoporosis in a Veteran Population With Multiple Risk Factors for Bone Loss on Androgen Deprivation Therapy. *J. Urol.* **182**, 2257–2264 (2009).
250. Lee, H., MCGovern, K., Finkelstein, J. S. & Smith, M. R. Changes in Bone Mineral Density and Body Composition during Initial and Long-Term Gonadotropin-Releasing Hormone Agonist Treatment for Prostate Carcinoma. *Cancer*, **104**, 1633–1637 (2005).
251. Lepor, H. Optimizing the Role of Hormonal Therapy in the Management of Prostate Cancer. *Rev. Urol.* **7**, S1 (2005).
252. Walker, L. M., Tran, S. & Robinson, J. W. Luteinizing hormone-releasing hormone agonists: A quick reference for prevalence rates of potential adverse effects. *Clinical Genitourinary Cancer* **11**, 375–384 (2013).
253. Irani, J., Salomon, L., Oba, R., Bouchard, P. & Mottet, N. Efficacy of venlafaxine, medroxyprogesterone acetate, and cyproterone acetate for the treatment of vasomotor hot flashes in men taking gonadotropin-releasing hormone analogues for prostate cancer: a double-blind, randomised trial. *Lancet Oncol.* **11**, 147–154 (2010).
254. Loprinzi, C. L. *et al.* A phase III randomized, double-blind, placebo-controlled trial of gabapentin in the management of hot flashes in men (N00CB). *Ann. Oncol.* **20**, 542–549 (2009).
255. Lee, M. S., Kim, K. H., Shin, B. C., Choi, S. M. & Ernst, E. Acupuncture for treating hot flashes in men with prostate cancer: A systematic review. *Supportive Care in Cancer* **17**, 763–770 (2009).
256. Braga-Basaria, M. *et al.* Metabolic syndrome in men with prostate cancer undergoing long-term androgen-deprivation therapy. *J. Clin. Oncol.* **24**, 3979–3983 (2006).
257. Nobes, J. P., Langley, S. E. M., Klopper, T., Russell-Jones, D. & Laing, R. W. A prospective, randomized pilot study evaluating the effects of metformin and lifestyle intervention on patients with prostate cancer receiving androgen deprivation therapy. *BJU Int.* **109**, 1495–1502 (2012).
258. Alibhai, S. M. H. *et al.* Impact of androgen deprivation therapy on cardiovascular

- disease and diabetes. *J. Clin. Oncol.* **27**, 3452–3458 (2009).
259. Keating, N. L., O'Malley, A. J. & Smith, M. R. Diabetes and cardiovascular disease during androgen deprivation therapy for prostate cancer. *J. Clin. Oncol.* **24**, 4448–4456 (2006).
260. Keating, N. L., O'Malley, A. J., Freedland, S. J. & Smith, M. R. Diabetes and cardiovascular disease during androgen deprivation therapy: Observational study of veterans with prostate cancer. *J. Natl. Cancer Inst.* **102**, 39–46 (2010).
261. Grundy, S. M. *et al.* Diagnosis and management of the metabolic syndrome: An American Heart Association/National Heart, Lung, and Blood Institute scientific statement. *Circulation* **112**, 2735–2752 (2005).
262. Smith, M. R. *et al.* Sarcopenia during androgen-deprivation therapy for prostate cancer. *J. Clin. Oncol.* **30**, 3271–3276 (2012).
263. Haseen, F., Murray, L. J., Cardwell, C. R., O'Sullivan, J. M. & Cantwell, M. M. The effect of androgen deprivation therapy on body composition in men with prostate cancer: Systematic review and meta-analysis. *J. Cancer Surviv.* **4**, 128–139 (2010).
264. Levy, M. E. *et al.* Physical Function Changes in Prostate Cancer Patients on Androgen Deprivation Therapy: A 2-Year Prospective Study. *Urology* **71**, 735–739 (2008).
265. Geerkens, M. J. M., Pouwels, N. S. A. & Beerlage, H. P. The effectiveness of lifestyle interventions to reduce side effects of androgen deprivation therapy for men with prostate cancer: a systematic review. *Quality of Life Research* **29**, 843–865 (2020).
266. Baumann, F. T., Zopf, E. M. & Bloch, W. Clinical exercise interventions in prostate cancer patients—a systematic review of randomized controlled trials. *Supportive Care in Cancer* **20**, 221–233 (2012).
267. Saigal, C. S. *et al.* Androgen deprivation therapy increases cardiovascular morbidity in men with prostate cancer. *Cancer* **110**, 1493–1500 (2007).
268. Lu-Yao G, Stukel TA, Yao SL. Changing patterns in competing causes of death in men with prostate cancer: a population based study. *J Urol.* **171**, 2285-90 (2004).
269. Bosco, C. *et al.* Quantifying Observational Evidence for Risk of Fatal and Nonfatal Cardiovascular Disease Following Androgen Deprivation Therapy for Prostate Cancer: A Meta-analysis. *European Urology* **68**, 386–396 (2015).
270. Zhao, J. *et al.* Androgen deprivation therapy for prostate cancer is associated with cardiovascular morbidity and mortality: A meta-analysis of population-based observational studies. *PLoS One* **9**, (2014).
271. Nguyen, P. L. *et al.* Association of androgen deprivation therapy with cardiovascular death in patients with prostate cancer: A meta-analysis of randomized trials. *JAMA - Journal of the American Medical Association* **306**, 2359–2366 (2011).
272. Levine, G. N. *et al.* Androgen-deprivation therapy in prostate cancer and cardiovascular risk: A science advisory from the American heart association, American cancer society, and American urological association. *Circulation* **121**, 833–840 (2010).
273. Storey, D. J. *et al.* Clinically relevant fatigue in men with hormonesensitive prostate cancer on long-term androgen deprivation therapy. *Ann. Oncol.* **23**, 1542–1549 (2012).
274. Alibhai, S. M. H. *et al.* Impact of androgen-deprivation therapy on physical function and quality of life in men with nonmetastatic prostate cancer. *J. Clin. Oncol.* **28**, 5038–5045 (2010).
275. Nead, K. T. *et al.* Androgen deprivation therapy and future Alzheimer's disease risk. *J. Clin. Oncol.* **34**, 566–571 (2016).
276. Moffat, S. D. *et al.* Longitudinal assessment of serum free testosterone concentration predicts memory performance and cognitive status in elderly men. *J. Clin. Endocrinol. Metab.* **87**, 5001–5007 (2002).
277. Green, H. J. *et al.* Altered cognitive function in men treated for prostate cancer with

- luteinizing hormone-releasing hormone analogues and cyproterone acetate: A randomized controlled trial. *BJU Int.* **90**, 427–432 (2002).
278. Nelson, C. J., Lee, J. S., Gamboa, M. C. & Roth, A. J. Cognitive effects of hormone therapy in men with prostate cancer: A review. *Cancer* **113**, 1097–1106 (2008).
279. Cherrier, M. M. & Higano, C. S. Impact of androgen deprivation therapy on mood, cognition, and risk for AD. *Urologic Oncology: Seminars and Original Investigations* **38**, 53–61 (2020).
280. Alibhai, S. M. H. *et al.* Impact of androgen-deprivation therapy on cognitive function in men with nonmetastatic prostate cancer. *J. Clin. Oncol.* **28**, 5030–5037 (2010).
281. Smith, M. R. *et al.* Denosumab in Men Receiving Androgen-Deprivation Therapy for Prostate Cancer. *N. Engl. J. Med.* **361**, 745–755 (2009).
282. Higano, C. S. Sexuality and intimacy after definitive treatment and subsequent androgen deprivation therapy for prostate cancer. *Journal of Clinical Oncology* **30**, 3720–3725 (2012).
283. Bolla, M. *et al.* Duration of Androgen Suppression in the Treatment of Prostate Cancer. *N. Engl. J. Med.* **360**, 2516–2527 (2009).
284. Smith, J. C. *et al.* The effects of induced hypogonadism on arterial stiffness, body composition, and metabolic parameters in males with prostate cancer. *J. Clin. Endocrinol. Metab.* **86**, 4261–4267 (2001).
285. Smith, M. R., Lee, H. & Nathan, D. M. Insulin Sensitivity during Combined Androgen Blockade for Prostate Cancer. *J. Clin. Endocrinol. Metab.* **91**, 1305–1308 (2006).
286. Boxer, R. S., Kenny, A. M., Dowsett, R. & Taxel, P. The effect of 6 months of androgen deprivation therapy on muscle and fat mass in older men with localized prostate cancer. *Aging Male* **8**, 207–212 (2005).
287. Galvão, D. A. *et al.* Changes in muscle, fat and bone mass after 36 weeks of maximal androgen blockade for prostate cancer. *BJU Int.* **102**, 44–47 (2008).
288. Smith, M. R. *et al.* Changes in Body Composition during Androgen Deprivation Therapy for Prostate Cancer. *J. Clin. Endocrinol. Metab.* **87**, 599–603 (2002).
289. Smith, M. R. *et al.* Metabolic changes during gonadotropin-releasing hormone agonist therapy for prostate cancer: Differences from the classic metabolic syndrome. *Cancer* **112**, 2188–2194 (2008).
290. Greenspan, S. L. *et al.* Bone loss after initiation of androgen deprivation therapy in patients with prostate cancer. *J. Clin. Endocrinol. Metab.* **90**, 6410–6417 (2005).
291. Berruti, A. *et al.* Changes in bone mineral density, lean body mass and fat content as measured by dual energy x-ray absorptiometry in patients with prostate cancer without apparent bone metastases given androgen deprivation therapy. *J. Urol.* **167**, 2361–2367 (2002).
292. Smith, M. R. Changes in fat and lean body mass during androgen-deprivation therapy for prostate cancer. *Urology* **63**, 742–745 (2004).
293. Chen, Z. *et al.* Low bone density and high percentage of body fat among men who were treated with androgen deprivation therapy for prostate carcinoma. *Cancer* **95**, 2136–2144 (2002).
294. Basaria, S. *et al.* Long-term effects of androgen deprivation therapy in prostate cancer patients. *Clin. Endocrinol. (Oxf)*. **56**, 779–786 (2002).
295. Kirby, M., Hirst, C. & Crawford, E. D. Characterising the castration-resistant prostate cancer population: A systematic review. *International Journal of Clinical Practice* **65**, 1180–1192 (2011).
296. Nørgaard, M. *et al.* Skeletal Related Events, Bone Metastasis and Survival of Prostate Cancer: A Population Based Cohort Study in Denmark (1999 to 2007). *J. Urol.* **184**, 162–

- 167 (2010).
297. Imbriaco, M. *et al.* A new parameter for measuring metastatic bone involvement by prostate cancer: The bone scan index. *Clin. Cancer Res.* **4**, 1765–1772 (1998).
 298. Charhon, S. A. *et al.* Histomorphometric analysis of sclerotic bone metastases from prostatic carcinoma with special reference to osteomalacia. *Cancer* **51**, 918–924 (1983).
 299. CLARKE, N. W., McCLURE, J. & GEORGE, N. J. R. Morphometric Evidence for Bone Resorption and Replacement in Prostate Cancer. *British Journal of Urology* **68**, 74–80 (1991).
 300. Garnero, P. *et al.* Markers of bone turnover for the management of patients with bone metastases from prostate cancer. *Br. J. Cancer* **82**, 858–864 (2000).
 301. Abrahamsson, P.-A. Pathophysiology of Bone Metastases in Prostate Cancer. *Eur Urol Suppl* **3**, 3-9 (2004)
 302. Berruti A, Dogliotti L, Tucci M, Tarabuzzi R, Fontana D, Angeli A. Metabolic bone disease induced by prostate cancer: rationale for the use of bisphosphonates. *J. Urol.* **166**, 2023–2031 (2001).
 303. Coleman, RE. Skeletal complications of malignancy. *Cancer* **80**, (1997).
 304. Yong, C., Onukwugha, E. & Mullins, C. D. Clinical and economic burden of bone metastasis and skeletal-related events in prostate cancer. *Current Opinion in Oncology* **26**, 274–283 (2014).
 305. Lage MJ, Barber BL, Harrison DJ, Jun S. The cost of treating skeletal-related events in patients with prostate cancer. *Am J Manag Care*, **14(5)**, 317-22 (2008)
 306. Lothgren, M. *et al.* Cost per patient and potential budget implications of denosumab compared with zoledronic acid in adults with bone metastases from solid tumours who are at risk of skeletal-related events: An analysis for Austria, Sweden and Switzerland. *Eur. J. Hosp. Pharm.* **20**, 227–231 (2013).
 307. Hussain, A. *et al.* Risk of skeletal related events among elderly prostate cancer patients by site of metastasis at diagnosis. *Cancer Med.* **5**, 3300–3309 (2016).
 308. Saad, F. *et al.* Long-term efficacy of zoledronic acid for the prevention of skeletal complications in patients with metastatic hormone-refractory prostate cancer. *J. Natl. Cancer Inst.* **96**, 879–882 (2004).
 309. Simon Tchekmedyian, N., Chen, Y. M. & Saad, F. Disease progression increases the risk of skeletal-related events in patients with bone metastases from castration-resistant prostate cancer, lung cancer, or other solid tumors. *Cancer Invest.* **28**, 849–855 (2010).
 310. Berruti, A. *et al.* Predictive factors for skeletal complications in hormone-refractory prostate cancer patients with metastatic bone disease. *Br. J. Cancer* **93**, 633–638 (2005).
 311. DePuy, V. *et al.* Effects of skeletal morbidities on longitudinal patient-reported outcomes and survival in patients with metastatic prostate cancer. *Support. Care Cancer* **15**, 869–876 (2007).
 312. Saad F, Gleason DM, Murray R, et al. Long-Term Efficacy of Zoledronic Acid for the Prevention of Skeletal Complications in Patients With Metastatic Hormone-Refractory Prostate Cancer. *J. Natl. Cancer Inst.* **96**, 879–882 (2004).
 313. Woodward, E. *et al.* Skeletal complications and survival in renal cancer patients with bone metastases. *Bone* **48**, 160–6 (2011).
 314. Krupski, T. L. *et al.* Health Care Cost Associated With Prostate Cancer, Androgen Deprivation Therapy and Bone Complications. *J. Urol.* **178**, 1423–1428 (2007).
 315. Guise, T. A. *et al.* Basic mechanisms responsible for osteolytic and osteoblastic bone metastases. *Clinical Cancer Research* **12**, 6213s-6216s (2006).

316. Upadhyay, J. *et al.* Membrane type 1-matrix metalloproteinase (MT1-MMP) and MMP-2 immunolocalization in human prostate: Change in cellular localization associated with high-grade prostatic intraepithelial neoplasia. *Clin. Cancer Res.* **5**, 4105–4110 (1999).
317. Vu, T. H. *et al.* MMP-9/gelatinase B is a key regulator of growth plate angiogenesis and apoptosis of hypertrophic chondrocytes. *Cell* **93**, 411–422 (1998).
318. Morgia, G. *et al.* Matrix metalloproteinases as diagnostic (MMP-13) and prognostic (MMP-2, MMP-9) markers of prostate cancer. *Urol. Res.* **33**, 44–50 (2005).
319. Conley-LaComb, M. K. *et al.* Pharmacological targeting of CXCL12/CXCR4 signaling in prostate cancer bone metastasis. *Mol. Cancer* **15**, 68 (2016).
320. Mehrad, B., Keane, M. P. & Strieter, R. M. Chemokines as mediators of angiogenesis. *Thrombosis and Haemostasis* **97**, 755–762 (2007).
321. Cooper, C. R. *et al.* Skeletal Complications of Malignancy Stromal Factors Involved in Prostate Carcinoma Metastasis to Bone. *Cancer.* **97** (Supp3) p739-747 (2003)
322. Chu, K. *et al.* Cadherin-11 promotes the metastasis of prostate cancer cells to bone. *Mol. Cancer Res.* **6**, 1259–1267 (2008).
323. Huang, C. F. *et al.* Cadherin-11 increases migration and invasion of prostate cancer cells and enhances their interaction with osteoblasts. *Cancer Res.* **70**, 4580–4589 (2010).
324. Paget, S. The distribution of secondary growths in cancer of the breast. 1889. *Cancer metastasis Rev.* **8**, 98–101 (1989).
325. Logothetis, C., Morris, M. J., Den, R. & Coleman, R. E. Current perspectives on bone metastases in castrate-resistant prostate cancer. *Cancer Metastasis Rev.* **37**, 189–196 (2018).
326. Kingsley, L. A., Fournier, P. G. J., Chirgwin, J. M. & Guise, T. A. Molecular biology of bone metastasis. *Molecular Cancer Therapeutics* **6**, 2609–2617 (2007).
327. Wang, M., Xia, F., Wei, Y. & Wei, X. Molecular mechanisms and clinical management of cancer bone metastasis. *Bone Res.* **8**, (2020).
328. Logothetis, C. J. & Lin, S. H. Osteoblasts in prostate cancer metastasis to bone. *Nat. Rev. Cancer* **5**, 21–28 (2005).
329. Guise, T. A., Yin, J. J. & Mohammad, K. S. Role of endothelin-1 in osteoblastic bone metastases. in *Cancer* **97**, 779–784 (John Wiley and Sons Inc., 2003).
330. Guise, T. A. & Mundy, G. R. Cancer and Bone*. *Endocr. Rev.* **19**, 18–54 (1998).
331. Dong, Z. *et al.* Prostate cancer cell-derived urokinase-type plasminogen activator contributes to intraosseous tumor growth and bone turnover. *Neoplasia* **10**, 439–449 (2008).
332. Andreasen, P. A., Egelund, R. & Petersen, H. H. The plasminogen activation system in tumor growth, invasion, and metastasis. *Cellular and Molecular Life Sciences* **57**, 25–40 (2000).
333. Zoni, E. & van der Pluijm, G. The role of microRNAs in bone metastasis. *J. Bone Oncol.* **5**, 104–108 (2016).
334. Liu, C. M. *et al.* Exosomes from the tumor microenvironment as reciprocal regulators that enhance prostate cancer progression. *International Journal of Urology* **23**, 734–744 (2016).
335. Ye, Y. *et al.* Exosomal miR-141-3p regulates osteoblast activity to promote the osteoblastic metastasis of prostate cancer. *Oncotarget* **8**, 94834–94849 (2017).
336. Harris, A. L. Hypoxia - A key regulatory factor in tumour growth. *Nature Reviews Cancer* **2**, 38–47 (2002).
337. Kingsley, L. A., Fournier, P. G. J., Chirgwin, J. M. & Guise, T. A. Molecular Biology of Bone Metastasis. *Mol Cancer Ther* **6**, 2609–2626 (2007).

338. Arnett, T. Regulation of bone cell function by acid–base balance. *Proc. Nutr. Soc.* **62**, 511–520 (2003).
339. Nadler, M. *et al.* Osteoporosis knowledge, health beliefs, and healthy bone behaviours in patients on androgen-deprivation therapy (ADT) for prostate cancer. *BJU Int.* **111**, 1301–1309 (2013).
340. Walker, L. M., Tran, S., Wassersug, R. J., Thomas, B. & Robinson, J. W. Patients and partners lack knowledge of androgen deprivation therapy side effects. *Urol. Oncol. Semin. Orig. Investig.* **31**, 1098–1105 (2013).
341. Santini, D. *et al.* Bone health management in the continuum of prostate cancer disease: a review of the evidence with an expert panel opinion. *ESMO Open.* **5** (2): e000652 (2020)
342. Coleman, R. *et al.* Bone health in cancer: ESMO Clinical Practice Guidelines y behalf of the ESMO Guidelines Committee. *Ann. Oncol.* **31**, 1650–1663 (2020).
343. Lee CE, Leslie WD, Czaykowski P, Gingerich J, Geirnaert M, Lau YK. A comprehensive bone-health management approach for men with prostate cancer receiving androgen deprivation therapy. *Curr Oncol.* **18**(4):e163-72 (2011)
344. Saylor, P. J. *et al.* Bone health and bone-targeted therapies for prostate cancer: ASCO endorsement of a cancer care ontario guideline. *J. Clin. Oncol.* **38**, 1736–1743 (2020).
345. Brown, J. E. *et al.* Guidance for the assessment and management of prostate cancer treatment-induced bone loss. A consensus position statement from an expert group. *J. Bone Oncol.* **25**, (2020).
346. Damji, A. N., Bies, K., Alibhai, S. M. H. & Jones, J. M. Bone health management in men undergoing ADT: examining enablers and barriers to care. *Osteoporos. Int.* **26**, 951–959 (2015).
347. Agarwal, M. M. *et al.* Factors affecting bone mineral density in patients with prostate carcinoma before and after orchidectomy. *Cancer* **103**, 2042–2052 (2005).
348. Datta M, S. G. Calcium and vitamin D supplementation during androgen deprivation therapy for prostate cancer: a critical review. *Oncologist* **17**, 1171–1179 (2012).
349. Bourke, L. *et al.* Exercise for men with prostate cancer: A systematic review and meta-analysis. *European Urology* **69**, 693–703 (2016).
350. Ndjavera, W. *et al.* Exercise-induced attenuation of treatment side-effects in patients with newly diagnosed prostate cancer beginning androgen-deprivation therapy: a randomised controlled trial. *BJU Int.* **125**, 28–37 (2020).
351. Cormie, P. *et al.* Exercise maintains sexual activity in men undergoing androgen suppression for prostate cancer: A randomized controlled trial. *Prostate Cancer Prostatic Dis.* **16**, 170–175 (2013).
352. Cruz-Jentoft, A. J. *et al.* Sarcopenia: European consensus on definition and diagnosis. *Age Ageing* **39**, 412–423 (2010).
353. Fried, L. P. *et al.* Frailty in older adults: Evidence for a phenotype. *Journals Gerontol. - Ser. A Biol. Sci. Med. Sci.* **56**, (2001).
354. Vermeulen, J., Neyens, J. C., Van Rossum, E., Spreeuwenberg, M. D. & De Witte, L. P. Predicting ADL disability in community-dwelling elderly people using physical frailty indicators: A systematic review. *BMC Geriatr.* **11**, 33 (2011).
355. National institute of health and care excellence (NICE). *Prostate cancer: diagnosis and management. Clinical guideline CG175.* (2014).
356. Bourke, L. *et al.* A multi-centre investigation of delivering national guidelines on exercise training for men with advanced prostate cancer undergoing androgen deprivation therapy in the UK NHS. *PLoS One* **13**, e0197606 (2018).
357. Reale, S. *et al.* Embedding supervised exercise training for men on androgen

- deprivation therapy into standard prostate cancer care: a feasibility and acceptability study (the STAMINA trial). *Sci. Reports* 2021 111 **11**, 1–12 (2021).
358. Home | STAMINA. Available at: <https://www.stamina.org.uk/>. (Accessed: 17th June 2021)
359. Green, J. R. Bisphosphonates: Preclinical Review. *Oncologist* **9**, 3–13 (2004).
360. Drake, M. T., Clarke, B. L. & Khosla, S. Bisphosphonates: Mechanism of action and role in clinical practice. *Mayo Clinic Proceedings* **83**, 1032–1045 (2008).
361. Pazianas, M., Van Der Geest, S. & Miller, P. Bisphosphonates and bone quality. *Bonekey Rep.* **3**, 529 (2014).
362. Allen, M. R. Recent Advances in Understanding Bisphosphonate Effects on Bone Mechanical Properties. *Current Osteoporosis Reports* **16**, 198–204 (2018).
363. Serpa Neto, A. *et al.* Bisphosphonate therapy in patients under androgen deprivation therapy for prostate cancer: A systematic review and meta-analysis. *Prostate Cancer and Prostatic Diseases* **15**, 36–44 (2012).
364. Smith, M. R. *et al.* Randomized controlled trial of early zoledronic acid in men with castration-sensitive prostate cancer and bone metastases: Results of CALGB 90202 (Alliance). *J. Clin. Oncol.* **32**, 1143–1150 (2014).
365. James, N. D. *et al.* Addition of docetaxel, zoledronic acid, or both to first-line long-term hormone therapy in prostate cancer (STAMPEDE): Survival results from an adaptive, multiarm, multistage, platform randomised controlled trial. *Lancet* **387**, 1163–1177 (2016).
366. Kennel, K. A. & Drake, M. T. Adverse Effects of Bisphosphonates: Implications for Osteoporosis Management. *Mayo Clin. Proc.* **84**, 632–638 (2009).
367. Aragon-Ching, J. B. *et al.* Higher incidence of Osteonecrosis of the Jaw (ONJ) in patients with metastatic castration resistant prostate cancer treated with anti-angiogenic agents. *Cancer Invest.* **27**, 221–226 (2009).
368. Dodson, T. B. The Frequency of Medication-related Osteonecrosis of the Jaw and its Associated Risk Factors. *Oral Maxillofac Surg Clin North Am.* **27**, 509-16. (2015)
369. Ruggiero, S. *et al.* Practical Guidelines for the Prevention, Diagnosis, and Treatment of Osteonecrosis of the Jaw in Patients With Cancer. *J. Oncol. Pract.* **2**, 7–14 (2006).
370. Smith, M. R. *et al.* Effects of Denosumab on Bone Mineral Density in Men Receiving Androgen Deprivation Therapy for Prostate Cancer. *J. Urol.* **182**, 2670–2676 (2009).
371. Fizazi, K. *et al.* Denosumab versus zoledronic acid for treatment of bone metastases in men with castration-resistant prostate cancer: A randomised, double-blind study. *Lancet* **377**, 813–822 (2011).
372. Smith, M. R., Fallon, M. A., Lee, H. & Finkelstein, J. S. Raloxifene to prevent gonadotropin-releasing hormone agonist-induced bone loss in men with prostate cancer: A randomized controlled trial. *J. Clin. Endocrinol. Metab.* **89**, 3841–3846 (2004).
373. Smith, M. R. *et al.* Toremifene to reduce fracture risk in men receiving androgen deprivation therapy for prostate cancer. *J. Urol.* **184**, 1316–1321 (2010).
374. Consensus development conference: Diagnosis, prophylaxis, and treatment of osteoporosis. in *The American Journal of Medicine* **94**, 646–650 (Am J Med, 1993).
375. Johnell O, Kanis JA, . An estimate of the worldwide prevalence and disability associated with osteoporotic fractures. *Osteoporos. Int.* **17**, 1726–1733 (2006).
376. British Orthopaedic Association. *The care of patients with fragility fractures.* (2007). <https://www.bgs.org.uk/sites/default/files/content/attachment/2018-05-02/Blue%20Book%20on%20fragility%20fracture%20care.pdf>
377. National Osteoporosis Guideline Group. *Osteoporosis Clinical guideline for prevention*

and treatment: Executive Summary. (2018).
<https://www.sheffield.ac.uk/NOGG/NOGG%20Guideline%202017.pdf>

378. Burge RT, Worley D, Johansen A, et al. The cost of osteoporotic fractures in the UK: projections for 2000–2020. *J. Med. Econ.* **4**, 51–52 (2001).
379. Sernbo I, Johnell O, . Consequences of a hip fracture: a prospective study over 1 year. *Osteoporos. Int.* **3**, 148–153 (1993).
380. Schousboe, J. T. Epidemiology of Vertebral Fractures. *J. Clin. Densitom.* **19**, 8–22 (2016).
381. Ensrud, K. E. & Schousboe, J. T. Clinical practice. Vertebral fractures. *N. Engl. J. Med.* **364**, 1634–42 (2011).
382. Bernabei, R., Martone, A. M., Ortolani, E., Landi, F. & Marzetti, E. Screening, diagnosis and treatment of osteoporosis: a brief review. *Clin. Cases Miner. Bone Metab.* **11**, 201–207 (2014).
383. Compston, J. Glucocorticoid-induced osteoporosis: an update. *Endocrine* **61**, 7–16 (2018).
384. Silverman, S. *et al.* International management of bone health in glucocorticoid-exposed individuals in the observational GLOW study. *Osteoporosis International* **26**, 419–420 (2014).
385. Fardet, L., Petersen, I. & Nazareth, I. Prevalence of long-term oral glucocorticoid prescriptions in the UK over the past 20 years. *Rheumatology (Oxford)*. **50**, 1982–1990 (2011).
386. Van Staa, T. P., Leufkens, H. G. M. & Cooper, C. The epidemiology of corticosteroid-induced osteoporosis: A meta-analysis. *Osteoporosis International* **13**, 777–787 (2002).
387. Van Staa, T. P., Leufkens, H. G. M., Abenhaim, L., Zhang, B. & Cooper, C. Use of oral corticosteroids and risk of fractures. *J. Bone Miner. Res.* **15**, 993–1000 (2000).
388. Dempster, D. W. Perspectives bone histomorphometry in glucocorticoid-induced osteoporosis. *J. Bone Miner. Res.* **4**, 137–141 (1989).
389. Wu, Z., Bucher, N. L. & Farmer, S. R. Induction of peroxisome proliferator-activated receptor gamma during the conversion of 3T3 fibroblasts into adipocytes is mediated by C/EBPbeta, C/EBPdelta, and glucocorticoids. *Mol. Cell. Biol.* **16**, 4128–4136 (1996).
390. Weinstein, R. S., Jilka, R. L., Michael Parfitt, A. & Manolagas, S. C. Inhibition of osteoblastogenesis and promotion of apoptosis of osteoblasts end osteocytes by glucocorticoids potential mechanisms of their deleterious effects on bone. *J. Clin. Invest.* **102**, 274–282 (1998).
391. Yao, W. *et al.* Sclerostin-antibody treatment of glucocorticoid-induced osteoporosis maintained bone mass and strength. *Osteoporos. Int.* **27**, 283–294 (2016).
392. Sato, A. Y. *et al.* Glucocorticoids induce bone and muscle atrophy by tissue-specific mechanisms upstream of E3 ubiquitin ligases. *Endocrinology* **158**, 664–677 (2017).
393. Jänne, M., Hogeveen, K. N., Deol, H. K. & Hammond, G. L. Expression and regulation of human sex hormone-binding globulin transgenes in mice during development. *Endocrinology* **140**, 4166–4174 (1999).
394. Vanderschueren D, Laurent MR, Claessens F, et al. Sex steroid actions in male bone. *Endocr Rev.* **35**(6):906-960. (2014).
395. Perrien, D. S. *et al.* Inhibin A is an endocrine stimulator of bone mass and strength. *Endocrinology* **148**, 1654–1665 (2007).
396. Golds G, Houdek D, Arnason T. Male Hypogonadism and Osteoporosis: The Effects, Clinical Consequences, and Treatment of Testosterone Deficiency in Bone Health. *Int J Endocrinol.* 4602129 (2017).
397. Ucer, S. *et al.* The Effects of Androgens on Murine Cortical Bone Do Not Require AR or

- ER α Signaling in Osteoblasts and Osteoclasts. *J. Bone Miner. Res.* **30**, 1138–1149 (2015).
398. Chiang, C. *et al.* Mineralization and Bone Resorption Are Regulated by the Androgen Receptor in Male Mice. *J. Bone Miner. Res.* **24**, 621–631 (2009).
399. Sinnesael, M. *et al.* Androgen receptor (AR) in osteocytes is important for the maintenance of male skeletal integrity: Evidence from targeted AR disruption in mouse osteocytes. *J. Bone Miner. Res.* **27**, 2535–2543 (2012).
400. Sobel, V., Schwartz, B., Zhu, Y.-S., Cordero, J. J. & Imperato-McGinley, J. Bone Mineral Density in the Complete Androgen Insensitivity and 5 α -Reductase-2 Deficiency Syndromes. *J. Clin. Endocrinol. Metab.* **91**, 3017–3023 (2006).
401. Marcus, R. *et al.* The Contribution of Testosterone to Skeletal Development and Maintenance: Lessons from the Androgen Insensitivity Syndrome. *J. Clin. Endocrinol. Metab.* **85**, 1032–1037 (2000).
402. Sjögren, K. *et al.* Elevated aromatase expression in osteoblasts leads to increased bone mass without systemic adverse effects. *J. Bone Miner. Res.* **24**, 1263–1270 (2009).
403. Rochira, V. & Carani, C. Aromatase deficiency in men: A clinical perspective. *Nature Reviews Endocrinology* **5**, 559–568 (2009).
404. Sanyal, A. *et al.* Regulation of bone turnover by sex steroids in men. *J. Bone Miner. Res.* **23**, 705–714 (2008).
405. Mellström, D. *et al.* Older men with low serum estradiol and high serum SHBG have an increased risk of fractures. *J. Bone Miner. Res.* **23**, 1552–1560 (2008).
406. Mellström, D. *et al.* Free testosterone is an independent predictor of BMD and prevalent fractures in elderly men: MrOS Sweden. *J. Bone Miner. Res.* **21**, 529–535 (2006).
407. Cauley, J. A. *et al.* Sex steroid hormones in older men: Longitudinal associations with 4.5-year change in hip bone mineral density - The osteoporotic fractures in men study. *J. Clin. Endocrinol. Metab.* **95**, 4314–4323 (2010).
408. Amin, S. *et al.* Estradiol, Testosterone, and the Risk for Hip Fractures in Elderly Men from the Framingham Study. *Am. J. Med.* **119**, 426–433 (2006).
409. Meier C, Nguyen TV, Handelsman DJ, Schindler C, Kushnir MM, Rockwood AL, Meikle AW, Center JR, Eisman JA, Seibel MJ. Endogenous sex hormones and incident fracture risk in older men: the Dubbo Osteoporosis Epidemiology Study. *Arch Intern Med.* **168**(1):47-54. (2008)
410. Orwoll, E. *et al.* Endogenous testosterone levels, physical performance, and fall risk in older men. *Arch. Intern. Med.* **166**, 2124–2131 (2006).
411. Van Staa, T. P., Dennison, E. M., Leufkens, H. G. M. & Cooper, C. Epidemiology of fractures in England and Wales. *Bone* **29**, 517–522 (2001).
412. Berger, C. *et al.* Peak bone mass from longitudinal data: Implications for the prevalence, pathophysiology, and diagnosis of osteoporosis. *J. Bone Miner. Res.* **25**, 1948–1957 (2010).
413. Walsh, J. S. & Eastell, R. Osteoporosis in men. *Nature Reviews Endocrinology* **9**, 637–645 (2013).
414. Eleftheriou, K. I. *et al.* Bone structure and geometry in young men: The influence of smoking, alcohol intake and physical activity. *Bone* **52**, 17–26 (2013).
415. Fatayerji, D. & Eastell, R. Age-related changes in bone turnover in men. *J. Bone Miner. Res.* **14**, 1203–1210 (1999).
416. Riggs, B. L. *et al.* A population-based assessment of rates of bone loss at multiple skeletal sites: Evidence for substantial trabecular bone loss in young adult women and men. *J. Bone Miner. Res.* **23**, 205–214 (2008).

417. Clarke, B. L. *et al.* Predictors of bone mineral density in aging healthy men varies by skeletal site. *Calcif. Tissue Int.* **70**, 137–145 (2002).
418. Jones, G., Nguyen, T., Sambrook, P., Kelly, P. J. & Eisman, J. A. Progressive loss of bone in the femoral neck in elderly people: Longitudinal findings from the Dubbo osteoporosis epidemiology study. *BMJ* **309**, 691 (1994).
419. Hannan, M. T. *et al.* Risk factors for longitudinal bone loss in elderly men and women: The Framingham Osteoporosis Study. *J. Bone Miner. Res.* **15**, 710–720 (2000).
420. Parfitt, A. M. Age-related structural changes in trabecular and cortical bone: Cellular mechanisms and biomechanical consequences. *Calcif. Tissue Int.* **36**, S123–S128 (1984).
421. Seeman, E. During aging, men lose less bone than women because they gain more periosteal bone, not because they resorb less endosteal bone. *Calcified Tissue International* **69**, 205–208 (2001).
422. Riggs, B. L. *et al.* Population-based study of age and sex differences in bone volumetric density, size, geometry, and structure at different skeletal sites. *J. Bone Miner. Res.* **19**, 1945–1954 (2004).
423. Burghardt, A. J., Kazakia, G. J., Ramachandran, S., Link, T. M. & Majumdar, S. Age- and gender-related differences in the geometric properties and biomechanical significance of intracortical porosity in the distal radius and tibia. *J. Bone Miner. Res.* **25**, 983–993 (2010).
424. Aaron JE, Makins NB, S. K. The microanatomy of trabecular bone loss in normal aging men and women. *Clin Orthop Relat. Res.* **215**, 260–271 (1987).
425. Silva, M. J. & Gibson, L. J. Modeling the mechanical behavior of vertebral trabecular bone: Effects of age-related changes in microstructure. *Bone* **21**, 191–199 (1997).
426. Orwoll, E. *et al.* Testosterone and estradiol among older men. *J. Clin. Endocrinol. Metab.* **91**, 1336–1344 (2006).
427. Khosla, S. *et al.* Relationship of Serum Sex Steroid Levels and Bone Turnover Markers with Bone Mineral Density in Men and Women: A Key Role for Bioavailable Estrogen 1. *J. Clin. Endocrinol. Metab.* **83**, 2266–2274 (1998).
428. Leder, B. Z., LeBlanc, K. M., Schoenfeld, D. A., Eastell, R. & Finkelstein, J. S. Differential effects of androgens and estrogens on bone turnover in normal men. *J. Clin. Endocrinol. Metab.* **88**, 204–210 (2003).
429. Falahati-Nini, A. *et al.* Relative contributions of testosterone and estrogen in regulating bone resorption and formation in normal elderly men. *J. Clin. Invest.* **106**, 1553–1560 (2000).
430. Von Mühlen, D., Laughlin, G. A., Kritz-Silverstein, D., Bergstrom, J. & Bettencourt, R. Effect of dehydroepiandrosterone supplementation on bone mineral density, bone markers, and body composition in older adults: The DAWN trial. *Osteoporos. Int.* **19**, 699–707 (2008).
431. Amin, S. *et al.* High serum IGFBP-2 is predictive of increased bone turnover in aging men and women. *J. Bone Miner. Res.* **22**, 799–807 (2007).
432. Tobias, J. H., Chow, J. W. & Chambers, T. J. Opposite effects of insulin-like growth factor-I on the formation of trabecular and cortical bone in adult female rats. *Endocrinology* **131**, 2387–2392 (1992).
433. Liu, J. M. *et al.* IGF-1 as an early marker for low bone mass or osteoporosis in premenopausal and postmenopausal women. *J. Bone Miner. Metab.* **26**, 159–164 (2008).
434. Epstein, S. *et al.* The influence of age on bone mineral regulating hormones. *Bone* **7**, 421–425 (1986).
435. Boonen, S. *et al.* Age-related (type II) femoral neck osteoporosis in men: Biochemical

- evidence for both hypovitaminosis D- and androgen deficiency-induced bone resorption. *J. Bone Miner. Res.* **12**, 2119–2126 (1997).
436. World Health Organisation. *Assessment of fracture risk and its application to screening for postmenopausal osteoporosis. Report of a WHO Study Group.* (1994). https://apps.who.int/iris/bitstream/handle/10665/39142/WHO_TRS_843_eng.pdf?sequence=1&isAllowed=y
437. De Laet, C. E. D. H. *et al.* Hip fracture prediction in elderly men and women: Validation in the Rotterdam study. *J. Bone Miner. Res.* **13**, 1587–1593 (1998).
438. Binkley, N., Adler, R. & Bilezikian, J. P. Osteoporosis diagnosis in men: The T-score controversy revisited. *Curr. Osteoporos. Rep.* **12**, 403–409 (2014).
439. Marshall, D., Johnell, O. & Wedel, H. Meta-analysis of how well measures of bone mineral density predict occurrence of osteoporotic fractures. *Br. Med. J.* **312**, 1254–1259 (1996).
440. Johnell, O. *et al.* Predictive value of BMD for hip and other fractures. *J. Bone Miner. Res.* **20**, 1185–1194 (2005).
441. Siris, E. S. *et al.* Bone mineral density thresholds for pharmacological intervention to prevent fractures. *Arch. Intern. Med.* **164**, 1108–1112 (2004).
442. Stone, K. L. *et al.* BMD at Multiple Sites and Risk of Fracture of Multiple Types: Long-Term Results From the Study of Osteoporotic Fractures. *J. Bone Miner. Res.* **18**, 1947–1954 (2003).
443. World Health Organisation and University of Sheffield, . Fracture Risk Assessment Tool (FRAX). Available at: <https://www.sheffield.ac.uk/FRAX/reference.aspx>. (Accessed: 20th November 2020)
444. Kanis, J. A. *et al.* Development and use of FRAX® in osteoporosis. *Osteoporosis International* **21**, 407–413 (2010).
445. World Health Organisation. *WHO scientific group on the assessment of osteoporosis at primary health care level.* (2004). <https://www.who.int/chp/topics/Osteoporosis.pdf>
446. Kanis, J. A. *et al.* A systematic review of intervention thresholds based on FRAX: A report prepared for the National Osteoporosis Guideline Group and the International Osteoporosis Foundation. *Archives of Osteoporosis* **11**, (2016).
447. Compston, J. *et al.* UK clinical guideline for the prevention and treatment of osteoporosis. *Arch. Osteoporos.* **12**, (2017).
448. The National Institute for Health and Care. Guide to the methods of technology appraisal. *Nice* 1–93 (2018).
449. Devlin, N. J. & Brooks, R. EQ-5D and the EuroQol Group: Past, Present and Future. *Applied Health Economics and Health Policy* **15**, 127–137 (2017).
450. Shepstone, L. *et al.* Screening in the community to reduce fractures in older women (SCOOP): a randomised controlled trial. *Lancet* **391**, 741–747 (2018).
451. Rubin, K. H. *et al.* Effectiveness of a two-step population-based osteoporosis screening program using FRAX: the randomized Risk-stratified Osteoporosis Strategy Evaluation (ROSE) study. *Osteoporos. Int.* **29**, 567–578 (2018).
452. Turner, D. A. *et al.* The Cost-Effectiveness of Screening in the Community to Reduce Osteoporotic Fractures in Older Women in the UK: Economic Evaluation of the SCOOP Study. *J. Bone Miner. Res.* **33**, 845–851 (2018).
453. Harvey, N. C. *et al.* Falls Predict Fractures Independently of FRAX Probability: A Meta-Analysis of the Osteoporotic Fractures in Men (MrOS) Study. *J. Bone Miner. Res.* **33**, 510–516 (2018).
454. Kennedy, C. C. *et al.* A Frailty Index predicts 10-year fracture risk in adults age 25 years and older: results from the Canadian Multicentre Osteoporosis Study (CaMos).

Osteoporos. Int. **25**, 2825–2832 (2014).

455. Li, G., Papaioannou, A., Thabane, L., Cheng, J. & Adachi, J. D. Frailty Change and Major Osteoporotic Fracture in the Elderly: Data from the Global Longitudinal Study of Osteoporosis in Women 3-Year Hamilton Cohort. *J. Bone Miner. Res.* **31**, 718–724 (2016).
456. McCloskey, E. V. *et al.* A Meta-Analysis of Trabecular Bone Score in Fracture Risk Prediction and Its Relationship to FRAX. *J. Bone Miner. Res.* **31**, 940–948 (2016).
457. Jefferies, E. R. *et al.* Admissions to hospital due to fracture in England in patients with prostate cancer treated with androgen-deprivation therapy – do we have to worry about the hormones? *BJU Int.* **118**, 416–422 (2016).
458. Saylor, P. J., Kaufman, D. S., Michaelson, M. D., Lee, R. J. & Smith, M. R. Application of a Fracture Risk Algorithm to Men Treated With Androgen Deprivation Therapy for Prostate Cancer. *J. Urol.* **183**, 2200–2205 (2010).
459. Neubecker, K., Adams-Huet, B., Farukhi, I. M., Delapena, R. C. & Gruntmanis, U. Predictors of Fracture Risk and Bone Mineral Density in Men with Prostate Cancer on Androgen Deprivation Therapy. *J. Osteoporos.* **2011**, 1–6 (2011).
460. James, H. *et al.* Comparison of fracture risk assessment tool score to bone mineral density for estimating fracture risk in patients with advanced prostate cancer on androgen deprivation therapy. *Urology* **84**, 164–168 (2014).
461. Adler, R. A., Hastings, F. W. & Petkov, V. I. Treatment thresholds for osteoporosis in men on androgen deprivation therapy: T-score versus FRAX™. *Osteoporos. Int.* **21**, 647–653 (2010).
462. Kojima, I. *et al.* Efficacy of zoledronic acid in older prostate cancer patients undergoing androgen deprivation therapy. *Osteoporos. Sarcopenia* **5**, 128–131 (2019).
463. Miyazawa, Y. *et al.* Effect of androgen-deprivation therapy on bone mineral density in Japanese patients with prostate cancer. *In Vivo (Brooklyn)*. **32**, 409–412 (2018).
464. Dhanapal, V. & Reeves, D. J. Bone health management in prostate cancer patients receiving androgen deprivation therapy. *J Oncol Pharm Pract.* **18**(1):84-90 (2018).
465. Brown, J. E. *et al.* Baseline fracture risk in men with prostate cancer starting the STAMPEDE trial. *Ann. Oncol.* **30**, v334–v335 (2019).
466. Kawahara, T. *et al.* Bone management in Japanese patients with prostate cancer: Hormonal therapy leads to an increase in the FRAX score. *BMC Urol.* **16**, 32 (2016).
467. Ojeda, S. *et al.* Deprivación andrónica en cáncer de próstata y riesgo de fractura a largo plazo. *Actas Urol. Esp.* **41**, 491–496 (2017).
468. Bauer DC. Osteoporotic fractures: ignorance is bliss? *Am J Med.* **109**(4):338-9 (2000)
469. Harrington, J. T., Broy, S. B., Derosa, A. M., Licata, A. A. & Shewmon, D. A. Hip fracture patients are not treated for osteoporosis: A call to action. *Arthritis Care Res.* **47**, 651–654 (2002).
470. Feldstein, A. C. *et al.* The near absence of osteoporosis treatment in older men with fractures. *Osteoporos. Int.* **16**, 953–962 (2005).
471. Klop, C. *et al.* Anti-osteoporosis drug prescribing after hip fracture in the UK: 2000–2010. *Osteoporos. Int.* **26**, 1919–1928 (2015).
472. National Osteoporosis Foundation. Report: *Medicare cost of osteoporotic fractures*. (2021 update). <https://www.milliman.com/en/insight/medicare-cost-of-osteoporotic-fractures-2021-updated-report>
473. Watts, N. B. *et al.* Osteoporosis in men: An Endocrine Society clinical practice guideline. *Journal of Clinical Endocrinology and Metabolism* **97**, 1802–1822 (2012).
474. Chalitsios, C. V., Shaw, D. E. & McKeever, T. M. A retrospective database study of oral

- corticosteroid and bisphosphonate prescribing patterns in England. *Prim. Care Respir. Med.* **30**, 1–8 (2020).
475. Boonen, S. *et al.* Fracture Risk and Zoledronic Acid Therapy in Men with Osteoporosis. *N. Engl. J. Med.* **367**, 1714–1723 (2012).
476. Orwoll, E. *et al.* Alendronate for the Treatment of Osteoporosis in Men. *N. Engl. J. Med.* **343**, 604–610 (2000).
477. Boonen, S. *et al.* Once-weekly risedronate in men with osteoporosis: Results of a 2-Year, placebo-controlled, double-blind, multicenter study. *J. Bone Miner. Res.* **24**, 719–725 (2009).
478. Shimon, I. *et al.* Alendronate for osteoporosis in men with androgen-repleted hypogonadism. *Osteoporos. Int.* **16**, 1591–1596 (2005).
479. Cummings, S. R. *et al.* Denosumab for Prevention of Fractures in Postmenopausal Women with Osteoporosis. *N. Engl. J. Med.* **361**, 756–765 (2009).
480. Orwoll, E. *et al.* A randomized, placebo-controlled study of the effects of denosumab for the treatment of men with low bone mineral density. *J. Clin. Endocrinol. Metab.* **97**, 3161–3169 (2012).
481. Langdahl, B. L. *et al.* A 24-month study evaluating the efficacy and safety of denosumab for the treatment of men with low bone mineral density: Results from the ADAMO trial. *J. Clin. Endocrinol. Metab.* **100**, 1335–1342 (2015).
482. Cummings, S. R. *et al.* Vertebral Fractures After Discontinuation of Denosumab: A Post Hoc Analysis of the Randomized Placebo-Controlled FREEDOM Trial and Its Extension. *J. Bone Miner. Res.* **33**, 190–198 (2018).
483. Kendler, D. L. *et al.* Effects of teriparatide and risedronate on new fractures in postmenopausal women with severe osteoporosis (VERO): a multicentre, double-blind, double-dummy, randomised controlled trial. *Lancet* **391**, 230–240 (2018).
484. Neer, R. M. *et al.* Effect of Parathyroid Hormone (1-34) on Fractures and Bone Mineral Density in Postmenopausal Women with Osteoporosis. *N. Engl. J. Med.* **344**, 1434–1441 (2001).
485. Orwoll, E. S. *et al.* The effect of teriparatide [human parathyroid hormone (1-34)] therapy on bone density in men with osteoporosis. *J. Bone Miner. Res.* **18**, 9–17 (2003).
486. Rachner, T. D., Khosla, S. & Hofbauer, L. C. Osteoporosis: Now and the future. *The Lancet* **377**, 1276–1287 (2011).
487. Scottish Medicines Consortium: Romosozumab. (2020). Available at: <https://www.scottishmedicines.org.uk/media/5567/romosozumab-evenity.pdf> (Accessed: 2nd December 2020)
488. Hussain, A., Lee, R. J., Graff, J. N. & Halabi, S. The evolution and understanding of skeletal complication endpoints in clinical trials of tumors with metastasis to the bone. *Critical Reviews in Oncology/Hematology* **139**, 108–116 (2019).
489. Overview | Advanced breast cancer: diagnosis and treatment | Guidance | NICE. <https://www.nice.org.uk/guidance/cg81>. Accessed November 2020.
490. Overview | Early and locally advanced breast cancer: diagnosis and management | Guidance | NICE. <https://www.nice.org.uk/guidance/ng101>. Accessed November 2020.
491. Cianferotti, L. *et al.* The prevention of fragility fractures in patients with non-metastatic prostate cancer: A position statement by the international osteoporosis foundation. *Oncotarget* **8**, 75646–75663 (2017).
492. Santini, D. *et al.* Bone health management in the continuum of prostate cancer disease: a review of the evidence with an expert panel opinion. (2020). doi:10.1136/esmooopen-2019-000652
493. Szulc, P., Marchand, F., Duboeuf, F. & Delmas, P. D. Cross-sectional assessment of age-

- related bone loss in men: The MINOS study. *Bone* **26**, 123–129 (2000).
494. Khosla, S. *et al.* Effects of sex and age on bone microstructure at the ultradistal radius: A population-based noninvasive in vivo assessment. *J. Bone Miner. Res.* **21**, 124–131 (2006).
495. De Laet, C. *et al.* Body mass index as a predictor of fracture risk: A meta-analysis. *Osteoporos. Int.* **16**, 1330–1338 (2005).
496. Burger, H. *et al.* Risk factors for increased bone loss in an elderly population: The Rotterdam Study. *Am. J. Epidemiol.* **147**, 871–879 (1998).
497. Meyer, H. E., Sjøgaard, A. J., Falch, J. A., Jørgensen, L. & Emaus, N. Weight change over three decades and the risk of osteoporosis in men. *Am. J. Epidemiol.* **168**, 454–460 (2008).
498. Nielson, C. M. *et al.* BMI and fracture risk in older men: The osteoporotic fractures in men study (MrOS). *J. Bone Miner. Res.* **26**, 496–502 (2011).
499. King, C. M., Hamilton, G. A., Cobb, M., Carpenter, D. & Ford, L. A. Association Between Ankle Fractures and Obesity. *J. Foot Ankle Surg.* **51**, 543–547 (2012).
500. Premaor, M. O. *et al.* The association between fracture site and obesity in men: A population-based cohort study. *J. Bone Miner. Res.* **28**, 1771–1777 (2013).
501. Atkins, G. J. *et al.* Metabolism of vitamin D3 in human osteoblasts: Evidence for autocrine and paracrine activities of 1 α ,25-dihydroxyvitamin D3. *Bone* **40**, 1517–1528 (2007).
502. Gielen, E. *et al.* Calcium and Vitamin D Supplementation in Men. *J. Osteoporos.* **2011**, 1–6 (2011).
503. Crowe, F. L. *et al.* Trends in the incidence of testing for Vitamin D deficiency in primary care in the UK: A retrospective analysis of the Health Improvement Network (THIN), 2005-2015. *BMJ Open* **9**, (2019).
504. Li, H. *et al.* A prospective study of plasma vitamin D metabolites, vitamin D receptor polymorphisms, and prostate cancer. *PLoS Med.* **4**, 562–571 (2007).
505. Annweiler, C., Schott, A. M., Berrut, G., Fantino, B. & Beauchet, O. Vitamin D-related changes in physical performance: A systematic review. *J. Nutr. Heal. Aging* **13**, 893–898 (2009).
506. Visser, M., Deeg, D. J. H. & Lips, P. Low Vitamin D and High Parathyroid Hormone Levels as Determinants of Loss of Muscle Strength and Muscle Mass (Sarcopenia): The Longitudinal Aging Study Amsterdam. *J. Clin. Endocrinol. Metab.* **88**, 5766–5772 (2003).
507. Alibhai, S. M. H. *et al.* Bone health and bone-targeted therapies for nonmetastatic prostate cancer a systematic review and meta-analysis. *Ann. Intern. Med.* **167**, 341–350 (2017).
508. Myllyharju, J. & Kivirikko, K. I. Collagens and collagen-related diseases. *Annals of Medicine* **33**, 7–21 (2001).
509. Hardy, R. & Cooper, M. S. Bone loss in inflammatory disorders. *Journal of Endocrinology* **201**, 309–320 (2009).
510. Sutter, S. *et al.* Abnormalities in cortical bone, trabecular plates, and stiffness in postmenopausal women treated with glucocorticoids. *J. Clin. Endocrinol. Metab.* **99**, 4231–4240 (2014).
511. Eastell, R. *et al.* Bone turnover markers: Are they clinically useful? *European Journal of Endocrinology* **178**, R19–R31 (2018).
512. Kanis, J. A. *et al.* A meta-analysis of prior corticosteroid use and fracture risk. *J. Bone Miner. Res.* **19**, 893–899 (2004).
513. Kanis, J. A., Johansson, H., Oden, A. & McCloskey, E. V. Guidance for the adjustment of

- FRAX according to the dose of glucocorticoids. *Osteoporos. Int.* **22**, 809–816 (2011).
514. Pack, A. M. Antiepileptic drugs and bone disease. *Clinical Reviews in Bone and Mineral Metabolism* **2**, 159–165 (2004).
515. Lexell, J. Human aging, muscle mass, and fiber type composition. in *Journals of Gerontology - Series A Biological Sciences and Medical Sciences* **50**, 11–16 (Oxford University Press, 1995).
516. Verdijk, L. B. *et al.* Satellite cell content is specifically reduced in type II skeletal muscle fibers in the elderly. *Am. J. Physiol. - Endocrinol. Metab.* **292**, (2007).
517. Clark, B. C. & Manini, T. M. What is dynapenia? *Nutrition* **28**, 495–503 (2012).
518. Malmstrom, T. K., Miller, D. K., Simonsick, E. M., Ferrucci, L. & Morley, J. E. SARC-F: a symptom score to predict persons with sarcopenia at risk for poor functional outcomes. *J. Cachexia. Sarcopenia Muscle* **7**, 28–36 (2016).
519. Cawthon, P. M. *et al.* Frailty in older men: Prevalence, progression, and relationship with mortality. *J. Am. Geriatr. Soc.* **55**, 1216–1223 (2007).
520. Wolfson, L., Judge, J., Whipple, R. & King, M. Strength is a major factor in balance, gait, and the occurrence of falls. in *Journals of Gerontology - Series A Biological Sciences and Medical Sciences* **50**, 64–67 (Oxford University Press, 1995).
521. Visser, M. & Schaap, L. A. Consequences of sarcopenia. *Clinics in Geriatric Medicine* **27**, 387–399 (2011).
522. Gariballa, S. & Alessa, A. Sarcopenia: Prevalence and prognostic significance in hospitalized patients. *Clin. Nutr.* **32**, 772–776 (2013).
523. Borst, S. E. Interventions for sarcopenia and muscle weakness in older people. *Age and Ageing* **33**, 548–555 (2004).
524. Brooks, S. V. & Faulkner, J. A. Skeletal muscle weakness in old age: Underlying mechanisms. *Med. Sci. Sports Exerc.* **26**, 432–439 (1994).
525. Von Haehling, S., Morley, J. E. & Anker, S. D. An overview of sarcopenia: facts and numbers on prevalence and clinical impact. *J. Cachexia. Sarcopenia Muscle* **1**, 129–133 (2010).
526. Rolland, Y., Van Kan, G. A., Gillette-Guyonnet, S. & Vellas, B. Cachexia versus sarcopenia. *Curr. Opin. Clin. Nutr. Metab. Care* **14**, 15–21 (2011).
527. Argilés, J. M., Campos, N., Lopez-Pedrosa, J. M., Rueda, R. & Rodriguez-Mañas, L. Skeletal Muscle Regulates Metabolism via Interorgan Crosstalk: Roles in Health and Disease. *Journal of the American Medical Directors Association* **17**, 789–796 (2016).
528. Prado, C. M. *et al.* Prevalence and clinical implications of sarcopenic obesity in patients with solid tumours of the respiratory and gastrointestinal tracts: a population-based study. *Lancet Oncol.* **9**, 629–635 (2008).
529. Kazemi-Bajestani, S. M. R., Mazurak, V. C. & Baracos, V. Computed tomography-defined muscle and fat wasting are associated with cancer clinical outcomes. *Seminars in Cell and Developmental Biology* **54**, 2–10 (2016).
530. Joglekar, S., Nau, P. N. & Mezhir, J. J. The impact of sarcopenia on survival and complications in surgical oncology: A review of the current literature. *Journal of Surgical Oncology* **112**, 503–509 (2015).
531. Wang, B. *et al.* Cancer-related fatigue and biochemical parameters among cancer patients with different stages of sarcopenia. *Support. Care Cancer* **28**, 581–588 (2020).
532. Wildiers, H. *et al.* International society of geriatric oncology consensus on geriatric assessment in older patients with cancer. *Journal of Clinical Oncology* **32**, 2595–2603 (2014).
533. Cruz-Jentoft, A. J. *et al.* Sarcopenia: European consensus on definition and diagnosis.

Age Ageing **39**, 412–423 (2010).

534. Cruz-Jentoft, A. J. *et al.* Sarcopenia: Revised European consensus on definition and diagnosis. *Age and Ageing* **48**, 16–31 (2019).
535. Muscaritoli, M. *et al.* Consensus definition of sarcopenia, cachexia and pre-cachexia: Joint document elaborated by Special Interest Groups (SIG) ‘cachexia-anorexia in chronic wasting diseases’ and ‘nutrition in geriatrics’. *Clin. Nutr.* **29**, 154–159 (2010).
536. Fielding, R. A. *et al.* Sarcopenia: An Undiagnosed Condition in Older Adults. Current Consensus Definition: Prevalence, Etiology, and Consequences. International Working Group on Sarcopenia. *J. Am. Med. Dir. Assoc.* **12**, 249–256 (2011).
537. Vermeulen, A., Goemaere, S. & Kaufman, J. M. Sex hormones, body composition and aging. *Aging Male* **2**, 8–15 (1999).
538. Szulc, P., Claustrat, B., Marchand, F. & Delmas, P. D. Increased Risk of Falls and Increased Bone Resorption in Elderly Men with Partial Androgen Deficiency: The MINOS Study. *J. Clin. Endocrinol. Metab.* **88**, 5240–5247 (2003).
539. Matsumoto, A. M. Andropause: Clinical implications of the decline in serum testosterone levels with aging in men. *Journals of Gerontology - Series A Biological Sciences and Medical Sciences* **57**, (2002).
540. Minetto, M. A., D’Angelo, V., Arvat, E. & Kesari, S. Diagnostic work-up in steroid myopathy. *Endocrine* **60**, 219–223 (2018).
541. Cheung, A. S. *et al.* Androgen deprivation causes selective deficits in the biomechanical leg muscle function of men during walking: a prospective case-control study. *J. Cachexia. Sarcopenia Muscle* **8**, 102–112 (2017).
542. Ikeda, T. *et al.* Prognostic impact of sarcopenia in patients with metastatic hormone-sensitive prostate cancer. *Jpn. J. Clin. Oncol.* **50**, 933–939 (2020).
543. Ohtaka, A. *et al.* Sarcopenia is a poor prognostic factor of castration-resistant prostate cancer treated with docetaxel therapy. *Prostate Int.* **7**, 9–14 (2019).
544. Stangl-Kremser, J. *et al.* Assessment of body composition in the advanced stage of castration-resistant prostate cancer: special focus on sarcopenia. *Prostate Cancer Prostatic Dis.* **23**, 309–315 (2020).
545. Cushen, S. J. *et al.* Impact of body composition parameters on clinical outcomes in patients with metastatic castrate-resistant prostate cancer treated with docetaxel. *Clin. Nutr. ESPEN* **13**, e39–e45 (2016).
546. Boyle, H. J. *et al.* Updated recommendations of the International Society of Geriatric Oncology on prostate cancer management in older patients. *European Journal of Cancer* **116**, 116–136 (2019).
547. Clegg, A., Young, J., Iliffe, S., Rikkert, M. O. & Rockwood, K. Frailty in elderly people. in *The Lancet* **381**, 752–762 (Elsevier B.V., 2013).
548. Handforth, C. *et al.* The prevalence and outcomes of frailty in older cancer patients: A systematic review. *Ann. Oncol.* **26**, 1091–1101 (2015).
549. Mitnitski, A. B., Mogilner, A. J., MacKnight, C. & Rockwood, K. The accumulation of deficits with age and possible invariants of aging. *ScientificWorldJournal.* **2**, 1816–1822 (2002).
550. Welsh, T. J., Gordon, A. L. & Gladman, J. R. Comprehensive geriatric assessment - A guide for the non-specialist. *International Journal of Clinical Practice* **68**, 290–293 (2014).
551. Repetto, L. *et al.* Comprehensive Geriatric Assessment Adds Information to Eastern Cooperative Oncology Group Performance Status in Elderly Cancer Patients: An Italian Group for Geriatric Oncology Study. *J. Clin. Oncol.* **20**, 494–502 (2002).
552. Mohile, S. G. *et al.* A pilot study of the vulnerable elders survey-13 compared with the

- comprehensive geriatric assessment for identifying disability in older patients with prostate cancer who receive androgen ablation. *Cancer* **109**, 802–810 (2007).
553. Bylow, K. *et al.* Obese frailty, physical performance deficits, and falls in older men with biochemical recurrence of prostate cancer on androgen deprivation therapy: A case-control study. *Urology* **77**, 934–940 (2011).
554. Bylow, K., Mohile, S. G., Stadler, W. M. & Dale, W. Does Androgen-deprivation therapy accelerate the development of frailty in older men with prostate cancer? A conceptual review. *Cancer* **110**, 2604–2613 (2007).
555. Droz, J. P. *et al.* Management of prostate cancer in older patients: Updated recommendations of a working group of the International Society of Geriatric Oncology. *The Lancet Oncology* **15**, (2014).
556. Baird, R. *et al.* An Association of Cancer Physicians' strategy for improving services and outcomes for cancer patients. *Ecancermedicalscience* **10**, (2016).
557. Kalsi, T. *et al.* Are the UK oncology trainees adequately informed about the needs of older people with cancer. *Br. J. Cancer* **108**, 1936–1941 (2013).
558. Macmillan Cancer Support, D. of H. and A. U. Cancer Services Coming of Age: Learning from the Improving Cancer Treatment and Support for Older People Project. p1–44 (2012).
https://www.macmillan.org.uk/documents/aboutus/health_professionals/olderpeople_sproject/cancerservicescomingofage.pdf
559. Macmillan Cancer Support. *Older people living with cancer Designing the future health care workforce*. <https://www.macmillan.org.uk/assets/workforce-report.pdf>. (2014).
560. WHO: Body mass index (BMI). Available at: <https://www.euro.who.int/en/health-topics/disease-prevention/nutrition/a-healthy-lifestyle/body-mass-index-bmi>. (Accessed: 25th January 2021)
561. Duren, D. L. *et al.* Body composition methods: Comparisons and interpretation. *J. Diabetes Sci. Technol.* **2**, 1139–1146 (2008).
562. Chumlea, W. C. & Guo, S. S. Bioelectrical Impedance and Body Composition: Present Status and Future Direction (Nutr Rev 1994;52:123–31). *Nutrition Reviews* **52**, 323–325 (1994).
563. Perera, S. *et al.* Gait Speed Predicts Incident Disability: A Pooled Analysis. *Journals Gerontol. - Ser. A Biol. Sci. Med. Sci.* **71**, 63–71 (2015).
564. Cooper, R., Kuh, D. & Hardy, R. Objectively measured physical capability levels and mortality: Systematic review and meta-analysis. *BMJ (Online)* **341**, 639 (2010).
565. Studenski, S. *et al.* Physical Performance Measures in the Clinical Setting. *J. Am. Geriatr. Soc.* **51**, 314–322 (2003).
566. Langley, F. & Mackintosh, S. Functional Balance Assessment of Older Community Dwelling Adults: A Systematic Review of the Literature. *Internet J. Allied Heal. Sci. Pract.* **5**, (2007).
567. Ferrucci, L. *et al.* Age-related change in mobility: Perspectives from life course epidemiology and geroscience. *Journals of Gerontology - Series A Biological Sciences and Medical Sciences* **71**, 1184–1194 (2016).
568. Bohannon, R. W. Hand-grip dynamometry predicts future outcomes in aging adults. *J. Geriatr. Phys. Ther.* **31**, 3–10 (2008).
569. Syddall, H. E., Martin, H. J., Harwood, R. H., Cooper, C. & Aihie Sayer, A. The SF-36: A simple, effective measure of mobility-disability for epidemiological studies. *J. Nutr. Heal. Aging* **13**, 57–62 (2009).
570. Sayer, A. A. *et al.* Falls, sarcopenia, and growth in early life: Findings from the hertfordshire cohort study. *Am. J. Epidemiol.* **164**, 665–671 (2006).

571. Gale, C. R., Martyn, C. N., Cooper, C. & Sayer, A. A. Grip strength, body composition, and mortality. *Int. J. Epidemiol.* **36**, 228–235 (2007).
572. Rantanen, T. *et al.* Muscle strength and body mass index as long-term predictors of mortality in initially healthy men. *Journals Gerontol. - Ser. A Biol. Sci. Med. Sci.* **55**, (2000).
573. Syddall, H., Cooper, C., Martin, F., Briggs, R. & Sayer, A. A. Is grip strength a useful single marker of frailty? *Age Ageing* **32**, 650–656 (2003).
574. Clinical Assessment Recommendations | American Society of Hand Therapists (ASHT). Available at: <https://www.asht.org/practice/clinical-assessment-recommendations>. (Accessed: 29th January 2021)
575. Mathiowetz, V., Weber, K., Volland, G. & Kashman, N. Reliability and validity of grip and pinch strength evaluations. *J. Hand Surg. Am.* **9**, 222–226 (1984).
576. Peolsson, A., Hedlund, R. & Oberg, B. Intra- and inter-tester reliability and reference values for hand strength. *J. Rehabil. Med.* **33**, 36–41 (2001).
577. Bohannon, R. W. Grip strength: A summary of studies comparing dominant and nondominant limb measurements. *Percept. Mot. Skills* **96**, 728–730 (2003).
578. Mathiowetz, V., Rennells, C. & Donahoe, L. Effect of elbow position on grip and key pinch strength. *J. Hand Surg. Am.* **10**, 694–697 (1985).
579. Richards, L. G., Olson, B. & Palmiter-Thomas, P. How Forearm Position Affects Grip Strength. *Am. J. Occup. Ther.* **50**, 133–138 (1996).
580. Spijkerman, D. C. M., Snijders, C. J., Stijnen, T. & Lankhorst, G. J. Standardization of grip strength measurements. Effects on repeatability and peak force. *Scand. J. Rehabil. Med.* **23**, 203–206 (1991).
581. Jung, M. C. & Hallbeck, M. S. Quantification of the effects of instruction type, verbal encouragement, and visual feedback on static and peak handgrip strength. *Int. J. Ind. Ergon.* **34**, 367–374 (2004).
582. Watanabe, T. *et al.* The short-term reliability of grip strength measurement and the effects of posture and grip span. *J. Hand Surg. Am.* **30**, 603–609 (2005).
583. Jasper, I., Häbussler, A., Baur, B., Marquardt, C. & Hermsdörfer, J. Circadian variations in the kinematics of handwriting and grip strength. *Chronobiol. Int.* **26**, 576–594 (2009).
584. Guralnik, J. M., Ferrucci, L., Simonsick, E. M., Salive, M. E. & Wallace, R. B. Lower-Extremity Function in Persons over the Age of 70 Years as a Predictor of Subsequent Disability. *N. Engl. J. Med.* **332**, 556–562 (1995).
585. Ostir, G. V., Volpato, S., Fried, L. P., Chaves, P. & Guralnik, J. M. Reliability and sensitivity to change assessed for a summary measure of lower body function: Results from the Women's Health and Aging Study. *J. Clin. Epidemiol.* **55**, 916–921 (2002).
586. Studenski, S. *et al.* Physical performance measures in the clinical setting. *J. Am. Geriatr. Soc.* **51**, 314–322 (2003).
587. Buatois, S. *et al.* A Simple Clinical Scale to Stratify Risk of Recurrent Falls in Community-Dwelling Adults Aged 65 Years and Older. *Phys. Ther.* **90**, 550–560 (2010).
588. Blazer, D. G. A Short Physical Performance Battery Assessing Lower Extremity Function: Association With Self-Reported Disability and Prediction of Mortality and Nursing Home Admission. *Artic. J. Gerontol.* **M85**. (1994).
589. Guralnik, J. M. *et al.* A short physical performance battery assessing lower extremity function: Association with self-reported disability and prediction of mortality and nursing home admission. *Journals Gerontol.* **49**, 85-94. (1994).
590. Perera, S., Mody, S. H., Woodman, R. C. & Studenski, S. A. Meaningful change and responsiveness in common physical performance measures in older adults. *J. Am. Geriatr. Soc.* **54**, 743–749 (2006).

591. Bylow, K. *et al.* Falls and Physical Performance Deficits in Older Patients With Prostate Cancer Undergoing Androgen Deprivation Therapy. *Urology* **72**, 422–427 (2008).
592. Clay, C. A. *et al.* Physical Function in Men With Prostate Cancer on Androgen Deprivation Therapy. *Phys. Ther.* **87**, 1325–1333 (2007).
593. Gewandter, J. S. *et al.* Associations between a patient-reported outcome (PRO) measure of sarcopenia and falls, functional status, and physical performance in older patients with cancer. *J. Geriatr. Oncol.* **6**, 433–441 (2015).
594. Stone KL, Seeley DG, Lui L-Y, *et al.* BMD at multiple sites and risk of fracture of multiple types: long-term results from the Study of Osteoporotic Fractures. *J. bone Miner. Res.* **18**, 1947–1954 (2003).
595. Marshall D, Johnell O, W. H. Meta-analysis of how well measures of bone mineral density predict occurrence of osteoporotic fractures. *BMJ* **312**, 1254–1259 (1996).
596. Gluer CC. Monitoring skeletal change by radiological techniques. *J. bone Miner. Res.* **14**, 1952–1962 (1999).
597. Blake, G. M. & Fogelman, I. The role of DXA bone density scans in the diagnosis and treatment of osteoporosis. *Postgrad. Med. J.* **83**, 509–17 (2007).
598. Shepherd, J. A., Baim, S., Bilezikian, J. P. & Schousboe, J. T. Executive Summary of the 2013 International Society for Clinical Densitometry Position Development Conference on Body Composition. *J. Clin. Densitom.* **16**, 489–495 (2013).
599. Broy, S. B. *et al.* Fracture Risk Prediction by Non-BMD DXA Measures: The 2015 ISCD Official Positions Part 1: Hip Geometry. *J. Clin. Densitom.* **18**, 287–308 (2015).
600. Silva, B. C. *et al.* Fracture Risk Prediction by Non-BMD DXA Measures: The 2015 ISCD Official Positions Part 2: Trabecular Bone Score. *J. Clin. Densitom.* **18**, 309–330 (2015).
601. Kelly, T. L., Berger, N. & Richardson, T. L. DXA body composition: Theory and practice. in *Applied Radiation and Isotopes* **49**, 511–513 (Elsevier Sci Ltd, 1998).
602. Laskey, M. A. Dual-energy X-ray absorptiometry and body composition. *Nutrition* **12**, 45–51 (1996).
603. Genant, H. K. *et al.* Noninvasive assessment of bone mineral and structure: State of the art. *J. Bone Miner. Res.* **11**, 707–730 (2009).
604. Blake, G. M., Griffith, J. F., Yeung, D. K. W., Leung, P. C. & Fogelman, I. Effect of increasing vertebral marrow fat content on BMD measurement, T-Score status and fracture risk prediction by DXA. *Bone* **44**, 495–501 (2009).
605. Bolotin, H. H., Sievänen, H. & Grashuis, J. L. Patient-Specific DXA Bone Mineral Density Inaccuracies: Quantitative Effects of Nonuniform Extraosseous Fat Distributions. *J. Bone Miner. Res.* **18**, 1020–1027 (2003).
606. Research, I. of M. (US) C. on M. N., Carlson-Newberry, S. J. & Costello, R. B. Dual-Energy X-Ray Absorptiometry: Research Issues and Equipment. (1997).
607. Beck, T. Measuring the structural strength of bones with dual-energy X-ray absorptiometry: principles, technical limitations, and future possibilities. *Osteoporosis international.* **14 Suppl 5**, (2003).
608. Yu, E. W., Thomas, B. J., Brown, J. K. & Finkelstein, J. S. Simulated increases in body fat and errors in bone mineral density measurements by DXA and QCT. *J. Bone Miner. Res.* **27**, 119–124 (2012).
609. Zmuda JM, Cauley JA, Glynn NY, F. J. Posterior and lateral dual-energy X-ray absorptiometry for the assessment of vertebral osteoporosis and bone loss among older men. *J. Bone Miner. Res.* **15**, 1417–1424 (2000).
610. Melton LJ III, Atkinson EJ, O'Connor MK, *et al.* Bone density and fracture risk in men. *J. bone Miner. Res.* **13**, 1915–1923 (1998).

611. Wong, A. K. O. A comparison of peripheral imaging technologies for bone and muscle quantification: A technical review of image acquisition. *Journal of Musculoskeletal Neuronal Interactions* **16**, 265–282 (2016).
612. Kalender WA. X-ray computed tomography. *Phys. Med. Biol.* **51**, R29–R43 (2006).
613. Krug R, Burghardt AJ, Majumdar S, L. T. High-resolution imaging techniques for the assessment of osteoporosis. *Radiol. Clin. North Am.* **48**, 601–621 (2010).
614. Burghardt AJ, Link TM, M. S. High-resolution computed tomography for clinical imaging of bone microarchitecture. *Clin. Orthop. Relat. Res.* **469**, 2179–2193 (2011).
615. Boutroy S, Bouxsein ML, Munoz F, D. P. In vivo assessment of trabecular bone microarchitecture by high-resolution peripheral quantitative computed tomography. *J. Clin. Endocrinol. Metab.* **90**, 6508–6515 (2005).
616. Laib A, Hauselmann HJ, R. P. In vivo high resolution 3DQCT of the human forearm. *Technol. Heal. care* **6**, 329–337 (1998).
617. Tjong W, Kazakia GJ, Burghardt AJ, M. S. The effect of voxel size on high-resolution peripheral computed tomography measurements of trabecular and cortical bone microstructure. *Med. Phys.* **39**, 1893–903 (2012).
618. Nishiyama KK, Macdonald HM, Buie HR, et al. Postmenopausal women with osteopenia have higher cortical porosity and thinner cortices at the distal radius and tibia than women with normal aBMD: an in vivo HR-pQCT study. *J. bone Miner. Res.* **25**, 882–890 (2010).
619. MacNeil JA, B. S. Accuracy of high-resolution peripheral quantitative computed tomography for measurement of bone quality. *Med. Eng. Phys.* **29**, 1096–1105 (2007).
620. MacNeil JA, B. S. Improved reproducibility of high-resolution peripheral quantitative computed tomography for measurement of bone quality. *Med. Eng. Phys.* **30**, 792–799 (2008).
621. Sekhon K, Kazakia GJ, Burghardt AJ, et al. Accuracy of volumetric bone mineral density measurement in high-resolution peripheral quantitative computed tomography. *Bone* **45**, 473–479 (2009).
622. Cheung, A. M. et al. High-resolution peripheral quantitative computed tomography for the assessment of bone strength and structure: A review by the canadian bone strength working group. *Curr. Osteoporos. Rep.* **11**, 136–146 (2013).
623. Graeff, C. et al. Monitoring Teriparatide-Associated Changes in Vertebral Microstructure by High-Resolution CT In Vivo: Results From the EUROFOR Study. *J. Bone Miner. Res.* **22**, 1426–1433 (2007).
624. Parashar, S. K. & Sharma, J. K. A review on application of finite element modelling in bone biomechanics. *Perspect. Sci.* **8**, 696–698 (2016).
625. Huiskes, R. & Chao, E. Y. S. A survey of finite element analysis in orthopedic biomechanics: The first decade. *J. Biomech.* **16**, 385–409 (1983).
626. Burr, D. B. The use of finite element analysis to estimate the changing strength of bone following treatment for osteoporosis. *Osteoporos. Int.* **27**, 2651–2654 (2016).
627. Ruffoni, D. & Van Lenthe, G. H. 3.10 Finite element analysis in bone research: A computational method relating structure to mechanical function. *Compr. Biomater. II* **169** (2017).
628. Morgan, E. F. & Keaveny, T. M. Dependence of yield strain of human trabecular bone on anatomic site. *J. Biomech.* **34**, 569–577 (2001).
629. Bevill, G. & Keaveny, T. M. Trabecular bone strength predictions using finite element analysis of micro-scale images at limited spatial resolution. *Bone* **44**, 579–584 (2009).
630. MacNeil, J. A. & Boyd, S. K. Bone strength at the distal radius can be estimated from high-resolution peripheral quantitative computed tomography and the finite element

- method. *Bone* **42**, 1203–1213 (2008).
631. van Rietbergen, B., Weinans, H., Huiskes, R. & Odgaard, A. A new method to determine trabecular bone elastic properties and loading using micromechanical finite-element models. *J. Biomech.* **28**, 69–81 (1995).
632. Van Rietbergen, B. Micro-FE analyses of bone: State of the art. in *Advances in Experimental Medicine and Biology* **496**, 21–30 (Kluwer Academic/Plenum Publishers, 2001).
633. Frey, P., Sarter, B. & Gautherie, M. Fully automatic mesh generation for 3-D domains based upon voxel sets. *Int. J. Numer. Methods Eng.* **37**, 2735–2753 (1994).
634. Cheung, A. S. *et al.* Differing Effects of Zoledronic Acid on Bone Microarchitecture and Bone Mineral Density in Men Receiving Androgen Deprivation Therapy: A Randomized Controlled Trial. *J. Bone Miner. Res.* **35**, 1871–1880 (2020).
635. Aggarwal, R. R. *et al.* High-resolution peripheral quantitative computed tomography (HR-pQCT) to detect compartmental bone loss on androgen deprivation therapy (ADT): A feasibility study. *J. Clin. Oncol.* **35**, 209–209 (2017).
636. Piot, A., Chapurlat, R. D., Claustrat, B. & Szulc, P. Relationship Between Sex Steroids and Deterioration of Bone Microarchitecture in Older Men: The Prospective STRAMBO Study. *J. Bone Miner. Res.* **34**, 1562–1573 (2019).
637. Royal Osteoporosis Society. *Reporting dual energy X-ray absorptiometry scans in adult fracture risk assessment: Standards for quality*, 2019. <https://theros.org.uk/media/xhfhyy52/ros-reporting-dxa-scans-in-adult-fracture-risk-assessment-august-2019.pdf>
638. Leib, E. S., Lenchik, L., Bilezikian, J. P., Maricic, M. J. & Watts, N. B. Position statements of the International Society for Clinical Densitometry: Methodology. in *Journal of Clinical Densitometry* **5**, (Humana Press, 2002).
639. Engelke, K. *et al.* Short-term in vivo precision of BMD and parameters of trabecular architecture at the distal forearm and tibia. *Osteoporos. Int.* **23**, 2151–2158 (2012).
640. Whittier, D. E. *et al.* Guidelines for the assessment of bone density and microarchitecture in vivo using high-resolution peripheral quantitative computed tomography. *Osteoporos. Int.* **31**, 1607–1627 (2020).
641. Meehan, M. & Penckofer, S. The Role of Vitamin D in the Aging Adult. *J. Aging Gerontol.* **2**, 60–71 (2014).
642. Weaver, C. M. *et al.* Calcium plus vitamin D supplementation and risk of fractures: an updated meta-analysis from the National Osteoporosis Foundation. *Osteoporos Int* **27**, 367–376 (2016).
643. Yao, P. *et al.* Vitamin D and Calcium for the Prevention of Fracture: A Systematic Review and Meta-analysis. *JAMA network open* **2**, e1917789 (2019).
644. Owen, P. J., Daly, R. M., Livingston, P. M. & Fraser, S. F. Lifestyle guidelines for managing adverse effects on bone health and body composition in men treated with androgen deprivation therapy for prostate cancer: An update. *Prostate Cancer and Prostatic Diseases* **20**, 137–145 (2017).
645. Grossmann, M. *et al.* Bone and metabolic health in patients with non-metastatic prostate cancer who are receiving androgen deprivation therapy. *Med. J. Aust.* **194**, 301–306 (2011).
646. Nguyen PL, Alibhai SM, Basaria S, D'Amico AV, Kantoff PW, Keating NL, Penson DF, Rosario DJ, Tombal B, Smith MR. Adverse effects of androgen deprivation therapy and strategies to mitigate them. *Eur Urol.* **67**:825-36 (2015)
647. Marshall, D. T. *et al.* Vitamin D3 supplementation at 4000 international units per day for one year results in a decrease of positive cores at repeat biopsy in subjects with

- low-risk prostate cancer under active surveillance. *J. Clin. Endocrinol. Metab.* **97**, 2315–2324 (2012).
648. Kanis, J. A., Johnell, O., Oden, A., Johansson, H. & McCloskey, E. FRAX™ and the assessment of fracture probability in men and women from the UK. *Osteoporos. Int.* **19**, 385 (2008).
649. Ettinger, B. *et al.* Performance of FRAX in a Cohort of Community Dwelling, Ambulatory Older Men: The Osteoporotic Fractures in Men (MrOS) Study. *Osteoporos. Int.* **24**, 1185 (2013).
650. Kanis, J. A. *et al.* FRAX and fracture prediction without bone mineral density. <https://doi.org/10.3109/13697137.2015.1092342> **18**, 2–9 (2015).
651. Moe, E. L. *et al.* Falls and frailty in prostate cancer survivors on androgen deprivation therapy. *J. Clin. Oncol.* **34**, 134–134 (2016).
652. Winters-Stone, K. M. *et al.* Falls and Frailty in Prostate Cancer Survivors: Current, Past, and Never Users of Androgen Deprivation Therapy. *J. Am. Geriatr. Soc.* **65**, 1414–1419 (2017).
653. Cheung, A. S. *et al.* Relationships between insulin resistance and frailty with body composition and testosterone in men undergoing androgen deprivation therapy for prostate cancer. *Eur. J. Endocrinol.* **175**, 229–237 (2016).
654. Boyle, H. J. *et al.* Updated recommendations of the International Society of Geriatric Oncology on prostate cancer management in older patients. *European Journal of Cancer* **116**, 116–136 (2019).
655. Soyupek, F., Soyupek, S., Perk, H. & Özorak, A. Androgen deprivation therapy for prostate cancer: Effects on hand function. *Urol. Oncol. Semin. Orig. Investig.* **26**, 141–146 (2008).
656. Gonzalez, B. D. *et al.* Changes in physical functioning and muscle strength in men receiving androgen deprivation therapy for prostate cancer: a controlled comparison. *Support. Care Cancer* **24**, 2201–2207 (2016).
657. Newton, R. U. *et al.* Timing of exercise for muscle strength and physical function in men initiating ADT for prostate cancer. *Prostate Cancer Prostatic Dis.* **23**, 457–464 (2020).
658. Bylow, K. *et al.* Falls and Physical Performance Deficits in Older Patients With Prostate Cancer Undergoing Androgen Deprivation Therapy NIH Public Access. *Urology* **72**, 422–427 (2008).
659. Puthoff, M. L. Outcome measures in cardiopulmonary physical therapy: short physical performance battery. *Cardiopulm. Phys. Ther. J.* **19**, 17–22 (2008).
660. Guralnik, J. M. *et al.* A short physical performance battery assessing lower extremity function: Association with self-reported disability and prediction of mortality and nursing home admission. *Journals Gerontol.* **49**, (1994).
661. Sayers, S. P., Guralnik, J. M., Newman, A. B., Brach, J. S. & Fielding, R. A. Concordance and discordance between two measures of lower extremity function: 400 meter self-paced walk and SPPB. *Aging Clin. Exp. Res.* **18**, 100–106 (2006).
662. Golan, R., Scovell, J. M. & Ramasamy, R. Age-related testosterone decline is due to waning of both testicular and hypothalamic-pituitary function. *Aging Male* **18**, 201–204 (2015).
663. Araujo, A. B. & Wittert, G. A. Endocrinology of the aging male. *Best Practice and Research: Clinical Endocrinology and Metabolism* **25**, 303–319 (2011).
664. Couillard, C. *et al.* Contribution of Body Fatness and Adipose Tissue Distribution to the Age Variation in Plasma Steroid Hormone Concentrations in Men: The HERITAGE Family Study*. *J. Clin. Endocrinol. Metab.* **85**, 1026–1031 (2000).
665. Atkins, J. L. & Wannamathee, S. G. Sarcopenic obesity in ageing: Cardiovascular

- outcomes and mortality. *Br. J. Nutr.* **124**, 1102–1113 (2020).
666. Addison, O., Marcus, R. L., Lastayo, P. C. & Ryan, A. S. Intermuscular fat: A review of the consequences and causes. *International Journal of Endocrinology* **2014**, (2014).
667. Argilés, J. M., Busquets, S., Stemmler, B. & López-Soriano, F. J. Cachexia and sarcopenia: Mechanisms and potential targets for intervention. *Current Opinion in Pharmacology* **22**, 100–106 (2015).
668. Hamilton, E. J. *et al.* Increase in visceral and subcutaneous abdominal fat in men with prostate cancer treated with androgen deprivation therapy. *Clin. Endocrinol. (Oxf)*. **74**, 377–383 (2011).
669. Morote, Juan, *et al.* . The metabolic syndrome and its components in patients with prostate cancer on androgen deprivation therapy. *J. Urol.* **93**, 1963–1969 (2015).
670. Mårin P, Odén B, Björntorp P. Assimilation and mobilization of triglycerides in subcutaneous abdominal and femoral adipose tissue in vivo in men: Effects of androgens. *J. Clin. Endocrinol. Metab.* **80**, 239–243 (1995).
671. Fui, M. N. T., Dupuis, P. & Grossmann, M. Lowered testosterone in male obesity: Mechanisms, morbidity and management. *Asian Journal of Andrology* **16**, 223–231 (2014).
672. Kaufman, J. M. & Vermeulen, A. The decline of androgen levels in elderly men and its clinical and therapeutic implications. *Endocrine Reviews* **26**, 833–876 (2005).
673. Lee, C. M. Y., Huxley, R. R., Wildman, R. P. & Woodward, M. Indices of abdominal obesity are better discriminators of cardiovascular risk factors than BMI: a meta-analysis. *Journal of Clinical Epidemiology* **61**, 646–653 (2008).
674. Foulkes, S. J., Daly, R. M. & Fraser, S. F. The clinical importance of quantifying body fat distribution during androgen deprivation therapy for prostate cancer. *Endocrine-Related Cancer* **24**, R35–R48 (2017).
675. Cheung, A. S. *et al.* Cardiovascular risk and bone loss in men undergoing androgen deprivation therapy for non-metastatic prostate cancer: Implementation of standardized management guidelines. *Andrology* **1**, 583–589 (2013).
676. Buttigliero, C. *et al.* The fat body mass increase after adjuvant androgen deprivation therapy is predictive of prostate cancer outcome. *Endocrine* **50**, 223–230 (2015).
677. Efstathiou, J. A. *et al.* Obesity and mortality in men with locally advanced prostate cancer: Analysis of RTOG 85-31. *Cancer* **110**, 2691–2699 (2007).
678. Cao, Y. & Ma, J. Body mass index, prostate cancer-specific mortality, and biochemical recurrence: A systematic review and meta-analysis. *Cancer Prevention Research* **4**, 486–501 (2011).
679. Schakman, O., Gilson, H., Kalista, S. & Thissen, J. P. Mechanisms of muscle atrophy induced by glucocorticoids. *Horm. Res.* **72**, 36–41 (2009).
680. Hamilton, E. J. *et al.* Structural decay of bone microarchitecture in men with prostate cancer treated with androgen deprivation therapy. *J. Clin. Endocrinol. Metab.* **95**, E456–63 (2010).
681. Berruti, A. *et al.* Changes in bone mineral density, lean body mass and fat content as measured by dual energy x-ray absorptiometry in patients with prostate cancer without apparent bone metastases given androgen deprivation therapy. *J. Urol.* **167**, 2361–2367 (2002).
682. Hughes, V. A. *et al.* Longitudinal muscle strength changes in older adults: Influence of muscle mass, physical activity, and health. *Journals Gerontol. - Ser. A Biol. Sci. Med. Sci.* **56**, (2001).
683. Palumbo, C. *et al.* Changes in body composition and lipid profile in prostate cancer patients without bone metastases given Degarelix treatment: the BLADE prospective

- cohort study. *Prostate Cancer Prostatic Dis.* 1–8 (2021).
684. Cormie, P. *et al.* Can supervised exercise prevent treatment toxicity in patients with prostate cancer initiating androgen-deprivation therapy: A randomised controlled trial. *BJU Int.* **115**, 256–266 (2015).
685. Saylor, P. J., Keating, N. L. & Smith, M. R. Prostate cancer survivorship: Prevention and treatment of the adverse effects of androgen deprivation therapy. *Journal of General Internal Medicine* **24**, 389 (2009).
686. Peterson, M. D., Sen, A. & Gordon, P. M. Influence of resistance exercise on lean body mass in aging adults: A meta-analysis. *Med. Sci. Sports Exerc.* **43**, 249–258 (2011).
687. Alberga, A. S. *et al.* Age and androgen-deprivation therapy on exercise outcomes in men with prostate cancer. *Support. Care Cancer* **20**, 971–981 (2012).
688. Nilsen, T. S. *et al.* Effects of strength training on body composition, physical functioning, and quality of life in prostate cancer patients during androgen deprivation therapy. *Acta Oncol. (Madr).* **54**, 1805–1813 (2015).
689. Nilsen, T. S. *et al.* Effects of strength training on muscle cellular outcomes in prostate cancer patients on androgen deprivation therapy. *Scand. J. Med. Sci. Sports* **26**, 1026–1035 (2016).
690. Winters-Stone, K. M. *et al.* Resistance exercise reduces body fat and insulin during androgen-deprivation therapy for prostate cancer. *Oncol. Nurs. Forum* **42**, 348–356 (2015).
691. Taaffe, D. R. *et al.* Effects of Different Exercise Modalities on Fatigue in Prostate Cancer Patients Undergoing Androgen Deprivation Therapy: A Year-long Randomised Controlled Trial. *Eur. Urol.* **72**, 293–299 (2017).
692. Bourke, L. *et al.* Lifestyle changes for improving disease-specific quality of life in sedentary men on long-term androgen-deprivation therapy for advanced prostate cancer: A randomised controlled trial. *Eur. Urol.* **65**, 865–872 (2014).
693. Alibhai, S. M. H. *et al.* Protocol for a phase III RCT and economic analysis of two exercise delivery methods in men with PC on ADT 11 Medical and Health Sciences 1117 Public Health and Health Services. *BMC Cancer* **18**, 1–18 (2018).
694. Smith, M. R., Fallon, M. A. & Goode, M. J. Cross-sectional study of bone turnover during bicalutamide monotherapy for prostate cancer. *Urology* **61**, 127–131 (2003).
695. García-Fontana, B. *et al.* Sclerostin serum levels in prostate cancer patients and their relationship with sex steroids. *Osteoporos. Int.* **25**, 645–651 (2014).
696. Mittan, D. *et al.* Bone loss following hypogonadism in men with prostate cancer treated with GnRH analogs. *J. Clin. Endocrinol. Metab.* **87**, 3656–3661 (2002).
697. Khosla, S., Melton, L. J. & Riggs, B. L. Estrogen and the Male Skeleton. *J. Clin. Endocrinol. Metab.* **87**, 1443–1450 (2002).
698. Carani, C. *et al.* Effect of Testosterone and Estradiol in a Man with Aromatase Deficiency. *N. Engl. J. Med.* **337**, 91–95 (1997).
699. Taxel, P. *et al.* The effect of micronized estradiol on bone turnover and calciotropic hormones in older men receiving hormonal suppression therapy for prostate cancer. *J. Clin. Endocrinol. Metab.* **87**, 4907–4913 (2002).
700. Tannock, I. F. *et al.* Docetaxel plus Prednisone or Mitoxantrone plus Prednisone for Advanced Prostate Cancer. *N. Engl. J. Med.* **351**, 1502–1512 (2004).
701. Vale, C. L. *et al.* Addition of docetaxel or bisphosphonates to standard of care in men with localised or metastatic, hormone-sensitive prostate cancer: A systematic review and meta-analyses of aggregate data. *Lancet Oncol.* **17**, 243–256 (2016).
702. James, N. D. *et al.* Addition of docetaxel, zoledronic acid, or both to first-line long-term hormone therapy in prostate cancer (STAMPEDE): Survival results from an adaptive,

- multiarm, multistage, platform randomised controlled trial. *Lancet* **387**, 1163–1177 (2016).
703. Ekenstam, E., Stålenheim, G. & Hällgren, R. The acute effect of high dose corticosteroid treatment on serum osteocalcin. *Metabolism* **37**, 141–144 (1988).
704. Reid, I. R. *et al.* Low Serum Osteocalcin Levels in Glucocorticoid-Treated Asthmatics. *J. Clin. Endocrinol. Metab.* **62**, 379–383 (1986).
705. Leclerc, N., Noh, T., Khokhar, A., Smith, E. & Frenkel, B. Glucocorticoids inhibit osteocalcin transcription in osteoblasts by suppressing Egr2/Krox20-binding enhancer. *Arthritis Rheum.* **52**, 929–939 (2005).
706. Heinrichs, A. A. J. *et al.* Identification of Multiple Glucocorticoid Receptor Binding Sites in the Rat Osteocalcin Gene Promoter. *Biochemistry* **32**, 11436–11444 (1993).
707. Strömstedt, P. E., Poellinger, L., Gustafsson, J. A. & Carlstedt-Duke, J. The glucocorticoid receptor binds to a sequence overlapping the TATA box of the human osteocalcin promoter: a potential mechanism for negative regulation. *Mol. Cell. Biol.* **11**, 3379–3383 (1991).
708. Varsavsky, M. *et al.* Bone turnover markers in patients with prostate carcinoma: Influence of sex steroids levels. *J. Bone Miner. Metab.* **32**, 65–70 (2014).
709. Miyazawa, Y. *et al.* Evaluation of Bone Turnover / Quality Markers and Bone Mineral Density in Prostate Cancer Patients Receiving Androgen Deprivation Therapy with or without Denosumab. (2017). doi:10.21873/anticancerres.11737
710. Mödder, U. I. *et al.* Relation of age, gender, and bone mass to circulating sclerostin levels in women and men. *J. Bone Miner. Res.* **26**, 373–379 (2011).
711. Polyzos, S. A. *et al.* Serum sclerostin levels positively correlate with lumbar spinal bone mineral density in postmenopausal women-the six-month effect of risedronate and teriparatide. *Osteoporos. Int.* **23**, 1171–1176 (2012).
712. Arasu, A. *et al.* Serum sclerostin and risk of hip fracture in older caucasian women. *J. Clin. Endocrinol. Metab.* **97**, 2027–2032 (2012).
713. Szulc, P., Bertholon, C., Borel, O., Marchand, F. & Chapurlat, R. Lower fracture risk in older men with higher sclerostin concentration: A prospective analysis from the MINOS study. *J. Bone Miner. Res.* **28**, 855–864 (2013).
714. Mödder, U. II *et al.* Regulation of circulating sclerostin levels by sex steroids in women and in men. *J. Bone Miner. Res.* **26**, 27–34 (2011).
715. Galea, G. L. *et al.* Sost down-regulation by mechanical strain in human osteoblastic cells involves PGE2 signaling via EP4. *FEBS Lett.* **585**, 2450–2454 (2011).
716. Sapir-Koren, R. & Livshits, G. Is interaction between age-dependent decline in mechanical stimulation and osteocyte-estrogen receptor levels the culprit for postmenopausal-impaired bone formation? *Osteoporosis International* **24**, 1771–1789 (2013).
717. Hudson, B. D. *et al.* SOST inhibits prostate cancer invasion. *PLoS One* **10**, (2015).
718. Sebastian, A., Hum, N., Hudson, B. & Loots, G. Cancer–Osteoblast Interaction Reduces Sost Expression in Osteoblasts and Up-Regulates lncRNA MALAT1 in Prostate Cancer. *Microarrays* **4**, 503–519 (2015).
719. Mcdonald, M. M. & Delgado-Calle, J. Sclerostin: an emerging target for the treatment of cancer-induced bone disease. *Curr Osteoporos Rep.* **15**(6) (2017)
720. Yavropoulou, M. P., van Lierop, A. H., Hamdy, N. A. T., Rizzoli, R. & Papapoulos, S. E. Serum sclerostin levels in Paget’s disease and prostate cancer with bone metastases with a wide range of bone turnover. *Bone* **51**, 153–157 (2012).
721. Dai, J. *et al.* Bone morphogenetic protein-6 promotes osteoblastic prostate cancer bone metastases through a dual mechanism. *Cancer Res.* **65**, 8274–8285 (2005).

722. Cai, J. *et al.* MicroRNA-374a activates Wnt/ β -catenin signaling to promote breast cancer metastasis. *J. Clin. Invest.* **123**, 566–579 (2013).
723. Zhan, T., Rindtorff, N. & Boutros, M. Wnt signaling in cancer. *Oncogene* **36**, 1461–1473 (2017).
724. Appelman-Dijkstra, N. M. & Papapoulos, S. E. Sclerostin Inhibition in the Management of Osteoporosis. *Calcified Tissue International* **98**, 370–380 (2016).
725. Delgado-Calle, J. *et al.* Genetic deletion of Sost or pharmacological inhibition of sclerostin prevent multiple myeloma-induced bone disease without affecting tumor growth. *Leukemia* **31**, 2686–2694 (2017).
726. Eda, H. *et al.* Regulation of Sclerostin Expression in Multiple Myeloma by Dkk-1: A Potential Therapeutic Strategy for Myeloma Bone Disease. *J. Bone Miner. Res.* **31**, 1225–1234 (2016).
727. Zhu, M. *et al.* Sclerostin induced tumor growth, bone metastasis and osteolysis in breast cancer. *Sci. Rep.* **7**, (2017).
728. Sato, A. Y. *et al.* Protection From Glucocorticoid-Induced Osteoporosis by Anti-Catabolic Signaling in the Absence of Sost/Sclerostin. *J. Bone Miner. Res.* **31**, 1791–1802 (2016).
729. O'Brien, C. A. *et al.* Glucocorticoids act directly on osteoblasts and osteocytes to induce their apoptosis and reduce bone formation and strength. *Endocrinology* **145**, 1835–1841 (2004).
730. Gifre, L. *et al.* Effect of glucocorticoid treatment on Wnt signalling antagonists (sclerostin and Dkk-1) and their relationship with bone turnover. *Bone* **57**, 272–276 (2013).
731. Brabnikova Maresova, K., Pavelka, K. & Stepan, J. J. Acute effects of glucocorticoids on serum markers of osteoclasts, osteoblasts, and osteocytes. *Calcif. Tissue Int.* **92**, 354–361 (2013).
732. Van Lierop, A. H. *et al.* Circulating sclerostin levels are decreased in patients with endogenous hypercortisolism and increase after treatment. *J. Clin. Endocrinol. Metab.* **97**, (2012).
733. Jacobsson, M., van Raalte, D. H., Heijboer, A. C., den Heijer, M. & de Jongh, R. T. Short-Term Glucocorticoid Treatment Reduces Circulating Sclerostin Concentrations in Healthy Young Men: A Randomized, Placebo-Controlled, Double-Blind Study. *JBMR Plus* **4**, e10341 (2020).
734. Nadler, M. *et al.* Osteoporosis knowledge, health beliefs, and healthy bone behaviours in patients on androgen-deprivation therapy (ADT) for prostate cancer. *BJU Int.* **111**, 1301–1309 (2013).
735. Lassemlante, A. C. M., Skinner, T. L., Hooper, J. D., Prins, J. B. & Wright, O. R. L. Osteoporosis-Related Health Behaviors in Men With Prostate Cancer and Survivors: Exploring Osteoporosis Knowledge, Health Beliefs, and Self-Efficacy. *Am. J. Mens. Health* **11**, 13–23 (2017).
736. Hu, J., Aprikian, A. G., Vanhuyse, M. & Dragomir, A. Contemporary population-based analysis of bone mineral density testing in men initiating androgen deprivation therapy for prostate cancer. *JNCCN J. Natl. Compr. Cancer Netw.* **18**, 1374–1381 (2020).
737. Ito, K., Elkin, E. B., Girotra, M. & Morris, M. J. Cost-effectiveness of fracture prevention in men who receive androgen deprivation therapy for localized prostate cancer. *Ann. Intern. Med.* **152**, 621–629 (2010).
738. Cianferotti, L. *et al.* The prevention of fragility fractures in patients with non-metastatic prostate cancer: A position statement by the international osteoporosis foundation. *Oncotarget* **8**, 75646–75663 (2017).

739. Reid DM *et al.* Guidance for the management of breast cancer treatment-induced bone loss: a consensus position statement from a UK Expert Group. *Cancer Treat. Rev.* **34 Suppl 1**, (2008).
740. Hadji, P. *et al.* Management of Aromatase Inhibitor-Associated Bone Loss (AIBL) in postmenopausal women with hormone sensitive breast cancer: Joint position statement of the IOF, CABS, ECTS, IEG, ESCEO, IMS, and SIOG. *J. Bone Oncol.* **7**, 1 (2017).
741. Early and locally advanced breast cancer: diagnosis and management NICE guideline. (2018). <https://www.nice.org.uk/guidance/ng101>
742. Hussain, S. A., Weston, R., Stephenson, R. N., George, E. & Parr, N. J. Immediate dual energy X-ray absorptiometry reveals a high incidence of osteoporosis in patients with advanced prostate cancer before hormonal manipulation. *BJU Int.* **92**, 690–694 (2003).
743. Ziaran, S., Goncalves, F. M. & Sn, J. B. Complex metabolic and skeletal changes in men taking long-term androgen deprivation therapy. *Clin. Genitourin. Cancer* **11**, 33–38 (2013).
744. Smith MR, McGovern FJ, Fallon MA, Schoenfeld D, Kantoff PW, Finkelstein JS. Low bone mineral density in hormone-naïve men with prostate carcinoma. *Cancer.* **91**, 2238-45 (2001)
745. Snyder, P. J. *et al.* Effect of Testosterone Treatment on Volumetric Bone Density and Strength in Older Men With Low Testosterone: A Controlled Clinical Trial. *JAMA Intern. Med.* **177**, 471–479 (2017).
746. Evan YY *et al.* Long-term dynamics of bone mineral density during intermittent androgen deprivation for men with nonmetastatic, hormone-sensitive prostate cancer. *J. Clin. Oncol.* **30**, 1864–1870 (2012).
747. Spry, N. A. *et al.* Long-term effects of intermittent androgen suppression therapy on lean and fat mass: a 33-month prospective study. *Prostate Cancer Prostatic Dis.* **2013** *161* **16**, 67–72 (2012).
748. Ilias, I., Zoumakis, E. & Ghayee, H. An Overview of Glucocorticoid Induced Osteoporosis. *J. Clin. Rheumatol.* **5**, (2018).
749. DW, D. Bone histomorphometry in glucocorticoid-induced osteoporosis. *J. Bone Miner. Res.* **4**, 137–141 (1989).
750. Paggiosi MA, Peel NF, Eastell R. The impact of glucocorticoid therapy on trabecular bone score in older women. *Osteoporos Int.* **26**(6):1773-80 (2015)
751. KG, S. *et al.* Trabecular Bone Score in Patients With Chronic Glucocorticoid Therapy-Induced Osteoporosis Treated With Alendronate or Teriparatide. *Arthritis Rheumatol.* **68**, 2122–2128 (2016).
752. Sode, M., Burghardt, A. J., Pialat, J.-B., Link, T. M. & Majumdar, S. Quantitative characterization of subject motion in HR-pQCT images of the distal radius and tibia. *Bone* **48**, 1291 (2011).
753. Kawano, H. *et al.* Suppressive function of androgen receptor in bone resorption. *Proc. Natl. Acad. Sci.* **100**, 9416–9421 (2003).
754. D, V. *et al.* Bone and mineral metabolism in aged male rats: short and long term effects of androgen deficiency. *Endocrinology* **130**, 2906–2916 (1992).
755. Benito, M. *et al.* Deterioration of Trabecular Architecture in Hypogonadal Men. *J. Clin. Endocrinol. Metab.* **88**, 1497–1502 (2003).
756. L, D. C. *et al.* Comparison of trabecular bone microarchitecture and remodeling in glucocorticoid-induced and postmenopausal osteoporosis. *J. Bone Miner. Res.* **16**, 97–103 (2001).
757. Kontulainen, S. A. *et al.* Strength indices from pQCT imaging predict up to 85% of

- variance in bone failure properties at tibial epiphysis and diaphysis. *J. Musculoskelet. Neuronal Interact.* **8**, 401–409 (2008).
758. C, G. *et al.* High resolution quantitative computed tomography-based assessment of trabecular microstructure and strength estimates by finite-element analysis of the spine, but not DXA, reflects vertebral fracture status in men with glucocorticoid-induced osteoporosis. *Bone* **52**, 568–577 (2013).
759. CC, G. *et al.* Comparative effects of teriparatide and risedronate in glucocorticoid-induced osteoporosis in men: 18-month results of the EuroGIOPs trial. *J. Bone Miner. Res.* **28**, 1355–1368 (2013).
760. J., S. E. *et al.* Cortical and trabecular bone microarchitecture predicts incident fracture independently of DXA bone mineral density and FRAX in older women and men: The Bone Microarchitecture International Consortium (BoMIC). *lancet. Diabetes Endocrinol.* **7**, 34 (2019).
761. Taoka, T. *et al.* Factors influencing visualization of vertebral metastases on MR imaging versus bone scintigraphy. *Am. J. Roentgenol.* **176**, 1525–1530 (2001).
762. Chambers, A. F., Groom, A. C. & MacDonald, I. C. Dissemination and growth of cancer cells in metastatic sites. *Nature Reviews Cancer* **2**, 563–572 (2002).
763. Wang, M., Xia, F., Wei, Y. & Wei, X. Molecular mechanisms and clinical management of cancer bone metastasis. *Bone Res.* **8**(1):30 (2020)
764. Hussain, M. H. A. *et al.* Prostate-specific antigen progression predicts overall survival in patients with metastatic prostate cancer: Data from Southwest Oncology Group trials 9346 (intergroup study 0162) and 9916. *J. Clin. Oncol.* **27**, 2450–2456 (2009).
765. Brown, J. E. & Sim, S. Evolving role of bone biomarkers in castration-resistant prostate cancer. *Neoplasia* **12**, 685–696 (2010).
766. Ramiah, V., George, D. J. & Armstrong, A. J. Clinical endpoints for drug development in prostate cancer. *Curr. Opin. Urol.* **18**, 303–308 (2008).
767. Garnero, P. Markers of bone turnover in prostate cancer. *Cancer Treat. Rev.* **27**, 187–192 (2001).
768. Koizumi, M., Yonese, J., Fukui, I. & Ogata, E. The serum level of the amino-terminal propeptide of type I procollagen is a sensitive marker for prostate cancer metastasis to bone. *BJU Int.* **87**, 348–351 (2001).
769. Koopmans, N., de Jong, I. J., Breeuwsma, A. J. & van der Veer, E. Serum Bone Turnover Markers (PINP and ICTP) for the Early Detection of Bone Metastases in Patients With Prostate Cancer: A Longitudinal Approach. *J. Urol.* **178**, 849–853 (2007).
770. Jung, K. *et al.* Comparison of 10 serum bone turnover markers in prostate carcinoma patients with bone metastatic spread: Diagnostic and prognostic implications. *Int. J. Cancer* **111**, 783–791 (2004).
771. Lara, P. N. *et al.* Serum Biomarkers of Bone Metabolism in Castration-Resistant Prostate Cancer Patients With Skeletal Metastases: Results From SWOG 0421. *JNCI J. Natl. Cancer Inst.* **106**, (2014).
772. Coleman, R. E. *et al.* Predictive value of bone resorption and formation markers in cancer patients with bone metastases receiving the bisphosphonate zoledronic acid. *J. Clin. Oncol.* **23**, 4925–4935 (2005).
773. Brown, J. E. *et al.* Bone turnover markers as predictors of skeletal complications in prostate cancer, lung cancer, and other solid tumors. *J. Natl. Cancer Inst.* **97**, 59–69 (2005).
774. Rajpar, S. *et al.* Urinary N-telopeptide (uNTx) is an independent prognostic factor for overall survival in patients with bone metastases from castration-resistant prostate cancer. *Ann. Oncol.* **21**, 1864–1869 (2010).

775. Lipton, A. *et al.* Normalization of bone markers is associated with improved survival in patients with bone metastases from solid tumors and elevated bone resorption receiving zoledronic acid. *Cancer* **113**, 193–201 (2008).
776. Lein, M. *et al.* Serial Markers of Bone Turnover in Men with Metastatic Prostate Cancer Treated with Zoledronic Acid for Detection of Bone Metastases Progression. *Eur. Urol.* **52**, 1381–1387 (2007).
777. Lein, M. *et al.* Bone turnover markers as predictive tools for skeletal complications in men with metastatic prostate cancer treated with zoledronic acid. *Prostate* **69**, 624–632 (2009).
778. Danila, D. C. *et al.* Circulating tumor cell number and prognosis in progressive castration-resistant prostate cancer. *Clin. Cancer Res.* **13**, 7053–7058 (2007).
779. Sundling, K. E. & Lowe, A. C. Circulating Tumor Cells: Overview and Opportunities in Cytology. *Advances in Anatomic Pathology* **26**, 56–63 (2019).
780. Helo, P. *et al.* Circulating prostate tumor cells detected by Reverse transcription-PCR in men with localized or castration-refractory prostate cancer: Concordance with CellSearch assay and association with bone metastases and with survival. *Clin. Chem.* **55**, 765–773 (2009).
781. Krebs, M. G., Hou, J. M., Ward, T. H., Blackhall, F. H. & Dive, C. Circulating tumour cells: Their utility in cancer management and predicting outcomes. *Therapeutic Advances in Medical Oncology* **2**, 351–365 (2010).
782. Cescon, D. W., Bratman, S. V., Chan, S. M. & Siu, L. L. Circulating tumor DNA and liquid biopsy in oncology. *Nat. Cancer* **1**, 276–290 (2020).
783. Colden, M. *et al.* MicroRNA-466 inhibits tumor growth and bone metastasis in prostate cancer by direct regulation of osteogenic transcription factor RUNX2. *Cell Death Dis.* **8**, e2572 (2017).
784. Jia, J., Huang, B., Zhuang, Z. & Chen, S. Circulating tumor DNA as prognostic markers for late stage NSCLC with bone metastasis. *Int. J. Biol. Markers* **33**, 222–230 (2018).
785. Lian JB, Stein GS, van Wijnen AJ, Stein JL, Hassan MQ, Gaur T, Zhang Y. MicroRNA control of bone formation and homeostasis. *Nat Rev Endocrinol*, **8**(4):212-27 (2012)
786. Zhao, H. *et al.* The key role of extracellular vesicles in the metastatic process. *Biochimica et Biophysica Acta - Reviews on Cancer* **1869**, 64–77 (2018).
787. Probert, C. *et al.* Communication of prostate cancer cells with bone cells via extracellular vesicle RNA; a potential mechanism of metastasis. *Oncogene* **38**, 1751–1763 (2019).
788. Hashimoto, K. *et al.* Cancer-secreted hsa-miR-940 induces an osteoblastic phenotype in the bone metastatic microenvironment via targeting ARHGAP1 and FAM134A. *Proc. Natl. Acad. Sci. U. S. A.* **115**, 2204–2209 (2018).
789. Tholey, A. & Becker, A. Top-down proteomics for the analysis of proteolytic events - Methods, applications and perspectives. *Biochimica et Biophysica Acta - Molecular Cell Research* **1864**, 2191–2199 (2017).
790. Kohli, M. *et al.* Surface-enhanced laser desorption/ionization time-of-flight mass spectrometry (SELDI-TOF MS) for determining prognosis in advanced stage hormone relapsing prostate cancer. *Cancer Biomarkers* **2**, 249–258 (2006).
791. Le, L. *et al.* Identification of serum amyloid A as a biomarker to distinguish prostate cancer patients with bone lesions. *Clin. Chem.* **51**, 695–707 (2005).
792. Iglesias-Gato, D. *et al.* The proteome of prostate cancer bone metastasis reveals heterogeneity with prognostic implications. *Clin. Cancer Res.* **24**, 5433–5444 (2018).
793. Westbrook, J. A. *et al.* CAPG and gipc1: Breast cancer biomarkers for bone metastasis development and treatment. *J. Natl. Cancer Inst.* **108**, 1–10 (2016).

794. Li, X. Q. *et al.* ITGBL1 is a Runx2 transcriptional target and promotes breast cancer bone metastasis by activating the TGF β signaling pathway. *Cancer Res.* **75**, 3302–3313 (2015).
795. Nutter, F. *et al.* Different molecular profiles are associated with breast cancer cell homing compared with colonisation of bone: Evidence using a novel bone-seeking cell line. *Endocr. Relat. Cancer* **21**, 327–341 (2014).
796. Holen, I. *et al.* IL-1 drives breast cancer growth and bone metastasis in vivo. *Oncotarget* **7**, 75571–75584 (2016).
797. Westbrook, J. A. *et al.* Identification and validation of DOCK4 as a potential biomarker for risk of bone metastasis development in patients with early breast cancer. *J. Pathol.* **247**, 381–391 (2019).
798. Li, Y. *et al.* A mandatory role of nuclear PAK4-LIFR axis in breast-to-bone metastasis of ER α -positive breast cancer cells. *Oncogene* **38**, 808–821 (2019).
799. Tiedemann, K. *et al.* Exosomal Release of L-Plastin by Breast Cancer Cells Facilitates Metastatic Bone Osteolysis. *Transl. Oncol.* **12**, 462–474 (2019).
800. Sutherland, A. *et al.* The Role of Prolactin in Bone Metastasis and Breast Cancer Cell-Mediated Osteoclast Differentiation. *J. Natl. Cancer Inst.* **108**, (2016).
801. Tikik, K. *et al.* Circulating prolactin and in situ breast cancer risk in the European EPIC cohort: A case-control study. *Breast Cancer Res.* **17**, 49 (2015).
802. Sun, H. Q., Yamamoto, M., Mejillano, M., Yin, H. L. & Gelsolin, a multifunctional actin regulatory protein. *J. Biol. Chem.* **274**, 33179–82 (1999).
803. De Corte, V. *et al.* Increased importin-beta-dependent nuclear import of the actin modulating protein CapG promotes cell invasion. *J. Cell Sci.* **117**, 5283–92 (2004).
804. Winder, S. J. & Ayscough, K. R. Actin-binding proteins. *J. Cell Sci.* **118**, 651–4 (2005).
805. Sahlas, D. J., Milankov, K., Park, P. C. & De Boni, U. Distribution of snRNPs, splicing factor SC-35 and actin in interphase nuclei: immunocytochemical evidence for differential distribution during changes in functional states. *J. Cell Sci.* **105** (Pt 2, 347–57 (1993).
806. Scheer, U., Hinssen, H., Franke, W. W. & Jockusch, B. M. Microinjection of actin-binding proteins and actin antibodies demonstrates involvement of nuclear actin in transcription of lampbrush chromosomes. *Cell* **39**, 111–122 (1984).
807. Xu, S.-G., Yan, P.-J. & Shao, Z.-M. Differential proteomic analysis of a highly metastatic variant of human breast cancer cells using two-dimensional differential gel electrophoresis. *J. Cancer Res. Clin. Oncol.* **136**, 1545–1556 (2010).
808. Renz, M., Betz, B., Niederacher, D., Bender, H. G. & Langowski, J. Invasive breast cancer cells exhibit increased mobility of the actin-binding protein CapG. *Int. J. Cancer* **122**, 1476–1482 (2007).
809. Dahl, E. *et al.* Systematic identification and molecular characterization of genes differentially expressed in breast and ovarian cancer † †. *J. Pathol. J Pathol* **205**, 21–28 (2005).
810. Shao, F., Zhang, R., Don, L. & Ying, K. Overexpression of Gelsolin-Like Actin-Capping Protein Is Associated with Progression of Lung Adenocarcinoma. *Tohoku J. Exp. Med.* **225**, 95–101 (2011).
811. Ha, E. S. *et al.* Identification of proteins expressed differently among surgically resected stage I lung adenocarcinomas. *Clin. Biochem.* **46**, 369–377 (2013).
812. Zhu, W. Y. *et al.* Prognostic Evaluation of CapG, Gelsolin, P-gp, GSTP1, and Topo-II Proteins in Non-Small Cell Lung Cancer. *Anat. Rec.* **295**, 208–214 (2012).
813. Wu, W. *et al.* Function of the macrophage-capping protein in colorectal carcinoma. *Oncol. Lett.* **14**, 5549–5555 (2017).

814. Tsai, T.-J. *et al.* Capping Actin Protein Overexpression in Human Colorectal Carcinoma and Its Contributed Tumor Migration. *Anal. Cell. Pathol.* **2018**, 1–6 (2018).
815. Thompson, C. C. *et al.* Pancreatic cancer cells overexpress gelsolin family-capping proteins, which contribute to their cell motility. *Gut* **56**, 95–106 (2007).
816. Glaser, J. *et al.* Macrophage Capping Protein CapG Is a Putative Oncogene Involved in Migration and Invasiveness in Ovarian Carcinoma. *Biomed Res. Int.* **2014**, 1–8 (2014).
817. Nomura, H. *et al.* Clinical significance of gelsolin-like actin-capping protein expression in oral carcinogenesis: An immunohistochemical study of premalignant and malignant lesions of the oral cavity. *BMC Cancer* **8**, 1–8 (2008).
818. Du, M. *et al.* Chromatin interactions and candidate genes at ten prostate cancer risk loci. *Sci. Rep.* **6**, 1–13 (2016).
819. Li, B. K. *et al.* Influence of suppression of CapG gene expression by siRNA on the growth and metastasis of human prostate cancer cells. *Genet. Mol. Res.* **14**, 15769–15778 (2015).
820. Li, T. *et al.* Gelsolin-like actin-capping protein is associated with patient prognosis, cellular apoptosis and proliferation in prostate cancer. *Biomark. Med.* **10**, 1251–1260 (2016).
821. Huang, S. *et al.* CAPG enhances breast cancer metastasis by competing with PRMT5 to modulate STC-1 transcription. *Theranostics* **8**, 2549–2564 (2018).
822. Brown, J. E. & Wood, S. L. Novel mediators of breast cancer bone metastasis—insights from studies of gene-regulation and the global proteome. *Ann. Transl. Med.* **6**, S71–S71 (2018).
823. Katoh, M. GIPC gene family (Review). *Int. J. Mol. Med.* **9**, 585–589 (2002).
824. Katoh, M. Functional proteomics, human genetics and cancer biology of GIPC family members. *Exp. Mol. Med.* **45**, e26-9 (2013).
825. Reed, B. C. *et al.* GLUT1CBP(TIP2/GIPC1) interactions with GLUT1 and myosin VI: evidence supporting an adapter function for GLUT1CBP. *Mol. Biol. Cell* **16**, 4183–201 (2005).
826. Buss, F. & Kendrick-Jones, J. How are the cellular functions of myosin VI regulated within the cell? *Biochem. Biophys. Res. Commun.* **369**, 165–75 (2008).
827. Caswell, P. T., Vadrevu, S. & Norman, J. C. Integrins: masters and slaves of endocytic transport. *Nat. Rev. Mol. Cell Biol.* **10**, 843–853 (2009).
828. Arden, S. D., Puri, C., Au, J. S.-Y., Kendrick-Jones, J. & Buss, F. Myosin VI is required for targeted membrane transport during cytokinesis. *Mol. Biol. Cell* **18**, 4750–61 (2007).
829. Valdembrì, D. *et al.* Neuropilin-1/GIPC1 Signaling Regulates $\alpha 5\beta 1$ Integrin Traffic and Function in Endothelial Cells. *PLoS Biol.* **7**, e1000025 (2009).
830. Ligensa, T. *et al.* A PDZ domain protein interacts with the C-terminal tail of the insulin-like growth factor-1 receptor but not with the insulin receptor. *J. Biol. Chem.* **276**, 33419–27 (2001).
831. Lin, D. C. *et al.* APPL1 Associates with TrkA and GIPC1 and Is Required for Nerve Growth Factor-Mediated Signal Transduction. *Mol. Cell. Biol.* **26**, 8928–8941 (2006).
832. Lou, X., Yano, H., Lee, F., Chao, M. V. & Farquhar, M. G. GIPC and GAIP Form a Complex with TrkA: A Putative Link between G Protein and Receptor Tyrosine Kinase Pathways. *Mol. Biol. Cell* **12**, 615–627 (2001).
833. Blobel, G. C., Liu, X., Fang, S. J., How, T. & Lodish, H. F. A Novel Mechanism for Regulating Transforming Growth Factor β (TGF- β) Signaling. *J. Biol. Chem.* **276**, 39608–39617 (2001).
834. Kirikoshi, H. & Katoh, M. Expression of human GIPC1 in normal tissues, cancer cell lines,

- and primary tumors. *Int. J. Mol. Med.* **9**, 509–513 (2002).
835. Knudsen, K. A., Soler, A. P., Johnson, K. R. & Wheelock, M. J. Interaction of alpha-actinin with the cadherin/catenin cell-cell adhesion complex via alpha-catenin. *J. Cell Biol.* **130**, 67–77 (1995).
836. Awan, A. *et al.* 5T4 Interacts with TIP-2/GIPC, a PDZ Protein, with Implications for Metastasis. *Biochem. Biophys. Res. Commun.* **290**, 1030–1036 (2002).
837. Muders, M. H. *et al.* Expression and regulatory role of GAIP-interacting protein GIPC in pancreatic adenocarcinoma. *Cancer Res.* **66**, 10264–10268 (2006).
838. Yavelsky, V. *et al.* Native human autoantibodies targeting GIPC1 identify differential expression in malignant tumors of the breast and ovary. (2008). doi:10.1186/1471-2407-8-247
839. Rudchenko, S. *et al.* A human monoclonal autoantibody to breast cancer identifies the PDZ domain containing protein GIPC1 as a novel breast cancer-associated antigen. *BMC Cancer* **8**, 248 (2008).
840. Muders, M. H. *et al.* Targeting GIPC/Synectin in Pancreatic Cancer Inhibits Tumor Growth. *Clin. Cancer Res.* **15**, 4095–4103 (2009).
841. Paek, A. R. & You, H. J. GAIP-interacting protein, C-terminus is involved in the induction of zinc-finger protein 143 in response to insulin-like growth factor-1 in colon cancer cells. *Mol. Cells* **32**, 415–9 (2011).
842. Chittenden, T. W. *et al.* Therapeutic Implications of GIPC1 Silencing in Cancer. *PLoS One* **5**, e15581 (2010).
843. Wu, D., Haruta, A. & Wei, Q. GIPC1 interacts with MyoGEF and promotes MDA-MB-231 breast cancer cell invasion. *J. Biol. Chem.* **285**, 28643–50 (2010).
844. Favre-Bonvin, A., Reynaud, C., Kretz-Remy, C. & Jalinot, P. Human Papillomavirus Type 18 E6 Protein Binds the Cellular PDZ Protein TIP-2/GIPC, Which Is Involved in Transforming Growth Factor Signaling and Triggers Its Degradation by the Proteasome. *J. Virol.* **79**, 4229–4237 (2005).
845. Coleman R, Cameron D, Dodwell D, Bell R, Wilson C, Rathbone E, *et al.* Adjuvant zoledronic acid in patients with early breast cancer: final efficacy analysis of the AZURE (BIG 01/04) randomised open- label phase 3 trial. *Lancet Oncol.* **15**, 997–1006 (2014).
846. Singer, A. *et al.* Impact of the adaptor protein GIPC1/Synectin on radioresistance and survival after irradiation of prostate cancer. *Strahlentherapie und Onkol.* **188**, 1125–1132 (2012).
847. Côté, J.-F. & Vuori, K. Identification of an evolutionarily conserved superfamily of DOCK180-related proteins with guanine nucleotide exchange activity. *J. Cell Sci.* **115**, 4901–13 (2002).
848. Brugnera, E. *et al.* Unconventional Rac-GEF activity is mediated through the Dock180-ELMO complex. *Nat. Cell Biol.* **4**, 574–582 (2002).
849. Hanawa-Suetsugu, K. *et al.* Structural basis for mutual relief of the Rac guanine nucleotide exchange factor DOCK2 and its partner ELMO1 from their autoinhibited forms. *Proc. Natl. Acad. Sci.* **109**, 3305–3310 (2012).
850. Webb, D. J., Parsons, J. T. & Horwitz, A. F. Adhesion assembly, disassembly and turnover in migrating cells – over and over and over again. *Nat. Cell Biol.* **4**, E97–E100 (2002).
851. Lauffenburger, D. A. & Horwitz, A. F. Cell migration: A physically integrated molecular process. *Cell* **84**, 359–369 (1996).
852. Katoh, H. Activation of Rac1 by RhoG regulates cell migration. *J. Cell Sci.* **119**, 56–65 (2005).
853. Kobayashi, M., Harada, K., Negishi, M. & Katoh, H. Dock4 forms a complex with SH3YL1

- and regulates cancer cell migration. *Cell. Signal.* **26**, 1082–1088 (2014).
854. Nobes, C. D. & Hall, A. Rho GTPases control polarity, protrusion, and adhesion during cell movement. *J Cell Biol.* 1999;144(6):1235–44. GTPases control polarity, protrusion, and adhesion during cell movement. *J. Cell Biol.* **144**, 1235–1244 (1999).
855. Hiramoto-Yamaki, N. *et al.* Ephexin4 and EphA2 mediate cell migration through a RhoG-dependent mechanism. *J. Cell Biol.* **190**, 461–477 (2010).
856. Abraham, S. *et al.* ARTICLE A Rac/Cdc42 exchange factor complex promotes formation of lateral filopodia and blood vessel lumen morphogenesis. *Nat. Commun.* **6**, (2015).
857. Wu, X. *et al.* Rac1 activation and subsequent β -catenin phosphorylation controls nuclear localization of β -catenin during canonical Wnt signaling. *Cell* **133**, 340–353 (2009).
858. Yang, K. *et al.* The evolving roles of canonical WNT signaling in stem cells and tumorigenesis: Implications in targeted cancer therapies. *Lab. Investig.* **96**, 116–136 (2016).
859. Kikuchi, A. Roles of Axin in the Wnt Signalling Pathway. *Cell. Signal* **11**, 777–788 (1999).
860. Upadhyay, G. *et al.* Molecular association between β -catenin degradation complex and Rac guanine exchange factor DOCK4 is essential for Wnt/ β -catenin signaling. *Oncogene* **27**, 5845–5855 (2008).
861. Xu X, Jin T. ELMO proteins transduce G protein-coupled receptor signal to control reorganization of actin cytoskeleton in chemotaxis of eukaryotic cells. *Small GTPases* **10**, 271–279 (2019).
862. Schlessinger, K., Hall, A. & Tolwinski, N. Wnt signaling pathways meet Rho GTPases. *Genes Dev.* **23**, 265–277 (2009).
863. Dasari, T. *et al.* Design of novel lead molecules against RhoG protein as cancer target—a computational study. *J. Biomol. Struct. Dyn.* **35**, 3119–3139 (2017).
864. Gadea, G., Sanz-Moreno, V., Self, A., Godi, A. & Marshall, C. J. DOCK10-Mediated Cdc42 Activation Is Necessary for Amoeboid Invasion of Melanoma Cells. *Curr. Biol.* **18**, 1456–1465 (2008).
865. Sanz-Moreno, V. *et al.* Rac Activation and Inactivation Control Plasticity of Tumor Cell Movement. *Cell* **135**, 510–523 (2008).
866. Laurin, M. *et al.* Rac-specific guanine nucleotide exchange factor DOCK1 is a critical regulator of HER2-mediated breast cancer metastasis. *Proc. Natl. Acad. Sci.* **110**, 7434–7439 (2013).
867. Feng, H. *et al.* Phosphorylation of dedicator of cytokinesis 1 (Dock180) at tyrosine residue Y722 by Src family kinases mediates EGFRvIII-driven glioblastoma tumorigenesis. *Proc. Natl. Acad. Sci.* **109**, 3018–3023 (2012).
868. Yajnik V, Paulding C, et al. DOCK4, a GTPase activator, is disrupted during tumorigenesis. *Cell* **112**, 673–684 (2003).
869. Yu, J. R. *et al.* TGF- β /smad signaling through DOCK4 facilitates lung adenocarcinoma metastasis. *Genes Dev.* **29**, 250–261 (2015).
870. Valastyan, S. & Weinberg, R. A. Tumor metastasis: molecular insights and evolving paradigms. *Cell* **147**, 275–92 (2011).
871. Pavlovic, M. *et al.* Enhanced MAF Oncogene Expression and Breast Cancer Bone Metastasis. *J. Natl. Cancer Inst.* **107** (2015).
872. El-Haibi, C. P., Singh, R., Sharma, P. K., Singh, S. & Lillard, J. W. CXCL13 mediates prostate cancer cell proliferation through JNK signalling and invasion through ERK activation. *Cell Prolif* **44**, (2011).
873. Horoszewicz, J. S. *et al.* LNCaP model of human prostatic carcinoma. *Cancer Res.* **43**,

- 1809–1818 (1983).
874. Veldscholte, J. *et al.* A mutation in the ligand binding domain of the androgen receptor of human LNCaP cells affects steroid binding characteristics and response to anti-androgens. *Biochem. Biophys. Res. Commun.* **173**, 534–40 (1990).
875. Vlietstra, R. J., van Alewijk, D. C., Hermans, K. G., van Steenbrugge, G. J. & Trapman, J. Frequent inactivation of PTEN in prostate cancer cell lines and xenografts. *Cancer Res.* **58**, 2720–3 (1998).
876. Tomlins, S. A. *et al.* Distinct classes of chromosomal rearrangements create oncogenic ETS gene fusions in prostate cancer. *Nature* **448**, 595–599 (2007).
877. Baena, E. *et al.* ETV1 directs androgen metabolism and confers aggressive prostate cancer in targeted mice and patients. *Genes Dev.* **27**, 683–98 (2013).
878. Sato, N. *et al.* A metastatic and androgen-sensitive human prostate cancer model using intraprostatic inoculation of LNCaP cells in SCID mice. *Cancer Res.* **57**, 1584–9 (1997).
879. Lim, D. J. *et al.* Growth of an androgen-sensitive human prostate cancer cell line, LNCaP, in nude mice. *Prostate* **22**, 109–18 (1993).
880. Thalmann, G. N. *et al.* Androgen-independent cancer progression and bone metastasis in the LNCaP model of human prostate cancer. *Cancer Res.* **54**, 2577–81 (1994).
881. Wu, T. T. *et al.* Establishing human prostate cancer cell xenografts in bone: induction of osteoblastic reaction by prostate-specific antigen-producing tumors in athymic and SCID/bg mice using LNCaP and lineage-derived metastatic sublines. *Int. J. cancer* **77**, 887–94 (1998).
882. Thalmann, G. N. *et al.* LNCaP progression model of human prostate cancer: Androgen-independence and osseous metastasis. *Prostate* **44**, 91–103 (2000).
883. Lin, D. L. *et al.* Bone metastatic LNCaP-derivative C4-2B prostate cancer cell line mineralizes in vitro. *Prostate* **47**, 212–221 (2001).
884. Kaighn, M. E., Narayan, K. S., Ohnuki, Y., Lechner, J. F. & Jones, L. W. Establishment and characterization of a human prostatic carcinoma cell line (PC-3). *Invest. Urol.* **17**, 16–23 (1979).
885. Ching, K. Z. *et al.* Expression of mRNA for epidermal growth factor, transforming growth factor- α and their receptor in human prostate tissue and cell lines. *Mol. Cell. Biochem.* **126**, 151–8 (1993).
886. van Bokhoven, A., Varella-Garcia, M., Korch, C., Hessels, D. & Miller, G. J. Widely used prostate carcinoma cell lines share common origins. *Prostate* **47**, 36–51 (2001).
887. Tai, S. *et al.* PC3 is a cell line characteristic of prostatic small cell carcinoma. *Prostate* **71**, 1668–1679 (2011).
888. Pettaway, C. A. *et al.* Selection of highly metastatic variants of different human prostatic carcinomas using orthotopic implantation in nude mice. *Clin. Cancer Res.* **2**, 1627–36 (1996).
889. Stephenson, R. A. *et al.* Metastatic model for human prostate cancer using orthotopic implantation in nude mice. *J. Natl. Cancer Inst.* **84**, 951–7 (1992).
890. Wong, S. K. *et al.* Prostate Cancer and Bone Metastases: The Underlying Mechanisms. *Int. J. Mol. Sci.* **20**, (2019).
891. Kwiatkowski, D. J. Functions of gelsolin: motility, signaling, apoptosis, cancer. *Curr. Opin. Cell Biol.* **11**, 103–108 (1999).
892. Richmond, A. & Yingjun, S. Mouse xenograft models vs GEM models for human cancer therapeutics. *DMM Disease Models and Mechanisms* **1**, 78–82 (2008).
893. Zhu, Y. *et al.* Proteome Profiling of 1 to 5 Spiked Circulating Tumor Cells Isolated from Whole Blood Using Immunodensity Enrichment, Laser Capture Microdissection,

Nanodroplet Sample Processing, and Ultrasensitive nanoLC–MS. *Anal. Chem.* **90**, 11756–11759 (2018).

894. Picotti, P. & Aebersold, R. Selected reaction monitoring–based proteomics: workflows, potential, pitfalls and future directions. *Nat. Methods* **2012 9**, 555–566 (2012).
895. Brady L, Kriner M, Coleman I, et al. Inter- and intra-tumor heterogeneity of metastatic prostate cancer determined by digital spatial gene expression profiling. *Nat Commun.* **3**;1426 (2021).